

Does HPV-16 seropositivity correlate with T-cell
distribution providing additional prognostic
information in infected HNSCC patients?

Tosief Zahoor MBBS MRCS DOHNS

MD by thesis

The University of Hull and The University of York
Hull York Medical School

March 2016

Abstract

It is widely accepted that infection with Human Papilloma Virus (HPV) confers better outcomes and survival rates in head and neck squamous cell carcinoma (HNSCC) patients (80% 5-year survival) compared with HPV-negative counterparts (50% 5-year survival), regardless of treatment modality. It is hypothesised that the increased immune response against HPV infection contributes to better survival, however the exact mechanisms involved remain unknown. The HPV oncoproteins E6 and E7 have been shown to be involved in tumourigenesis of HNSCC, particularly those originating in the oropharynx and oral cavity. These proteins appear to act through inactivating both the p53 and retinoblastoma (pRb) genes, as silencing of these viral proteins results in re-expression of these two suppressor pathways. In order to show a causative role of HPV infection and tumorigenesis a biologically active infection needs to be shown, this was done by the use of multi-modal diagnostic techniques using p16 IHC as a surrogate marker and ISH as a confirmatory test.

HPV seropositivity in HNSCC has been quoted to range between 24-67% with the exact role in prognosis not defined. HPV-oncoproteins were expressed to use against human sera in an in-house developed ELISA. This study found a high percentage of healthy controls displaying an antibody response to the HPV E7 oncoprotein, therefore the use of an antibody response as an indicator of HPV16 infection alone is not valid. However, seropositivity may be useful as a prognostic indicator when correlated with other immune markers.

Tumour infiltrating cells and CD8⁺ve:FoxP3 ratio have been associated with improved outcomes regardless of tumour subset. This study found TIL were higher in HPV+ compared to HPV- HNSCC and CD8⁺ve:FoxP3 ratio was higher in HPV positive HNSCC. CD4⁺ve cells are associated with increased survival outcomes, this study found high levels of CD4⁺ve cells associated with >3year prognosis. Improved adaptive immunity plays a role in the favourable prognosis of patients with HPV-16 positive HNSCC, further knowledge of which may lead to the development of combined targeted immunotherapy thus reducing current treatment associated morbidity, such as that associated with radiotherapy.

Table of Contents

Abstract	2
List of Figures	9
List of Tables	13
List of Abbreviations	14
Acknowledgements	17
Author Declaration	18
Chapter 1. Introduction	19
1.1 Epidemiology of head and neck squamous cell carcinoma	19
1.2 Anatomy of the Head and Neck Region	21
1.2.1 Boundaries of the Head and Neck.....	21
1.2.2 Oral Cavity.....	21
1.2.3 Oropharynx.....	22
1.2.4 Nasopharynx.....	23
1.2.5 Hypopharynx	23
1.2.6 Larynx	24
1.3 Cervical Lymph Nodes	24
1.3.1 Distribution of Cervical Lymph Nodes.....	25
1.3.2 Drainage Patterns of Cervical Lymph Nodes	25
1.4 Aetiology of Head and Neck squamous cell carcinoma	28
1.4.1 Tobacco	28
1.4.1.1 Smoking.....	28
1.4.1.2 Snuff, Oral tobacco or Smokeless tobacco	32
1.4.2 HPV & Smoking.....	33
1.4.3 Alcohol.....	34
1.4.4 Betel Quid (Paan)	35
1.4.5 HPV and Betel Quid.....	37
1.4.6 Other Risk factors	37
1.5 Staging of HNSCC	38
1.5.1 TNM Staging System.....	38
1.5.2 Stages of Cancer	39
1.6 Treatment options for HNSCC	40

1.7 Human Papilloma Virus-16 associated HNSCC	41
1.7.1 Introduction to the Human Papilloma Viruses	42
1.7.2 The Structure of HPV-16.....	45
1.7.3 The HPV Life Cycle.....	46
1.7.4 HPV-16 Oncoproteins.....	50
1.7.5 HPV-16 E6	53
1.7.6. HPV-16 E7	54
1.7.7 Trends in HPV related HNSCC	57
1.8 The role of HPV in oncogenesis	59
1.8.1 Role of E6 and E7 in Oncogenesis.....	61
1.9 HPV and The Immune Response	64
1.9.1 Local Immune factors.....	64
1.9.2 Systemic Immune factors	66
1.9.3 Poor prognostic indicators in HNSCC.....	69
1.10 HPV Detection methods.....	74
1.10.1 Direct HPV tests	74
1.10.1.1 Polymerase Chain Reaction.....	74
1.10.1.2 In Situ Hybridisation	75
1.10.1.3 Southern Blotting Assay	76
1.10.2 Indirect Tests Correlating with HPV	77
1.10.2.1 Immunohistochemical staining for p16.....	77
1.10.2.2 Serum Antibodies against HPV	78
1.11 Aims of Thesis.....	79
Chapter 2. Material & Methods	81
2.1 Purification of Genomic DNA.....	81
2.1.1 Phenol Chloroform extraction.....	81
2.2 Amplification of genomic DNA using PCR	83
2.2.1 Primer Design	83
2.2.2 Structure of HPV 16	84
2.2.3 Genomic sequence patterns with primers	85
2.2.4 Protein Tags.....	87
2.2.5 Expression Vectors.....	88
2.2.6 PCR Template	90
2.2.7 PCR Reaction.....	90
2.2.8 Isolation and analysis of PCR products	92

2.2.9 Preparing the Agarose gel	92
2.2.10 Analysis of PCR products	92
2.2.11 Purification of PCR Products	94
2.2.12 Purification of DNA Fragments	95
2.3 <i>Escherichia Coli</i> Competent Cell Production	96
2.4 Expression in Bacteria and Purification of Recombinant plasmids	98
2.4.1 Restriction Enzyme digest of Plasmid Vectors and DNA Fragments.....	98
2.4.2 Ligation Reactions	98
2.4.3 Transformation of Recombinant Plasmid in E-Coli.....	99
2.4.4 Pouring Agar Plates.....	100
2.4.5 Isolation of Recombinant Plasmid by Mini-preparation.....	100
2.5 Expression of Recombinant HPV-16 Proteins	102
2.5.1 E.coli Host Strains	102
2.5.2 Induction and Optimisation of Expression	102
2.5.3 Cell Lysis and Protein Extraction	104
2.6 Protein Purification By Immobilised Metal Affinity Chromatography (IMAC)	104
2.7 Protein Purification by Ammonium Sulphate Precipitation	105
2.8 Dialysis	106
2.9 Preparation of Sodium Dodecyl Sulfate (SDS)-polyacrylamide gel electrophoresis	107
2.9.1 Sample preparation for SDS gels.....	110
2.9.2 Running SDS-PAGE.....	110
2.10 Western Blotting.....	112
2.11 P16 Immunohistochemistry	115
2.11.1 Staining procedure for the Manual use of CINtec® Histology Kit.....	115
2.11.2 Deparaffinisation and Rehydration.....	116
2.11.3 Staining protocol	117
2.11.3.1 Epitope Retrieval.....	117
2.11.3.2 Peroxidase-Blocking Reagent.....	117
2.11.3.3 Primary Antibody	118
2.11.3.4 Visualisation Agent.....	118
2.11.3.5 Substrate-Chromogen Solution (DAB)	118
2.11.3.6 Counterstaining with Hematoxylin.....	119
2.11.3.7 Mounting	119
2.12 Hematoxylin and Eosin Staining.....	119

2.13 Enzyme Linked Immunosorbent Assay (ELISA).....	120
2.14 Ethical approval	122
Chapter 3. Molecular Biology-Expression of HPV-16 Oncoproteins	123
3.1 Introduction.....	123
3.2 Optimisation of PCR	123
3.2.1 Explanation for lack of E2	128
3.3 Transformation of PCR Products E6 and E7 His tag	129
3.4 Recombinant pGEX-E6 and pGEX-E7 Synthesis and Transformation	132
3.5 <i>BamHI</i> and <i>EcoRI</i> Restriction Enzyme Digests	133
3.6 Expression in Bacteria and Purification of Recombinant Proteins	140
3.6.1 Expression and purification of HPV-16 E2NT	140
3.6.2 Expression and purification of HPV-16 E2LCT	145
3.6.3 Expression and purification of HPV-16 E2	147
3.6.4 Expression and purification of HPV-16 E6	149
3.6.5 Expression and Purification of HPV-16 E7	152
3.7 Discussion.....	156
Chapter 4. Enzyme Linked Immunosorbent Assays of antibodies against HPV oncoproteins in Human Sera.....	159
4.1 Introduction.....	159
4.2 Optimization of the ELISA method	160
4.2.1 Binding Control for E7	160
4.2.2 Optimisation of E7 concentrations and serum dilutions.....	164
4.2.3 Reducing non-specific binding.....	166
4.2.4 Determination of optimum blocking reagents and diluents in Human sera.	169
4.2.5 Use of BSA as a diluent.....	173
4.3 Optimising serum concentrations.....	175
4.4 Determining positive cut off value	178
4.5 Use of the optimised E7 ELISA to determine E7 antibody titres in control and HNSCC patient serum	178
4.6 E7 Antibody titres for Oropharyngeal SCC	182
4.7 E7 Antibody titres for Oral Cavity SCC	184
4.8 E7 Antibody titres for Laryngeal SCC.....	185
4.9 E7 Antibody titres for Hypopharyngeal SCC	187
4.10 Development of the HPV-E6 ELISA	189

4.11 Using the optimised E6 ELISA to determine E6 antibody titres in control and HNSCC patient serum.....	191
4.12 Increasing concentrations of plate bound E6	195
4.13 Discussion	198
Chapter 5 - P16 Immunohistochemistry and In-Situ Hybridisation for HPV 16/18 detection in HNSCC FFPE sections	206
5.1 Introduction.....	206
5.1.1 P16 ^{INK4a} staining patterns	208
5.2 Methods.....	210
5.2.1 P16 immunohistochemistry.....	210
5.2.2. In situ hybridisation of HPV16.....	211
5.3 Results	213
5.3.1 Analysis of p16 immunohistochemistry	214
5.3.2 Analysis of in-situ hybridisation for the presence of HPV in HNSCC.....	217
5.3.3 Molecular Classification of HPV status	217
5.4 Discussion.....	219
Chapter 6 - Clinical Correlations of Tumour Infiltrating Lymphocytes and Peripheral Circulating Cytokines with HPV Status and Survival in HNSCC	226
6.1 Introduction.....	226
6.2 Method.....	228
6.3 Results	231
6.3.1. TIL in HPV-positive HNSCC versus HPV-negative HNSCC.....	231
6.3.2. Th1 and Th2 cytokines in HPV-positive HNSCC versus HPV-negative HNSCC	235
6.3.3. Anti-E7 antibody levels in HPV-positive HNSCC compared to HPV-negative HNSCC	237
6.3.4 Survival Curves in HPV-positive HNSCC versus HPV-negative HNSCC	238
6.3.5 Survival Outcomes Regardless of HPV status	240
6.4 Survival Outcomes in Oropharyngeal SCC	241
6.4.1 Tumour infiltrating lymphocytes and Anti-E7 antibodies in OPSCC.....	242
6.4.2 Th1 and Th2 cytokines in OPSCC	245
6.5 Discussion.....	246
Chapter 7. Concluding Remarks	251

References	260
Appendix 1. TNM Staging of HNSCC	276
Appendix 2. Buffers and Solutions.....	280
Appendix 3: Current on-going Trials in De-escalation of Treatment in HNSCC	282
Appendix 4. Ammonium sulphate precipitation tables.....	284

List of Figures

Fig. 1.1	Incidence of head and neck cancer worldwide and in the UK	20
Fig. 1.2	Boundaries of subsections of the Head and Neck	22
Fig. 1.3	Distribution of cervical lymph nodes	25
Fig. 1.4	Link between cigarette smoking and cancer	30
Fig. 1.5	The Papillomavirus Phylogenetic tree	43
Fig. 1.6	Structure of HPV-16	45
Fig. 1.7	The HPV viral life cycle	46
Fig. 1.8	HPV integration into basal cell keratinocyte and infection cycle	48
Fig. 1.9a-b	(a)Normal Cell cycle (b) Interruption of cell cycle by HPV-16 E7	56
Fig. 1.10	Normal cell cycle control and check points	57
Fig. 2.1	Centrifugation of the phenol/ chloroform extracted DNA	82
Fig. 2.2	Complete genome of HPV-16	84
Fig. 2.3a-c	Genomic sequence for HPV-16 oncoproteins E2, E6 and E7	85
Fig. 2.4	The pET-28a vector	89
Fig. 2.5	pGEX-6P1 fusion vector with cloning and restriction sites.	89
Fig. 2.6	PCR reaction and temperature changes with DNA replication.	91
Fig. 2.7	Lambda DNA/EcoRI Hind III Marker	93
Fig. 2.8	Midbase 1kb DNA ladder	94
Fig. 2.9	SDS-PAGE system set up	111
Fig. 2.10	Set up of Western Blotting membrane between electrodes.	115
Fig. 3.1	Optimisation PCR for GST and HIStag for E2, E6 and E7.	124
Fig. 3.2	PCR optimisation for E2 and E6	125
Fig. 3.3	Optimisation of PCR by addition of Mg ²⁺ and DMSO	127
Fig. 3.4	Optimisation of E2 PCR by use of ReddyMix PCR Mastermix	128
Fig. 3.5.	Purified PCR products for E6 His Tag and E7 His Tag	129
Fig. 3.6.	Restriction enzyme digests of pET28a vector	130
Fig. 3.7.	Agarose gel for double cut pET28a, double cut E6 and E7 His Tag	131
Fig. 3.8	Agarose gel for E6 and E7 GST tag on 1.2% agarose gel	133
Fig. 3.9	Restriction enzyme digests on pGEX-6p1 vector	134
Fig. 3.10	Restriction enzyme digested pGEX-6p1, E6 _{BE} and E7 _{BE} .	135

Fig. 3.11	Repeated PCR for E6-GST and E7-GST	136
Fig. 3.12	Restriction enzyme digested pGEX-6p1, E6 _{BE} and E7 _{BE}	137
Fig. 3.13	BamHI and EcoRI digested pGEX6p1 with E6 and E7 inserts	140
Fig. 3.14	SDS-PAGE of protein expression of HPV-E2NT	141
Fig. 3.15	Recombinant HPV-16 E2NT purified by IMAC	142
Fig. 3.16	Ammonium sulphate ppt of 10mM imidazole elute E2NT	144
Fig. 3.17	HPV-16 E2LCT and HPV-16 E2 soluble and insoluble phases	145
Fig. 3.18	Purification of HPV-16 E2LCT with IMAC	146
Fig. 3.19	E2LCT expressed in BL21 pLysS purification with IMAC	147
Fig. 3.20	Purification of HPV-16 E2 soluble phase by IMAC	148
Fig. 3.21	HPV-16 E2 expressed in BL21 pLysS	149
Fig. 3.22	HPV-16 E6 purified with IMAC	150
Fig. 3.23	HPV-16 E6 purification by ammonium sulphate precipitation	151
Fig. 3.24	E6 protein product illustrated by Western Blotting	152
Fig. 3.25	Expression of recombinant HPV-16 E7 protein	153
Fig. 3.26	HPV-16 E7 First Purification Step by IMAC	154
Fig. 3.27	HPV-16 E7 Ammonium sulphate precipitation of 100mM Elute	155
Fig. 3.28	E7 protein illustrated by Western Blotting	155
Fig. 4.1	Binding control for HPV-E7 on ELISA assay	161
Fig. 4.2a-b	Absorbance for ELISA using varying conc. of E7 and MAHAb	162
Fig. 4.3	Binding control of E7 with Anti-E7	163
Fig. 4.4a-b	Optimum conc. of HPV-E7 determined by healthy controls	165
Fig. 4.5	Assay set up for reducing non-specific binding of detection antibody and optimising use of Anti-GAM/GAH-HRP	167
Fig. 4.6 a-b	Comparison of blocking buffers, diluents and detection with variable dilutions of GAM- or GAH-HRP	169
Fig. 4.7a-b	Optimising diluents with human sera	171
Fig. 4.8 a-b	Optimum diluent and blocking agent to use with human sera	172
Fig. 4.9 a-b	Comparison of 1% BSA versus 1% NFDM as diluent	174
Fig. 4.10	Variable serum dilutions added to E7 and CB as negative control to assess binding of antibodies within sera	176
Fig. 4.11a-b	Increased serum dilutions of controls and patients	177
Fig. 4.12	Patient and control samples and distribution of sub site of cancer	178

Fig. 4.13	Average absorbance for patient and controls at 1:500 and 1:5000 dilutions against E7	179
Fig. 4.14a-b	Distribution of E7 seropositivity for early versus late HNSCC	181
Fig. 4.15	Absorbance values for all subgroups of HNSCC	182
Fig. 4.16a-b	Absorbance of anti-E7 for early versus late OPSCC.	183
Fig. 4.17a-b	Absorbance of anti-E7 OCSCC and comparison of nodal status	185
Fig. 4.18a-b	Absorbance of anti-E7 for early versus late laryngeal SCC	187
Fig. 4.19	Anti-E7 levels for early versus late stage HPSCC and nodal status	188
Fig. 4.20	Optimisation of use of E6 protein and testing negative control	190
Fig. 4.21	Absorbance values for E6 and binding control for E6 antigen	190
Fig. 4.22 a-b	Healthy control and patient absorbance levels for E6 by ELISA	192
Fig. 4.23	Absorbance values for control and patient sample when tested against E6 and negative control CB	193
Fig. 4.24	Absorbance values for a single patient sample and negative controls with 0.75µg/ml of E6	194
Fig. 4.25a-b	(a) E6 binding control (b) patient samples tested against variable E6 conc. and negative control CB	196
Fig. 4.26a-b	E6 used at a conc. of 5µg/ml with negative control of CB	198
Fig. 5.1	CINtec [®] Staining Atlas of p16 staining patterns	208
Fig. 5.2	Molecular classification of HNSCC p16 IHC and ISH	209
Fig. 5.3a-b	a) H&E staining HNSCC b) p16 IHC HNSCC	211
Fig. 5.4	Photomicrograph of OPSCC showing ISH positive HPV-DNA	213
Fig. 5.5	Distribution of patient samples available for IHC analysis	214
Fig. 5.6a-d	p16 IHC staining patterns	215
Fig. 5.7	IHC samples per subtype and p16 positive samples	216
Fig. 5.8	ISH samples per subset tested	217
Fig. 5.9	Diagnostic algorithms for detection of biologically active HPV in FFPE HNSCC samples	223
Fig. 6.1	Flow chart for HPV diagnostic tests and Ethical approval codes	229
Fig. 6.2	Patient samples available with complete data set	231
Fig. 6.3a-b	TIL in HPV+ve (a) HNSCC compared to HPV-ve (b)HNSCC.	233
Fig. 6.4	CD4:CD8 ratio amongst HPV+ve and HPV-ve HNSCC	234
Fig. 6.5	CD8 ⁺ :FoxP3 ratio amongst HPV+ versus HPV- HNSCC	235

Fig. 6.6a-b	Th1 and Th2 cytokines in HPV+ (a) and HPV- (b) HNSCC	237
Fig. 6.7	E7 antibody status and prognosis in HPV+ve and HPV-ve HNSCC	238
Fig. 6.8	Kaplan Meier survival curves for HPV+ve and HPV-ve HNSCC	239
Fig. 6.9	DFS in good (≥ 3 -years) compared to poor prognosis (< 3 -years)	240
Fig. 6.10	Five year DFS in HPV+ versus HPV- OPSCC	242
Fig 6.11a-d	CD4 ⁺ , CD8 ⁺ , FoxP3 and anti-E7 in HPV+ve vs. HPV-ve OPSCC	243
Fig. 6.12	CD4 ⁺ :CD8 ⁺ ratio amongst the HPV+ve vs. HPV-ve	244
Fig. 6.13	CD8 ⁺ :FoxP3 ratio amongst HPV+ vs. HPV- OPSCC	244
Fig. 6.14a-b	Th1 and Th2 cytokines in HPV+ and HPV- OPSCC	245

List of Tables

Table 1.1	Cervical Lymph Node Metastases by Primary Cancer site	27
Table 1.2	Stage grouping for oral cavity, oropharyngeal, hypopharyngeal and laryngeal cancers	40
Table 1.3	Differences between HPV positive and HPV negative HNSCC	42
Table 1.4	Summary of Oncoprotein Function	51
Table 1.5	Direct HPV Detection Methods	77
Table 2.1	Primer design for His-tag fusion proteins	87
Table 3.1	Combinations for restriction digests with <i>BamHI</i> and <i>EcoRI</i>	134
Table 3.2	Ammonium sulphate precipitates and volume of salt required	143
Table 4.1	Distribution of Grade of Laryngeal SCC	186
Table 5.1	Molecular classifications of HNSCC samples based on p16 IHC and ISH	219
Table 5.2	Concordance rates between p16 positivity and DNA ISH	224
Table 6.1	Levels of TIL, cytokines and E7 Ab on DFS survival	241
Table 6.2	Th1 and Th2 cytokines in OPSCC	246

List of Abbreviations

Ab	Antibody
ADH	Alcohol dehydrogenase enzyme
AJCC	American Joint Committee on Cancer
APC	Antigen presenting cell
BSA	Bovine serum albumin
CD	Cluster of differentiation cell
CDK	Cyclin-dependant kinase
CI	Confidence interval
CIN	Cervical intraepithelial neoplasia
CTL	Cytolytic T-lymphocyte
DNA	Deoxyribo-nucleic acid
DSS	Disease specific survival
DFS	Disease free survival
E-Coli	<i>Escherichia coli</i>
EGFR	Epidermal growth factor receptor
ELISA	Enzyme linked immunosorbent assay
FFPE	Formalin fixed paraffin embedded
Fox-P3	Forkhead Box P3
GAH-HRP	Goat-anti human horse radish peroxidase
GAM-HRP	Goat-anti mouse horse radish peroxidase
GST	Glutathione-S-transferases
HDAC	Histone deacetylase
H&E	Haematoxylin and Eosin
HNSCC	Head and neck squamous cell carcinoma
HP	Hypopharynx/hypopharyngeal
HPV	Human papillomavirus
HPV+	Human papillomavirus positive
HPV-	Human papillomavirus negative
IFN-γ	Interferon-gamma

IL	Interleukin
IHC	Immunohistochemistry
IMAC	Immobilized metal affinity chromatography
IPTG	Isopropyl thio-b-D-galactoside
ISH	In-situ hybridization
LB	Luria Bertania
MHC	Major histocompatibility complex
MNPN	3-methylnitrosamino propionaldehyde
NFDM	Non-fat dried milk
OC	Oral cavity
OP	Oropharynx/oropharyngeal
OPSCC	Oropharyngeal squamous cell carcinoma
OR	Odds ratio
ORF	Open reading frame
OS	Overall survival
PAH	Polyaromatic hydrocarbons
PAP	Papanicolaou smear test
PBS	Phosphate buffered saline
PCR	Polymerase Chain Reaction
PD-1	Programmed Cell Death Protein 1
PD-L1	Programmed Cell Death Ligand 1
PDX	Patient derived xenograft
pRb	Retinoblastoma protein
PVDF	Polyvinylidene fluoride
RNA	Ribonucleic acid
SBA	Southern blotting assay
SCC	Squamous cell carcinoma
TIL	Tumour infiltrating lymphocyte
TNF	Tumour necrosis factor
UICC	Union for International Cancer Control
WHO	World Health Organization
Wt-p53	Wild-type p53
VIN	Vulval intraepithelial neoplasia

*Dedicated to my Father without whose support this work would not
have been possible*

Acknowledgements

I would like to thank my supervisors immensely without whom this work would not have been possible. I would like to thank Dr Victoria Green for her help and support with guidance of laboratory techniques and help with development of tests, in particular in the development of the in-house ELISA, also for her help in the guidance and development of the thesis. I would like to thank Professor John Greenman for his immense support and help in the development of the thesis idea and for help with analysis of results and guidance in general on all aspects of the thesis. I would like to thank Professor Nicholas Stafford for his help and support throughout this work and I would also like to thank Dr Kevin Morgan for his help on the work on Western blotting and DNA extraction.

Author Declaration

“I can confirm that this work is original and that if any passage(s) or diagram(s) have been copied from academic papers, books, the Internet or any other sources these are clearly identified by the use of quotation marks and the reference(s) is fully cited. I certify that, other than where indicated, this is my own work and does not breach the regulations of HYMS, the University of Hull or the University of York regarding plagiarism or academic conduct in examinations. I have read the HYMS Code of Practice on Academic Misconduct, and state that this piece of work is my own and does not contain any unacknowledged work from any other sources. I confirm that any patient information obtained to produce this piece of work has been appropriately anonymised”.

Chapter 1. Introduction

1.1 Epidemiology of head and neck squamous cell carcinoma

Head and neck carcinoma is the fifth most common cancer worldwide and is the sixth most common cause of cancer related mortality (WHO, 2012). There were an estimated 686,300 cases of head and neck cancer worldwide, with a mortality of 54.6% in 2012. In the UK there were 9600 cases, with an incidence rate of 18.4/100,000, with over 3000 deaths related to head and neck cancer in 2012 (WHO, 2012). Compared to all cancers worldwide (excluding skin), head and neck cancer has both an incidence and mortality of 5% (WHO, 2012). The majority of head and neck cancers are squamous cell carcinoma by far (Marur et al., 2010), with the largest subtype being the oral cavity, including the lip and oropharynx (see Fig.1.1).

The incidence of laryngeal cancer has declined in the UK by 20% since the 1990's, however the rates have leveled off in the last five years. The reason for falling rates can be attributed to increasing awareness of risk factors such as smoking and alcohol consumption, and health campaigns to reduce such risk factors. On the contrary the rates of oral and oropharyngeal cancer have increased substantially over this period. Rates of oral cancer have increased by around 30%, and have been linked to increasing migration from the Indian subcontinent, with associated customary risk factors, such as chewing betel quid. The largest increase has been observed in the oropharyngeal category with rates having more than doubled in the last 30 years, the causative factors have changed, with high risk human papillomavirus (HPV), namely

HPV-16 and HPV-18, being the major causative factors in the younger sub-population rather than alcohol and smoking.

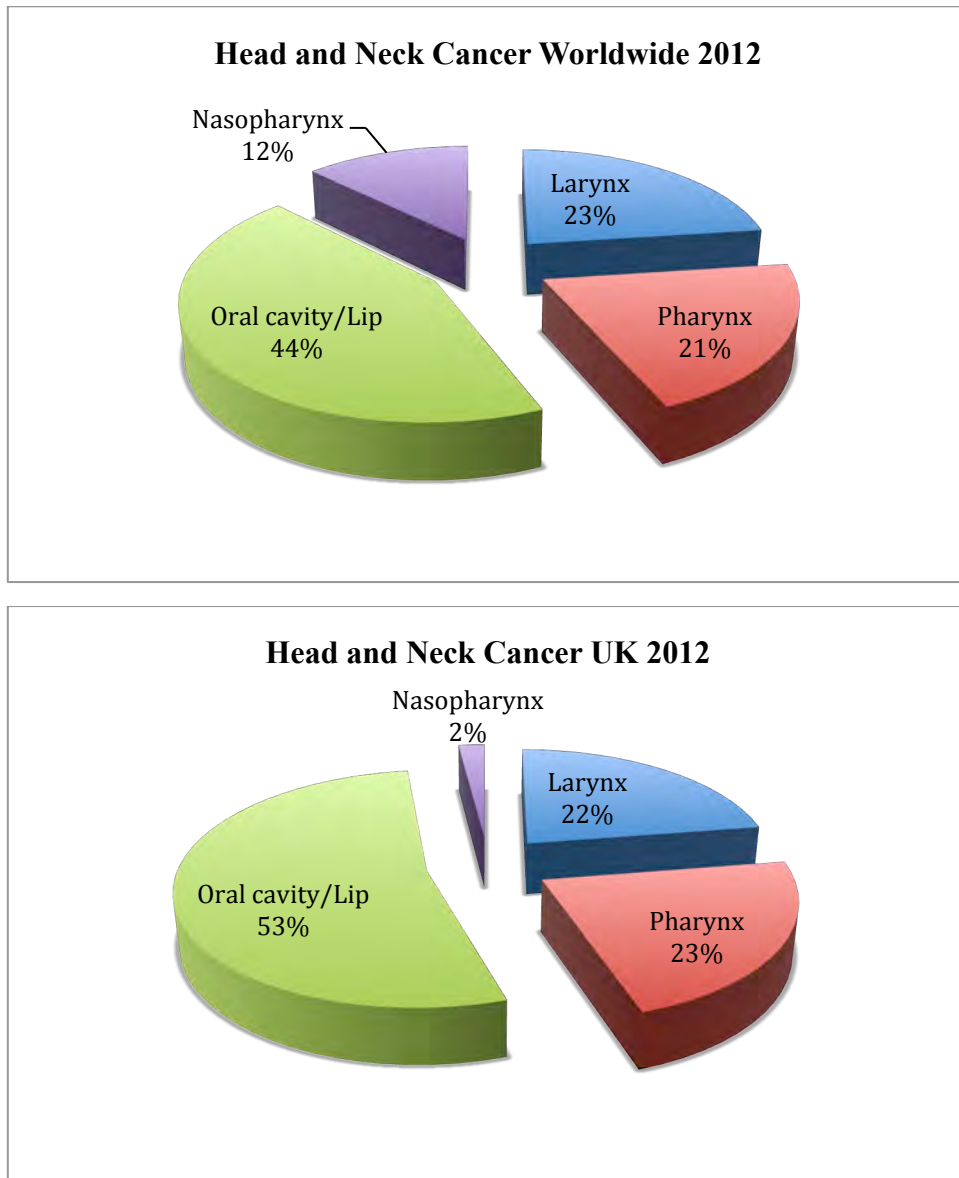


Figure 1.1 Incidence of sub-site of head and neck cancer worldwide and in the UK, Adapted from GLOBOCAN 2012 (WHO, 2012).

Primary recurrence of HNSCC has remained the same over the last 30 years at around 30% in the USA and Western Europe (Kreimer et al., 2005). There has been recent

evidence that rates of recurrence have reduced in HNSCC that are positive for high risk HPV (Rubenstein et al., 2011), suggesting that it is vital in understanding the nature of these tumours to help extrapolate prognostic indicators or factors to all HNSCC's.

HPV is a major cause of oropharyngeal squamous cell carcinoma (OPSCC). Accounting for 40-80% of cases in the western world (D'Souza et al., 2007, Termine et al., 2008, Chaturvedi et al., 2011). Although patients with HPV positive OPSCC tend to present at a later stage with advanced disease, that is usually poorly differentiated (which is usually associated with poorer outcomes), studies have reported improved outcomes when matched to HPV-negative disease of the same stage (Ward et al., 2014).

1.2 Anatomy of the Head and Neck Region

1.2.1 Boundaries of the Head and Neck

For anatomical classification the head and neck region is broadly categorised into the sections as shown in Fig.1.2.

1.2.2 Oral Cavity

The oral cavity extends from the lips and cheeks externally to the anterior pillars of the fauces internally, where it continues into the oropharynx. The mouth can be subdivided into the vestibule external to the teeth and the oral cavity proper internal to the teeth. The palate forms the roof of the mouth and separates the oral and nasal cavities. The floor of the mouth is formed by the mylohyoid muscles and is occupied

mainly by the tongue. The lateral walls of the mouth are defined by the cheeks and retromolar regions. Three pairs of major salivary glands (parotid, submandibular and sublingual) and numerous minor salivary glands (labial, buccal, palatal, lingual) open into the mouth (Standring, 2009).

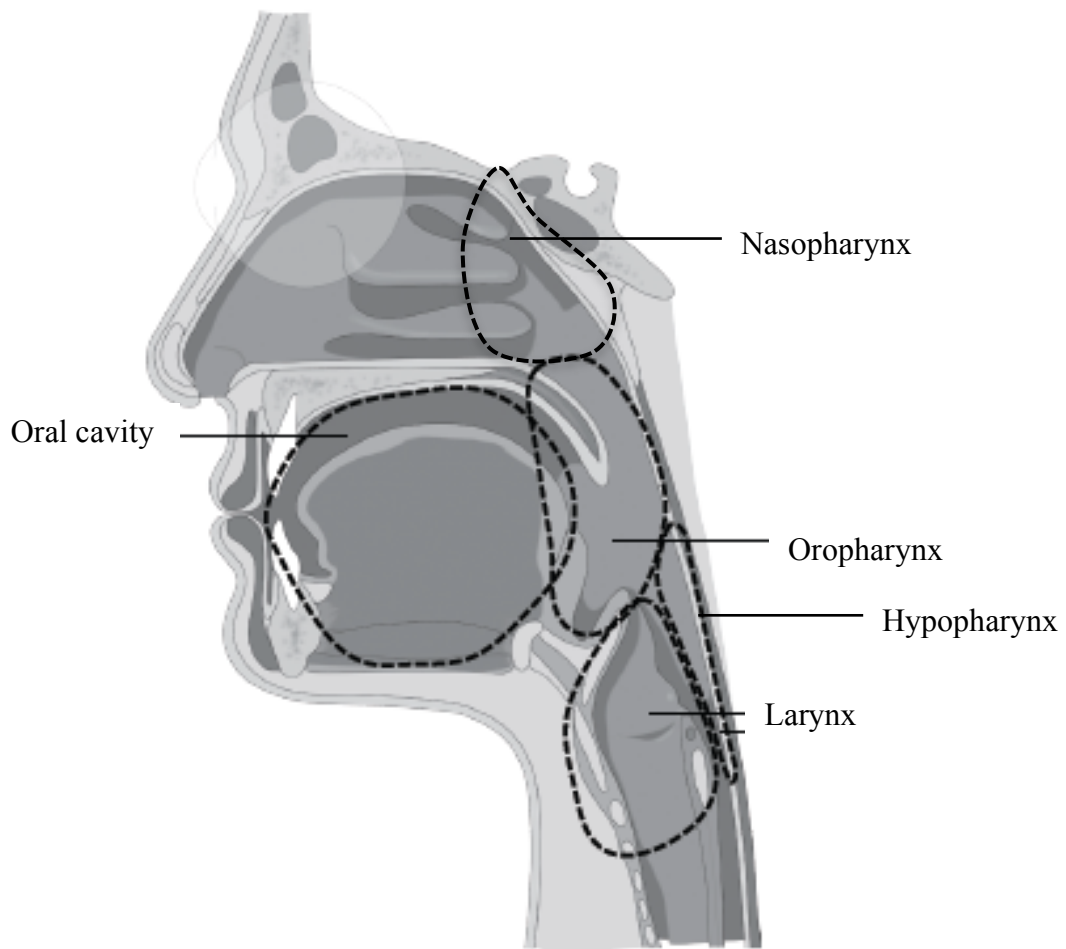


Figure 1.2 Boundaries of subsections of the Head and Neck

1.2.3 Oropharynx

The oropharynx is a three dimensional structure, bounded superiorly by the lower edge of the soft palate and the hyoid bone inferiorly. The anterior tonsillar pillars or palatoglossal folds and the base of tongue form the anterior border. The superior and middle pharyngeal constrictor muscles and their overlying mucosa form the posterior border.

Inferiorly, the posterior one third of the tongue, or the base of the tongue, continues the anterior border of the oropharynx. The vallecula, which is the space between the base of the tongue and the epiglottis, forms the inferior border of the oropharynx. This is typically at the level of the hyoid bone. Within the lateral walls of the oropharynx are the paired palatine tonsils, sitting in a fossa separated anteriorly by the palatoglossal folds and posteriorly by the palatopharyngeal folds.

1.2.4 Nasopharynx

The nasopharynx is the superior most aspect of the pharynx. It extends from the base of skull superiorly to the lower edge of the soft palate inferiorly. The anterior border is formed by the posterior choanae and posterior septum. It contains the adenoids. Laterally it is bounded by the pharyngeal walls that contain the eustacian tube orifice.

1.2.5 Hypopharynx

The hypopharynx is bounded superiorly by the hyoid bone or the tip of the epiglottis and inferiorly by the upper esophageal sphincter (UES), or cricopharyngeus muscle.

The anterior boundary of the hypopharynx consists largely of the laryngeal inlet, which includes the epiglottis and the paired aryepiglottic folds and arytenoid

cartilages. The posterior surface of the arytenoid cartilages and the posterior plate of the cricoid cartilage complete the anteroinferior border of the hypopharynx.

Lateral to the arytenoid cartilages, the hypopharynx consists of the paired piriform sinuses, which are bounded laterally by the thyroid cartilage.

1.2.6 Larynx

The larynx is located within the anterior aspect of the **neck**, anterior to the inferior portion of the pharynx and superior to the **trachea**. Its functions include protection of the upper airway and also voice production. It is split vertically into three areas; the supraglottis, the glottis and the subglottis.

The supraglottis is composed of the epiglottis (both the lingual and the laryngeal surfaces), aryepiglottic folds (laryngeal surfaces only), arytenoids, and the false vocal cords. The inferior limit of the supraglottis is a horizontal plane through the lateral margin of the ventricle at its junction with the superior surface of the true vocal cord.

The glottis is composed of the true vocal cords (both the superior and inferior surfaces) and includes the anterior and posterior commissures. The inferior boundary of the glottis is a horizontal plane 1 cm inferior to the inferior limit of the supraglottis.

The subglottis extends from the inferior limit of the glottis to the inferior edge of the cricoid cartilage.

1.3 Cervical Lymph Nodes

Head and neck cancers can metastasise to locoregional lymph nodes, which are the cervical lymph nodes, and often there is a set pattern to metastasis depending on the sub-site of cancer.

1.3.1 Distribution of Cervical Lymph Nodes

The evaluation of drainage patterns from the upper aerodigestive tract has led to the identification of cervical nodal groups at risk of metastasis. These have been divided into seven groups or levels (Figure 1.3), however this is not all-inclusive as several groups such as the supraclavicular, parotid and retropharyngeal space nodes are not accounted for in this system.

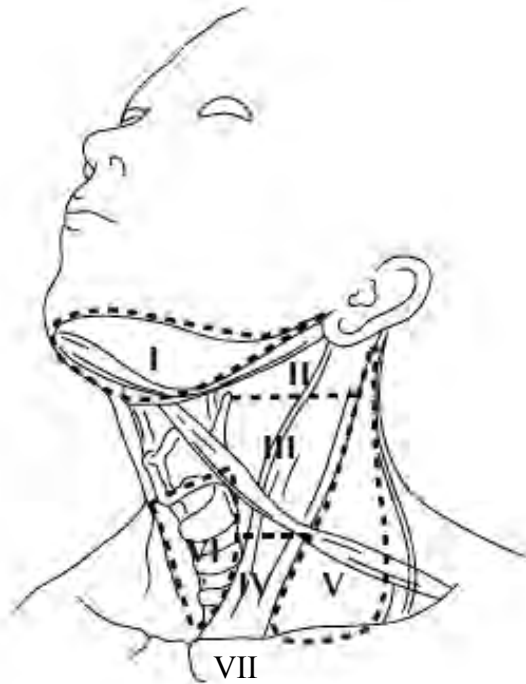


Figure 1.3 Distribution of cervical lymph nodes

1.3.2 Drainage Patterns of Cervical Lymph Nodes

Level I – Submandibular and submental triangles

The submental and submandibular nodes drain the lower lip, lateral parts of anterior two thirds of tongue, floor of mouth, medial cheek mucosa, nasal cavity and the paranasal sinuses. The nodes of this group in turn drain into the jugular chain.

Level II – The Upper jugular region

The nodes of this level drain the oropharynx including the palatine and lingual tonsils, base of tongue, the valleculae, supraglottis, the upper oesophagus and the nasopharynx

Level III – The middle jugular region

This level drains the posterior first third tongue, submandibular and submental nodes and the larynx. Also receives efferents from the upper jugular nodes.

Level IV – The Lower Jugular region

The lower jugular nodes receive efferents from the transverse cervical, anterior cervical and superior deep cervical nodes. In addition they drain the hypopharynx, subglottis, cranial portion trachea and the thyroid gland.

Level V – The posterior triangle

The posterior triangle receive lymphatics from the scalp, auricle and mastoid nodes. In addition they drain the lateral neck and shoulder.

Level VI – The anterior compartment

The Thyroid gland, subglottis and the caudal portion of the trachea drain into the central compartment of the neck.

Level VII Upper mediastinal

These further drain the Thyroid gland and upper chest. The upper deep cervical lymph nodes act as a pathway of spread for malignant tumours of the supraglottis. Up to 40% of these tumours will have undergone metastatic spread at the time of clinical presentation. The glottis is poorly endowed with lymphatic vessels and 95% of tumours confined to the glottis will present with dysphonia or airway obstruction. Subglottic tumours usually spread to the paratracheal lymph nodes which are deep seated in the neck, although spread may be early, the usual presenting symptom is airway obstruction or voice change. Table 1.1 illustrates the common primary site for cancer metastasis depending upon the site of the primary cancer.

Table 1.1 Cervical Lymph Node Metastases by Primary Cancer site

Lymph Node Level	Primary Cancer site
Level I	Lip, oral cavity, skin, salivary gland
Level II	Oral cavity, Oropharynx, Nasopharynx, Larynx, Salivary gland
Level III	Oral cavity, Oropharynx, Hypopharynx, Larynx, Thyroid
Level IV	Oropharynx, Hypopharynx, Larynx, Cervical oesophagus, Thyroid

Level V	Nasopharynx, Scalp, Breast, Lung, Gastrointestinal tract
Level VI	Thyroid
Level VII	Thyroid, superior mediastinum

1.4 Aetiology of Head and Neck squamous cell carcinoma

The aetiology of HNSCC, like most cancers, is multifactorial and dependent on both environmental and genetic factors. The significance of these factors is dependent upon the site affected, here the most important risk factors will be considered.

1.4.1 Tobacco

Tobacco is a major risk factor for HNSCC, the effects of tobacco consumption in addition to heavy alcohol consumption and poor diet account for greater than 90% of all HNSCC (Johnson, 2001). The majority of tobacco is smoked in the Western world however it can be taken in other forms when considering worldwide aetiology associated with tobacco use.

1.4.1.1 Smoking

Smoking is a recognised risk factor for developing HNSCC as well as other cancers, the relative risk of developing HNSCC is dose dependent and cumulative over the years. Smoking cessation reduces the risk and this is around 70% after 10 years of abstaining.

There are over sixty recognized carcinogens in each puff of a cigarette (Sebelius, 2010), which can be broadly classified into the following groups; polycyclic aromatic hydrocarbons (PAH), N-nitrosamines, aromatic amines, aldehydes, volatile organic hydrocarbons and metals. The aldehydes and volatile hydrocarbons are at highest quantity, with average of 10-1000µg per cigarette. However the most potent of the carcinogens are the PAH, N-nitrosamines and aromatic amines, these are at minute quantities in comparison, with an average of 0.1-200ng per cigarette.

The majority of carcinogens require activation to allow them to form covalent bonds with DNA; forming DNA adducts. This process is initiated by cytochrome P450 enzymes, however some carcinogens can bind directly to DNA without activation. In particular cytochrome P450 1A1 and 1B1 which are inducible through cigarette smoke by interactions with the aryl hydrocarbon receptor, are important in the metabolic activation of PAH's (Sebelius, 2010).

The inducibility of these enzymes contributes to the susceptibility to cancer formation. In response to activation of these metabolic carcinogens there is also a competing detoxification process which converts the carcinogens into harmless inactive forms, this process is activated by a number of enzymes which include glutathione-S-transferases (GSTs), uridine-5'-disphosphate-glucuronosyltransferases (UGTs), epoxide hydrolases and sulfatases (Sebelius, 2010). The balance between activation and detoxification of carcinogens determines overall susceptibility to cancer, those with higher rate of activation of cytochrome p450 and reduced rates of detoxification are at highest risk. There are 3 recognised pathways of causal relationship between smoking and carcinogenesis, these are illustrated in Fig. 1.4:

1. Exposure to carcinogens in tobacco
2. Formation of covalent bonds between the carcinogens and DNA (DNA adduct formation)
3. Resulting accumulation of permanent somatic mutations in critical genes

There are a number of cellular repair mechanisms that can remove DNA adducts and maintain a normal DNA structure. These include direct repair of DNA bases by alkyltransferases, excision of the DNA damage by base and nucleotide excision repair, mismatch repair and double strand break repair. If DNA repair enzymes are overwhelmed or for any other reason cannot function, DNA adducts can persist and increase the likelihood of DNA somatic mutations. Inherited polymorphic variants of DNA repair enzymes are also associated with a reduction in DNA repair and hence increased risk of developing cancer (Sebelius, 2010).

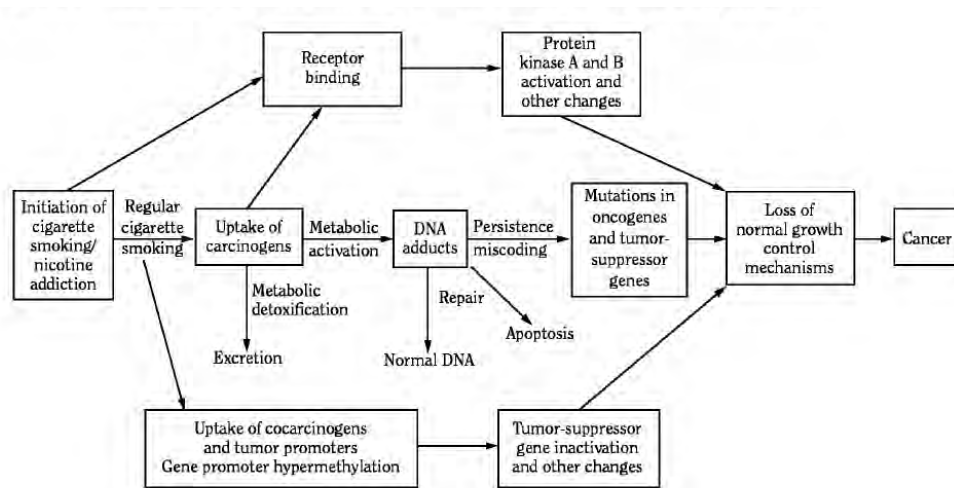


Figure 1.4 Link between cigarette smoking and cancer through carcinogens in tobacco smoke (Sebelius, 2010).

Most of the work on carcinogenesis from tobacco has been carried out on lung cancer however these findings can be extrapolated to laryngeal cancer. The majority of damage is caused by metabolically active PAHs, in addition to other genetic mutations they cause mutations in the tumour suppressor gene TP53 and KRAS protein coding gene, a mutation in which can aid carcinogenesis, these result in increased risk of carcinogenesis (Sebelius, 2010). Overall pathogenesis is caused by genetic mutations that result in loss of normal cellular growth and apoptotic pathways leading to unregulated cellular growth.

Reduction of cancer risk with smoking cessation supports the role of tumour promoters and other epigenetic factors in tobacco carcinogenesis. One such important epigenetic pathway is the enzymatic hypermethylation of promoter regions of genes, if this occurs in tumour-suppressor genes, gene silencing can occur which can result in unregulated cell proliferation.

Gillison *et al.*, found no difference in hazards ratio for p16 positive versus negative patients for secondary primary tumours; the hazards ratio is the rate at which the hazard occurs for a defined event, which in this case was the development of a secondary primary tumour. The only strong confounding factor was smoking with the hazard increasing by 1.5% per pack-year (HR 1.015 95% CI 1.005-1.026) or 1.5% per year of smoking (HR 1.015 95% CI 0.994-1.037) (Gillison et al., 2012). The overall survival was also determined by smoking status at diagnosis, the hazard of death was more than two-fold in those who smoked more than 10 years versus ≤ 10 years (HR 2.10; 95%CI 1.35-3.25), this equated to an absolute difference of around 30% in 5 year overall survival (Gillison et al., 2012).

There have been a number of studies which have shown a direct relationship between the duration of smoking and the risk of carcinogenesis, in particular of the head and neck region, and this risk is further confounded when alcohol is taken concurrently (Blot et al., 1988, Bundgaard et al., 1995, Lewin et al., 1998). Bundgaard *et al.*, showed that the odds ratio of smoking alone to smoking and drinking alcohol jumped from 5.8 to 80.7 (Bundgaard et al., 1995), in addition to the duration of smoking and risk of developing cancer it has also been shown that amount of tobacco consumed is also positively correlated with the risk of cancer (Tuyns et al., 1988). The effects of smoking cessation show reducing risk with increasing years of cessation, a number of studies have quoted no further increase in risk from 10-20 years of cessation (Blot et al., 1988, Spitz et al., 1988, Lewin et al., 1998).

1.4.1.2 Snuff, Oral tobacco or Smokeless tobacco

Smokeless tobacco can be categorized into; chewing tobacco and Snuff. Chewing tobacco is placed between the cheek and gum or teeth and the nicotine is absorbed through the oral mucosa, snuff is a finely ground or shredded tobacco that has been cured and fermented, thus increasing the potency of carcinogens, it is either placed between the lower lip and gum, or inhaled into the nasal cavity. In the USA the use of chewing tobacco has declined over the last 15 years by 30.6%, however the use of oral snuff has increased by 51.8% due to the growing popularity of its use amongst teenagers and young adolescents (Hoffmann and Djordjevic, 1997). The results of the National Drug survey in North America found that an estimated 8.6 million Americans aged 12 years and over used smokeless tobacco in 2009, the highest use was seen in men aged between 18-24 (NSDUH, 2010).

A case-controlled study in which 1056 patients and 1252 controls were examined found a significant increased risk of HNSCC in users of smokeless tobacco for 10 years or more (OR=4.06, 95% CI 1.31-12.6) compared to never users (Zhou et al., 2013). Compared to never cigarette smokers the risk of HNSCC was significantly elevated in those that had used smokeless tobacco 20 or more times (OR=4.21, 95% CI 1.01-17.6)(Zhou et al., 2013). A meta-analysis from Europe and North America found that the relative risk of oral cancer from smokeless tobacco use was 1.8 (95% CI 1.1-2.9) (Boffetta et al., 2008).

1.4.2 HPV & Smoking

Smoking is not a strong co-factor for the development of the HPV positive oropharyngeal cancer subset of HNSCC, however, there is confounding evidence that it can alter the treatment of this type of cancer making HPV positive tumours less likely to respond to treatment (Gillison et al., 2012, Ang et al., 2010b).

It has been established that HPV positive versus HPV negative patients have a better outcome in terms of survival, the exact mechanisms of which are unknown. However Hafkamp *et al.*, (Hafkamp et al., 2008) showed that smoking in HPV positive patients resulted in worse outcomes and that smoking status was the highest compounding factor when comparing outcomes. Although HPV positive patients generally have improved outcomes when compared to HPV negative patients, this may be related to the fact that HPV positive patients tend to be younger and have less of a cumulative history of tobacco and alcohol consumption which are statistically significant $p=0.002$ and 0.011 respectively (Hafkamp et al., 2008).

Gillison *et al.*, found that after accounting for a number of co-factors including tumour p16 status, smoking remained the most important predictor of survival, when evaluated as a continuous variable, the hazard of death increased by 1% per pack-year and approximately 2% per year of smoking (Gillison *et al.*, 2012). The magnitude of tobacco effect increasing risk of relapse or risk of death was seen to increase with each year of smoking, this risk was found to be similar in both HPV-positive (hazard ratio 1.01 95% CI 1.00-1.02) versus HPV-negative patients (hazard ratio 1.01;95% CI 1.00-1.03) (Ang *et al.*, 2010b).

1.4.3 Alcohol

Alcohol or ethanol itself is not known to be carcinogenic, however it is well established that consumption of large quantities of alcohol has a dose dependent relationship with regards to risk of HNSCC, this is amplified when the synergistic effect of smoking is added (Blot *et al.*, 1988). The major risk for oral cancer amongst non-smokers is alcohol intake however, it is presently unclear whether the type of alcoholic beverage affects oral cancer risk after adjustment for amount and concentration consumed (Castellsague *et al.*, 2004). There are a number of theories associated with the risk of alcohol intake and increased risk in the development cancer, one such is the solvent affect of alcohol in combination with smoking or oral tobacco used, this brings known carcinogens in tobacco in closer contact with the mucosal surface, however this theory is not supported by the fact that the effects of alcohol remain for a certain period of time after cessation of drinking. Another theory is that acetaldehyde, a metabolite of alcohol once broken down by the alcohol dehydrogenase enzyme (ADH) forms DNA adducts and hence affects DNA synthesis and repair (Brooks and Theruvathu, 2005). A number of studies stated varied and

contradictory risks of oral cancer with different phenotypes of ADH, however a pooled analysis found no significant difference in risk related to the different phenotypes of ADH when adjusted for age, gender and smoking status (Brennan et al., 2004). There is evidence that resveratrol in grapes, and thus wine has chemopreventive activity, one such study showed that the relative risks of development of HNSCC in subjects who drank >21 units per week was less in those who consumed greater than 30% wine (Gronbaek et al., 1998).

1.4.4 Betel Quid (Paan)

Betel quid is most often used in the South Asian countries and often in migrant communities that have originated from there. Approximately 200 million persons chew betel regularly throughout the western Pacific basin and south Asia (Norton, 1998), and up to 600 million worldwide including migrant communities (Jeng et al., 2001). Betel quid is composed of the betel vine leaf, lime (calcium hydroxide), areca nut and with or without tobacco. This is often then supplemented with various spices such as saffron and cardamom, depending on the part of the world it has originated from. Areca nut is the fourth most commonly used psychoactive substance in the world after tobacco, alcohol and caffeine-containing beverages (Sullivan and Hagen, 2002). The betel quid or paan is either chewed and saliva spat out or it is simply placed between the cheek and gums. Betel quid is chewed for its psychostimulating effects (Norton, 1998), Areca-nut in particular is reported to have varied and widespread, predominantly stimulant effects (Chu, 2001).

A higher incidence of oral, oropharyngeal and hypopharyngeal cancers are observed in the regions where betel quid chewing is endemic. Of the 267,000 new oral cancers

estimated to occur globally, 128 000 (48%) occur in South and South-East Asia; of the 123 000 cases of oropharyngeal and hypopharyngeal cancer estimated to occur globally annually, 63 000 (51.2%) are accounted for in South and South-East Asia (Parkin DM, 2003).

Carcinogens in betel quid arise from areca nut, this fruit contains areca alkaloids which give rise to the N-nitrosamines, the most potent of which are 3-methylnitrosamino propionaldehyde (MNPN), the addition of tobacco increases the concentration of areca derived N-nitrosamines. The carcinogenic effects are most likely similar to that of tobacco where DNA adducts are formed leading to somatic mutations and loss of cell cycle control (International Agency for Research on Cancer, 2004).

The risks of carcinogenesis and death from betel quid are also like smoking, dose dependent and are cumulative over the years. It was found by Lee et al that there was a 31.4-fold higher risk of death in heavy users of betel quid (duration >30 years, with >30 quids consumed per day) compared to milder users (duration <10 years, with daily consumption <15 quids)(Lee et al., 2005). A case control study (148 patients with oral cancer, 260 controls) found a six-fold increase in risk of oral cancer in betel-quid chewers with tobacco, the odds ratio for risk from chewing betel quid alone was 1.7 (95% CI, 0.9-3.3) (Dikshit and Kanhere, 2000). The incidence of oral cancer in those that smoke tobacco, drink alcohol and chew betel quid is 123-fold higher than non-using counterparts (Ko et al., 1995).

1.4.5 HPV and Betel Quid

Betel quid is thought to exert its mutagenic effects on the oral mucosa by single strand DNA break, although further studies are needed to delineate any relationship between HPV 16 positivity and betel quid chewing, Chen *et al.*, (Chen et al., 2002) found that betel quid and HPV 16 were independent risk factors for oral cancer with odds ratio of 11.21 and 17.06 respectively when adjusted for age, gender and smoking history. They extrapolated that the synergistic effects of both would result in a much higher risk of oral cancer.

1.4.6 Other Risk factors

There are a number of other risk factors that are associated with HNSCC, these include Maté, marijuana, preserved foods, oral hygiene and health, acid reflux and ancestral. Maté is a hot beverage that is prepared by steeping dried leaves of *yerba mate* in hot water. There are a number of studies that have associated this with the development of oesophageal cancer and HNSCC, however as Maté also has some anticarcinogenic effects, it is argued that the PAH that it contains may arise from the production process of burning rather than native to Maté. Marijuana induces a higher risk of HNSCC compared to smoking tobacco, it contains a higher concentration of tar and aromatic hydrocarbons. Occupational exposure to wood dust is a known risk factor for nasopharyngeal cancer, industrial exposure to wood, nickel dust or formaldehyde are also risk factors for the development of cancers of the paranasal sinuses and nasal cavity (Luce et al., 2002).

1.5 Staging of HNSCC

1.5.1 TNM Staging System

Staging allows for the determination of primary treatment for the patient with established cancer. The TNM system is one of the most widely used cancer staging systems and has been developed by the Union for International Cancer Control (UICC) and the American Joint Committee on Cancer (AJCC). Most medical facilities use the TNM system as their main method for cancer reporting which allows for worldwide concordance on staging of cancers.

There are four different types of TNM staging 1)**Clinical Staging** determines how much cancer there is based on the physical examination, imaging tests and biopsies of affected areas 2)**Pathological Staging which** can only be determined from individual patients who have had surgery to remove a tumour or explore the extent of the cancer. Pathologic staging combines the results of both the clinical staging with surgical results. Once the pathological staging is determined after the resection of the primary tumour, it can add to decisions about whether any adjuvant therapy is required, 3)**Post-Therapy or Post-Neoadjuvant Therapy Staging** determines how much cancer remains after a patient is first treated with systemic (chemotherapy or hormone therapy) and/or radiation therapy prior to their surgery or where no surgery is performed. This can be assessed by clinical staging guidelines and/or pathologic staging guidelines, 4)**Restaging** is used to determine the extent of the disease if a cancer comes back after treatment. Restaging helps determine the best treatment options for cancer that has returned.

The TNM system is based on the size and/or extent of the primary tumor (**T**), the amount of spread to nearby lymph nodes (**N**), and the presence of metastasis (**M**). A number is added to each letter to indicate the size and/or extent of the primary tumor and the degree of cancer spread.

Primary Tumor (T)

TX: Primary tumor cannot be evaluated

T0: No evidence of primary tumor

Tis: Carcinoma in situ (CIS; abnormal cells are present but have not spread to neighboring tissue; although not cancer, CIS is precancerous)

T1, T2, T3, T4: Size and/or extent of the primary tumor

Regional Lymph Nodes (N)

NX: Regional lymph nodes cannot be evaluated

N0: No regional lymph node involvement

N1, N2, N3: Degree of regional lymph node involvement

Distant Metastasis (M)

MX: Distant metastasis cannot be evaluated

M0: No distant metastasis

M1: Distant metastasis is present

The T stage is dependable on the sub site of the primary cancer, although a higher assigned number indicates a greater extent of cancer the defined boundaries are different for each sub site (see Appendix 1).

1.5.2 Stages of Cancer

The combination of TNM staging together with the natural history of the tumour can be grouped in to 'Stages' of cancer (see Table 1.2). This is a means of

communicating the extent of cancer to other healthcare professionals to assist in therapeutic decisions and also in determining prognosis.

Stage	Tumour stage	Nodal stage	Metastatic stage
Stage 0	Tis	N0	M0
Stage I	T1	N0	M0
Stage II	T2	N0	M0
Stage III	T1, T2	N1	M0
	T3	N0, N1	M0
Stage IVA	T1, T2, T3	N2	M0
	T4a	N0, N1, N2	M0
Stage IVB	T4b	Any N	M0
	Any T	N3	M0
Stage IVC	Any T	Any N	M1

Table 1.2 Stage grouping for oral cavity, oropharyngeal, hypopharyngeal and laryngeal cancers adapted from UICC:TNM Classification of Malignant Tumours (UICC, 2009)

1.6 Treatment options for HNSCC

The treatment options for head and neck cancer can be broadly classified into surgery, chemotherapy, radiotherapy or a combination of these.

Surgery can be performed either on the primary site or areas of metastasis such as cervical lymph nodes with the addition of adjuvant radiotherapy or chemoradiotherapy. In England and Wales 46% of oropharyngeal carcinomas were treated surgically in 2013 (DAHNO, 2013) with the remainder having the main primary treatment of chemoradiotherapy. Chemotherapy is usually used as adjuvant

or neoadjuvant and the main therapeutic agent used is cisplatin. Radiotherapy is the use of ionised radiation focused on the tumour to induce cell death, it is either used independently or more increasingly in combination with chemotherapy.

Radiotherapy has a significant amount of co-morbidity associated with it, with side effects including xerostomia (dry mouth), localized skin reactions or skin burns, dysphagia (difficulty swallowing) or worse; dependence on artificial feeding via a gastrostomy tube. Late toxicity is worse with chemoradiotherapy than radiotherapy alone (Denis et al., 2003, Caudell et al., 2009). At present all patients receive the same form of treatment whether or not they have a HPV positive or negative tumour, the extent of the treatment is based on the stage of disease and nodal status (Appendix 1).

1.7 Human Papilloma Virus-16 associated HNSCC

Traditionally Head and Neck cancers have been grouped together with the exception of nasopharyngeal cancer given their common aetiology and treatment outcomes. However, considerable differences exist not just within the cancer sub site but also with type and stage of cancer at each site. One such group is the HPV positive HNSCC group, which has been established as a distinct disease entity, there are a number of differences between HPV-positive and HPV-negative HNSCC, these are described in Table 1.3. HPV cancers tend to occur with smaller risk of alcohol and smoking, the biology and pathophysiology is different to smoking & alcohol related SCC. There is evidence of p53 degradation and inactivation of the retinoblastoma pathway (Rb), with up regulation of p16 protein. Whereas traditional HNSCC is

related to smoking and alcohol, p53 is absent or mutated and down regulation of CDKN2A occurs which encodes p16 (McKaig et al., 1998).

Table 1.3 Differences between HPV positive and HPV negative HNSCC

	HPV Positive	HPV Negative
Incidence	Increasing	Decreasing
Age	Younger	Older
Gender	3:1 men	3:1 men
Risk Factors	Sexual behavior	Tobacco & Alcohol
Co-Factors	Marijuana, immunosuppression	Diet, Oral Hygiene
Anatomic Site	Lingual and palatine tonsils	All sites
Molecular genetic findings	P16 ↑ Rb ↓ P53 wild type	P16 ↓ Rb ↑ P53 mutated
Pathological Findings		
Primary	Basaloid	Keratinised
Lymph Node mets	Cystic	Solid
Survival Outcomes	Better	Worse

1.7.1 Introduction to the Human Papilloma Viruses

Human Papilloma Viruses are from the Papillomaviridae family of viruses, these are small non-enveloped, double-stranded DNA viruses that infect the mucosal and cutaneous epithelia by breaks on the surface that expose the basal cell layer. There are over one hundred different types, and were first discovered in the early 20th century when it was identified that skin warts or papillomas could be transferred between individuals by an infectious agent (World-Health-Organization, 2007). The individual types are classified based on their DNA sequence homology, furthermore,

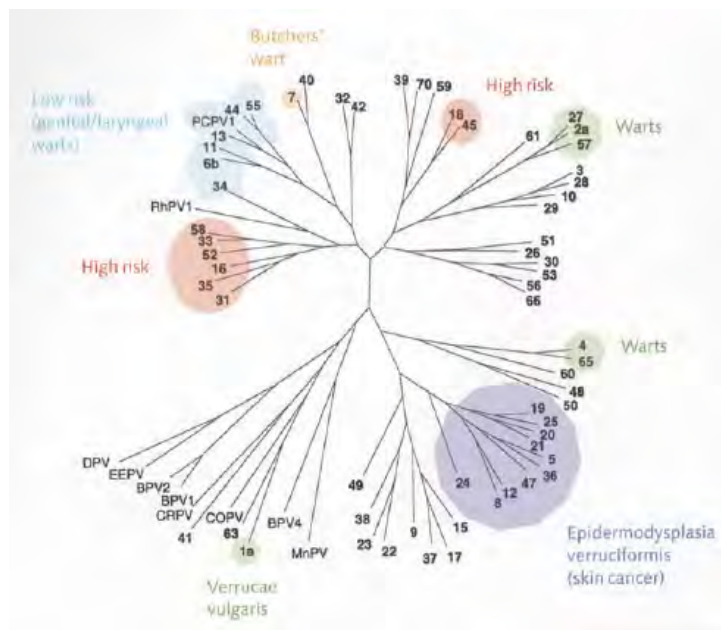


Figure 1.5 The papillomavirus family tree. Phylogenetic tree illustrating types of papillomavirus and types of lesions caused. The high risk HPVs are associated with predilection to carcinoma formation within the anogenital tract and the head and neck region. Adapted from Julie Burns and Norman Maitland 2005 (Maitland, 2005)

phylogenetic trees can also be related to the specific pathologies caused (Fig. 1.5).

HPV's have been found in higher eukaryotes with little change to viral genomic organization (Maitland, 2005). The majority of HPV's cause benign hyperproliferative lesions such as warts and verrucae, however a number of HPV's have been associated with the predilection for the anogenital mucosa, with a small number being implicated in the development of carcinogenesis; in particular research has led to the discovery that >99% of cervical cancer is associated with high risk HPV's, in particular HPV-16 and HPV-18 (Doorbar et al., 2012, Maitland, 2005). These high-risk HPVs are also implicated in the development of non-anogenital cancers, in particular skin and oropharyngeal cancer.

HPVs are obligate intracellular parasites with a specific tropism for squamous epithelium, the lifetime of these viruses is closely associated with the differentiation of host epithelial cells. The HPV virus only has eight open reading frames and therefore integrates itself into the host genome, so that it can maintain replication by using cellular functions. HPV has evolved so that it infects epithelial cells, these usually do not divide once they have left the basal cell layer and often lose their nucleus after differentiation, however HPV keeps cells in a state of continuous replication even once they have left the basal cell layer, therefore infected epithelia have a much higher rate of nucleated and dividing cells in all layers.

HPV's are classified into supergroups by their homologous gene structure, in particular genitally transmitted viruses such as HPV-16 belong to supergroup A or Alpha papillomaviruses. All papillomaviruses types have a predilection to infect a particular surface of the body, e.g. HPV type 1 tends to affect the soles of the feet, HPV-type 2 palms of the hands where it may cause benign proliferative warts or papillomas. Differences in viral genomic regulatory sequences and coding potential are likely to cause the different biological characteristics of the different HPV's.

The low risk types e.g. HPV-6 and HPV-11 induce benign proliferative lesions such as warts. On the contrary high risk HPVs (including HPV-16 and HPV-18, -31, -33, -35) are recognised for their oncogenic potential. In particular HPV-16 and HPV-18 are associated with anogenital and upper respiratory tract tumours (Fakhry and Gillison, 2006). At least 15 types of HPV are thought to have oncogenic potential, however >90% HPV-HNSCC are thought to be caused by HPV 16, the same type

which is associated with HPV-associated anogenital cancers (Fakhry and Gillison, 2006).

1.7.2 The Structure of HPV-16

HPVs are small (7900 base pairs), non-enveloped, double stranded DNA viruses that infect mucosal and cutaneous epithelia through tiny cuts and abrasions that expose cells of the basal layer. They establish productive infections in keratinocytes of skin and mucous membranes only. The HPV-16 virus has eight open reading frames and is encased in major and minor capsid proteins, L1 and L2, it also encodes six viral proteins each with a specific role (see Fig.1.6).

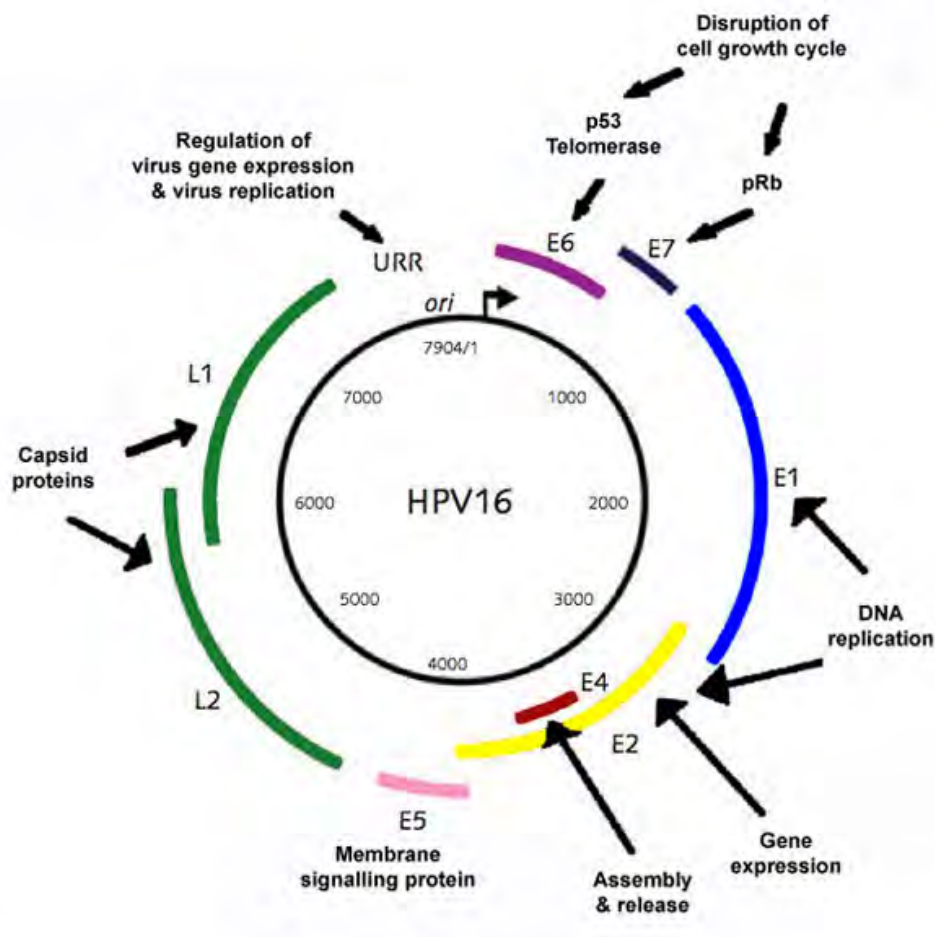


Figure 1.6 Structure of HPV-16 Adapted from www.microbiologybytes.com

1.7.3 The HPV Life Cycle

The life cycle of HPV is well defined; the virus undergoes five main stages in order to maintain survival and cause disease progression (Fig. 1.7).

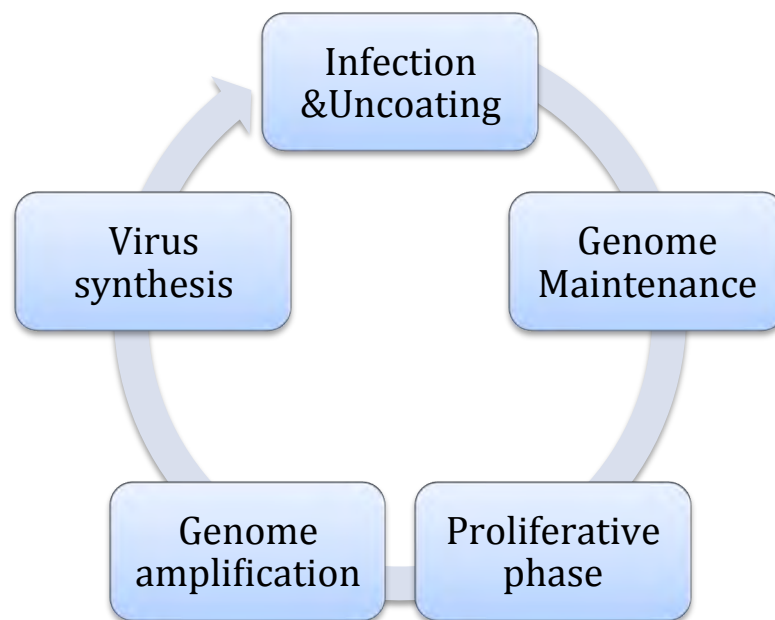


Figure 1.7 The HPV viral life cycle

Infection and Uncoating

The virus needs to infect cells of the basal cell layer, usually by a break in the skin or area of abrasion that may not be apparent. The virus then infects the epithelial stem cell in order to integrate within the host cell DNA, the infection cycle and integration is illustrated in Fig. 1.8, this also shows the viral proteins involved during each stage. Much controversy exists over the cell surface receptor that allows the initial attachment of the virus to the cell. Most studies suggest dependence on heparin sulphate (Giroglou et al., 2001). Internalisation of bound virus is a slow process and occurs through endocytosis. The virus is uncoated by breaking of the intracapsomeric

disulphide bonds which allows the viral DNA to enter the host cell nucleus (Li et al., 1998).

Genome Maintenance

Following infection and uncoating the virus maintains a low copy number episome (10-200 copies per cell) in the basal layer of epithelium. Viral gene expression is not well defined but E1 and E2 proteins are made to keep viral DNA as an episome. Viral early proteins (E1, E2, E6 and E7) are expressed at low levels (Doorbar, 2005).

Proliferative phase

The proliferative phase increases the number of basal cells with viral genome/episomes. In uninfected epithelium, basal cells exit the cell cycle soon after migrating into the suprabasal layers and undergo terminal differentiation to form different components of the epithelium creating a physical barrier against environmental factors. With HPV infection, normal cell cycle progression is abolished and normal terminal differentiation terminated.

Viral oncoproteins E6 and E7 expressed in these cells stimulate cell cycle progression by associating with cell cycle regulators (Munger et al., 2001). E6 complements E7 by preventing apoptosis and increasing the number of chance errors of host cell DNA to go unchecked (Stacey et al., 2000). Furthermore E6 of high risk HPV can also, independently of E7, induce proliferation of suprabasal cells through C-terminal of PD2-ligand domain, this may contribute to metastatic tumours by disrupting normal cell adhesion (Thomas et al., 2002)

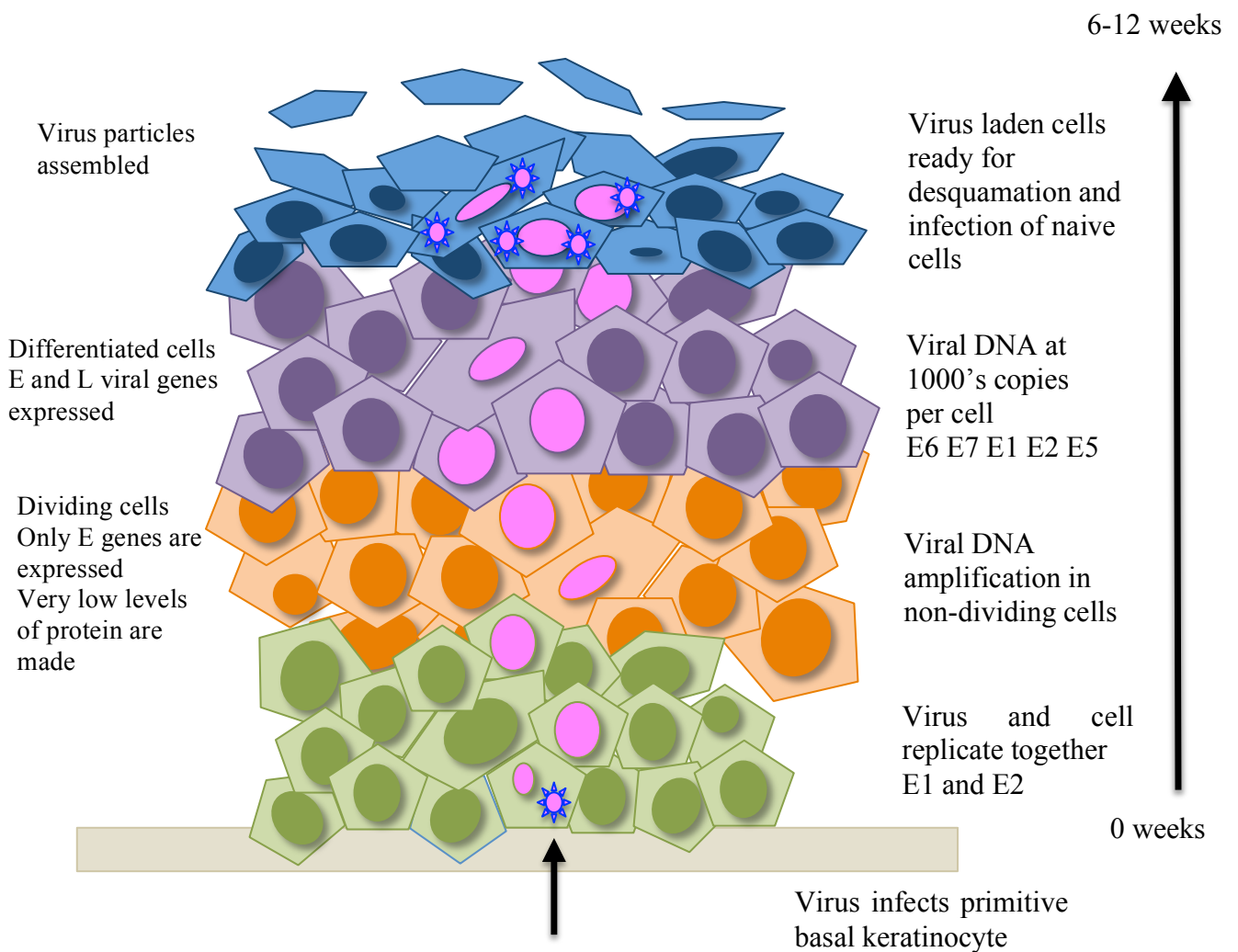


Figure 1.8 HPV integration into basal cell keratinocyte and infection cycle. HPV will only infect and replicate in fully differentiated squamous epithelium. The initial viral particle infects a basal keratinocyte due to a break/microtrauma in the skin. The plasmid is maintained in low copy numbers in the proliferative phase of the epithelium, the virus is maintained at around 10-200 copies per cell. The regulation of oncogenic viral proteins is tightly controlled by the virus, as long as the epithelium cells are dividing the viral oncoproteins E6 and E7 are expressed at low levels. As the squamous epithelium matures and cell division ceases the viral replication and activation of all its genes occurs and genome numbers increase to 1000s per cell. Malignant transformation occurs when control of expression of E6 and E7 is lost and gene expression becomes unregulated. The time taken from infection to development of infectious virus particles can take between 3-6 weeks, with the full cycle extending up to 12 weeks. Adapted from M Stanley (Stanley, 2012)

Genome Amplification

In order to form infectious virions the HPV virus must amplify its viral genome. For HPV-16 this occurs in the middle/upper epithelial layers following increased activity in the late promoter. The late promoter is the open reading frame E7, it is thought up regulation of this leads to increased expression of proteins involved in viral DNA replication (E1, E2, E4 and E5). Amplification begins in cells in the proliferative phase and this is thought to involve early viral gene products, however, the exact functions of these gene products are not yet full understood (Doorbar, 2005).

E2 binds to the HPV upstream regulatory region, this recruits E1 DNA helicase to the viral origin of replication. The E1/E2 initiation complex on the viral origin may allow replication of the viral genome in the absence of cellular DNA replication. The current model suggests a slight increase in the late promoter leads to an increase in E1/E2 and a subsequent increase in the genome copy number. The new genome facilitates further increases in E1 and E2, which further increase genome replication and thus the viral genome copies increase in number (Ozbun and Meyers, 1998).

Viral Synthesis

HPV has two structural proteins expressed in the upper layers of infected tissue once the viral genome amplification is completed. L2 is a minor coat protein produced in cells that produce E4 and L1 is expressed after L2, allowing assembly of infectious particles in upper layers. HPV is around ~8000 base pairs in a capsid that contains ~360 copies of L1 protein, ~12 copies of L2 organised into a 72 capsomere isocohedral shell. Virus particles can assemble in the absence of L2 however it is

thought that these proteins facilitate packaging and infectivity (Doorbar et al., 1997, Florin et al., 2002).

In order to be successful the virus must be able to escape from the host cell and survive extra cellularly prior to re-infection. HPV is non-lytic therefore it is not released until the infected cell reaches the epithelial surface. HPV is resistant to desiccation however survival may be enhanced if it is shed within cornified squamous epithelium. HPV may avoid detection by the immune system as HPV antigens remain intracellular until it reaches the upper layer of the epithelium, furthermore the virus has molecular mechanisms that avoid detection (Doorbar, 2005).

1.7.4 HPV-16 Oncoproteins

The HPV-16 oncoproteins play a key event and are pivotal in the progression of infection to neoplasia. The dysregulation of production of E6 and E7 leads to increased cell proliferation in lower epithelial cells and the inability of the host DNA to repair secondary defects. Expression of viral proteins can prevent expression of cellular proteins that lead to differentiation of epithelial cells, thus preventing formation of normal epithelial cells (Table 1.4).

The viral capsid proteins are L1 and L2, the functions of which, along with the remaining HPV proteins are summarized in Table 1.4. The papillomavirus E1 protein is the 'initiator' protein for viral DNA replication and plays a pivotal role in maintenance of the viral genome as an episome during the viral life cycle.

Table 2.4 Summary of Oncoprotein Function

Protein	Function
L1	Viral major capsid structural protein
L2	Viral minor capsid structural coat protein
E1	Viral DNA Replication
E2	Viral gene expression and viral DNA replication
E4	Virus assembly and release
E5	Membrane protein, Growth factor signaling
E6	Disruption of cellular growth and genetic instability through p53
E7	Disruption of cellular growth and genetic instability through Rb

The HPV-16 E2 gene controls viral gene expression and viral DNA replication, it is thus responsible for regulation of HPV-16 production. The E2 gene is interrupted during viral integration into the host genome, most cervical cancers contain chromosomally integrated copies of the HPV genome in which the E2 gene has been disrupted, absence or mutations of E2 increase HPV-16 immortalisation (Romanczuk and Howley, 1992). The role of E2 varies amongst other HPV viruses and can also have a proliferative response rather than restraining as in HPV-16.

The SiHa cells are a HPV-16 transformed cell line that contain a single copy of disrupted E2 gene, it has been shown by Sanchez-Perez *et al.*, (Sanchez-Perez et al., 1997) that expression of E2 in this cell line induces apoptosis, thus showing regulatory function of E2. There is also some evidence that the E2 protein induces apoptosis in non-HPV-16 infected cell lines such as that of HPV-32 (Frattini et al., 1997).

The E2 gene activates transcription of E6 and E7 from the p97 promoter located at the 3' end of the HPV-16 long control region, any increase in levels of these proteins can result in an increase in the level of free E2F and this can in turn lead to cell death. Mutations in the long control region of HPV-16 block the binding of E2 to the promoter and prevent E2 mediated repression of E6 and E7 transcription. E2 can also influence cell proliferation independently of the E6 and E7 pathway. (Webster et al., 2000).

E2 and E7 induce apoptosis via the p53 dependent pathway, functional p53 is required for apoptosis via this route. Co-expression of E6 reduces apoptosis as E6 recruits E6-AP via the ubiquitin ligase pathway, resulting in p53 degradation (section 1.7.5). DNA binding of E2 is not required for induction of apoptosis, there are a number of mechanisms whereby increased levels of E7 could lead to apoptosis but the route from over expression of E2 is unclear. It has been previously shown that E2 induces apoptosis in non-HPV infected cell lines (Webster et al., 2000), this supports the theory that there is more than one route of inducing apoptosis by E2, one requiring E7 and the other not.

The hallmark of HPV associated carcinogenesis is the integration of viral DNA into the host genome with loss of E2 expression. E2 binds to and represses the viral promoter directing expression of E6 and E7 oncogenes. Reintroduction of and expression of exogenous E2 in HPV positive cancer cells results in cellular growth arrest. But if exogenous E6 and E7 are added this effect is reversed (Wells et al., 2000).

E4 is associated with viral assembly and release, although E4 proteins are expressed at low levels during the early phase of viral infection, expression of E4 increases significantly during the late phase of infection. The E4 protein is further thought to facilitate virion release into the environment by causing cytoskeleton disruption of keratinocytes. It has not been fully established how E4 causes DNA replication. E4 has also been shown to participate in arresting cells in the G2 phase of the cell cycle (Middleton et al., 2003).

E5 is an early viral protein that is involved in increasing viral episomal DNA and plays an early role in tumorigenesis. It is lost when viral DNA is integrated into the host genome. In addition to E1, E2 and E4, E5 is involved in viral DNA replication and helps to keep the viral episome in low copy number, it further enhances entry to the S phase of the cell cycle, bypassing cell cycle check points. E5 is also found to cause cell-cell fusion, which results in binucleated cells, which are a pre cursor to malignancy in cervical cancer (Ganguly, 2012).

During integration into the host genome the above named early proteins are disrupted leading to unregulated over expression of E6 and E7, this will be discussed in detail. Integration of viral DNA occurs at ‘fragile sites’, these are portions of chromosomal DNA which are susceptible to breakages and allow integration of foreign DNA.

1.7.5 HPV-16 E6

HPV-16 E6 causes its effects by degradation of p53. E6 causes ubiquitination of p53 via the protein ligase E6AP, thereby preventing p53 senescence. It is thought that E6

binds to two regions of p53, a carboxy-terminal region and a core region. E6 from low risk HPVs bind to the carboxy region only, they can exert their effects on p53 by causing sequestration of the protein in the cytoplasm, however are not potent enough to cause ubiquitination and subsequent degradation. Another way E6 interacts with p53 independent of E6AP is by preventing acetylation of p53 and therefore inhibition of p53 activating transcriptional promoters, seen in both E6 high and low risk (Scheffner et al., 1990, Scheffner et al., 1993).

1.7.6. HPV-16 E7

The p16 protein (p16) also known as p16^{INK4a} is a cyclin-dependant kinase (CDK) inhibitor. Its function is to inactivate the CDKs that phosphorylate the retinoblastoma protein (Rb), namely CDK-4 and CDK-6, thus preventing cells from entering the G1–S phase (Sano et al., 1998). The cell cycle is controlled via a number of pathways and cell cycle check points. One of these pathways is the retinoblastoma protein (pRb) pathway, this controls cell cycle progression and hence proliferation. Under normal circumstances the pRb binds to the transcription factor E2F, this has the effect of stopping transcription of a number of genes that encode for cell cycle progression and also of the CDK-inhibitor p16. Binding of the transcription factor E2F by pRb is one key mechanism to stop continuous cell replication and proliferation (Israels and Israels, 2000).

The CDKs phosphorylate pRB, which results in a conformational change and release of E2F from the pRB, thus allowing cells to enter the S phase of the cell cycle. When E2F is released from pRb this unblocks the transcription of p16 protein (Fig.1.9a & b). The production of p16 protein in turn inhibits the phosphorylation of Rb via

CDK-4 and -6 cyclin D complex. This shifts the balance from phosphorylated Rb (inactive and unable to bind E2F) to non-phosphorylated (active, able to bind E2F) pRb (Israels and Israels, 2000). This fine negative feedback control maintains the cell cycle (Fig. 1.10).

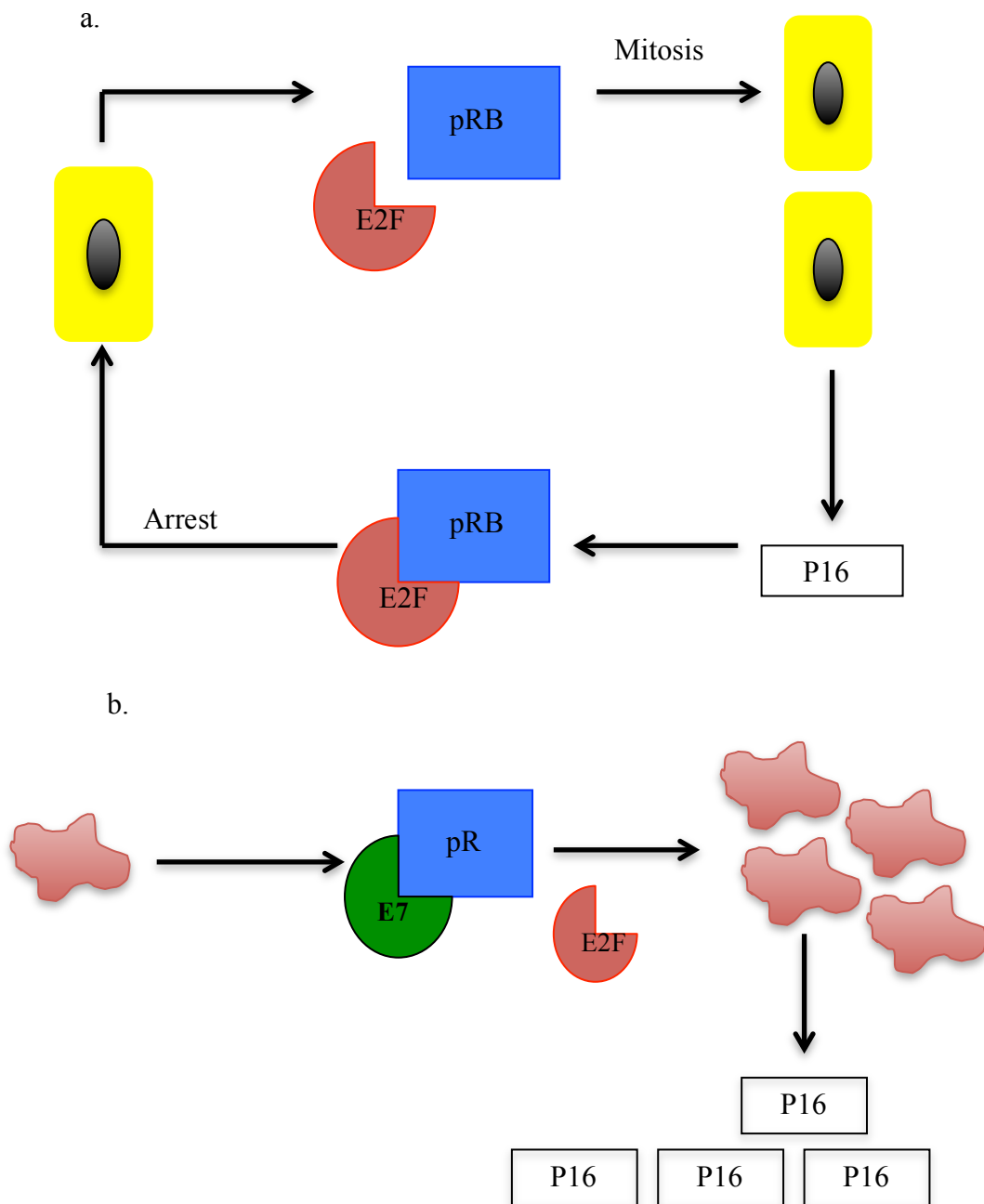


Figure 1.9a & b (a)Normal Cell cycle progression (Dividing Phase). Simplification of the dividing phase of the cell cycle and negative control feedback mechanism. (b) Interruption of the normal cell cycle by HPV-16 E7. There is uncontrolled division of neoplastic cells with high levels of by-product p16.

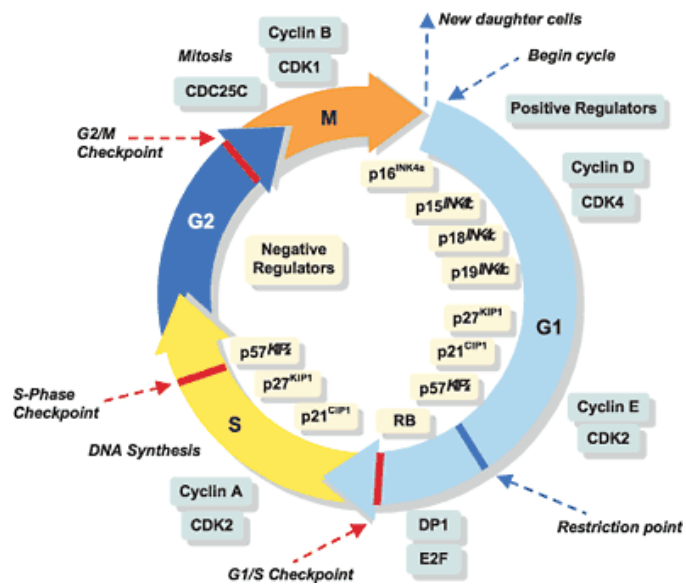


Fig. 1.10 Normal cell cycle control and check points. Illustration showing the cell cycle control phases from G1-M phase and control mechanisms to maintain controlled cell proliferation.

Chronic infection with high risk HPV, namely HPV 16 results in inactivation of the Rb pathway. The HPV oncogenic protein E7 interferes with Rb function and hence there is loss of control of Rb pathway, this results in uncontrolled proliferation of cells and over expression of p16 protein (Hamid et al., 2009). Over expression of p16 is a sensitive biomarker of tumour activity as high levels are expressed only when the oncogenic process has started rather than infection with high risk HPV alone. In terminally differentiated epithelial cells p16 levels are undetectable. In HPV mediated oncogenesis p16 levels are over expressed as the oncogenic E7 protein interferes with Rb and E2F binding.

1.7.7 Trends in HPV related HNSCC

The proportion of HPV-positive *vs.* HPV-negative HNSCC varies widely throughout the world as HNSCC is also dependent on other risk factors, such as tobacco and alcohol, and the relative proportion of these (Kreimer et al., 2005, Termine et al., 2008). For instance in the North Americas, the proportion of oropharyngeal tumours arising as a result of HPV infection ranges between 40 and 80%, whereas in Europe it varies between 20% in communities where smoking is taken to excess and up to 90% in countries such as Sweden where smoking habits are not as excess (Marur et al., 2010).

A study by Chaturverdi *et al.*, using Surveillance, Epidemiology and End Results program of the National Cancer Institute, USA (SEER) data suggested that HPV is currently the primary cause of tonsillar/oropharyngeal squamous cell carcinoma in North America and Europe (Chaturvedi et al., 2008). In North America in 1973 18% of all HNSCC were oropharynx (OP) compared to 31% in 2004 (Shiboski et al., 2005), and throughout the USA 60% of OP cancers are positive for HPV 16 (Marur et al., 2010). In Sweden oropharyngeal squamous cell carcinoma (OPSCC) caused by HPV-16 has steadily increased from 23% in 1970s to 57% in 1990s, to as high as 93% in 2007. A similar increase in incidence of HPV positive HNSCC has also been observed in the United Kingdom (Robinson and Macfarlane, 2003, Conway et al., 2006). The largest increase has been seen in the male Caucasian population age group 40-55 years. These data indicate that HPV infection is the primary cause of tonsillar SCC in North America and Europe.

It has traditionally been proposed that HPV associated HNSCC is related to risk factors of number of sexual partners, age at first consent, younger age, number of oral

sex partners and a higher risk in males. Although few, or no, oral sexual partners does not exclude the chance of disease, as a study reported between 8-40% of HPV positive oropharyngeal patients had no oral sex partners (Smith et al., 2004, Gillison et al., 2008). The increase in HPV associated HNSCC has mainly been within tonsillar and tongue base (oropharynx), although there are some HPV-positive tumours that have been found in the head and neck region excluding the oropharynx, the prevalence of these are not well documented.

1.8 The role of HPV in oncogenesis

Although greater than 95% of head and neck cancers are squamous cell cancers there is great heterogeneity amongst these. Various sub classes of HNSCC can be identified histologically, in particular RNA and DNA profiling have highlighted molecular heterogeneity (Leemans et al., 2011). There is a known favorable prognosis with HPV positivity in HNSCC. It has been found that p53 is mutated in 60-80% HNSCC, however in HPV positive HNSCC the p53 gene is often not mutated and the tumours often have wild type p53, the HPV oncoprotein E6 usually switches off this the p53 gene (Leemans et al., 2011). It is also known that the presence and type of p53 mutation affects prognosis (Westra et al., 2008), therefore it is not clear whether the more favourable outcome with HPV is secondary to the presence of wild type p53 or whether the HPV negative tumours have mutated p53 and hence an unfavourable outcome. As well as losing its function as a tumour suppressor gene, mutated p53 can inherit mutations which alter its function and cause negative effects, for example promoting tumourigenesis (Leemans et al., 2011).

HPV positive HNSCC has a different molecular profile to traditional HNSCC which is usually, but not exclusively, as a result of smoking and alcohol, and also genetic mutations or deletions in p53. The overall 5-year survival rate in HPV positive HNSCC has been shown to be 62% compared with 26% in HPV negative patients treated with radiotherapy (Lassen et al., 2009), furthermore improved outcomes were shown regardless of treatment options. Fischer *et al.* demonstrated 5 year survival rates of 26.8% in HPV negative and 57.1% in HPV positive OPSCC treated with surgery alone (Fischer et al., 2010).

In HPV negative HNSCC the prognosis is dependent upon stage and nodal status of disease, this is different to HPV positive HNSCC where prognosis is independent of stage and nodal status. The positive outcomes are increased for patients who are p16 positive, a surrogate marker for HPV, further providing evidence that the Rb pathway has been affected. The better prognosis for HPV positive patients is not thought to be related to the sensitivity to treatment since HPV cell lines have been shown to be more radioresistant than HPV negative HNSCC cell lines, suggesting that increased prognosis is likely secondary to the intrinsic nature of the tumour rather than increased radiosensitivity (Lajer and von Buchwald, 2010).

Spanos *et al.*, conducted a study in which they compared outcomes to radiotherapy in HPV positive and HPV negative tumours in immuno-competent and immuno-incompetent mice as well as responses to radiotherapy and cisplatin in human cancer cell lines (Spanos et al., 2009). For human and murine transformed cell lines, HPV positive tumours were more resistant to radiotherapy and cisplatin compared to HPV negative, however *in vivo*, HPV positive tumours were more sensitive to radiotherapy

and cisplatin compared to negative counterparts. Neither radiotherapy nor cisplatin cured immunoincompetent mice, transfer of wild type immune cells restored HPV-tumour clearance with cisplatin. This indicates that radiotherapy and cisplatin induce immune response and not that there is increased sensitivity intrinsically in the HPV positive tumours.

1.8.1 Role of E6 and E7 in Oncogenesis

P53 is a multifunctional transcription modulator and inducer of apoptosis. P53 becomes activated by acetylation and phosphorylation in response to DNA damage, nucleotide depletion or damage by hypoxia. It acts as a nuclear transcription factor to induce genes involved in cell cycle inhibition or apoptosis and can also induce apoptosis more directly by interacting with cytoplasmic proteins at mitochondrial sites (Kastan and Bartek, 2004). E6 abrogates the function of p53 therefore being a possible hypothesis into tumorigenesis by HPV 16 E6.

Unscheduled DNA synthesis activates cellular apoptotic pathways by a mechanism that has been termed 'trophic sentinel response', it is this response that is inactivated by the high risk E6, by switching off p53 and hence its ability to activate apoptosis. The retinoblastoma protein (pRB) is a regulator of cell cycle control, it interacts with the E2F family of transcription factors and regulates cell cycle and apoptosis.

E7 interacts mainly with unphosphorylated active pRB, resulting in the reversal of repression induced by the E2F genes, the expression of which are required for cell cycle progression from G1 to S phase. Once cells have left the basal layer and divide upwards they have usually exited the cell cycle and start to differentiate. However, the

presence of HPV E7 in the cells re-initiates or keeps the cell cycle active in these cells to keep a supply of proteins allowing S phase progression of the cell cycle. HPV E7 uncouples keratinocyte differentiation from cell cycle progression, this is central to HPV-induced transformation (see section 1.6.5).

There are a number of other interactions of E7 with cellular proteins that contribute to the inhibition of withdrawal from the cell cycle and may contribute to tumorigenesis that are independent of pRB, these are the following;

1. E7 binds to Mi2, a component of histone deacetylase (HDAC), this interaction is thought to mediate the interaction between high-risk HPV E7 and HDACs 1 and 2, allowing E7 to modulate the histone sequence with resultant possible modification of cellular genes needed for cell cycle dysregulation and possibly for immune invasion (Pim and Banks, 2010).
2. During keratinocyte differentiation loss of contact with the basal cell layer results in increasing levels of cyclin/CDK inhibitors p21 and p27, E7 can interact with p21 and p27 and reverse the inhibition of cyclin/CDKs (Missero et al., 1995, Martinez et al., 1999).
3. E7 also helps to drive cell survival by increasing Akt phosphorylation both by pRB dependent and independent pathways.

E7 has a number of properties that help it to modulate transcriptional activity, as well as being able to modify the histone machinery it has also been shown to modify insulin dependent cell signaling pathways, and is also associated with causing aneuploidy (Hashida and Yasumoto, 1991).

The viral E2 protein has been shown to inhibit the E7 mediated centrosome duplication errors by interacting with E7 directly. HPV E6 and E7 levels are low during normal or persistent infection. At some stage E2 loses its ability to repress the viral early promoter and levels of E6 and E7 rise to a high enough level to induce centrosome duplication and hence induce chromosomal abnormalities leading to carcinogenesis (Pim and Banks, 2010). Resulting aneuploidy may result in activation of DNA repair mechanisms that in turn result in viral integration into host DNA. Integration of viral DNA has been shown to occur frequently during cervical cancer progression, the same pathogenesis can be extrapolated to HNSCC.

E6 can contribute to oncogenesis independent of the p53 pathway. In normal differentiated cells, cells undergo a finite number of population doubling before apoptosis by activation of senescence pathways. Cells that survive this 'crisis point' are found to have activated telomerase, this is an enzyme complex that maintains telomeric repeats at the end of a chromosome (Hayflick, 1965). The mechanism involves transcriptional activation of the hTERT gene, which is a subunit of the telomerase complex. Tumour cells can also achieve this form of immortality by activation of the telomerase complex. The mechanism of telomerase activation by E6 and E7 is complex, however E6 activation is independent of E6AP binding and p53 degradation, it involves a mechanism of up regulation of the hTERT promoter through a number of cellular proteins (James et al., 2006). Recent reports have suggested that E6 can also bind directly with the telomerase complex (Liu et al., 2009), E7 is unable to directly activate telomerase activity itself however it augments the activity of E6.

1.9 HPV and The Immune Response

Unlike other viruses HPV has the ability to evade the immune system by maintenance of low viral protein levels in the cell, by expression of capsid proteins only in the outer layer of the epithelium thereby evading antigen presenting cells (APC). It also inhibits the interferon responsive elements and production of inhibitory cytokines. There are a number of local and systemic immune responses to HPV.

1.9.1 Local Immune factors

The natural history of HPV infection in the head and neck region is poorly characterised as most studies that have been performed looking at chromosomal alterations, gene expression patterns and expression of miRNA have been performed on cervical tissue and although there are some similarities there are also many differences. The mucosa of the head and neck is different to the rest of the body in that it is juxtaposed with lymphoid tissue, this is particularly true for the oropharyngeal region which encompasses the tonsils and base of tongue, both of which are lymphoid rich areas that provide adaptive immunity, especially in the early years, against inhaled and swallowed pathogens.

Studies on cervical tissue have shown that infection with HPV is usually cleared within the first couple of weeks to months by HPV specific T-cells, the contribution of both mucosal humoral and systemic responses to viral clearance remains under discussion. Persistent infection with HPV as a result of an inadequate initial T-cell response can lead to carcinogenesis by altering the E2 reading frame of HPV. The E2

viral oncoprotein usually suppresses levels of E6 and E7 viral proteins (Leemans et al., 2011). The reasons for inadequate immune response in some patients compared to others when matched for health status are a matter of further discussion and research.

HPV associated HNSCC arises in lymphoid tissue mainly in palatine and lingual tonsils, distinguished from non-HPV HNSCC by increased infiltration of lymphocytes within the stroma and tumour nests microscopically. Almost all transfected cells produce viral proteins (E6 and E7) that are highly immunogenic to the host and should be identified and targeted by the immune system. The question is therefore, how do virally infected tumours arise in an immune rich environment, whilst escaping the primary immune response. One mechanism of avoidance is proposed by the Programmed Cell Death Protein 1 (PD-1) and its corresponding ligand Programmed Cell Death Ligand 1 (PD-L1). CD8 is a glycoprotein co-receptor for the T cell receptor which is expressed on the surface of Killer T cells. The CD8 molecules bind to Class I Major histocompatibility complex (MHC) molecules on the surface of antigen presenting cells, the antigen is then presented on the MHC for recognition and destruction by the immune response. Activated CD8⁺ T Cells express the PD-1 receptor. Antigen induced expression by APC's is regulated by both co-stimulatory and co-inhibitory receptors and their corresponding ligands. After induction and stimulation of T-cells the resultant resolution of the immune response is initiated by the co-inhibitory factors, the aim of this is to prevent excess tissue damage and possible autoimmunity by the host immune response. The PD-L1 engages with the PD-1 receptor on CD8⁺ T-cells causing inhibition of the immune response. A recent study by Lyford-Pike *et al.* looked at the ratios of PD-1:PD-L1 in both HPV+

HNSCC and benign tonsillar pathologies (Lyford-Pike et al., 2013). They found over 70% of activated CD8⁺ TILs in HPV+ HNSCC expressed high levels of the PD-1 receptor compared to 35% of CD8⁺ T cells isolated from benign chronically inflamed tonsils, furthermore it was found that 70% of the tumour microenvironment in HPV+ HNSCC expressed PD-L1 which was juxtaposed to activated CD3⁺/CD8⁺ cells. Levels of PD-L1 are normally increased in normal tissue environment in response to localized increased levels of cytokines such as interferon- γ (IFN- γ), this helps to protect against excess tissue damage and autoimmunity. Lyford-Pike *et al.*, also found a significant increase in the levels of IFN- γ in CD8⁺ tumour infiltrating lymphocytes (TILs), and a 32-fold increase in tumours that expressed PD- L1, this showed that CD8⁺ TILs that are present in HPV+ HNSCC were activated and secreting IFN- γ which in turn is driving the expression of PD-L1, thus being a possible method of immune evasion by HPV as CD8⁺ PD-L1 cells are functionally anergic, and the tumour microenvironment can also up regulate the expression of PD-L1 by oncogenic mutations (Lyford-Pike et al., 2013). The initial infection by HPV occurs in the deep crypts of the tonsil, which are shown to be a PD-L1 rich area, thereby evading the host immune response. Blocking of PD-1 or PD-L1 by specific monoclonal antibodies can reverse the anergic state of tumour specific T-cells, therefore this can be targeted for immune therapy (Porichis et al., 2011, Hirano et al., 2005).

1.9.2 Systemic Immune factors

In addition to differences in the tumour infiltrating lymphocytes between HPV positive and negative tumours, the systemic immune response also appears to be altered in HPV positive tumours. In patients with HPV positive HNSCC Rubenstein *et al.*, (Rubenstein et al., 2011) found increasing levels of antibodies against E6 and

E7 with increasing stage of disease, it was also stated that these antibodies were a late marker of carcinogenesis. The same study looked at baseline IgG antibodies to E6 and E7 prior to treatment and at subsequent follow up intervals following treatment and found a higher level of antibody in the OP group compared to the oral cavity ($p=0.001$) or hypopharynx/larynx groups, they also found a higher level of E6, E7 or E6 & E7 with later stage disease. Compared to T1-2 tumours those with T3-4 tumours had higher levels of E6 antibody (ORs 6.8 vs 4.9 $p=0.05$). It was also demonstrated that antibody levels were higher for those with nodal involvement compared to those without nodal involvement (ORs 5.8 vs 2.1, $p=0.04$) (Rubenstein et al., 2011). In addition to the differences in the levels of E6 and E7 specific antibodies between different groups of patients, Rubenstein *et al.* found that there was increased overall and disease specific survival in baseline seropositive patients compared to baseline negative. In cervical cancer studies evidence has shown that decreases in antibody level between pre and post treatment follow up do better in terms of disease free survival and continuing remission.

The cytokine interleukin (IL) 10 has been associated with HPV related disease. IL-10 is a pleotropic cytokine (Bolpetti et al., 2010) produced by myeloid cells and lymphocytes, its actions display both immunostimulatory and immunoregulatory effects, in particular it inhibits the production of other cytokines such as IL-2, Interferon γ (IFN γ), IL-12, tumour necrosis factor (TNF) and it is also associated with down regulation of MHC I. Bolpetti *et al.* (Bolpetti et al., 2010) concluded production of IL-10 was a co-factor in tumour immune invasion via T cell regulatory pathway by HPV-HNSCC.

The mean CD8 count has also been shown to be higher in HPV-HNSCC ($p=0.04$) and also the CD4:CD8 ratio significantly lower ($p=0.02$) in patients with HPV-positive cancer (Wansom et al., 2010). No difference in other T or B cells in HPV positive or negative cancer patients has been demonstrated. Interestingly Wansom *et al.*, showed an overall increase in total white blood cell counts in non-HPV HNSCC who were also smokers compared to HPV positive HNSCC thereby further confirming that HPV down regulates the human immune response (Wansom et al., 2010).

Levels of peripheral lymphocytes are an indication of immune homeostasis and not a direct reflection of immune activation and response to HPV infection. Significance of increased T-cell lymphocytes in the peripheral blood of HPV-16 positive patients is not clearly elucidated. Although several studies have shown a link with CD8⁺ T cells in immunity against HPV-16, a mouse model showed that depletion of CD8 cells resulted in reduced tumour regression in HPV-mouse models compared to controls, indicating that CD8 was implicated in host response against HPV-HNSCC (Wansom et al., 2012).

Another theory of enhanced immunity with HPV-HNSCC is that HPV-E7 is highly antigenic, causing an enhanced immune response. Therefore dysplastic tumour cells that express E7 may be more readily recognised as foreign by the immune system. This is supported by DNA vaccine data that shows high levels of CD8 T-cells that are more aggressive towards E7 expressing tumour cells (Lin et al., 2007).

Clearance of HPV-16 is antigen dependent and immune mediated, concealing antigens may result in the evasion of the host immune response by HPV-16. Wansom

et al., found that an HPV-16 status combined with a high CD8 count and low CD4:CD8 ratio was a good predictor of improved outcomes with chemotherapy or chemoradiotherapy, this was shown both *in vivo* and in mouse model.(Wansom *et al.*, 2010)

1.9.3 Poor prognostic indicators in HNSCC

There are a myriad of T-regulatory and cytotoxic T cells within the tumour microenvironment and peripheral circulation, the functions of which are dependent on the complex interactions of inhibitory and stimulatory factors. A study done by Heusinkveld *et al.* looked at the local and systemic immune responses in patients with HNSCC and those who were HPV-16 positive. Nearly all patients with HPV-16 HNSCC had TILs within the tumour microenvironment, however only a proportion of these patients showed a systemic response (Heusinkveld *et al.*, 2012), therefore measurement of the peripheral immune response only is not representative of the HPV induced immune response. None of the HPV negative HNSCC patients had HPV-specific T-cells present within the tumour (Heusinkveld *et al.*, 2012). Immune infiltration into the tumour microenvironment is advantageous for survival, however in cervical cancer studies it has been shown that large polyclonal infiltrates of T-cells were largely inactive (de Vos van Steenwijk *et al.*, 2010), therefore rather than absolute numbers of immune cells within the tumour microenvironment it is important to assess the activity of such infiltrates.

A number of studies involving HNSCC have shown that varying levels of FoxP3 regulatory T cells and cytotoxic T cells have either no association with tumour control or the local tumour microenvironment control (Rajjoub *et al.*, 2007, Thurlow JK,

2010). In studies from other tumour sites, including breast, colorectal, pancreatic and gastric cancer, infiltration of T-lymphocytes into the tumour have been shown to have a poorer outcome, however these were adenocarcinomas and not squamous (Wilke et al., 2010), which most head and neck cancers are, therefore the exact role of infiltrating T-lymphocytes needs to be determined in HNSCC.

Other factors that have been shown to have a poor outcome with HNSCC include the epidermal growth factor receptor (EGFR), high levels of which are observed in OPSCC and associated with CD3⁺ T cell infiltration, these are cytotoxic T-cells, and are associated with poorer outcomes in OPSCC (Badoual et al., 2006).

Overexpressed levels of p53 are observed in a variety of human cancers including HNSCC, most p53 mutations are single base missense mutations, therefore the remainder of the protein accumulated is wild type p53 (wt-p53). Accumulated p53 is processed and presented to the surface as an epitope thereby increasing levels of cytolytic T-lymphocyte cells (CTL) (Sirianni et al., 2004). The tumour suppressor protein p53 has therefore been considered a target for immunotherapy, it was thought that by increasing levels of anti-p53 CTLs by immunotherapy this would prove beneficial in SCC. However, it was shown that there was an actual inverse relationship between p53 levels and levels of anti-p53 CTLs, highest levels were seen in those patients that had mutated p53 or did not accumulate p53 (Hoffmann et al., 2000). One theory postulated for this was that higher levels of anti-p53 CTLs were seen secondary to immunoselection for 'epitope loss' tumour cells. Sirianni *et al.* showed that the same effect could be seen in HNSCC tumours that were HPV-16 positive (Sirianni et al., 2004). HPV-16 E6 is known to cause degradation of both

wild type and mutant p53 and can enhance processing and presentation of p53 epitopes in mouse models (Vierboom et al., 2000).

Furthermore there is increased tumour recognition by T cells both *in vitro* and *in vivo* in those with degraded p53, due to E6 causing proteasomal degradation and processing of wt-p53. Anti-p53 T-cells recognise HPV-16 E6 expressing HNSCC that do not accumulate p53 peptide. E6 enhanced degradation of p53 is correlated with higher levels of anti-wt-p53 CTLs, levels of these are reduced in post operative follow up in patients with HPV-positive tumours however in HPV negative tumours levels of anti wt-p53 CTLs remain static, one theory is that in HPV positive tumours the antigen source is removed however in HPV negative tumours that contain accumulated p53, these can transfer the p53 peptide to dendritic cells which remain a source of antigenicity (Sirianni et al., 2004).

The composition of tumour infiltrating cells has also been variably described in studies. Wansom et al (Wansom et al., 2012) looked at the composition of tumour infiltrating lymphocytes in 46 subjects with oropharyngeal cancer. They concluded that there was no significant difference in the tumour infiltrates between HPV-16 positive and HPV-16 negative cancers. The average ratio of CD4/CD8 TILs was lower in HPV-16 positive OPSCC and the sum of CD4 and CD8 was higher, however, these findings were not statistically significant. A previous study by the same authors looked at peripheral circulating lymphocytes in HPV-positive and HPV-negative OPSCC. The study found CD8 levels were higher and CD4 levels lower in the peripheral blood of HPV-16 positive patients (Wansom et al., 2010). Furthermore no difference between FoxP3 (T-cell regulatory protein) counts were found in relation

to HPV-16 status, however it was found that the average ratio of FoxP3 to CD8 tended to be higher in the HPV negative group, however this was not statistically significant ($p=0.099$). They concluded that the CD4/CD8 ratio were significant predictors of outcome even after adjustment for HPV status ($p=0.0056$).

Wansom et al. found that overall survival was increased with higher levels of CD8 cells ($p=0.0615$), even after adjustment for HPV status and disease specific survival (DSS) was significantly associated with EGFR expression, HPV status, peripheral blood CD4/CD8 ratio and smoking history. With regards to tumour infiltrating markers, only CD4/CD8 ratio, FoxP3/CD8 ratio and the sum of CD4 plus CD8 cell infiltrates were significantly associated with DSS (Wansom et al., 2012). Higher levels of activated CD4 and FoxP3 cells in tumour stroma are associated with improved locoregional control and survival in mixed cohort of HNSCC (Badoual et al., 2006). Recently gene signatures of adaptive immunity in HNSCC have been shown to outperform HPV status monitoring in prognosis (Thurlow JK, 2010), however the heterogeneity in immune responses amongst HNSCC and HPV status are yet to be fully determined. It is thus more important to know the ratios of immune cells rather than actual levels, it has been reported that a higher CD8 to Treg ratio in tumour and stroma of oral cancer is associated with a favourable outcome (Watanabe et al., 2010). In unstratified OPSCC high TILs levels predicted for survival and correlated significantly with HPV-positive tumours ($p<0.001$) (Ward et al., 2014). The percentage of high, moderate and low TILs in HPV-positive tumours was 49%, 36% and 15% respectively; compared to 16%, 38% and 46% respectively in HPV-negative tumours.

Smoking status remained a significant predictor for overall and disease specific survival, even after adjusting for HPV-16 status and reduced survival benefit in HPV-positive patients. However levels of CD4, CD8 and FoxP3 tended to be higher in non-smokers even after adjustment for smoking and levels of TIL's still predicted for OS (Wansom et al., 2012).

The exact role of TIL in HNSCC remains to be determined, whilst it has been reported that TIL have a positive outcome on tumour status in HPV-positive patients, it has also been suggested that TIL are independent of HPV-status and are rather dependent on the tumour type, smoking history and EGFR expression (Wansom et al., 2012). Ward *et al.* reported that there was a significant difference in Kaplan-Meier survival curves within the HPV-positive OPSCC and TIL levels ($p < 0.001$). Patients that were HPV positive but with low TIL showed similar DSS to HPV-negative patients. However in HPV-negative tumours with high TILs there was no significant difference from HPV-negative tumours with low TILs levels (adjusted HR 0.47, $p = 0.17$) (Ward et al., 2014).

Positive outcomes in cancer are generally associated with early stage of disease with non or early nodal metastasis, however on the contrary outcomes for advance HPV-positive OPSCC have been shown to be positive even with advanced disease, as levels of TIL have not been associated with the stage of disease or as predictors of outcomes (Ward et al., 2014). One such plausible explanation for improved survival in HPV-positive versus HPV-negative tumors is that HPV tumours are virally driven and induce an adaptive immune response, usually with intact rather than mutated p53 and Rb.

1.10 HPV Detection methods

The presence of HPV virus does not indicate that it is the causative factor of carcinogenesis, molecularly active virus needs to be shown for this. HPV 16 becomes a causative factor when the oncogenic proteins E6 and E7 interfere with the cell cycle, this is the key to any detection method as it provides evidence of presence of HPV related carcinogenesis.

Currently there is no one specific test that elucidates a HPV positive cancer, rather there are a myriad of tests which when used in combination point to a higher possibility of a HPV positive cancer, the diagnostic challenges further add to the complexity of this disease process. Distinction between HPV positive and HPV negative HNSCC is important as it relates to prognostic differences and could lead to possible streamlined treatment for HPV positive patients. No consensus has been reached on the optimal way to identify HPV-positive SCC, most studies have used a number of methods, the most common including; immunohistochemical staining for p16, HPV *in situ* hybridization (HPV-ISH) and polymerase chain reaction (PCR).

1.10.1 Direct HPV tests

1.10.1.1 Polymerase Chain Reaction

The polymerase chain reaction (PCR) involves amplification of a specific sequence several orders of magnitude. First either DNA or RNA is extracted, and in the case of RNA, copied into complementary DNA before being denatured by heating to high

temperatures. Amplification of a specific sequence of interest is then achieved using several rounds of denaturing at 95°C, annealing of complimentary oligonucleotide primers at a lower temperature (c. 55°C, this is usually below the melting point) and DNA replication at an intermediate temperature (usually c. 72°C) by a heat resistant polymerase (Venuti and Paolini, 2012). PCR is highly sensitive and can detect a single copy of viral DNA per cell, furthermore it can be used on both fresh frozen samples and FFPE samples. However, it has less specificity than other methods and has a number of drawbacks, which include the inability to differentiate between cells infected with HPV or those that have undergone neoplastic change secondary to this, it also is unable to distinguish between episomal and integrated HPV; PCR is thus limited clinically on its own.

1.10.1.2 In Situ Hybridisation

This is the only molecular method that allows for reliable detection of HPV in relation to the topographical pathological lesions; a complementary labeled RNA or DNA probe is used to hybridize to a known target mRNA or DNA sequence. Briefly, commercially available HPV probes are used to bind to specific mRNA or DNA sequences at high temperatures, the excess probe is then washed away and the resultant hybridized probe which was labeled with either radio-, fluorescent- or antigen labeled bases is detected. Positively labeled nuclei are examined microscopically indicating presence of HPV in the tested specimen. ISH can detect clinically relevant HPV as it has specific markers for detecting integrated HPV. Although ISH has 100% specificity it is limited by its sensitivity which is around 83% (Venuti and Paolini, 2012), however, the advantages of ISH are that it can be used on

FFPE samples and also there are many commercially available kits. The disadvantages of ISH are that it is a laborious costly technique unlikely to be used for routine screening and is therefore reserved as a confirmatory test after initial screening for p16.

1.10.1.3 Southern Blotting Assay

Southern blotting involves extraction of the genomic DNA from a specimen following digestion with restriction enzymes. The digested product is then separated using agarose gel electrophoresis based on the size of the fragments. The separated DNA fragments are then transferred onto a nitro-cellulose or nylon membrane and hybridized with cloned complementary HPV genomic-labeled probes. The detection of the labeled DNA hybrids indicates that HPV is present within a given sample. The advantages of the Southern blotting assay (SBA) include the ability to differentiate between episomal and integrated HPV due to differences in fragments size, and also the ability to detect small copies of viral DNA (Venuti and Paolini, 2012). Although SBA has a higher specificity it is not as sensitive as other methods such as PCR. Furthermore SBA cannot be performed on formalin fixed paraffin (FFPE) samples due to the presence of cross-linked degraded nucleic acids and also it requires a large amount of DNA. This method has no clinical utilization at present.

There are a number of other direct HPV tests illustrated in Table 1.5, these are not routinely used in clinical practice due to various drawbacks.

Table 1.5 Direct HPV Detection Methods. Adapted from HPV Detection Methods in Head and Neck Cancer, Venuti & Paolini. Head and Neck Pathology (2012)(Venuti and Paolini, 2012)

Method	Specimen	Advantages	Disadvantages
Real-Time PCR	FFPE Fresh/Frozen Brushings/washings Any bodily Fluid	High sensitivity & specificity	False positive and false negative products No direct evidence of oncogene expression Labour-intensive
Reverse Transcriptase PCR	Fresh/frozen samples FFPE	Highly sensitive Detection of clinically relevant HPV	Time consuming Labour-intensive and technically challenging
Signal Amplification Methods	FFPE Fresh/Frozen OC brushings/washings	Easy to perform	False positives No typing No distinction between neoplastic HPV + cells and non-neoplastic HPV+ cells
PCR ISH	Fresh/frozen samples FFPE	High sensitivity and specificity	Labour-intensive and technically difficult No data on clinical use
DNA/RNA microarray	FFPE Fresh/Frozen OC brushings/Washings Saliva	Identification of gene profiles	High costs Predictive expression profiles still elusive

1.10.2 Indirect Tests Correlating with HPV

1.10.2.1 Immunohistochemical staining for p16

The oncogenic HPV protein E7 binds to the retinoblastoma protein (pRb) and causes increased expression of p16. Immunohistochemical staining for p16 has a sensitivity of almost 100%, however it is not 100% specific for HPV related SCC and can generate false positives, therefore it is used primarily as a screening tool. It has the advantages of being easy and cheap to perform and can be performed on FFPE.

Chronic infection with high risk HPV, namely HPV 16 results in inactivation of the pRb pathway and thus over expression of p16, which is a sensitive biomarker of tumour activity as high levels are expressed only when the oncogenic process has started rather than infection with high risk HPV alone, furthermore in terminally differentiated epithelial cells p16 levels are undetectable. In HPV-mediated oncogenesis p16 levels are over expressed as the oncogenic E7 protein interferes with pRb and E2F binding. P16 positive staining must take into account the cellular staining pattern, as p16 is a cellular protein that may be expressed at high levels in dysplastic and other lesions, albeit at differing levels. Therefore it is more important to measure the continuous staining pattern rather than staining alone.

1.10.2.2 Serum Antibodies against HPV

The same high risk HPVs involved in HNSCC can also infect or involve the anogenital tract. Therefore serological assays are not site specific and generally antibodies against the L1 and L2 capsid proteins do not differentiate between infection and neoplastic change. However in a large study where serum samples were collected from 900,000 referents, seropositivity measured with ELISA test against the capsid proteins was largely attributed to infection at the site of the tumour, with odds ratio of 37.5 for HPV-16 DNA compared to an odds ratio of 2.1 in HPV negative (Mork et al., 2001). Seropositivity to the HPV oncogenic proteins E6 and E7 can also be measured (Rubenstein et al., 2011).

HPV-DNA can also be detected in plasma, the clinical significance of this is largely undetermined. There is further scope for the possibility of detection of HPV in saliva, however research data on this is lacking.

1.11 Aims of Thesis

At present the explanation for improved survival outcomes in HPV-positive versus HPV-negative HNSCC remains unclear, it has been suggested that survival outcomes are multifactorial with a complex interplay of host and viral factors. HPV-positive HNSCC tends to have better outcomes regardless of treatment modality, which may possibly be due to the presence of the retinoblastoma and wild type p53 genes which are usually lost or mutated in conventional HNSCC. HPV-positive HNSCC is related to a lower risk of secondary cancers, this may be secondary to reduced field 'cancerisation'. Furthermore the presence of HPV inversely correlates to poor prognostic indicators such as epidermal growth factor receptor (EGFR) expression. Although survival outcomes are greatly improved in HPV-positive HNSCC compared to negative the treatment regimes remain the same, therefore many patients may be over treated.

Previously thought of as a homogenous group of cancers differing only by sub site of anatomy, HNSCC's are distinctly being sub-classified by genetic profiling and increasingly by immunoprofiling. HPV-positive HNSCC has distinctly been categorized as a separate disease entity, although much of the work done so far relates to oropharyngeal cancers, what is less understood is whether HPV has the same response in the remaining sub types and what specific immune factors correlate with outcomes. In particular what is not well understood is why some patients host an immune response to HPV and why some do not and how this contributes to cancer.

Whether HPV-positive non-oropharyngeal HNSCC is associated with a different immune profile and prognosis compared to HPV-negative HNSCC remains to be clarified. A study by Isayeva *et al.*, suggested that infection with HPV had no bearing on clinical outcome in HNSCC that did not originate from the base of tongue or tonsil (Isayeva *et al.*, 2012). This may perhaps be secondary to the anatomy of the OP in that it is an immune rich area compared to the other sub sites of the head and neck region. The authors concluded that not enough studies were available for comparison in non-oropharyngeal head and neck cancer.

The aim of this thesis is thus to correlate specific immune parameters patients have towards HPV-16 and compare these with clinical outcomes in terms of disease free survival. This study examined the role of seropositivity to the HPV-16 oncoproteins in HNSCC and also in the normal population given that most HPV infection is cleared. There are a number of tests available for diagnosing the presence of HPV infection, however in order to show HPV-induced carcinogenesis a molecularly active HPV infection needs to be present, the diagnosis of which is more challenging, this study examined the presence of molecular active HPV and the concordance between HPV testing. As demonstrated there are a number of studies with conflicting findings with regards to immune parameters in HPV-positive and HPV-negative cancers, the aim of this thesis was to examine a host of peripheral circulating and tumour infiltrating immune markers and the correlation of these with HPV status and survival outcomes.

Chapter 2. Material & Methods

2.1 Purification of Genomic DNA

2.1.1 Phenol Chloroform extraction

The UM-SCC-47 cell line, a squamous cell carcinoma of oral cavity origin was used to isolate HPV-16 DNA. The cell line was a generous gift from Dr T Carey (University of Michigan, USA) (Brenner et al., 2010). A 25cm² flask of cells was pelleted by centrifugation at 14,462 x g for 60 seconds (Techne Genofuge 16M). The supernatant was decanted carefully and cells were gently resuspended in 1ml of STE Buffer (Appendix 2). Proteinase K (Sigma Aldrich[®], Dorset, UK) was added to the cells at a final concentration of 2mg/ml and the solution was incubated overnight at 55°C to allow digestion of the cell membranes.

Following overnight incubation 500µl of the cell solution was transferred into two separate 1.5cm polypropylene tubes using a wide-bore pipette tip to avoid shearing of the DNA. Phenol and chloroform (250µl each; Sigma) were added to each tube and the solution was gently mixed for 5-10 minutes by inversion. The tubes were then centrifuged at 14,462 x g for 3 minutes (Techne, Genofuge 16M) to separate the mixture into three different phases; an upper aqueous phase containing the DNA/RNA, a central interphase containing proteins and a lower organic phase containing lipids (Fig. 2.1).

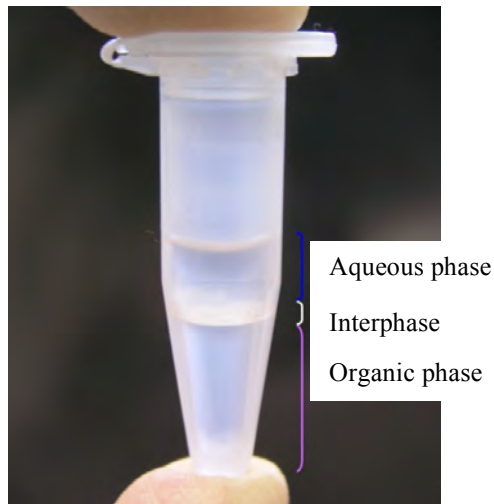


Figure 2.1 A polypropylene tube following centrifugation of the phenol/chloroform extracted DNA. At this stage three clear phases are visible: Top Phase – **Aqueous phase**; contains DNA/RNA, Middle Phase – **Interphase**; contains proteins, Bottom Phase – **Organic Phase**; contains lipids.

The aqueous phase was transferred into a clean 1.5cm polypropylene tube and the phenol/chloroform extraction was repeated as described above. After centrifugation the top aqueous phase containing DNA was again transferred to a new tube and 500 μ l of chloroform (Sigma) was added and mixed gently to remove any traces of phenol. The solution was centrifuged again at 14,462 x g for 3 minutes and the top DNA containing layer was transferred to a clean tube and 1ml of 100% ethanol was added to each 0.5ml of supernatant and mixed to precipitate the DNA. The DNA was pelleted by centrifugation at 14,462 x g for 3 minutes, the supernatant was discarded before the pellet was washed with 1.5ml of 70% ethanol. The tube was once again centrifuged at 14,462 x g for 3 minutes and the supernatant was decanted carefully so as not to disrupt the pellet. The DNA pellet was allowed to dry for 10-15 minutes and then dissolved in 1ml of Tris-EDTA Buffer (Appendix 2). The concentration of the DNA was determined using nano-spectrometry (see results chapter 3). The method of

phenol chloroform DNA extraction was based on methods described by Puissant *et al.*, and Chomczynski *et al.* (Puissant and Houdebine, 1990, Chomczynski and Sacchi, 1987, Chomczynski and Sacchi, 2006).

2.2 Amplification of genomic DNA using PCR

Polymerase chain reaction (PCR) was used to amplify target DNA templates, namely the oncoprotein sequence regions for HPV-E2, -E6 and -E7. DNA polymerase initiated the reaction by attaching a nucleotide onto a pre-existing 3'-OH group. A primer was required to which the first nucleotide could be attached, these were designed as described in section 2.2.1.

2.2.1 Primer Design

The *Oligonucleotide Properties Calculator*, which is an online tool, was used to design primers for the HPV-E2, -E6 and -E7 proteins respectively with additional restriction sites incorporated so that these could be later used to insert the genomic DNA into an expression vector. The length of the primers were kept between 18-26 base pairs; ensuring that the guanine (G) and cytosine (C) content was kept between 50-60%, this allowed for increased stability of binding of the primer to the DNA template. The melting temperature (T_m) of the primers was kept between 50-60°C and the T_m of both the forward and reverse primers for each set were kept within 2°C of each other to allow for simultaneous annealing. Long runs of the same nucleotide were avoided to prevent 'breathing' of the primer. It was also ensured that the 3' end of the primer ended in either G or C nucleotide, this is known as GC clamping and allowed for increased affinity of the primer to bind to the DNA template and allow for polymerisation in the correct direction. This is as the G-C bond is stronger than the

A-T bond as there are three hydrogen bonds between the G-C compared to two on the A-T. Mis-hybridisation was avoided by ensuring that the primer sequences were not similar to nearby genomic DNA sequence patterns by using the online Basic local alignment search tool (BLAST).

Primers were designed by identification of the target DNA template from the already established HPV-16 DNA sequence. Once designed the primers were manufactured by **Eurofins MWG Operon** (Ebersberg, Germany).

2.2.2 Structure of HPV 16

This is described in detail in section 1.7.2., HPV-16 is a non-enveloped double stranded DNA virus with 7900 base pairs. The oncoproteins E2, E6 and E7 are visible in the genomic sequence illustrated in Fig. 2.2.

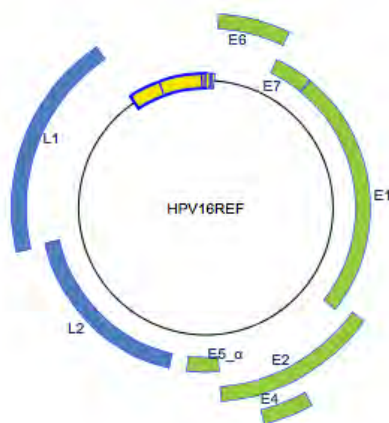


Figure 2.2 Complete genome of HPV-16 with illustrated oncoproteins E1-E7 and capsid proteins L1 and L2.

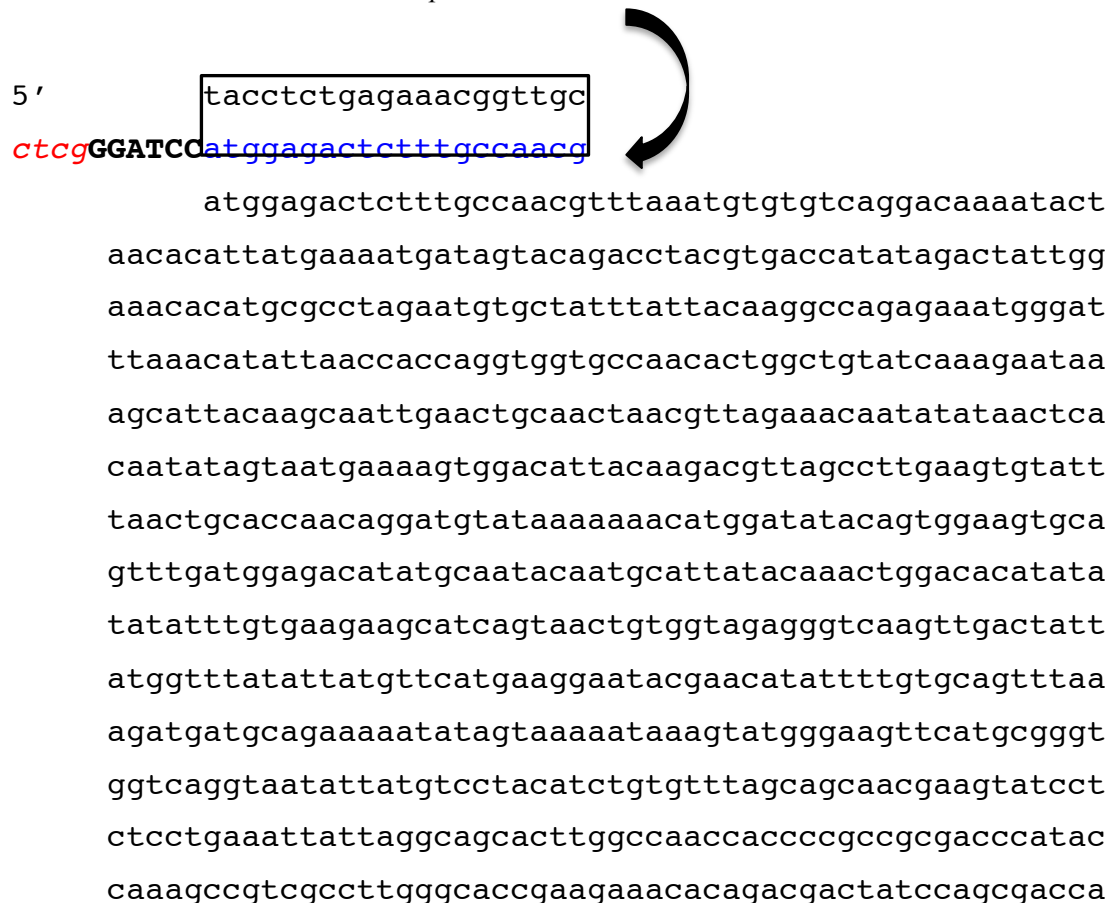
2.2.3 Genomic sequence patterns with primers

DNA sequence patterns were identified for the HPV oncoproteins E2, E6 and E7. Primers were designed as described in section 2.2.1. Figures 2.3a-c illustrate the genomic sequence pattern for each of the oncoproteins with attached primers and incorporated restriction sites for production of recombinant fusion GST tagged proteins. Protein tags were added to allow for incorporation of the genomic DNA into an expression vector (pGEX-6P1) to allow for later expression in bacterial medium and purification (see section 2.4).

Figure 2.3

(a)

The E2 forward primer attaches to the anti-sense strand of the DNA; upstream is the BamHI restriction site that allows insertion into the pGEX-6P1 vector.



agatcagagccagacaccggaaccctgccacaccactaagttggtgcaca
gagactcagtgacagtgctccaatcctcactgcatttaacagctcacacaa
aggacggattaactgtaatagtaaacactacacccatagtacatttaaagg
gatgctaataactttaaaatgtttaagatatagatttaaaaagcattgtacat
tgtatactgcagtgctcgtctacatggcattggacaggacataatgtaaaaca
taaaagtgcaattgttacacttacatgatagtgatggcaacgtgaccaa
ttttgtctcaagttaaaatacaaaaactattacagt

gtctactggatttatgtctatatga
cagatgacctaatacagatatactCTTAAGctgctc

(b) *The E6 forward primer attaches to the anti-sense strand of the DNA*



(c)



Figure 2.3a-c Genomic sequence for HPV-16 oncoproteins with attached reverse stop primer with the Eco R I restriction site for the pGEX 6P1 vector (bold). The stop codon is incorporated within the primer. The excess bases (italics) allow for increased efficiency for binding of restriction enzymes when used for cutting to allow incorporation into the expression vector. Also illustrated is the forward primer (BamHI) that attaches to the anti-sense helix (partly illustrated).

(a) Genomic sequence for HPV-E2

(b) Genomic sequence for HPV-E6

(c) Genomic sequence for HPV-E7

Primers were also designed for His-tag fusion proteins, these are illustrated in Table

2.1. Comparisons of GST versus His-Tag proteins are discussed in section 2.2.4.

Vector Tag	Primer with restriction sites	Sequence 5'→3'
E2 HISTAG	E2ForNCO	<i>ctcgtc</i> CCATGG AGACTCTTTGCCAACG
	E2RevNoStopXho	<i>gac</i> CTCGAG TATAGACATAAAATCCAGTAGACACTG
E6 HISTAG	E6ForNCO	<i>ctcgtc</i> CCATGG ATGCACCAAAGAGAACTGCAATG
	E6RevNoStopXho	<i>gac</i> CTCGAG CAGCTGGGTTTCTCTACGTG
E7 HISTAG	E7ForNCO	<i>ctcgtc</i> CCATGG ATGCATGGAGATACACCTACATTGC
	E7RevNoStopXho	<i>gac</i> CTCGAG TGGTTTCTGGGAACAGATGGG

Table 2.1 Restriction sites for the Nco R I and Xho I on the pET-28a vector are incorporated into the primer design (bold), excess bases (italics) are required to increase the specificity of cutting restriction enzymes. The pET-28a vector was used to allow for the His-Tag to be incorporated into the recombinant fusion proteins.

2.2.4 Protein Tags

The recombinant fusion proteins were tagged to allow for purification of the target protein by affinity purification. The purification method chosen was based on the specific biochemical properties conferred by the tag and the expression vector. The polyhistidine (His-tag) and the glutathione-S-transferase (GST) tags were selected based on their specific properties.

The His-tag is the most widely used and has several advantages; due to its small size the His-tag is less immunogenic when compared to other tags. Furthermore another advantage of the His-tag is that it does not require removal for downstream applications with the purified protein. It can also be placed at either the N- or C-terminus (Yip et al., 1989). Finally the His-tag allows for otherwise insoluble proteins to be purified using denaturing conditions.

The glutathione-S-transferase (GST) affinity tag is based on the strong affinity of GST for glutathione-covered matrices. GST isoforms are not normally found in bacteria, thus there is no competition from endogenous bacterial proteins for binding to purification resin with GST-fusion proteins expressed in bacteria. GST-fusion protein binding to glutathione is reversible and allows efficient elution of the bound GST-fusion protein with free glutathione (Smith and Johnson, 1988, Mannervik and Danielson, 1988).

2.2.5 Expression Vectors

A number of expression vectors are commercially available; this study used the pET-28a plasmid vector (Novagen, UK) for the insertion of a His-Tag to the recombinant fusion proteins and used the pGEX-6P1 plasmid vector (GE Healthcare, Buckinghamshire, UK) to insert a GST tag. Target genes in pET plasmids are cloned under control of strong bacteriophage T7 transcription and expression is induced by providing a source of T7 RNA polymerase in the host cell. T7 RNA polymerase is so selective and active that, when fully induced, almost all of the cell's resources are converted to target gene expression; the desired product can comprise more than 50% of the total cell protein a few hours after induction.

pET-28a Vector

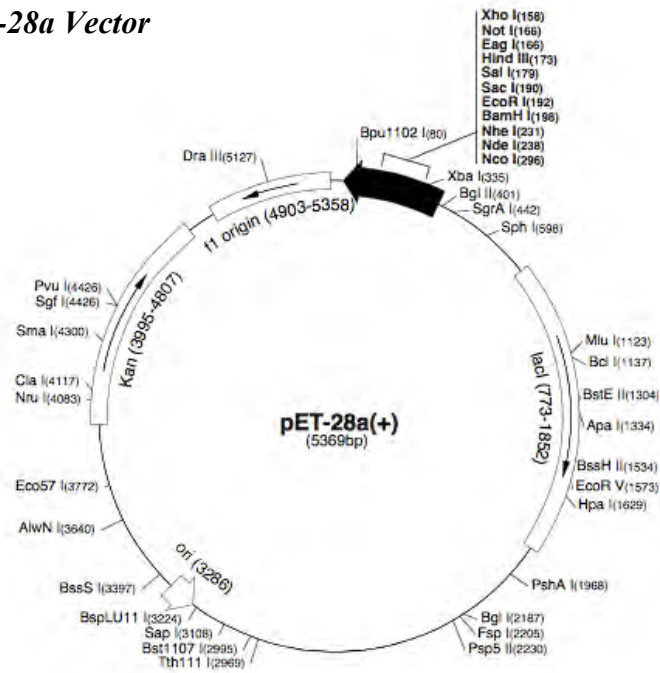


Figure 2.4 Adapted from Novagen. The pET-28a vector carries an N terminus His-Tag configuration. Shown are the restriction sites and direction of transcription.

pGEX-6P1 vector

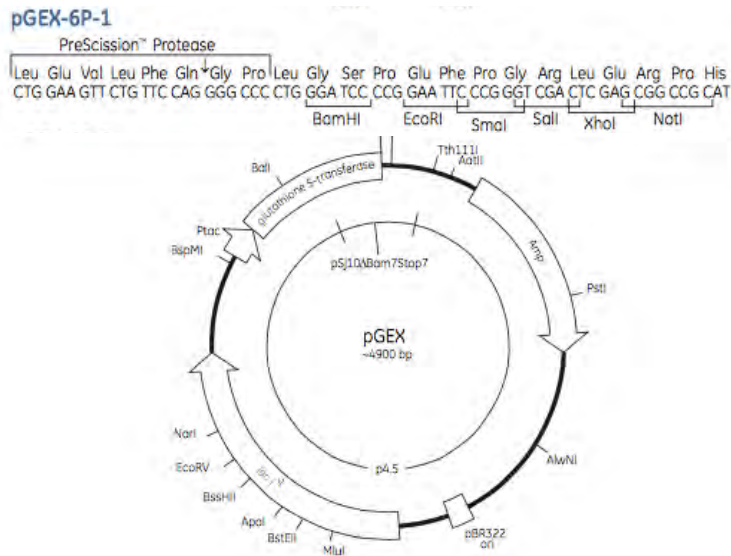


Figure 2.5 Adapted from GE Healthcare. Map of the pGEX-6P1 fusion vector with attached multiple cloning sites and restriction sites.

2.2.6 PCR Template

PCR was commenced in a standard fashion firstly by construction of the PCR templates. The concentration of the phenol-chloroform extracted genomic HPV-16 DNA had previously been determined to be $240\text{ng } \mu\text{l}^{-1}$ by nanospectrometry (see section 2.1). This was used at a dilution of 1:10 by adding $10\mu\text{l}$ of DNA to $90\mu\text{l}$ of dH_2O . A $50\mu\text{l}$ reaction template was composed by adding $1\mu\text{l}$ of DNA template to $0.5\mu\text{l}$ of each forward and reverse primers (see Table 2.1) at a final concentration of $1\mu\text{M}$ each. $5\mu\text{l}$ of $10 \times$ Phusion HF buffer (New England Biolabs(UK) Ltd, Hertfordshire, UK) was added, the HF buffer was used as this was the default buffer for high-fidelity amplification. Deoxynucleotides (dNTP)(New England Biolabs) were added at a concentration of 0.5mM ($0.5\mu\text{l}$). The solution was made up to $49\mu\text{l}$ with the addition of dH_2O . Mg^{2+} was added at a final concentration of 2mM , this was critical to achieve optimal activity with Phusion (PFU) DNA polymerase. Finally $1\mu\text{l}$ of PFU DNA polymerase (Thermoscientific) was added, this was in order to prevent any primer degradation caused by the $3' \rightarrow 5'$ exonuclease activity. All reaction components once mixed were set on ice and quickly transferred to the pre-heated thermo-cycler machine.

2.2.7 PCR Reaction

The thermo-cycler was set up as detailed in Fig. 2.4. The denaturing temperature was set at 95°C for 30 seconds, during this phase the double strands of DNA were separated by disruption of the hydrogen bonds between the base pairs. The separated DNA was cooled in the presence of excess primers, which allowed for hybridisation of the primers to the complementary DNA sequence. The annealing temperature was

set at 50°C, this had been determined previously during the primer design by using the online tool Oligonucleotide calculator to determine the T_m of the primers. The extension time was set at 60 seconds at 72°C, in general an extension time of 30seconds per kb of genomic DNA was used. The mixture was then incubated with DNA polymerase and the four deoxyribonucleoside triphosphates which allowed for DNA synthesis to occur from the primer site. The cycle was repeated numerous times to allow for DNA amplification with the newly formed DNA strands acting as templates and thus the yield of DNA sequence increased with time. A sample of the yielded DNA was placed on agarose gel to check for the presence of amplified DNA.

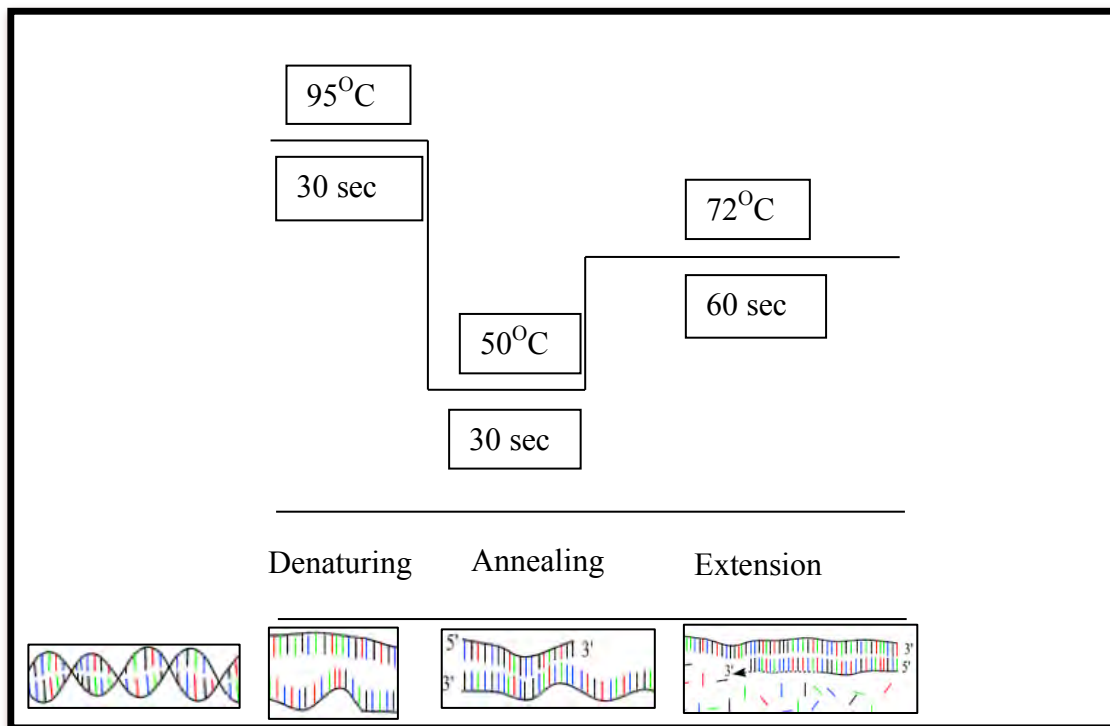


Figure 2.6 Diagram illustrating the temperature changes during a single cycle on the thermocycler during PCR reaction with corresponding DNA replication.

2.2.8 Isolation and analysis of PCR products

This was performed to check if DNA synthesis was achieved successfully for each of the HPV-16 templates. Once completed the PCR products were loaded onto an agarose gel and following electrophoresis visualised under ultra violet (UV) light to assess the purity and to allow a qualitative assessment of yield of the desired band.

2.2.9 Preparing the Agarose gel

This was made at a concentration of 1% (w/v) by adding 0.5g Agarose powder (Melford, Suffolk, UK) to 50ml of 1 x TAE buffer (40mM Tris, 20mM Acetic acid, 1mM EDTA [ThermoScientific]), this was heated to 95°C until the agarose powder was completely dissolved then 5µl of RedSafe™ nucleic acid staining solution (iNTRON Biotechnology, Korea) was added. The solution was then placed in a gel-casting tray with comb and allowed to set for approximately 1 hour.

The set agarose gel was submerged in a bath of 1 X TAE (Thermoscientific) and the comb was removed under buffer to prevent formation of air bubbles within the wells. Gel electrophoresis allows the DNA fragments to be separated by molecular size. As DNA is negatively charged the electrical current flows through the water bath and the DNA fragments traverse towards the positive electrode with the gel acting like a sieve separating the fragments. Fragments of a similar size form a band on the gel that is visible under UV light.

2.2.10 Analysis of PCR products

Each PCR product was made up to 12µl by combining 5µl of PCR product with 2µl of DNA Loading dye (Thermoscientific) to allow for visualisation of the product and with 5µl of dH₂O; the full 12µl was loaded in the well of the agarose gel. Two markers with known molecular weights were also loaded onto the gel, these were Lambda *EcoRI Hind III* (Thermoscientific) (Fig. 2.7) with base range of 21 226 to 564 bp and Midbase Ranger (Geneflow, Staffordshire, UK) (Fig. 2.8) with base range of 5000 bp to 300 bp. The voltage was set to 100v and the electrophoresis was allowed to run until clear separation of the control markers was seen, the gel was then observed under UV light to look for DNA bands at expected base pair levels compared to the control markers.

**Lambda DNA/EcoRI+HindIII Marker, 3,
ready-to-use**

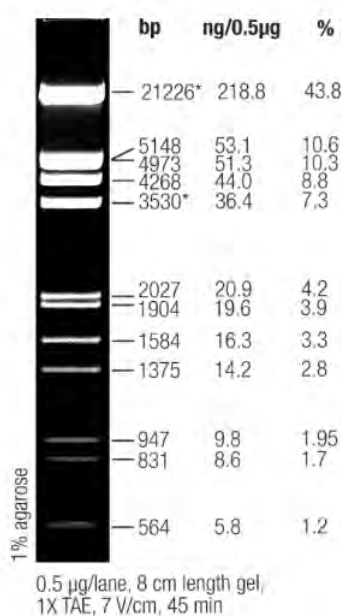


Figure 2.7 Lambda DNA/EcoRI Hind III Marker (Thermoscientific), range 21226 base pairs to 564 base pairs

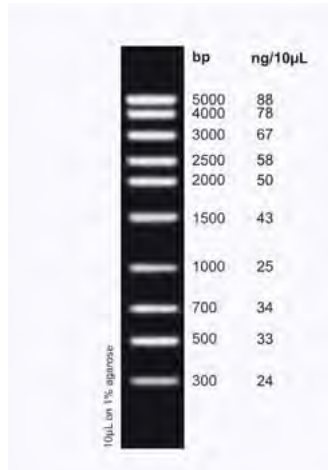


Figure 2.8 Midbase 1kb DNA ladder (Geneflow, Staffordshire, UK), range from 5000 base pairs to 300 base pairs.

2.2.11 Purification of PCR Products

Once bands of the correct size for DNA fragments were identified these were purified using the remaining PCR product by running this on an ultrapure agarose gel, this was so that impurities were reduced during harvest of the product. The ultrapure agarose gel was made by adding 0.6g Top vision Ultra pure gel (Thermoscientific) to 50ml of 1 x TAE buffer (Thermoscientific) to achieve a concentration of 1.2% (w/v), this was heated until all granules were melted. The gel was then cast as described in section 2.2.9.

The remaining PCR products were each mixed with 5µl of glycerol (Melford), this was to increase the mass of the PCR product to allow for easier insertion into the wells of the agarose gel. The total volume of PCR product was inserted into the gel for maximal recovery of PCR products. The gel was run at 100 volts in TAE buffer bath and the reaction was stopped once the bands on the marker were clearly

separated. The gel was visualized under UV light for the minimum amount of time so damage to the DNA was minimised, bands corresponding to the correct size were cut out and purified using the GeneJET Extraction kit (Thermoscientific) using a standard protocol.

2.2.12 Purification of DNA Fragments

The GeneJET Gel Extraction Kit (Thermo Scientific) was used for purification of DNA fragments, the kit is designed for rapid and efficient purification of DNA fragments from standard or low-melting point agarose gels run in TAE buffer.

The kit utilizes a proprietary silica-based membrane technology in the form of a convenient spin column and can be used to purify DNA fragments from 25 bp to 20 kb in size with recovery rates up to 95% (technologies, 2012) Each purification column has a binding capacity of up to 25 µg of DNA and can process up to 1 g of agarose gel. The isolated DNA is then ready for use in downstream applications such as restriction digest and ligation.

The weight of the gel containing the DNA fragments was determined using a 2 place balance (Ohaus, Switzerland). A 1:1 ratio of weight to volume of binding buffer was used for each gel containing DNA fragment. This was placed in a water bath at 50°C for 10 minutes, or until all the gel had dissolved. A 1:2 volume of 100% isopropanol was added to the solubilised gel, this was for optimization of DNA harvest as the DNA fragments were less than 500bp.

The solubilised gel solution was transferred to the GeneJET purification column 800µl at a time and centrifuged at 14,462 x g for 60 seconds between each volume

transfer. The flow through was discarded and the column placed back into the same collection tube. Once the total volume of solubilised gel solution had been applied to the column, a 100µl of Binding Buffer was added to the GeneJET purification column. Again this was placed back into the centrifuge at 14,462 x g for 60 seconds. The flow through was discarded and the column was placed back into the same collection tube. This step was repeated with 700µl of Wash Buffer. The empty GeneJET column was finally centrifuged for a further 60 seconds at 14,462 x g to remove any residual wash buffer. The column was then transferred into a fresh 1.5ml polypropylene tube. Elution Buffer (50µl) was placed onto the purification column and centrifuged for 60 seconds at 14,462 x g. The column was thus discarded and the flow through, i.e. purified DNA fragments were stored at -20°C, until analysis and further use.

2.3 *Escherichia Coli* Competent Cell Production

Competent *Escherichia coli* (*E-coli*) cells were produced using a standard protocol. Briefly fresh colonies of *E coli* competent cells (XL1-Blue strain) were plated out on LB agar plates in an aseptic manner and placed in the incubator set at 37°C for overnight growth. After overnight growth (c.16 hours) individual colonies were picked and placed in 5ml of LB broth (Melford LB Broth, pH 7.2) in 25ml polypropylene tubes in an aseptic manner. These were then left overnight in the shaking incubator set at 37°C, 220 RPM.

A 100ml of fresh LB broth was placed in a sterilized 500ml conical flask. This was inoculated with 0.5ml of the overnight culture of *E-coli*, this was to reduce the final concentration of stationary or dead cells to about 1:80 or 1:100 of the inoculum. The

conical flask was then placed into the shaking incubator for a further 3 hours, this was monitored regularly to ensure growth did not exceed $OD_{600nm} \sim 0.2$. This meant that cell are principally in the early exponential growth phase which produces the highest quality competent cells.

Once the optical density was achieved the flask was removed from the shaking incubator and placed on ice for 20 minutes to allow the culture to cool. Once cooled the 100ml culture was split equally between two pre-cooled 50ml Falcon tubes. The cultures were then centrifuged at $3000 \times g$ for 10 minutes to pellet the cells. The supernatant was decanted carefully not disrupting the pelleted cells. These were then gently suspended in 5ml of ice cold 0.1M $MgCl_2$, and left to incubate on ice for 5 minutes. The cells were then centrifuged once again at $3000 \times g$ for 5 minutes. The supernatant was decanted carefully and cells re-suspended gently in ice cold 0.1 M $CaCl_2$. Again the cells were left to incubate on ice for 5 minutes. These were then centrifuged again at $3000 \times g$ for 5 minutes and the supernatant decanted. The cells were finally re-suspended in 1ml of ice cold 0.1 M $CaCl_2$. Once re-suspended the cells were left on ice for 1.5 hours before being fully competent for use. The cell solution was then supplemented with 15% (v/v) glycerol to allow storage at $-80^\circ C$ to minimise crystallisation damage to cells, the cell solution was aliquoted in 1ml polypropylene tubes.

2.4 Expression in Bacteria and Purification of Recombinant plasmids

2.4.1 Restriction Enzyme digest of Plasmid Vectors and DNA Fragments

Restriction enzyme digests were performed on plasmid vectors and on inserts i.e. harvested DNA fragments to allow for ligation of cut plasmids at specific restriction sites and of cleaved DNA fragments. The pET28a vector was cut at restriction sites *Nco I* and *Xho I*. DNA fragments were also cleaved with the same restriction enzymes to allow for incorporation into the cut plasmids. Digests were performed by combining the plasmid vector with Tango 2x buffer (Fermentas), restriction enzymes *Nco I* and *Xho I* (Fermentas) and the solution was made up to a fixed volume with dH₂O. The same recipe was also used to double cut inserts at specific cleavage points. The reactions were placed in a water bath at 37°C for 90 minutes. The restriction digest products were then run on an agarose gel as described in section 2.2.11 to allow for isolation and purification of double cut plasmids and inserts. For each reaction the plasmid was cut with a single enzyme as control and the uncut plasmid was also analysed on the agarose gel to determine the identity of cut plasmids and as a control. Double cut plasmids and inserts were extracted and purified by the GeneJET Gel Extraction Kit (Thermoscientific) as described in section 2.2.12. The reasoning behind re-purification of cut plasmids was to allow for the greatest yield and purification of double cut plasmid and DNA fragments only.

2.4.2 Ligation Reactions

Recombinant plasmids were formed by ligation reactions of double cut plasmid and inserts. This allowed for replication of target viral DNA when the recombinant

plasmid was transformed into a bacterial vector (see section 2.4.3). Ligation reactions were performed using T4 DNA ligase (Fermentas). All reaction components were set on ice to prevent degradation of products and the T4 DNA ligase was added last to prevent premature catalyst of reactions. The vector to insert was added at a ratio of 1:3 and the NEBcalculator (an online tool) was used to calculate the molar mass and ratios of reaction components, 2 μ l of 10 x T4 DNA Ligase Buffer (Fermentas) was added, the solution was made up to 20 μ l by adding dH₂O, finally 1 μ l of T4 DNA ligase was added last and the reaction components were mixed by gently pipetting up and down. The solution was left at room temperature for 60minutes.

2.4.3 Transformation of Recombinant Plasmid in E-Coli

The recombinant plasmid was transformed into a bacterial host cell; *XL1-Blue E-coli*. These cells were used as the bacteria have a high yield and furthermore transformation rates are higher as compared with other bacterial cells. The XL1-Blue *E coli* cells were produced as described in section 2.3. The cells were removed from -80°C freezer and thawed on ice, a ratio of 1:10 of ligation reaction and *XL1-Blue E-coli* cells were used, therefore 10 μ l of ligation reaction was mixed with 100 μ l of *XL1-Blue E-coli* cells, this was placed back on ice for 30 minutes. The cells were removed from ice and heat shocked by placing in a water bath at 42°C for 75 seconds and then back onto ice for a further two minutes, this allowed for incorporation of the recombinant plasmids into the bacterial cells. To allow for optimisation of growth of transformed cells, 250 μ l of Luria Bertania (LB) broth was aliquoted to each of the polypropylene tubes containing transformed E-coli cells, these were then placed in a shaking incubator at 37°C, 220 RPM for 30 minutes. These were then plated out on the agar plates containing appropriate antibiotic and left to incubate overnight at 37°C

(Binder Incubator). Antibiotics were added to agar plates (see section 2.4.4) as plasmids contain an antibiotic resistant cassette, these vary depending on the plasmid; the pET-28a vector contains a Kanamycin resistant cassette and the pGEX-6p1 contains Ampicillin resistant cassette, thus bacterial cells containing plasmid survive and those without plasmid are killed off by the antibiotic.

2.4.4 Pouring Agar Plates

Agar plates containing appropriate antibiotic [kanamycin (Agar_{Km}) or ampicillin (Agar_{Ap})] were made at a concentration of 2% (w/v) by adding 3g of Agar (Melford) to 200ml of LB broth. The LB broth was made by adding 5g of High Salt LB (10g NaCl, 10g Tryptone, 5g Yeast Extract; Melford) to 200ml of dH₂O and vortexed (Rodwell Scientific Instruments Ltd). The pH was adjusted to 7.2 using hydrochloric acid or sodium hydroxide base as appropriate. Once the LB was fully dissolved it was decanted into a 1000ml Duran bottle and the agar added. The vessels were autoclaved at 120°C for 1 hour 45 minutes for sterilisation. Once cooled to less than 45°C, Kanamycin (Melford) was added at a concentration of 20µg/ml, and Ampicillin (Melford) at concentration of 50µg/ml. The solution was poured into petri dishes, approximately 20ml/plate and allowed to set.

2.4.5 Isolation of Recombinant Plasmid by Mini-preparation

Recombinant plasmids were isolated from bacterial culture to assess for plasmid growth and viability by plasmid Miniprep using the GeneJET Plasmid Miniprep Kit (Thermoscientific) with standard procedure.

A single colony picked from overnight growth on agar plates of transformed bacterial cells, was used to inoculate 5ml of LB broth in a 30ml polypropylene tube in an aseptic manner, appropriate antibiotic depending on plasmid was added. This was placed in a shaking incubator (Innova 44, New Brunswick Scientific, Connecticut, USA) at 37°C, 220 RPM for 16 hours. The bacterial cultures were harvested by centrifugation at 6800 x g in a micro-centrifuge in 1ml aliquots. The supernatant was decanted and the remaining medium was removed by gently tapping on blotting tissue. Care was taken not to disrupt the pellet.

Pelleted cells were re-suspended in 250µl of Resuspension solution (GeneJET Plasmid Miniprep Kit) and gently vortexed until no clumps remained. A further 250µl of the Lysis Solution provided was added to each polypropylene tube and mixed by inversion until the solution became viscous and clear. Vortexing was not used as this can shear the chromosomal DNA. After this 350µl of the Neutralisation Solution was added and mixed by inversion.

The solution was centrifuged for 5 minutes at 14,462 x g to pellet cell debris and chromosomal DNA. The supernatant was decanted into a GeneJet spin column (ThermoScientific) avoiding disruption of the precipitate. This was centrifuged for 60 seconds at 14,462 x g. The flow through was discarded and 500µl of Wash Solution was added and again centrifuged as before. This step was repeated twice to remove residual cell debris. A further centrifugation of the column was performed to remove wash solution residue. The GeneJET spin column was transferred to a fresh 1.5ml micro centrifuge tube and 50µl of the Elution Buffer was added to elute the plasmid DNA. The spin column was left to incubate for 2minutes and then centrifuged for a

further 2 minutes at 14,462 x g. The spin column was discarded and the flow-through containing the purified plasmid DNA was stored at -20°C until further use.

The purified recombinant plasmids were restriction digested as described in section 2.4.1, these were then run on an agarose gel (as described in section 2.2.11) to assess the presence of DNA fragments and to assess if the transformation had worked.

2.5 Expression of Recombinant HPV-16 Proteins

2.5.1 E.coli Host Strains

The BL21(DE3) and BL21(DE3)pLysS strains were used, both these strains contain a cloned T7 RNA polymerase gene which resides on the bacterial chromosome as a lamda lysogen and is inducible by IPTG. The pLysS strain in addition expresses T7 lysozyme, an inhibitor of T7 RNA polymerase, this has the effect of reducing basal level expression of genes which is useful when levels of heterogous toxic genes are to be reduced.

2.5.2 Induction and Optimisation of Expression

Recombinant pET15b, pET28a and pGEX6p1 plasmids were transformed into host strains (as described in section 2.4.3) and selected by the addition of variable antibiotics; these were Ampicillin at concentration of 50µg/ml for pET15b and pGEX6p1, and Kanamycin 20µg/ml for pET28a. In the case of pLysS, Chloramphenicol was also added at a concentration of 34µg/ml.

Transformed plasmids were grown on a LB agar plate supplemented with appropriate antibiotics for 16 hours at 37°C (Binder Incubator). Individual colonies were selected from the agar plates after overnight growth and used to inoculate 5ml of LB broth (Appendix 2, Melford) supplemented with required antibiotics. The cells were allowed to grow overnight at 37°C at 220 RPM in a shaking incubator (Innova®44, New Brunswick Scientific).

Sterile LB medium (500ml) was inserted in to a 2L Flask; this was supplemented with required antibiotics and inoculated with 0.01 volume of overnight culture. This was allowed to grow at specified temperatures ranging from 16-37°C, 220 RPM in the shaking incubator (Innova® 44) until required optical density OD₆₀₀ 0.6-1.0 was reached. Once optimum optical density was reached the culture was induced with 500µl of 1M IPTG (Melford) for a final concentration of 1mM and allowed to grow for 4-6 hours. A constant culture to total flask volume of 0.2 was maintained throughout.

After induction cells were harvested by centrifugation at 6,130 x g at 4°C (Sorvall® Refrigerated Superspeed Centrifuge) for 10 minutes. The supernatant was decanted and the pellet containing cells re-suspended in 10ml of Talon Buffer, 10mM Tris, 300mM NaCl, pH 8.0 (Appendix 2) and stored at -20°C.

In all cases the aim of optimisation was to increase the yield of soluble recombinant protein. Variable parameters included strain of *E coli*, plasmid, induction time and temperature were assessed.

2.5.3 Cell Lysis and Protein Extraction

The frozen down cell pellets were defrosted at room temperature and then kept on ice to prevent denaturation of proteins by proteases present within the cells. Sonification was used at 50 cycles pulsing for 2 minutes (Soniprobe, DAWE Instruments LTD, London, UK) to break down cell membranes to release proteins. The sonicated cell medium was centrifuged at 20,000 x g at 4°C for 45 minutes. After this time two clear phases could be seen; a top soluble protein phase and lower insoluble protein phase. Soluble and insoluble phases were analysed by SDS-PAGE (section 2.9). The soluble phase was carefully transferred to a clean 25ml polypropylene tube and stored at -20°C. The insoluble phase was resuspended gently in 10ml Talon buffer (Appendix 2) and stored at -20°C.

2.6 Protein Purification By Immobilised Metal Affinity Chromatography (IMAC)

Proteins were purified using Immobilised metal affinity chromatography (IMAC). This involves using an integrated column with metal containing resin that has affinity for certain protein tags, in this case the Nickel Resin (Qiagen) was used which has high affinity for His-Tag. Briefly, the column was washed through with four 10ml volumes of Talon buffer (Appendix 2) to remove industrial manufacturing residue. The column was then prepared using 5ml of resin slurry, which approximately equates to 2.5ml of resin once set. This was then set by four 10ml Talon Buffer washes. The soluble protein phase suspended in Talon buffer was washed through the column, a clean 25ml polypropylene tube was placed at the bottom of the column to collect subsequent elutes. These were the initial flow through, 10ml of talon buffer,

10ml Talon buffer with increasing imidazole concentrations, namely 10, 100 and 200mM. The purification is based on the His-tag proteins. These have a high affinity for Nickel present in the resin, and when washed through these bind to the nickel. Imidazole displaces His-Tag from Nickel and hence is used to elute purified protein. An SDS-PAGE (section 2.9) was run to identify optimum concentration of imidazole at which the proteins were displaced (Mateo et al., 2001, de Costa et al., 2016).

2.7 Protein Purification by Ammonium Sulphate Precipitation

This method is used to purify proteins by altering their solubility, a technique based on salting out. Based on the principle that proteins are less soluble at high salt concentrations. The concentration of salt needed for a protein to precipitate out of solution varies from protein to protein. Proteins are soluble in aqueous solution as they have hydrophilic amino acid side chains facing outwards that can interact with water and form hydrogen bonds. If enough of the surface of the protein is hydrophilic then it can be dissolved in water. Any compound that interferes with the interaction between the amino acid side chain and water affects the solubility of the protein. As the interactions between water becomes less marked the protein-protein interactions increase and hence the protein will aggregate and come out of solution. Provided that the temperature is maintained low (i.e. below 4^oC) the protein is not denatured and can be re-dissolved in buffer (Duong-Ly and Gabelli, 2014). Thus it is possible to remove a mixture of proteins from solution based on their hydrophilicity by gradually increasing the ammonium sulphate concentration.

Ammonium sulphate was used as it is water soluble, has no adverse effects on enzyme activity, and concentrated solutions of it reduce the availability of water

considerably. The Ammonium Sulphate Precipitation Table (Appendix 4) was used to calculate volumes of ammonium sulphate required based on concentration of precipitate and on the volume of cell lysate.

A known volume of cell free extract was placed in a 25ml flask in gentle vortex at 0°C. Ammonium sulphate was measured out and added slowly at known concentrations whilst the solution was stirring. It was important to add in the ammonium sulphate slowly as adding the full volume immediately meant that there would be an initial rise in the concentration with proteins precipitating out at the wrong concentration whilst allowing all of the solute to be dissolved (i.e. false positive). Once the total volume of ammonium sulphate was added the solution was left stirring on ice for a further 20 minutes. After this the solution was decanted into a precooled 15ml falcon tube and centrifuged at 1,900 x *g* between 12-20 minutes at 4°C. The supernatant was decanted back into the glass flask, kept on ice, and the whole process was repeated with increasing concentrations of ammonium sulphate. The pellet was re-suspended in 5ml of Talon buffer (Appendix 2) and stored at 4°C.

2.8 Dialysis

Dialysis was used to remove small molecular weight substances and contaminants such as reducing agents, non-reacted cross-linking or labeling reagents that may interfere with experimental procedure later. The principle of dialysis is based on passive and selective diffusion of small, unwanted molecules from macromolecules in solution (i.e. protein) through a semi permeable membrane. The dialysis membrane is made from regenerated cellulose, this has pores of varying size which allow smaller molecules to pass through freely into the buffer solution (dialysate) which is usually

200-500 times the volume of the sample. This creates a steep osmotic gradient allowing for diffusion. The rate of diffusion is dependent on a number of factors including the concentration of molecule, temperature, molecular weight of the molecule and the surface area of the dialysis membrane. Small molecules can form a microenvironment on the outer layer of the membrane (Nernst diffusion layer), stirring breaks up this microenvironment and hence maintains the concentration differential required for diffusion .

A 3L stock of Tris-Buffered saline (TBS), pH 8.0 (see appendix 2) was made up for the dialysate buffer. Dialysis membrane, 12,000 kDa MW cut off (Visking Tubing, Medicell International Ltd, London, UK) was cut into 30cm strips and placed in distilled water which was boiled for 3 minutes. The aim of this was to soften the membrane that is made of cellulose for ease of handling and use. A double knot was secured at one end of the membrane, the protein sample was slowly loaded into the membrane and secured with a double knot at the other end. The membrane was placed in 3L TBS Buffer on slow stirring at 4°C, this was to prevent heat denaturation of protein. The first phase of dialysis was continued for 16 hours and second phase of dialysis in fresh TBS buffer for 48-72hours.

2.9 Preparation of Sodium Dodecyl Sulfate (SDS)-polyacrylamide gel electrophoresis

The sodium dodecyl sulfate (SDS) polyacrylamide gel electrophoresis or SDS-PAGE is a method of separating proteins by electrophoresis. This can be used to determine the relative molecular mass and relative abundance of a protein within a sample. It also allows the assessment of the purity of proteins. SDS is an anionic detergent,

when this is combined with proteins it destroys the complex nature of proteins leaving individual polypeptide chains which bind SDS in proportion to their molecular mass. SDS coats protein with a uniform negative charge which masks the intrinsic charges of the R group, SDS binds fairly uniformly to linear proteins, therefore 1.4g of SDS binds to 1g of protein. Thereby the charge of the protein is proportional to the molecular mass, the final separation is therefore based on relative molecular mass of polypeptides. The overall negative charge allows the protein to be attracted to a positive electrode in an electric field underlying the principle of electrophoresis (Brunelle and Green, 2014, Smith, 1994).

Acrylamide is chemically inert, the concentration of acrylamide in SDS gels determines the range of polypeptides which can be separated. A gel of 7% (w/v) acrylamide separates polypeptides with molecular masses between 45 and 500 kDa. A denser gel such as the 12% (w/v) used here separates smaller polypeptides between 10-200kDa. A stacking gel is initially used to level the proteins at the same starting point, this is determined by the variable pH of the Laemmli buffer system, which is a discontinuous buffer system. Glycine can exist in different states, namely positive, neutral and negative. When the electric charge is switched on (see Fig 2.9) this forces the negatively charged glycine into the lower pH 6.8 stacking gel, this forces the charge state of glycine to change to neutral. The negatively charged chloride from Tris-HCL migrate quicker in the electric field ahead of glycine, separation of chloride from Tris creates a steep voltage gradient which drags the glycine behind it. This creates two migrating ion fronts. As all proteins have an electrophoretic charge in between the two extremes of charges proteins are concentrated into a narrow band. Once this band reaches the running gel of higher pH 8.8, the glycine now becomes

negatively charged and marches ahead leaving behind the protein, which is slowed down by the higher concentration of acrylamide gel, therefore bands of protein are separated.

The gel was cast by using two 1.5mm glass plates separated by a thin peripheral Teflon layer, these were sandwiched onto a casting block with the shorter plate innermost. The casting block was placed on a casting stand consisting of a rubber seal inferiorly ensuring a water-tight chamber was formed. A fill level was marked 0.5cm below the lower level of the well forming comb, it was to this level the separating gel was filled. The 12% (w/v) separating gel was mixed first by combining 6.0 ml 30% Acrylamide/0.8% bisacrylamide (Geneflow Ltd, Staffordshire, UK), 3.75ml 4x Tris-HCL/SDS pH 8.8 (see appendix x), 4.5g urea (Duchefa Biochemie, Haarlem, The Netherlands), 3.0ml dH₂O, 50µl 10% w/v ammonium persulfate (APS) (National Diagnostics, Hesse, UK) and 10µl TEMED (National Diagnostics). This was enough to prepare 4 gels. The solution was gently mixed by inversion and then quickly pipetted between the glass plates avoiding introduction of air bubbles, haste was required to avoid polymerization prior to loading the gel. The gel was leveled out by gently filling with dH₂O; the aim of this was to ensure proteins were run from the same starting point. The separating gel was allowed to polymerise prior to mixing of the stacking gel this took approximately 30 minutes (Smith, 1994).

The stacking gel was prepared by mixing 0.65ml 30% Acrylamide/0.8% bisacrylamide (Geneflow), 1.25ml 4x Tris-HCL/SDS pH 6.8 (Appendix 2), 1.5g urea (Duchefa Biochemie), 2.20ml dH₂O, 25µl 10% APS (National Diagnostics) and 5µl TEMED (National Diagnostics). The dH₂O was decanted carefully from the glass

plates and the stacking gel was gently pipetted between the glass plate 'sandwich', the comb was inserted and gel allowed to polymerise.

2.9.1 Sample preparation for SDS gels

Prior to analysis protein samples need to be unraveled/denatured to the primary structure, this was performed by preparing samples using 10 μ l 2x Urea/SDS Loading Buffer (Appendix 2) per 3 μ l protein sample. Once combined in a 1.5ml polypropylene tube the sample was made up to 20 μ l with dH₂O. This was placed in a heat box at 95^oC for 3 minutes. The loading buffer is a dissociating buffer that helps to break up hydrogen bonds between polypeptide chains at high temperatures allowing the polypeptide chains to unravel.

2.9.2 Running SDS-PAGE

The casting stand was removed from the casting block. The casting block containing the SDS gel between glass plates was placed in the electrophoresis tank and plates submerged in 1x SDS Running Buffer (Appendix 2), the comb was removed under buffer to avoid introduction of air bubbles within the wells. An unstained protein MW marker (Thermo Scientific) was loaded into the first well with subsequent wells containing 20 μ l of protein sample.

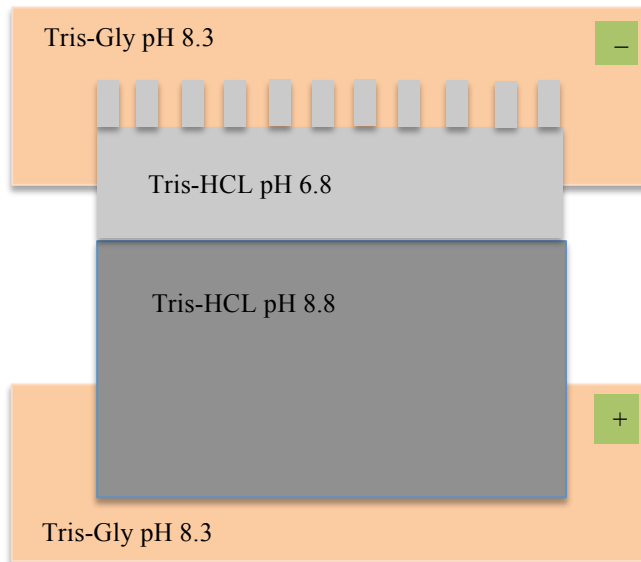


Figure 2.9 SDS-PAGE system set up. Figure illustrates the set up of an SDS-PAGE gel with the variable pH in the stacking gel (pH 6.8) and running gel (pH 8.8), also illustrated is the running buffer at pH 8.3.

The cathode electrode was connected to the bottom chamber and anode to the top chamber, with the electric current flowing in the direction of anode and dragging along the negatively charged proteins. The gels were run at 35mA per gel, this was to allow the protein samples and protein marker to migrate to the bottom of the gel without over heating the gels. Over heating can result in distortion of the gel, once the protein marker had reached the bottom of the gel, the gel was carefully removed from the tank and glass plates were carefully removed isolating the SDS gel which was then submerged in *Instant Blue* Coomassie blue protein (Expedeon, Cambridge, UK) stain to highlight separated proteins, this was left to develop for at least 24 hours prior to analysis, although the manufacturers guidelines advise leaving for minimum of 1 hour, best results were achieved after allowing colour development overnight.

2.10 Western Blotting

The aim of Western Blotting or immunoblotting is to allow the transfer of proteins from polyacrylamide gels which do not allow immuno-analysis of proteins onto a membrane which allows for the analysis and identification of proteins. There are two main phases to Western Blotting; the first involves the mobilisation of protein from the polyacrylamide gel onto a synthetic membrane support. After separation of proteins with SDS-polyacrylamide gel electrophoresis (PAGE), the proteins are transferred further by electrophoresis onto the supporting synthetic PVDF membrane (blotting phase).

The second phase allows for the detection of proteins on the synthetic membrane by probing with a protein specific antibody and subsequent visualisation with labelled proteins. This allows for probing and identification of proteins which otherwise would be inaccessible on polyacrylamide gels.

Phase 1

An SDS-PAGE gel was prepared as described in section 2.9; a 4% stacking and 12% separating gel was used respectively. Protein samples were prepared by placing varying concentrations of protein sample (neat, 1:2, 1:4 and 1:8) in sample loading buffer (Tris base, glycerol, SDS, Mercaptoethanol, Bromophenol blue, HCL acid, pH 6.8) and the protein was unraveled/denatured by placing in a heat box at 80°C for two minutes. A 10µl aliquot of sample was loaded into each well; a known molecular weight marker was also loaded onto the gel as a control point (PageRuler™Plus,

ThermoScientific). The gel was run at 45 mA in a water bath containing 1x glycine running buffer (Tris base, glycine and SDS).

Once the dye front had run to within 2 cm of the bottom of the plate the electrophoresis was stopped and gel removed from the water bath. The glass slides encasing the gel were carefully removed and the stacking gel was cut away from the separating gel containing the protein sample. This was then carefully transferred onto Polyvinylidene fluoride (PVDF) transfer membrane. The membrane is encased within two filter papers which in turn are placed between an electrode sandwich (see Fig.2.10). In electrophoretic transfer an electric field is used to transfer proteins from gels to membranes as the proteins are negatively charged this allows for the transfer of the proteins from the SDS-PAGE onto the PVDF membrane, the membrane sandwich is placed within a blotting machine (BioRAD Transblot Turbo Transfer System). The electrode on the blotting machine is run at a set protocol of 25 Volts for 30 minutes.

Phase 2

After completion of the electrode blotter the membrane was carefully removed from the sandwich and placed within a sterile tray. The membrane was submerged in 1% (w/v) bovine serum albumin (BSA), sterile and filtered, this was the blocking agent. This was left to incubate for 24hours at 4°C. After 24 hours the blocking agent-BSA was discarded and the membrane was then submerged with the primary antibody at a dilution of 1:200 in sterile 1% BSA. This was placed on an agitator (Stuart Scientific Mini Orbital Shaker SO5, United Kingdom) at 50 RPM and left to incubate for one hour at room temperature.

After incubation with the primary antibody the membrane containing proteins was washed three times; each wash consisted of a rinse with tris buffered saline with 0.1% TWEEN (TBS-T), and then being submerged in TBS-T for 10 minutes placed on the agitator at 50 RPM. After completion of three washes the secondary detection antibody (Mouse monoclonal HRP) was diluted at a concentration of 1:2000 in 1% BSA, a 10ml stock solution of this was used to submerge the PVDF membrane and again placed on the agitator as described above. After incubation for 1 hour the membrane was washed three times as described above.

Once the second round of washes were completed the membrane was removed from the sterile tray and placed onto a clear Perspex film, this was then coated with 1ml of chemiluminescent detector (SuperSignal West Pico, Thermo Scientific), and was allowed to develop for 5 minutes in the dark. Chemiluminescent substrate is an enhanced chemiluminescent (ECL) horseradish peroxidase (HRP) substrate for low-picogram-level detection by Western blot analysis. The secondary antibody is conjugated with HRP, chemiluminescence is a chemical reaction whereby the HRP acts as a catalyst for the chemical reaction and produces light as a by-product. The signal is captured on an X-ray film, development times vary between 5 sec to 5 minutes depending on the strength of signal (Kurien and Scofield, 2015, Gorr and Vogel, 2015).

The membrane was analysed by manual detection with an x-ray film. The procedure was carried out in a dark room to avoid contamination of the film. In brief, the procedure involves placing the membrane within a developer cassette, a clear x-ray film is then placed over the membrane and allowed to develop for varying lengths of

time (i.e. 1 min, 2 min, 5 min and 30min). The film is then washed in three stages; a developer stage, in acetic acid and finally in a fixating agent. After manual development the film was analysed by comparing highlighted bands against the known protein marker (Page Ruler™ Plus, Thermo Scientific).

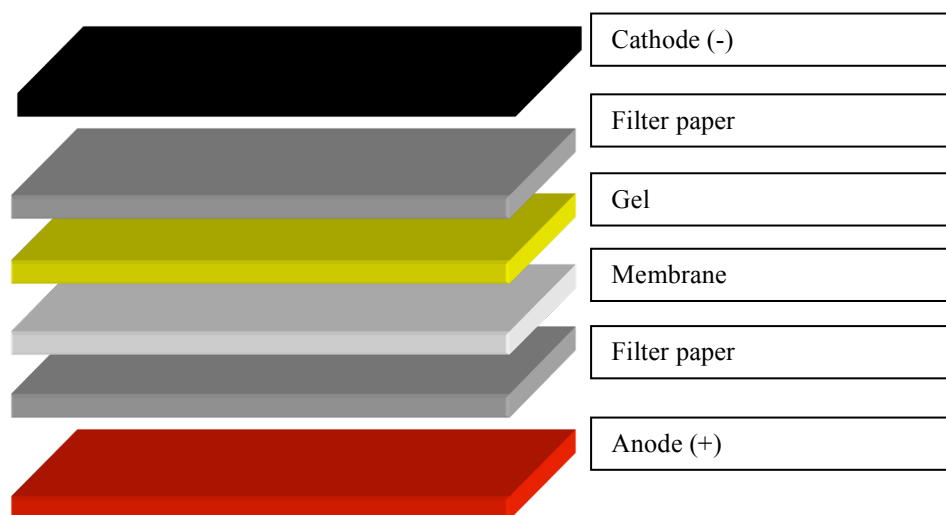


Figure 2.10 Set up of Western Blotting membrane between electrodes.

2.11 P16 Immunohistochemistry

2.11.1 Staining procedure for the Manual use of CINtec® Histology Kit

The CINtec® Histology Kit is a commercially available immunohistochemistry assay for the qualitative detection of p16^{INK4A} antigen in cervical biopsies that have been formalin fixed and paraffin embedded. Given the common aetiology and pathogenesis for HPV-positive cervical and HPV-positive HNSCC, the CINtec® Histology Kit was adapted to be used for the detection of p16INK4A/p16 in formalin

fixed paraffin embedded HNSCC samples in vitro. A manual staining procedure was used. The following steps were performed:

- Deparaffinisation and Rehydration
- Staining protocol
 - Epitope Retrieval
 - Peroxidase-Blocking Reagent
 - Primary Antibody
 - Visualisation Agent
 - Substrate-Chromagen Solution (DAB)
- Counterstaining with Hematoxylin
- Mounting

2.11.2 Deparaffinisation and Rehydration

Formalin fixed paraffin embedded slides (FFPE) were placed in a drying oven at 60°C for 20 minutes to remove excess water, melt the paraffin embedding material and to allow improved adherence of tissue to the slide. Deparaffinisation was then performed to remove remaining paraffin and embedding material. This was done by incubating slides at ambient temperatures (20-25°C) in serial baths of HistoClear for 2 minutes each, this step was repeated twice. The slides were then immersed in a fresh water bath containing dH₂O for 2 minutes. Once the paraffin and embedding material was removed the samples were rehydrated to allow for staining by immunohistochemistry. This was performed by immersing slides in reducing concentrations of ethanol, namely 100%, 90% and 70% for 2 minutes each. Finally the slides were immersed in a fresh bath of dH₂O for two minutes.

2.11.3 Staining protocol

2.11.3.1 Epitope Retrieval

Epitope retrieval solution (100mmol/L Tris buffer pH 9, 10mmol/L EDTA and 15mmol/L sodium azide) had been provided in the CINTec[®] Histology Kit at a concentration of 10x. This was diluted at a ratio of 1:10 with deionised water.

Plastic coplin jars containing the Epitope Retrieval solution (ERS) were immersed in a water bath set at 95-99^oC.

Once the ERS had reached the optimum temperature of 95-99^oC the deparaffinised slides were immersed into the solution, ensuring that each slide was completely covered by the ERS. The addition of the slides to the ERS reduced the temperature of the solution, therefore it was allowed for the ERS to warm to 95-99^oC before the timer was set for 10 minutes. After this period the slides still within the Coplin jars were removed from the water bath and allowed to cool in the epitope retrieval solution for 20 minutes at room temperature. The ERS was then decanted and the slides placed in wash buffer for 5 minutes (not provided in the kit, ROCHE, UK, Catalog No. 8550). The wash buffer was diluted at ratio of 1:10 with deionised water.

2.11.3.2 Peroxidase-Blocking Reagent

Slides were placed in plastic vertical slide holders and covered with 200 μ l of Peroxidase-Blocking Reagent (provided in the CINTec[®] Histology Kit, 3% hydrogen peroxide and 15mmol/L sodium azide). This was left to incubate for 5 minutes. After this period the slides were placed in a fresh wash buffer bath for 5 minutes.

2.11.3.3 Primary Antibody

Excess wash buffer was removed from the slides and each slide covered with 200 µl of primary antibody – Mouse Anti-Human p16^{INK4a} (provided in the CINtec[®] Histology Kit, Monoclonal mouse anti-Human p16^{INK4a} antibody, clone E6H4[®]). The slides were left to incubate for 30 minutes, after this period a further wash cycle was performed as described earlier.

2.11.3.4 Visualisation Agent

Excess wash buffer was then removed from the slides and the specimens covered with 200 µl of Visualisation Reagent (provided in the CINtec[®] Histology Kit, polymer reagent conjugated with horseradish peroxidase and affinity purified goat anti-Mouse Fab' antibody fragments), the slides were left to incubate for 30 minutes. After this period the slides were then re-immersed in a fresh wash buffer bath for 5 minutes; this step was repeated twice.

2.11.3.5 Substrate-Chromogen Solution (DAB)

Substrate-Chromogen solution (DAB) was prepared by adding 25µl of DAB Chromogen (provided in the CINtec[®] Histology Kit, 3,3'-diaminobenzidine chromogen solution) to 2mL of DAB Buffered Substrate (provided in the CINtec[®] Histology Kit, pH 7.5, containing <0.1% hydrogen peroxide). Slides were covered with 100 µl of DAB and left to incubate for 10 minutes, the slides were then gently rinsed with deionised water.

2.11.3.6 Counterstaining with Hematoxylin

Counterstaining was performed by immersing slides in a bath of Hematoxylin and incubating for 2 minutes. After this period slides were washed under a running tap until all excess Hematoxylin was removed. Slides were then rinsed in deionised water.

2.11.3.7 Mounting

A dehydration procedure was then performed prior to mounting slides in non-aqueous permanent mounting medium. Slides were incubated at ambient temperature (20-25°C) in 70% ethanol for 2 minutes, this step was repeated with 90% and 100% ethanol. After this the slides were placed in a HistoClear bath for 2 minutes, this step was repeat twice with a fresh HistoClear bath each time.

Histomount (National Diagnostics, Kingston upon Hull, UK) mounting medium was used to mount the stained IHC slides, these were then analysed manually under magnification of X10 and X40.

2.12 Hematoxylin and Eosin Staining

FFPE slides were stained with Hematoxylin and Eosin (H&E) for identification of tumour area for comparison with p16 staining (see section 4) (Pasyk and Hassett, 1989). FFPE slides were placed in a slide holder and dewaxed by placing in warm histoclear for 10 minutes. This step was repeated twice with fresh histoclear but for 30 seconds each. The slides were rehydrated by placing in 100% ethanol for 10

seconds, this was repeated twice by placing in 90% and 70% ethanol sequentially for 30 seconds each.

The slides were then gently rinsed under running tap water for one minute, care was taken not to place the slides directly in the flow of water to avoid disruption of the mounted tissue. The slides were then placed in Harris Hematoxylin solution for 5 minutes. After this period the slides were washed gently under running tap water until the colour of the water turned blue, this took around 1 minute. After this period slides were dipped in acid alcohol (1% concentrated HCL in 70% ethanol), this step was repeated ten times.

After dipping the slides in acid alcohol slides were gently rinsed under running tap water for 10 seconds. The slides were then immersed in Eosin stain for 2 minutes. Slides were then rinsed under running tap water for 1 minute.

A dehydration process was carried out prior to mounting (as described in section 2.11.3.7), slides were then mounted using Histomount (National Diagnostics) and stored away from direct sunlight to avoid fading.

2.13 Enzyme Linked Immunosorbent Assay (ELISA)

An in-house enzyme linked immunosorbent assay (ELISA) was developed for the detection of HPV-16 oncoproteins, namely E6 and E7. The ELISA was different to traditional, sandwich, ELISA in that the capture antibody was not bound to the Maxisorp plate but rather the antigen, i.e. E6 or E7 were bound to the plate and the antibodies, if present, were detected within the serum sample.

The harvested purified E7 protein (section 3) was diluted to a concentration of 5µg/ml in 0.05M carbonate buffer (pH 9.4) and 100µl was used to coat each well of a 96-well Maxisorp plate (Nunc). Following overnight incubation at 4°C, unbound protein was removed and each well was washed with 300µl of wash buffer (phosphate buffered saline (PBS) with 0.05% Tween 20) using an automated plate washer, residual wash buffer was removed by blotting the plate on a paper towel.

Non-fat dried milk (NFDM; 300µl; Marvel) diluted in PBS was used at differing concentrations to block the plate for 2 hours at 37°C and prevent non-specific binding of antibodies. Blocking buffer was removed and without washing 100µl of diluted human serum samples in 1% NFDM-PBS were added to duplicate wells and incubated at 37°C for 1 hour.

Following further washes 100µl of the secondary detection antibody, goat anti-human-HRP (Santa Cruz) diluted in PBS at a dilution of 1:10,000, was added to each well and incubated for 1 hour at 37°C. After this time a further wash cycle was performed.

Tetramethylbenzidine substrate solution (TMB; 100µl; Vector Laboratories) was added to each well, for 20 minutes at room temperature avoiding direct light, and a blue colour developed which was proportional to the amount of antibody present in the serum. Colour development was stopped by adding 50µl of stop solution (1M Sulphuric Acid), the plate was gently tapped to ensure thorough mixing and the absorbance of each well was measured immediately with wavelength of 450nm.

An average of the duplicate readings was taken and a positive HPV antibody response was determined as that which was two standard deviations above the cut off value (see section 4).

2.14 Ethical approval

National Research Ethics Service (NRES) approval was obtained for the use of archival HNSCC samples for IHC and ISH use – approval code 12/YH/0299. Furthermore samples that had been previously collected at the School of Biological Biomedical & Environmental Sciences (University of Hull), with Ethical approval of 05/Q1105/55, were used for the work on ELISA.

Clinical records were analysed at Castle Hill Hospital, Cottingham under the ethical approval code 12/YH/0299. All notes were anonymised by the use of Arabic numerals for each patient, no patient identifiable data was recorded and all data was kept on a secure server (University of Hull). The project was registered with the local Research and Development Department at Hull and East Yorkshire Hospitals NHS Trust, Research and Development Office, Office 13, Daisy Building, Castle Hill Hospital, and the study was granted NHS permission for research by the trust.

Chapter 3. Molecular Biology-Expression of HPV-16 Oncoproteins

3.1 Introduction

Although some HPV-16 oncoproteins are available commercially these were of variable quality and purity. Therefore it was proposed to isolate genomic HPV-16 DNA from a known HPV positive cell line, namely UMSCC 47 (Brenner et al., 2010) and express HPV-16 oncoproteins in-house.

HPV-16 viral oncoproteins each have a specific role in viral replication and oncogenesis; this is described in detail in section 1.7. For each of the HPV-16 proteins the aim was to optimise expression and purification so as to recover the greatest amount of biologically active, soluble, recombinant protein. Variable parameters included plasmid vector, protein tag, *E-coli* host strain and induction time.

3.2 Optimisation of PCR

PCR was used to amplify specific fragments of isolated genomic DNA as described in section 2.2. These fragments related to the viral oncoproteins, namely E2, E6 and E7. Primers were designed with both HIS-tag and GST-tag for each oncoprotein for purification following expression cloning into pET-28a and pGEX-6P1 respectively.

The PCR components were combined as described in section 2.2. Briefly, each mixture contained the genomic DNA template, forward and reverse primers, dNTP and DNA polymerase. The PCR thermal cycling was set at a 30 cycle repeat with each cycle having denaturation set at 95°C for 30 seconds, annealing at 50°C for 30 seconds and extension for 60 seconds at 72°C.

Preparative PCR products were placed onto an agarose gel (described in detail in section 2.2.10) and ran at 100 volts until clear separation of λ *EcoRI* and Mid Base ranger markers were seen. The DNA sequence for each oncoprotein was known, therefore the number of base pairs could be calculated; For E2 the base pairs were 1095, E6 477 base pairs and for E7 294 base pairs.

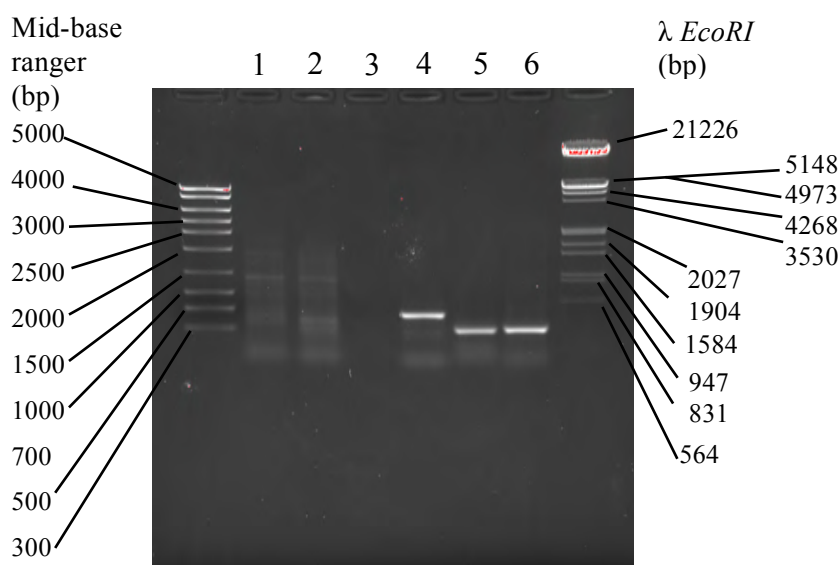


Figure 3.1 Optimisation PCR; The DNA sequence for each oncoprotein was known, therefore the number of base pairs could be calculated; For E2 the base pairs were 1095, E6 477 base pairs and for E7 294 base pairs. Corresponding bands could be seen for E6 HIS tag, and for both the GST and HIS tag E7 oncoprotein sequences. There were no visible bands identified for both the E2 protein sequences, indicating lack of amplification (representative of three repeats, 1% w/v agarose gel).

Lane 1-E2 GST tag
Lane 2-E2 HIS tag
Lane 3-E6 GST tag
Lane 4-E6 HIS tag
Lane 5-E7 GST tag
Lane 6-E7 HIS tag

The PCR was repeated under the same conditions regarding template mixtures however the annealing temperature was lowered from 50°C to 47°C, this was to increase the binding of the primers to genomic DNA. The potential unwanted result of reducing the annealing temperature was non-specific binding of primers, therefore the annealing temperature was kept close to the T_m (50°C). Furthermore the time allowed for annealing was also increased from 30 seconds to 60 seconds. Numerous repeats of the second optimisation were carried out varying the annealing temperature between 50-47°C and varying the annealing time between 30-60 seconds.

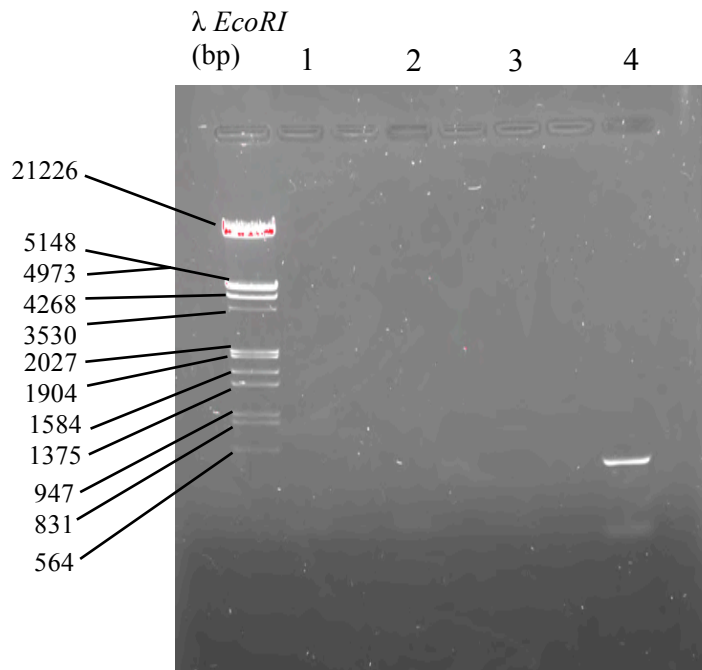


Figure 3.2 PCR optimised by reducing annealing temperature and increasing annealing time. Still no product was seen for either of the E2 fragment or for the E6 GST tag. E6 His Tag was still produced even though the annealing temperature was

reduced. This can be seen by the visible band just below the 564bp λ *EcoRI* marker (representative of three repeats, 1% w/v agarose gel).

Lane 1- E2 GST tag

Lane 2- E2 HIS tag

Lane 3- E6 GST tag

Lane 4- E6 HIS tag.

Unfortunately no PCR products for the E2 GST and His Tag proteins or for the E6 GST tag were observed. Therefore after no success with variable temperature and time, Magnesium (Mg^{2+}) and Dimethyl Sulfoxide (DMSO) were introduced into the PCR mix. DMSO reduces the T_m of DNA making it more labile to heat denaturation. DMSO aids in the denaturation of templates that have a high GC content, this is achieved by binding to the DNA at the cytosine residue, this increases the amplification of GC rich regions, which the primers were mostly composed of. DMSO also indirectly facilitates the annealing of primers to the DNA template. Phusion DNA polymerase is Mg^{2+} dependent, it stabilizes double strands of DNA and prevents complete denaturation of DNA. However excess magnesium can cause stabilisation of spurious annealing of primers to incorrect templates and thus reduce specificity (Tabor and Richardson, 1989, Strauss et al., 1982).

PCR was repeated for each of the E2 GST, E2 His Tag, and the E6 GST tag DNA sequences. A 50 μ l reaction template was set up as described in detail in section 2.2.6, DMSO was added at a concentration of 10% (w/v). A further reaction template was set up for each of the protein sequences with 1mM Mg^{2+} instead of DMSO to identify if either variable improved DNA replication in the PCR (Fig.3.3). The annealing temperature was kept at 47°C and time at 60 seconds, this is as shown in the first optimisation that E6 His Tag was replicated under these conditions (see Fig.3.2).

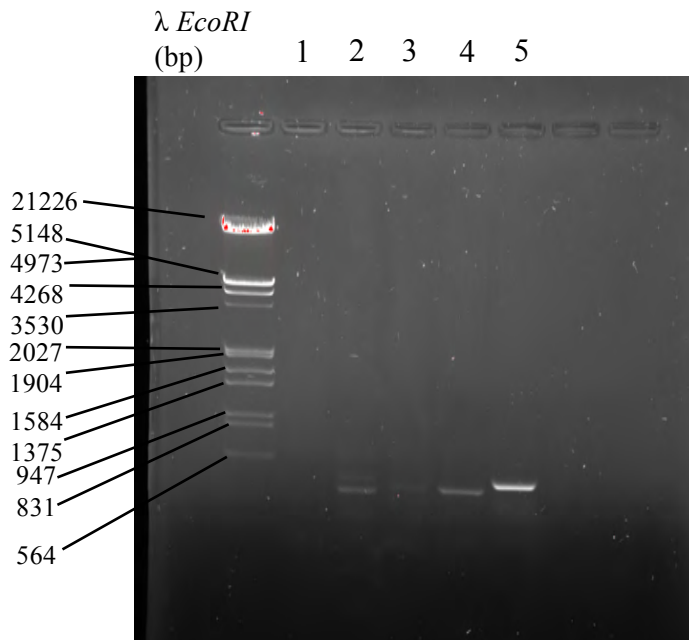


Figure 3.3 Optimisation of PCR by addition of Mg^{2+} and DMSO (1% w/v agarose gel). 1- E2 GST tag DMSO, 2- E2 GST tag Mg^{2+} , 3- E2 His tag DMSO, 4- E2 His tag Mg^{2+} , 5- E6 GST Mg^{2+} . No PCR product for each of the variable E2 parameters was seen, the visible band in each of the columns for E2 was below 564bp, and the E2 product is meant to be 1095bp. The bands may be accounted for by the fragmented E2 or by PCR by-products. For E6 GST tag, viable PCR product was obtained by the addition of Mg^{2+} .

Further attempts to amplify E2 DNA by PCR were undertaken using a different *ReddyMix PCR Mastermix 2X* (Thermoscientific). ReddyMix PCR Mastermix contains thermoprime *taq* DNA polymerase with 10x ReddyMix PCR buffer. This unique buffer has an inert red dye and a density reagent added, therefore after thermal cycling, a sample of the PCR mix can be removed and loaded onto an agarose gel. Furthermore the ReddyMix has enhanced enzyme stability that should give increased yield (ThermoScientific, 2012). A 50 μ l reaction was set up by the addition of 1 μ l of genomic DNA template, 0.5 μ l of each the forward and reverse primers for each of the GST and His tag E2 sequences, 25 μ l of ReddyMix PCR Mastermix 2X (Thermoscientific) and 23 μ l of dH₂O. Thirty PCR cycles were used: denaturation was set at 95°C for 30 seconds, annealing at 47°C for 60 seconds and extension for 60

seconds at 72°C. After this time the PCR products were loaded onto an agarose gel and run at 100volts until clear separation of the marker was seen.

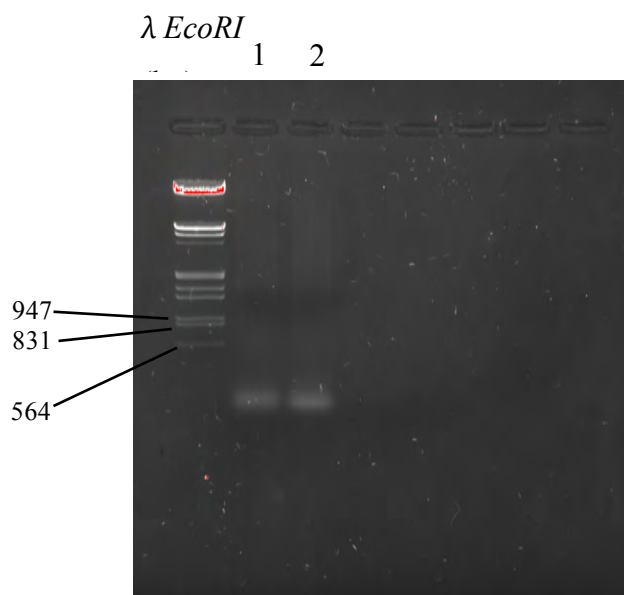


Figure 3.4 Optimisation of E2 PCR by use of ReddyMix PCR Mastermix(Thermoscientific). No viable PCR product was seen, visible bands below 564bp were likely PCR DNA fragments (representative of three repeats, 1% w/v agarose gel).

Lane 1- E2 GST

Lane 2- E2 His Tag

3.2.1 Explanation for lack of E2

Due to time constraints it was decided not to continue working with E2. If further work had been possible, new primers would have been designed as these may have been taking up some form of secondary structure that was preventing annealing and amplification. In addition genomic HPV DNA would have been isolated from other HNSCC cells lines as it may have been that the viral sequence within UMSCC47 had a mutated form of E2.

3.3 Transformation of PCR Products E6 and E7 His tag

PCR products for E6 and E7 His Tag proteins were isolated using the GeneJET Gel Extraction Kit (Thermo Scientific) as described in section 2.2.12. An agarose gel was run on purified products to ensure that viable products were still available. This is illustrated in Figure 3.5, which highlights available products for both E6-His Tag and E7-His Tag.

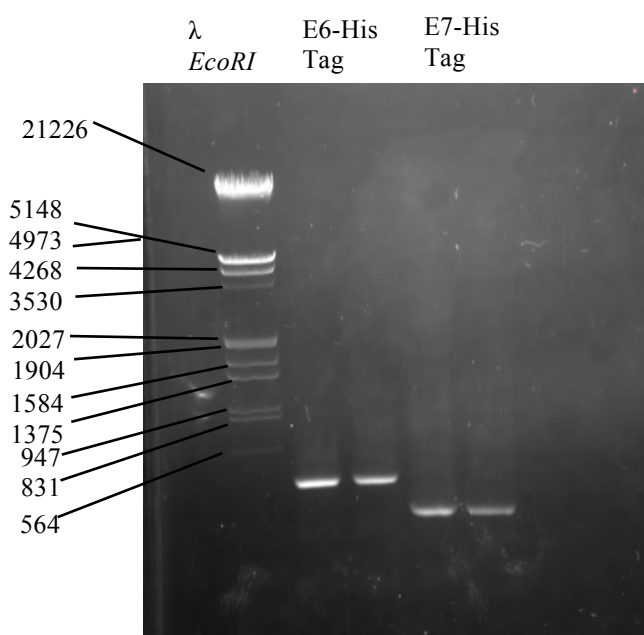


Figure 3.5. Purified PCR products for E6 His Tag and E7 His Tag are shown by the corresponding visible bands in Lane 1-2 for E6 and in Lane 3-4 for E7 in 1.2% w/v agarose gel (representative of two repeats).

Restriction enzyme digests were performed on the pET28a vector and on isolated PCR products for E6-His Tag and E7-His Tag as described in section 2.4.1. The pET 28a vector was double cut with each of the respective restriction enzymes *NcoI* and *XhoI*, 2 μ g of plasmid DNA was combined with 16 μ l of Tango 2x Buffer (Fermentas), 2 μ l of *Nco* and 2 μ l of *Xho* restriction enzymes were added and the solution made up to 80 μ l with dH₂O. For a control separate samples of the plasmid were also single cut

with each of the restriction enzymes, 1µl of pET 28a plasmid was added to 4µl of Tango 2x Buffer (Fermentas), 0.5µl of each of the restriction enzyme, either *NcoI* or *XhoI* were added, this was made up to 20µl by addition of dH₂O. Along each step a 1% agarose gel was run to ensure that products were still available prior to the next step being performed, this ensured if product was lost at any stage this could be identified and the step repeated.

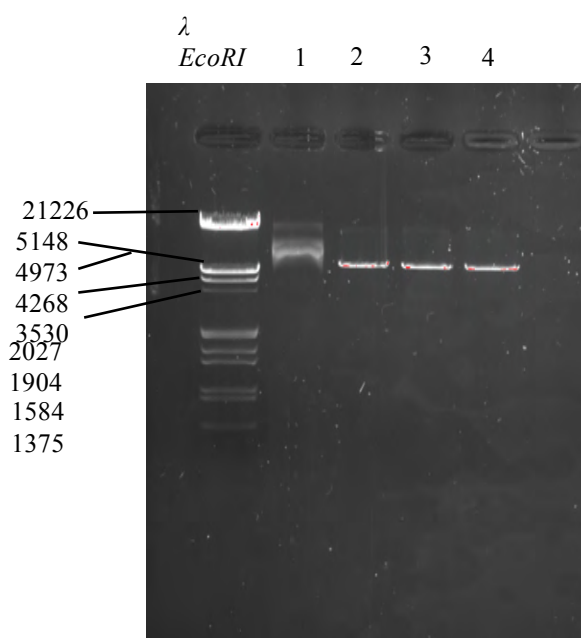


Figure 3.6. Restriction enzyme digests of pET28a vector. PET28a vector is known to be 5369bp in size, the uncut plasmid is visible in column 1, controls for each of the single cut plasmid are visible as bands in columns 2 and 3. Column 2 is pET28a single cut with *NcoI* restriction enzyme and column 3 with *XhoI*. Column 4 illustrates the double cut plasmid.

The PCR products were also digested with restriction enzyme; 46µl of each of the E6 His tag and E7 His tag products were combined with 12µl of Tango 2x Buffer (Fermentas) and 2µl each of the *NcoI* and *XhoI* enzymes. Once combined all products were placed in a water bath at 37°C for 90 minutes. The products were analysed to assess for restriction enzyme digestion by performance of a 1% w/v agarose gel, 5µl

of each product was combined with 5 μ l of dH₂O and 2 μ l of DNA loading dye (Thermoscientific). Double cut plasmid vector and E6 and E7 His tag fragments were purified using the GeneJET gel extraction kit (as described in section 2.2.12). The double cut plasmid and E6 and E7 were run on an ultrapure 1.2% w/v agarose gel as described in section 2.2.10.

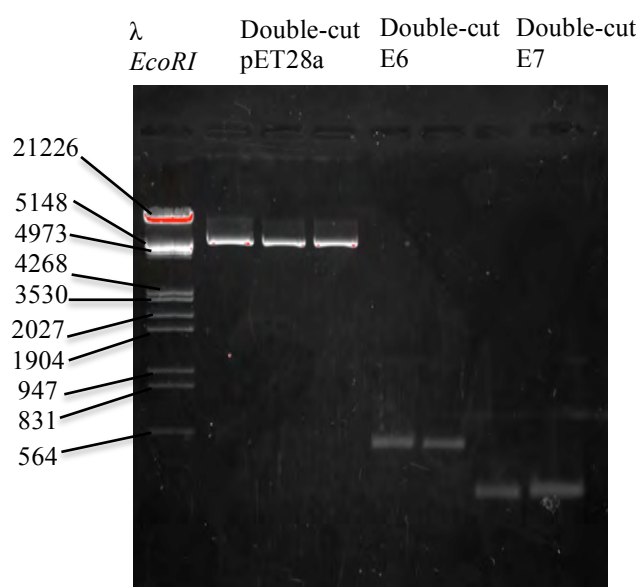


Figure 3.7. Ultrapure 1.2% agarose gel for purification of double cut pET28a and double cut E6 and E7 His Tag (representative of two repeats).

Ligation reactions for pET28a and E6 His Tag, and pET28a and E7 His Tag were carried out as described in section 2.4.2. The recombinant pET28-E6 and pET28-E7 plasmids were transformed into 100 μ l of competent *XLI Blue E.coli*, after transformation 250 μ l of Luria Broth (LB) was added to each aliquot of transformed cells and placed in a shaking incubator at 37 $^{\circ}$ C for 30 minutes, this was to optimise growth of transformed cells, this was repeated numerous times. The transformed cells with LB broth were then plated onto an Agar_{KM} plate and placed in an incubator at 37 $^{\circ}$ C for 16 hours. After numerous attempts only 2 viable colonies were present for pET28-E6 and no viable colonies were seen for pET28-E7. Individual colonies for

E6 were picked and placed aseptically in 5ml of LB broth with 20 μ g/ml Kanamycin (Km). These were placed in the shaking (220RPM) incubator at 37°C overnight. The cells from the *XLI-Blue* pET-E6 *E.coli* culture were pelleted by centrifugation at 14462 \times g. A total of 5ml of solution was centrifuged in 1ml aliquots (1-14 Sigma Centrifuge). The recombinant plasmid was then extracted from the *XLI-Blue E.coli* cells by mini-prepping using the GeneJET Plasmid Mini prep kit (Thermo Scientific). The recombinant plasmid pET28-E6 was then restriction digested as described in section 2.4.1 for isolation of HPV-16 E6 DNA fragment. This was then run on an agarose gel (1% w/v) at 100 volts to check for the presence of recombinant HPV-E6 DNA. No viable DNA fragment was identified, this was repeated four times and colonies appeared smeared on the agarose gel.

3.4 Recombinant pGEX-E6 and pGEX-E7 Synthesis and Transformation

PCR products for E6 and E7 GST tag were purified using the GeneJET gel extraction kit (Thermo Scientific), the same as described for E6 and E7 His Tag in section 3.1.3. Briefly 45 μ l of PCR product for each of E6 and E7 was combined with 5 μ l of pure glycerol (Melford), this was then loaded onto a 1.2% w/v ultra pure agarose gel, splitting across two wells as the maximum capacity per well was 25 μ l. The glycerol increased the density of the solution therefore allowing it to be placed into the gel wells with ease.

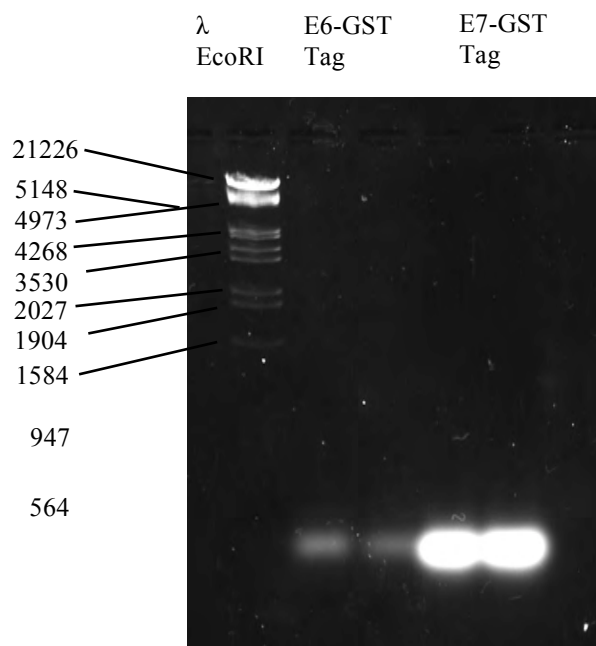


Figure 3.8 Purified products for E6 GST tag and E7 GST tag on 1.2% agarose gel. Visible bands for E6 GST are seen in columns 1-2, and for E7 GST in column 3-4.

3.5 *BamHI* and *EcoRI* Restriction Enzyme Digests

Restriction enzyme digests were performed on both the pGEX-6p1 plasmid vector and on the purified PCR products for E6-GST tag and E7-GST tag. The pGEX-6P1 vector was double cut with restriction enzymes *BamHI* (Thermo Scientific) and *EcoRI* (Thermo Scientific) by combining 2 μ l each of restriction enzymes with 2 μ l of pGEX-6P1 plasmid vector and 16 μ l of Tango 2x Buffer (Fermentas). The solution was made up to 80 μ l by the addition of 58 μ l of dH₂O and the reaction was carried out as described in section 2.4.1. The table below illustrates the combinations for the double cut plasmid and controls, and also for the E6-GST tag and E7-GST tag protein sequences for restriction enzyme digests.

Table 3.1 Combinations for restriction enzyme digests with *BamHI* and *EcoRI*

	Reaction	Plasmid (pGEX-6P1) μ l	Buffer-Tango 2x μ l	<i>BamHI</i> restriction enzyme μ l	<i>EcoRI</i> restriction enzyme μ l	dH ₂ O μ l	Total μ l
1	pGex-6P1 uncut (control)	0.5	4	-	-	15.5	20
2	Single <i>BamHI</i> (control)	0.5	4	0.5	-	15	20
3	Single <i>EcoRI</i> (control)	0.5	4	-	0.5	15	20
4	Double Cut pGEX-6P1	2	16	2	2	58	80
5	E6 _{GST tag}	46	12	2	2	-	62
6	E7 _{GST tag}	46	12	2	2	-	62

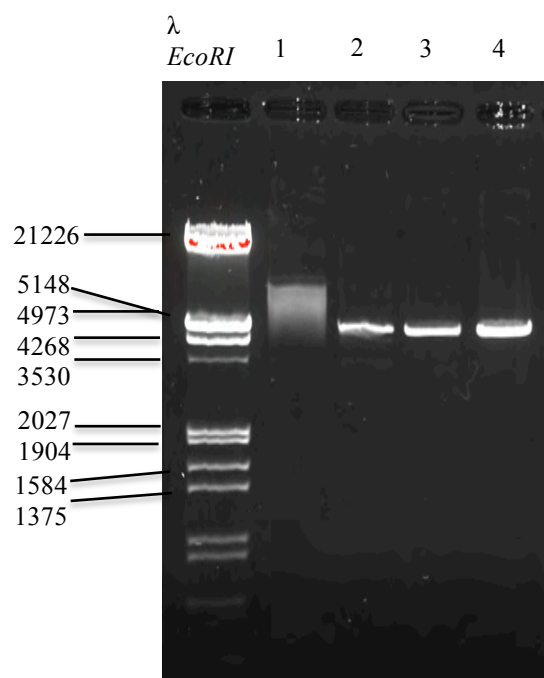


Figure 3.9 Restriction enzyme digests on pGEX-6p1 vector which is known to be 4900 bp in size, the uncut plasmid is visible in lane 1, lane 4 illustrates the double cut plasmid and controls for each of the single cut plasmid are visible as bands in lanes 2 and 3, lane 2 is pGEX-6p1 single cut with *BamHI* restriction enzyme and lane 3 with *EcoRI*.

Restriction enzyme digested products for E6-GST (E6_{BE}) and for E7-GST (E7_{BE}) were run on agarose gel to check for viable product after purification through the GeneJET gel extraction kit (Thermo Scientific). Figure 3.10 illustrates that no viable product for E6_{BE} and E7_{BE} were observed, however the double cut plasmid was still visible. This may have been due to loss of the DNA sequences through the purification column.

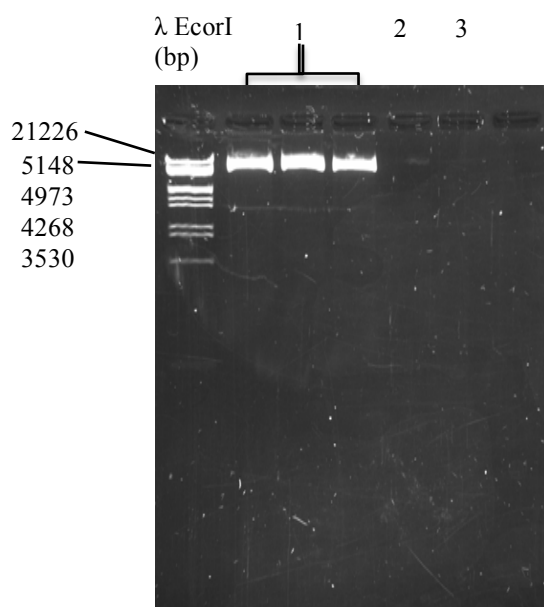


Figure 3.10 Restriction enzyme digested and purified pGEX-6p1, E6_{BE} and E7_{BE}. Lane 1 contains the double cut purified plasmid vector however there are no viable products in lanes 2 and 3 for each of E6_{BE} and E7_{BE} respectively.

The PCR for E6_{BE} and E7_{BE} was repeated under the same conditions as described in section 3.1. PCR products were purified once again using the GeneJET gel extraction kit, however the elution process was performed three times, instead of once, and during each elute a 5µl sample was taken off for analysis to assess the amount of DNA coming away from the purification column. A total volume of 15µl was therefore collected. Each 5µl elute sample was combined with 5µl of dH₂O and 2µl of

DNA loading dye and the sample was run on an agarose gel as described earlier, figure 3.11 illustrates the PCR products with number of elutions.

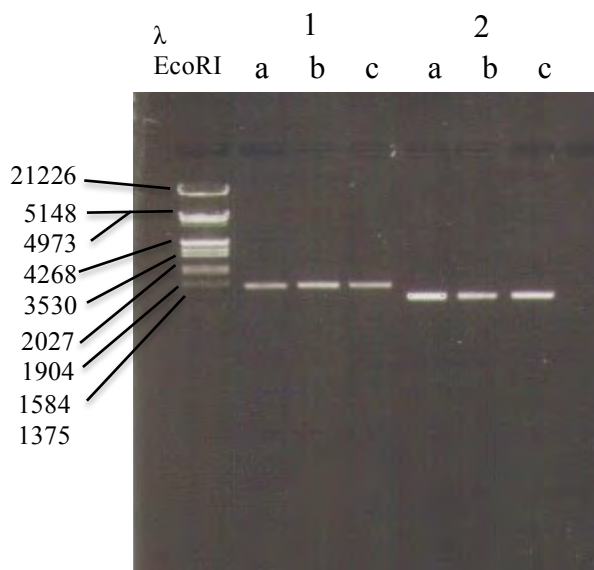


Figure 3.11 Repeated PCR for E6-GST and E7-GST (1% w/v agarose gel), A-C are the sequential elutions, as illustrated there is product from each elution.

Restriction enzyme digests were performed on the repeat PCR purified products and the digested pGEX-6p1, E6_{BE} and E7_{BE} were run on an ultra pure agarose gel to allow extraction using the GeneJET gel extraction kit, a total of 210µg of E6_{BE}, 470µg of E7_{BE} and 310µg of pGEX-6p1_{BE} were extracted. A final analytical gel was run for each sample, as described earlier, to quantify ligation reactions.

An analytical 1% (w/v) agarose gel was made as described earlier (2.2.11) and the wells were loaded with the 12µl digested pGEX-6p1, E6_{BE} and E7_{BE} by combining 5µl of the product, 5µl dH₂O and 2µl DNA Loading Dye (ThermoScientific). Once the gel was run for approximately 30 minutes at 100 volts until the expected bands were well separated; the gel was imaged with BioRAD Molecular Imager® Chemi DOC™ XRS⁺ with Image Lab™ Software.

The following image shows the digested pGEX-6p1, E6_{BE} and E7_{BE}. The concentration for the λ Hind Eco Marker (Fermentas) was known to be at a concentration of 0.5 μ g ml⁻¹. The vector to insert ratio was used at standard 1:3. Therefore the sizes were broadly; pGEX-6p1 which is 1904 base pairs at 0.04M, E6 at 0.06M and E7 at 0.1M.



Figure 3.12 Restriction enzyme digested vector pGEX-6p1, E6_{BE} and E7_{BE} on ultra-pure 1.2% agarose gel.
 Lane 1-2 – pGEX-6p1
 Lane 3 – E6
 Lane 4 – E7

Ligation reactions were set up as described earlier in section 2.4.2 by combining 2 μ l of pGEX-6p1 with 10 μ l of E6_{BE}, 2 μ l of DNA ligase buffer with 1 μ l of T4 DNA ligase, the reaction was made up to 20 μ l with the addition of dH₂O and left at room temperature for 1 hour. The same reaction was also performed for pGEX-6p1 and E7_{BE} instead with 4 μ l of vector added to 12 μ l of E7_{BE} insert.

Cells were transformed into XLI-Blue *E.coli* cells as described earlier in section 2.4.3, 250µl of LB broth was added to each aliquot of transformed cells and placed in a shaking incubator at 37°C for 30 minutes. The transformed cells with LB broth were then plated onto an Agar plates with Ampicillin at a concentration of 50µg ml⁻¹ and placed in an incubator at 37°C for 16 hours. Cultures were picked aseptically after 16 hours and placed in 5ml LB broth and 50µg ml⁻¹ ampicillin for overnight growth. The recombinant plasmids pGEX-E6 and pGEX-E7 were harvested and mini-prepped as described in section 3.3. The recombinant plasmid was thus restriction digested and separated on an agarose gel as described earlier. The colonies for both pGEX-E6 and pGEX-E7 were smeared on agarose gel, again this may be due to the RNase not working properly or a problem with the mini-prep kit. The experiment was repeated (n=4) under the same conditions, picking fresh colonies, changing variables such as using fresh TAE buffer and isolation reagents, unfortunately no distinct DNA band was given that could be used for further analysis.

In addition the experiment was repeated and as a control the uncut pGEX-6P1 plasmid was also transformed into XL1-Blue *E.coli* cells as described in section 2.4.3. After overnight growth few colonies were observed for pGEX-E6 and pGEX-E7 compared to the control plate of pGEX alone, this confirmed that the XL1-Blue *E.coli* cells were competent and that the problem lay with the ligation reactions and transformations. The antibiotic resistant cassette is on the pGEX plasmid, which will not replicate if the plasmid is non-circular. Therefore it was concluded that the ligation reaction had mostly likely worked inefficiently, the resultant transformed cells were therefore killed by the ampicillin as the plasmid was non-circular. However the few colonies that did survive from this repeat transformation were

aseptically transferred to 5ml of LB broth with $50\mu\text{g ml}^{-1}$ ampicillin and placed in a shaking incubator at 220RPM, 37°C overnight. The recombinant plasmid was harvested as described earlier in section 2.4.5, this time a different plasmid mini-prep kit was used – Nucleospin (Machery-Nagel, France).

Restriction enzyme digests were performed on recombinant pGEX-E6 and pGEX-E7 as described in section 2.4.1. The digested products were then ran on an analytical 1% (w/v) agarose gel as described in section 2.2.10 to check for presence of insert, i.e. E6 and E7. The results as shown in Figure 3.13 illustrate that despite the changes the recombinant pGEX-E6 failed to achieve production of the E6 insert. However there was product present for pGEX-E7, although there were multiple bands present on the gel. Bam-HI restriction enzyme is known to cause starring, i.e. if the product is over digested this can result in the plasmid being cut at numerous sites and hence the resultant variable sized bands.

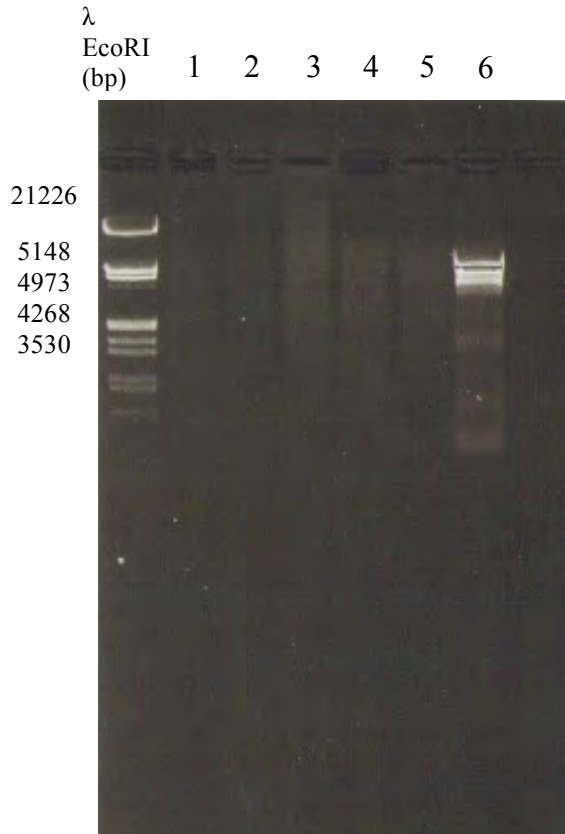


Figure 3.13 Restriction enzyme BamHI and EcoRI digested pGEX6p1 with E6 and E7 inserts on 1% (w/v) agarose gel. Lanes 1-4 illustrate no viable product is present for pGEX-E6, Lane 5 has no product for E7, however Lane 6 has viable pGEX-E7 product available.

3.6 Expression in Bacteria and Purification of Recombinant Proteins

Due to the inability of generating HPV E2 recombinant proteins a number of relevant expression constructs were sourced from Professor Norman Maitland (University of York): recombinant pET-E2, -E2NT, -E2LCT, pET15b-E6 and pET15b-E7.

3.6.1 Expression and purification of HPV-16 E2NT

The N-terminal domain of E2 was expressed in *E. coli* strain of BL21(DE3)pLysS after transformation with recombinant pET-E2NT plasmid. The bacteria were grown

in LB broth supplemented with Ampicillin (50µg/ml) and Chloramphenicol (34µg/ml) at 37°C until OD₆₀₀ 0.7-0.8 was reached after which time the cells were induced with 1mM IPTG for 4 hours and stored as described in section 2.5.2.

Approximately 30g of wet weight thawed cells were lysed by sonification and stored as described in section 2.5.3 into soluble and insoluble phases. SDS-PAGE analysis of both the soluble and insoluble phases was performed to check for protein expression (see Figure. 3.14), the insoluble phase was resuspended in 10ml of Talon buffer (Appendix 2).

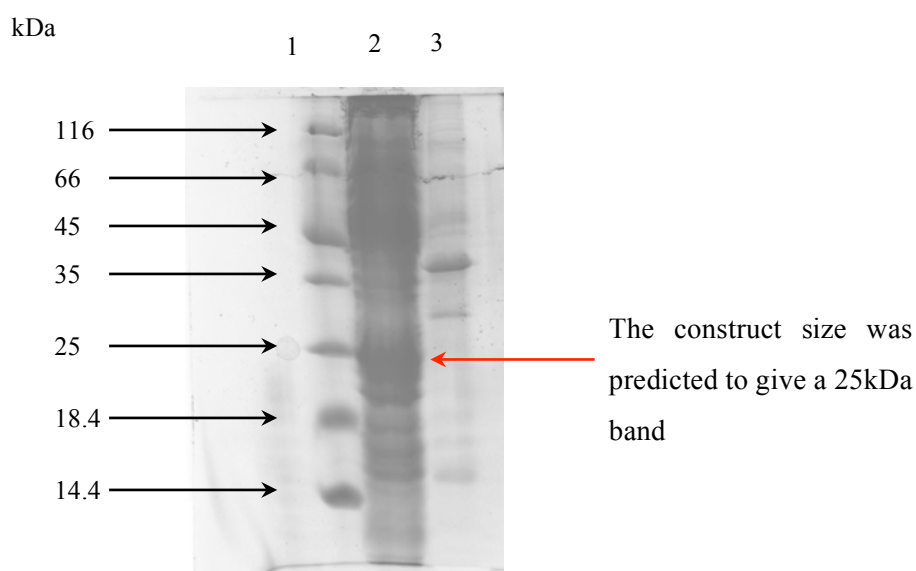


Figure 3.14 SDS-PAGE (12% acryl/urea stacking gel) showing the presence of protein expression of HPV-E2NT in the soluble phase of cell free extract after cell lysis. Lane 1 = unstained protein MW marker (Thermoscientific), Lane 2= soluble protein phase, Lane 3= insoluble protein phase. The HPV-E2NT protein is 255 amino acids and has a molecular weight of 25kDa.

The first purification process was performed by IMAC, the 10ml soluble phase was loaded onto an equilibrated IMAC column (2.5ml bed volume) as described in section 2.6. The first elute was stored as the flow through, the column was washed through

with 1 column volume (approx. 10ml) of Talon Buffer (10mM Tris, 300mM NaCl, pH 8.0). Subsequent washes with 1 column volume of Talon buffer with increasing concentrations of imidazole, namely 10, 100 and 200mM were used to elute the protein from the nickel resin in the column bed. The column washes were then analysed by SDS-PAGE (Fig. 3.15) to assess at which concentration of imidazole the protein was eluted most and also the strength of purification.

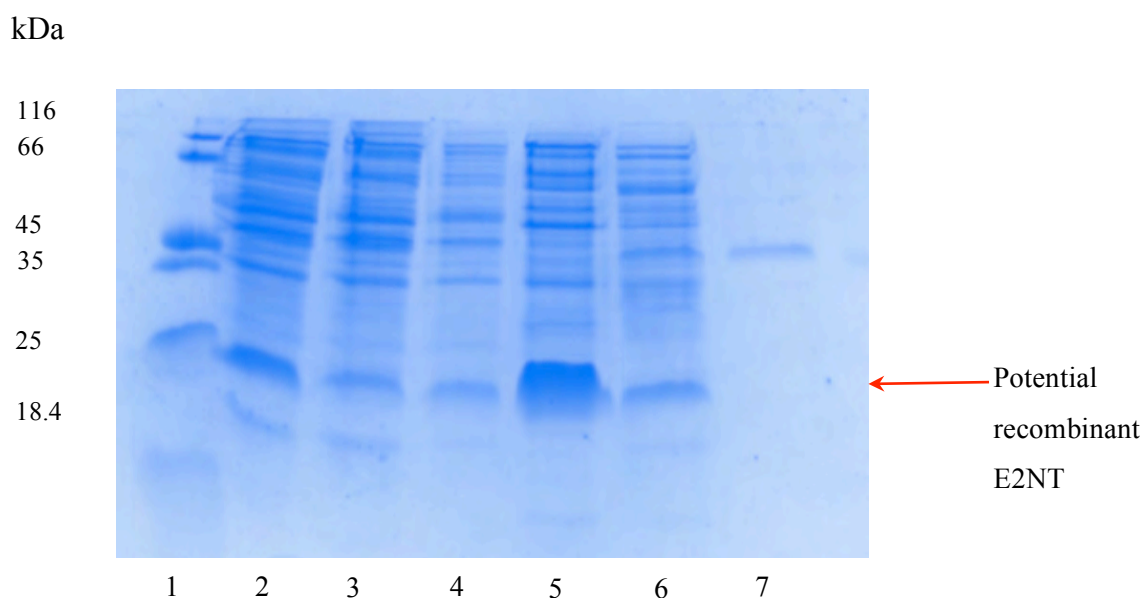


Figure 3.15 Recombinant HPV-16 E2NT was purified in a single immobilized metal affinity column chromatography step. A band at 25 kDa was observed, which is the correct molecular weight for potential recombinant E2NT on 15% (w/v) SDS-PAGE, stained with Coomassie Blue..

Lane 1 – Molecular weight marker (kDa)

Lane 2 – Cell free extract (CFE)

Lane 3 – Flow through

Lane 4 – Talon buffer wash

Lane 5 – Elute 10mM Imidazole

Lane 6 – Elute 100mM Imidazole

Lane 7 – Elute 200mM Imidazole

The greatest yield of protein was seen with the 10mM imidazole elute, this was further purified using ammonium sulphate precipitation as described in section 2.7,

10ml of 10mM imidazole elute was precipitated out using ammonium sulphate at concentrations of 15%, 30%, 45%, 60% and 100%. The sample was kept on vortex at 0°C and once the ammonium sulphate was fully dissolved the sample was centrifuged at 1900 x g, 4°C for 20 minutes, the supernatant was decanted back into the vortex and further precipitated with increasing concentrations of ammonium sulphate whilst the precipitates were suspended in 5ml of Talon buffer and stored at 4°C. The table below (Table 3.2) demonstrates the volumes of ammonium sulphate added for each precipitate. The precipitates were each run on an SDS-PAGE to analyse protein purification (Fig. 3.16).

Table 3.2 Ammonium sulphate precipitates and volume of salt required

Concentration of (NH₄)₂SO₄	Weight (g)
15%	0.84g
30%	0.88g
45%	0.94g
60%	0.99g
100%	3.14g

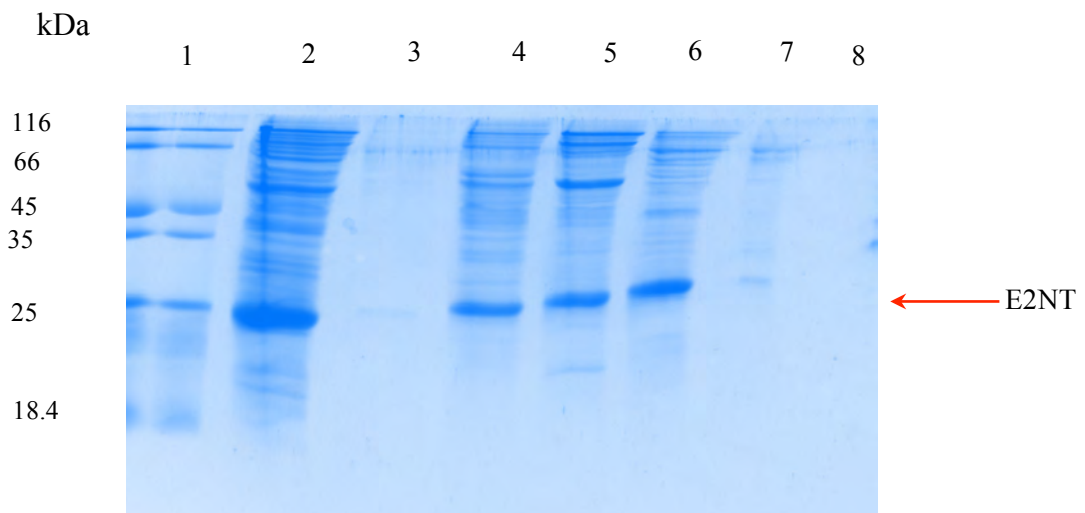


Figure 3.16 Ammonium sulphate precipitation of 10mM imidazole elute of HPV-16 E2NT, again a clear band is visible at 25kDa, i.e. recombinant E2NT (polyacrylamide gel electrophoresis stained by Coomassie blue). The second purification process removed contaminants from the purified protein as illustrated by clearer bands with increasing precipitate as compared to the IMAC purification alone.

Lane 1 – Molecular weight marker (kDa)

Lane 2 – Imidazole 10mM elute

Lane 3 – 15% precipitate

Lane 4 – 30% precipitate

Lane 5 – 45% precipitate

Lane 6 – 60% precipitate

Lane 7 – 100% precipitate

Lane 8 – Supernatant

The greatest yield of protein was observed at 30-60% ammonium precipitation.

Although the molecular weight of the highlighted band corresponded with E2NT on

analysis using Western Blotting, no E2 protein could be identified in the sample. The

experiment was repeated two further times, although the positive controls for the

Western Blotting worked no viable E2 protein was shown. Finally it was concluded

that although the protein was likely expressed, that the protein had degraded during

storage that was despite the addition of protease inhibitors in the lysate and storage at

4⁰C or it may be that the band was not E2.

3.6.2 Expression and purification of HPV-16 E2LCT

The long form of the E2 binding domain (E2LCT) was expressed in *E. coli* strain of BL21, transformed with recombinant pET-E2LCT plasmid. The bacteria were grown in LB broth supplemented with ampicillin (50µg/ml) at 37°C until OD₆₀₀ 0.8-1.0 was reached, cells were induced with 1mM IPTG and grown at 25°C for 4 hours and stored as described in section 2.5.2. Approximately 20g of wet weight cells were lysed by sonification and separated into soluble and insoluble phases as described earlier and run on 12% (w/v) SDS-PAGE (Fig. 3.17).

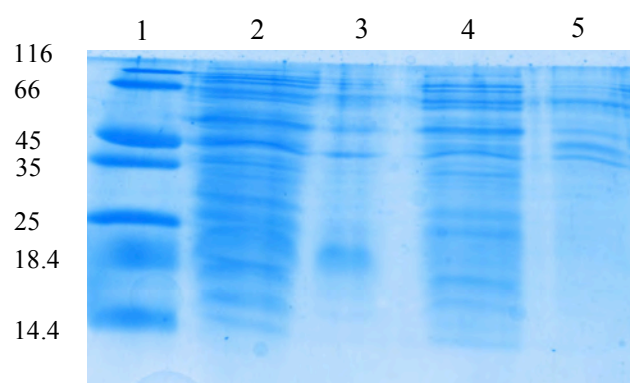


Figure 3.17 HPV-16 E2LCT and HPV-16 E2 soluble and insoluble phases. E2LCT is known to be 15kDa, although there is a visible band at around 15kDa in the soluble phase (Lane 2), the insoluble phase did not have a viable band at 15kDa (Lane 3). For the E2 protein this was less apparent on the soluble and insoluble phases, a band is expected to be seen at 43.6kDa, although a band is visible in the soluble phase (representative of two repeats), polyacrylamide gel electrophoresis stained by Coomassie blue.

Lane 1 – Molecular weight marker (kDa)

Lane 2 – Soluble E2LCT

Lane 3 – Insoluble E2LCT

Lane 4 – Soluble E2

Lane 5 – Insoluble E2

As demonstrated the majority of the protein was present in the soluble phase, this was purified by IMAC, as described for E2NT. Imidazole was used to elute protein from

the IMAC column in concentrations of 10, 100 and 200mM. The picture below (Fig. 3.18) illustrates that although a protein band was seen at 15kDa, no purified protein could be eluted with increasing concentrations of imidazole.

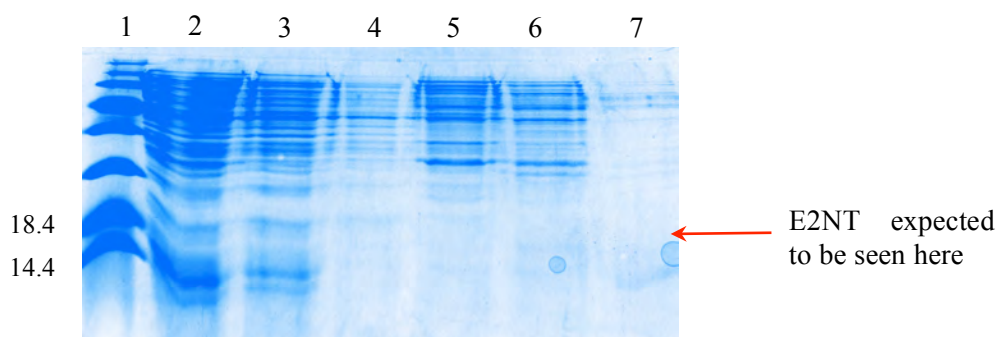


Figure 3.18 Purification of HPV-16 E2LCT with IMAC (representative of three repeats) shown by polyacrylamide gel electrophoresis stained by Coomassie blue.

Lane 1 – Molecular weight marker (kDa)

Lane 2 – Soluble cell free extract

Lane 3 – Flow through

Lane 4 – Talon wash

Lane 5 – 10mM imidazole elute

Lane 6 – 100mM imidazole elute

Lane 7 – 200mM imidazole elute

HPV-16 E2LCT was regrown with BL21 pLysS as described above. The soluble phase of protein was purified using IMAC as described above, the figure below (3.19) illustrates the eluted protein, although weak bands were present at 15kDa. Although protein bands had been shown to be present, no clear protein band could be expressed under the conditions described above; again after checking by Western Blotting no specific reactivity was observed.

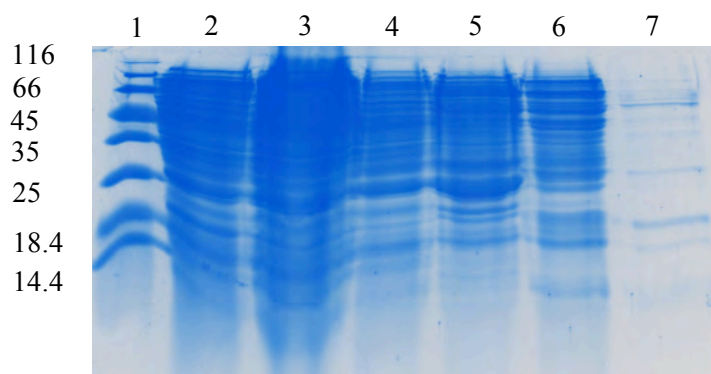


Figure 3.19 HPV-16 E2LCT purification with IMAC of cells expressed in BL21 pLysS shown by polyacrylamide gel electrophoresis stained by Coomassie blue.

Lane 1 – Molecular weight marker (kDa)

Lane 2 – Soluble cell free extract

Lane 3 – Flow through

Lane 4 – Talon wash

Lane 5 – 10mM imidazole elute

Lane 6 – 100mM imidazole elute

Lane 7 – 200mM imidazole elute

3.6.3 Expression and purification of HPV-16 E2

HPV-16 E2 was expressed in BL21 as described for E2LCT. Figure 3.17 above represents the soluble and insoluble phases of growth, there is a faint band visible at around 43kDa. The soluble phase was purified by IMAC as described above, figure 20 illustrates that no viable E2 product could be eluted with IMAC.

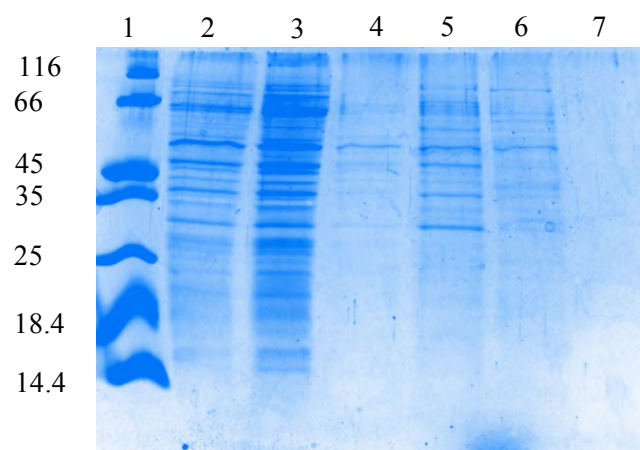


Figure 3.20 Purification of HPV-16 E2 soluble phase by IMAC illustrated by polyacrylamide gel electrophoresis stained by Coomassie blue. No viable product can be seen with imidazole elution which would be expected at 43.6kDa.

Lane 1 – Molecular weight marker (kDa)

Lane 2 – Soluble cell free extract

Lane 3 – Flow through

Lane 4 – Talon wash

Lane 5 – 10mM imidazole elute

Lane 6 – 100mM imidazole elute

Lane 7 – 200mM imidazole elute

The E2 protein was re-expressed in BL21 pLysS as described above, however after induction with 1mM IPTG the temperature was reduced to 16°C and cells allowed to grow overnight. Cells were extracted and lysed by sonification as described earlier, the soluble phase of E2 was purified using IMAC as described for E2LCT and run on 12% (w/v) SDS-PAGE (Fig. 3.21).

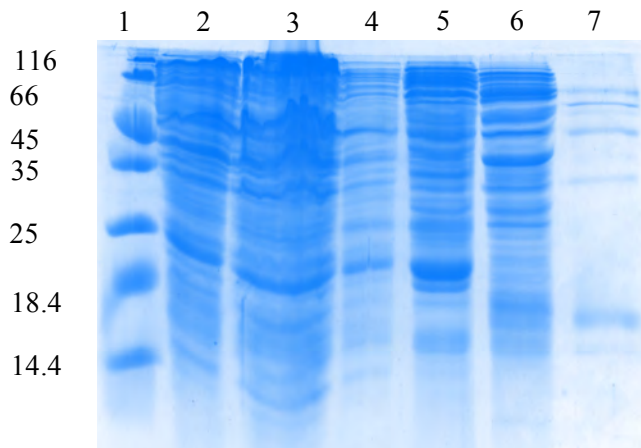


Figure 3.21 HPV-16 E2, expressed in BL21 pLysS. Soluble phase purification with IMAC, there is a visible band at around 43kDa in Lane 6 that would correspond with potential HPV-16 E2, polyacrylamide gel electrophoresis stained by Coomassie blue. Lane 1 – Molecular weight marker (kDa)
 Lane 2 – Soluble cell free extract
 Lane 3 – Flow through
 Lane 4 – Talon wash
 Lane 5 – 10mM imidazole elute
 Lane 6 – 100mM imidazole elute
 Lane 7 – 200mM imidazole elute

Western blotting was performed on the 100mM imidazole elute for E2, no viable protein could be identified. Again this is most likely due to degraded protein secondary to storage.

3.6.4 Expression and purification of HPV-16 E6

HPV-16 E6 was expressed from the host strain BL21 (DE3) pLysS after transformation of the *E-coli* strain with pET15b-E6 and selection with Ampicillin (50µg/ml) and Chloramphenicol (34µg/ml). E6 was expressed after induction of BL21 (DE3) pLysS with 1mM IPTG at 3 hours or when the OD₆₀₀ of 0.8-1 was reached. After induction growth continued at 25°C for 4 hours, cells were pelleted and stored as described in section 2.5.2.

The first purification step was carried out by IMAC as described earlier; approximately 28g of thawed wet cells were lysed by sonification. Protein from the soluble phase was eluted with Talon buffer containing imidazole at 10, 100 and 200mM from the IMAC column. A protein band was seen at 21kDa, the known MW of HPV-16 E6 at 10mM imidazole (see Fig. 3.22).

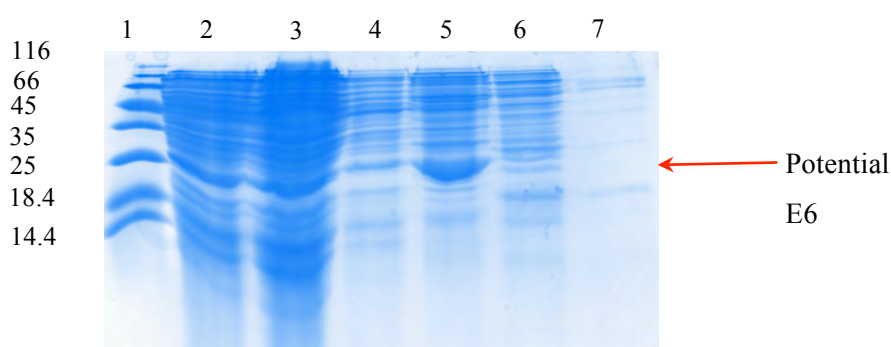


Figure 3.22 HPV-16 E6 purified with IMAC, a band visible at 21kDa is the potential recombinant protein (12% (w/v) SDS-PAGE, polyacrylamide gel electrophoresis stained by Coomassie blue.

Lane 1 – Molecular weight marker (kDa)

Lane 2 – Soluble cell free extract

Lane 3 – Flow through

Lane 4 – Talon wash

Lane 5 – 10mM imidazole elute

Lane 6 – 100mM imidazole elute

Lane 7 – 200mM imidazole elute

A secondary purification process was carried out by ammonium sulphate precipitation on the 10mM imidazole elute containing E6 as described in section 2.7. HPV-16 E6 was precipitated out by ammonium sulphate concentrations of 15, 30, 45, 60 and 100%. SDS-PAGE was performed on the precipitates that showed that E6 was precipitated out at concentrations between 30-60% ammonium sulphate (see Fig. 3.23). Lane 8 had no viable protein, this is expected as this was the supernatant after all protein had been precipitated out.

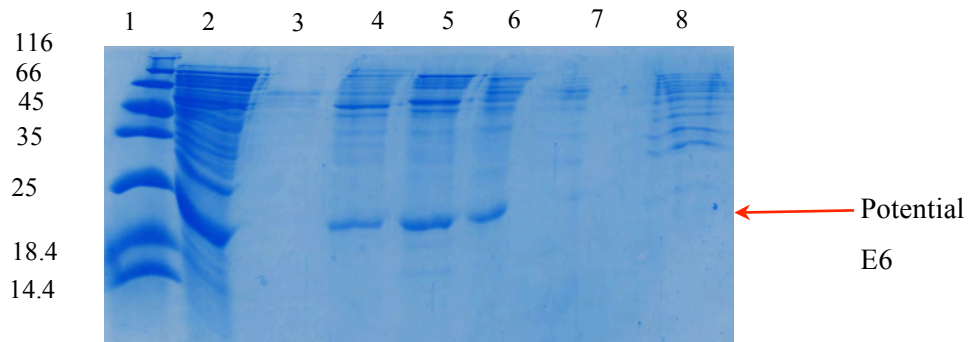


Figure 3.23 HPV-16 E6, secondary purification process by ammonium sulphate precipitation. Clear bands are visible in Lanes 4-6 at 21kDa corresponding with E6 (12% w/v SDS-PAGE, polyacrylamide gel electrophoresis stained by Coomassie blue).

Lane 1 – Molecular weight marker (kDa)

Lane 2 – Imidazole 10mM elute

Lane 3 – 15% precipitate

Lane 4 – 30% precipitate

Lane 5 – 45% precipitate

Lane 6 – 60% precipitate

Lane 7 – 100% precipitate

Lane 8 – Supernatant

To further purify the E6 protein and remove contaminants a further purification process was carried out using Vivaspin protein concentration columns (Sartorius Biotech, Germany). These are based on membrane centrifugation which allow proteins of only a certain MW to pass through during centrifugation, 5ml of E6 from elutes of 30-60% ammonium sulphate were each placed in the column and centrifuged at $3500 \times g$, 4°C for 10 minutes. The products were then analysed by SDS-PAGE to analyse protein purification, unfortunately no viable protein was centrifuged by the column as shown on SDS-PAGE and therefore the third purification process was abandoned. Western blotting was performed on the HPV-16 E6 protein purified by IMAC and ammonium sulphate precipitation, this was carried

out as described in section 2.12. The illustrations below depict the E6 protein (Fig. 3.24).

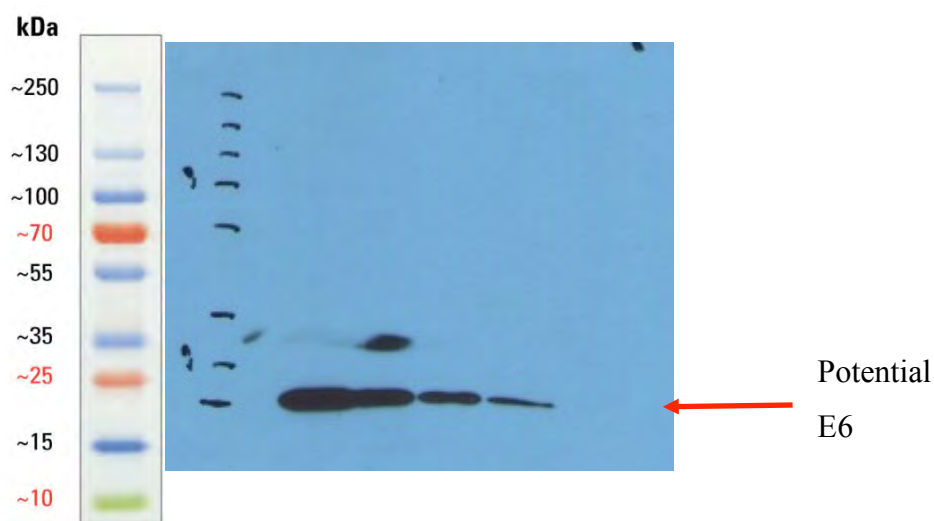


Figure 3.24 E6 protein product illustrated by Western blotting. The representative protein ladder (ThermoScientific pre-stained protein ladder) has been depicted from ThermoScientific product information sheet #26619.

3.6.5 Expression and Purification of HPV-16 E7

The HPV-16 E7 protein was expressed in E-coli strain BL21 (DE3) PLysS transformed with pET15b-E7 plasmid. Bacterial cultures were grown in LB broth media as described in section 2.5.2, once culture growth had reached $OD_{600} = 0.7$, bacterial cells were induced with 1mM IPTG and protein expression was continued for approximately 4 hours at 37°C.

Approximately 10g of thawed cells were lysed by sonification in Talon buffer (appendix 2) as described earlier. At this point a 12% SDS-PAGE gel was run for

each of the soluble and insoluble phases to identify presence of recombinant protein (See Figure 3.25), recombinant HPV-16 E7 protein was identified at 20kDa in the soluble phase.

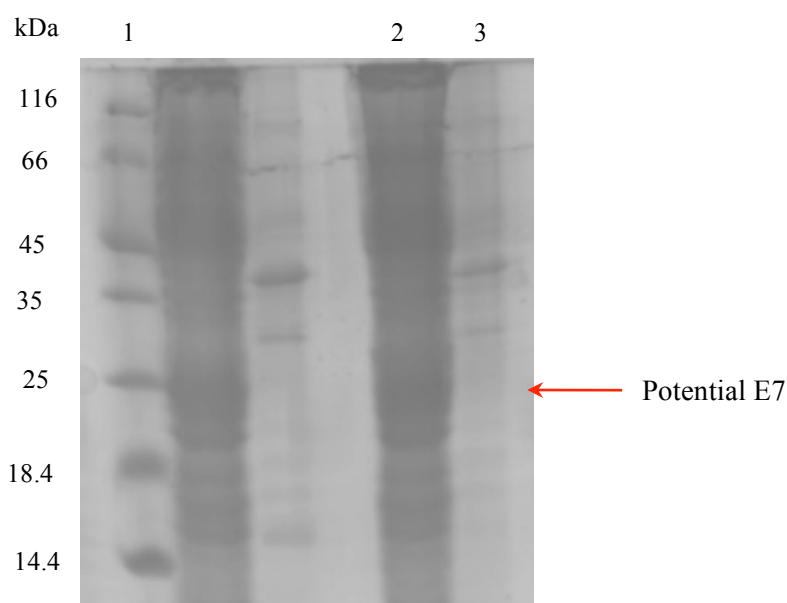


Figure 3.25 Expression of recombinant HPV-16 E7 protein. 12% Acryl/Urea SDS-PAGE and staining with Coomassie blue.

Lane 1 – Unstained molecular weight protein marker

Lane 2 – Soluble E7 Protein

Lane 3 – Insoluble E7 Protein

The first phase of protein purification was performed using IMAC the soluble protein phase as described in section 2.6. The clear lysate (approximately 10ml) was added to an equilibrated IMAC column with a 2.5ml bed volume of nickel resin. Protein was then eluted from the column with sequential 4 column volume washes with Talon adjusted to 10mM, 100mM and 200mM imidazole. The elute was immediately stored on ice to prevent protein denaturation. SDS-PAGE (12% w/v) gel was ran at this stage to identify concentration of imidazole at which maximum protein was eluted (see Fig.3.26).

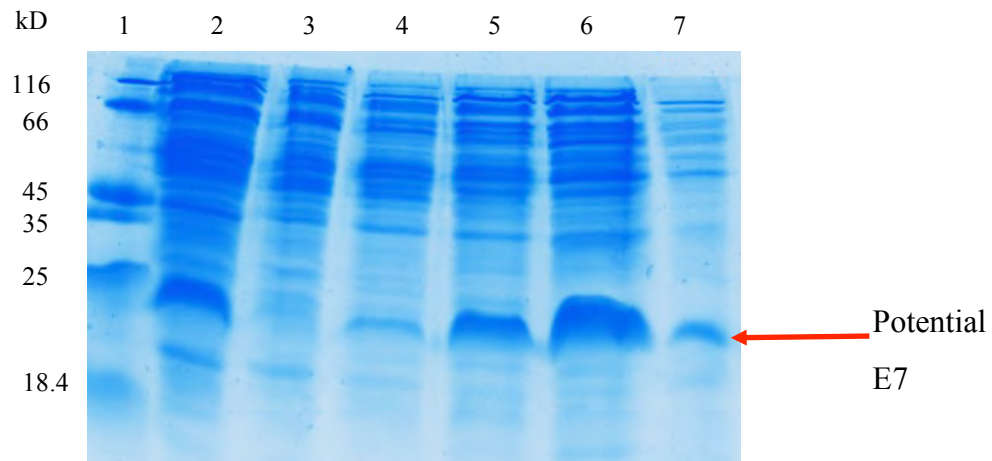


Figure 3.26 HPV-16 E7 First Purification Step by IMAC . 12% Acryl/urea SDS-PAGE stained with Coomassie Blue (representative of two repeats).

Lane 1 – Unstained protein molecular weight marker (ThermoScientific)

Lane 2 – Cell Free Extract (Soluble protein)

Lane 3 – Flow Through

Lane 4 - Talon buffer wash through

Lane 5 – Talon + 10mM imidazole

Lane 6 – Talon + 100mM imidazole

Lane 7 – Talon + 200mM imidazole

The 100mM elute was found to have the largest quantity of recombinant protein, this was used for the second purification process by ammonium sulphate precipitation as described earlier with precipitates at 15%, 30%, 45%, 60% and 100% saturation with $(\text{NH}_4)_2\text{SO}_4$ (see figure 3.27).

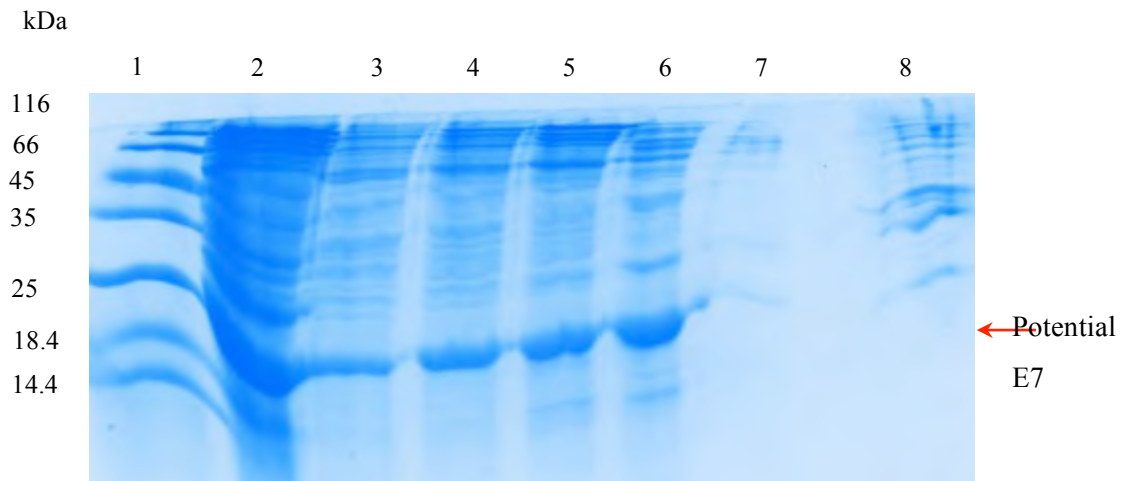


Figure 3.27 HPV-16 E7 Second purification step, Ammonium sulphate precipitation of 100mM Eluate. SDS-PAGE 12% urea stained with Coomassie Blue.

Lane 1 – Unstained protein molecular weight marker (ThermoScientific)

Lane 2 – 100mM Eluate

Lane 3 – 15% $(\text{NH}_4)_2\text{SO}_4$

Lane 4 – 30% $(\text{NH}_4)_2\text{SO}_4$

Lane 5 – 45% $(\text{NH}_4)_2\text{SO}_4$

Lane 6 – 60% $(\text{NH}_4)_2\text{SO}_4$

Lane 7 – 100% $(\text{NH}_4)_2\text{SO}_4$

Lane 8 – Supernatant

Pooled peak fractions of HPV-16 E7 at 60% were dialysed against TBS buffer, pH 8.0 (12 000 kDa MW cut off) at a factor of 4×10^4 . The presence of HPV-16 E7 was confirmed by Western Blotting as described in section 2.12 (Fig. 3.28).

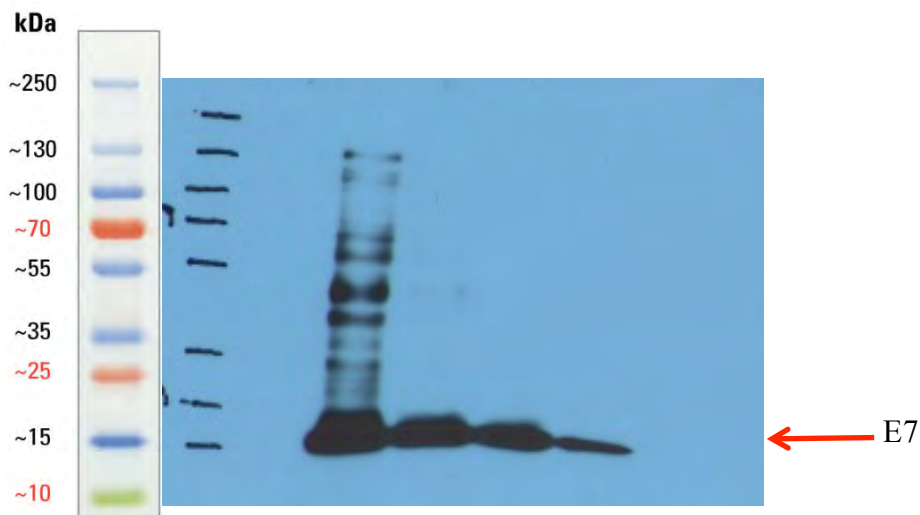


Figure 3.28 E7 protein (12.9kDa) as illustrated by Western blotting. The pre-stained protein ladder is also illustrated (ThermoScientific).

The concentration of protein was established by calculating the absorbance of the sample using the nano-drop spectrophotometer and using the formula below to calculate final concentration.

$$A = ECL$$

Where A = absorbance
 E = extinction co-efficient
 C = concentration
 L = length of light path (cm)

The extinction co-efficient of His-tag E7 was calculated at 6335 by using the PROTParam programme (ExpASy, Bioinformatics Resource Portal). Absorbance was calculated at 0.808 with the length of light path on the nano-spectrophotometer machine being 1cm, thus the final concentration of protein was calculated at 1.67mg/ml. Aliquots of purified protein were stored at -80°C in 10% (v/v) glycerol.

3.7 Discussion

The HPV-16 E6 and E7 proteins were successfully expressed in *E-coli* and purified by a two-stage purification process using IMAC and Ammonium sulphate precipitation. However after numerous attempts the expression of HPV-16 E2 remained unsuccessful. The E2 protein is known to suppress the viral oncoproteins E6 and E7 (Webster et al., 2000, Wells et al., 2000), most cervical cancer cell lines that have been used to express the HPV-16 oncoproteins have shown that the viral E2

gene has been disrupted (Baker et al., 1987), therefore it was possible that the UMSCC-47 cell line that was used in this study had a mutated form of the E2 gene.

Although the SDS-PAGE showed that there was possible expression of E2NT, with a band visible at 25kDa, this was not confirmed by Western Blotting. This may be due to protein degradation during storage. Due to time constraints no further expression of E2 was tried, however if time had allowed a different cell line and plasmid would have been tried.

The full length of the E6 protein was expressed as shown on Western blotting, the experiment was repeated numerous times, initially the protein was expressed with BL21 alone, no viable protein could be expressed, however with the addition of pLysS, which is a non-cloning vector and suppresses the T7 promoter by producing T7 lysosome which is an inhibitor of T7 RNA polymerase, E6 was expressed.

Previous studies have expressed E6 and E7 in E-coli cells (Di Bonito et al., 2006, Accardi et al., 2005), however the strains used were the JM109, unlike this study, which used the BL21 strain. The JM109 strain grows well and is transformed efficiently by a variety of methods. Because JM109 is recombinant and lacks the *E. coli* K restriction system, undesirable restriction of cloned DNA and recombination with host chromosomal DNA are prevented (Promega, 2016). The endonuclease A-mutation leads to an improved yield and quality of isolated plasmid DNA. However the BL21 competent cells were used as they contained pLysS, which suppressed the T7 promoter, if time had allowed further expressions with JM109 could have been trialed.

Di Bonito *et al.* also purified E6 and E7 by IMAC, difference is pooled fractions were neutralized to pH 8.8 by addition of Tris buffer and stored in urea buffer at -30°C. This study added 15 % (v/v) glycerol to the purified fractions for storage, however no buffer was used or the pH altered, this may have affected the storage and degradation of proteins, certainly in the case of E2NT (Di Bonito et al., 2006). The expressed and purified E6 and E7 proteins were stored at -20°C for application in ELISA.

Chapter 4. Enzyme Linked Immunosorbent Assays of antibodies against HPV oncoproteins in Human Sera

4.1 Introduction

An in-house Enzyme linked immunosorbent assay (ELISA) was developed for the detection of antibodies against HPV-16 oncoproteins, namely E6 and E7 in human serum samples. The direct ELISA used recombinant HPV-oncoproteins produced by *E.coli* immobilized on the plate (see section 3) as the capture target. The antibodies that were detected, if present, were from the serum of a series of patient samples. The aim was to measure levels of pre-treatment antibodies against two key oncoproteins produced by HPV.

HPV-E6 and -E7 oncoproteins are involved in the pathogenesis of HPV-associated cancer, they interfere with p53 and the Retinoblastoma protein (pRb) respectively, which are tumour suppressor proteins as described in section 1.7. E6 (Early protein 6) is a viral protein produced in cells infected with the Human Papillomavirus. E6 forms a complex with the host cell ubiquitin ligase E6AP (E6Associated Protein) generating a ligase activity that polyubiquitinates tumor suppressor p53 and targets it to 26S proteasome for degradation. As a result DNA damage and chromosomal instabilities increase, often leading to cell proliferation and cancer (Scheffner et al., 1993, Israels and Israels, 2000).

Anti-E7 response in sera has been used in HPV associated cervical cancer to monitor disease progression and response to treatment (Ravaggi et al., 2006, Park et al., 1998). It is believed that raised serum levels of antibodies against E7 confer improved outcomes in HPV positive HNSCC, in HNSCC it has previously been shown that antibodies are a late marker of disease (Rubenstein et al., 2011). The in-house ELISA was performed to establish levels of antibodies present against HPV-16 oncoproteins and whether these had a clinical reference with outcomes and stage of disease in HNSCC according to site of disease and also to assess if there was an antibody response in the normal population who may have been exposed to the virus.

4.2 Optimization of the ELISA method

The in-house ELISA was developed to ensure reproducibility and accuracy of results with low non-specific binding and few false positives. The ELISA was carried out as described in section 2.13, with the following steps taken for optimisation.

4.2.1 Binding Control for E7

In order to determine whether the His-tagged E7 protein was binding to the Maxisorp plate (Nunc) E7 protein diluted in carbonate buffer (0.05M) was added at varying dilutions (50µg/ml, 5µg/ml and 0.5µg/ml) to the Maxisorp plate (section 4.2), 100µl of diluted protein was added to triplicate wells (an average reading was taken) and the primary detection antibody used was the Mouse Anti-His antibody (MAH) as the E7 protein was His-tagged (see figure 4.1). This was used at dilutions of 2µg/ml, 1µg/ml and 0.5µg/ml (R&D) to determine the optimum concentration of antibody to detect E7-His tag as the manufacturers guidelines suggested 1-2µg/ml but for use in Western

Blotting. A goat-anti mouse HRP (Santa Cruz) was used as the detection antibody. Carbonate buffer (0.05M) alone was used to coat 12 wells of the 96-well plate as a negative control to check for non-specific binding instead of E7 protein. The MAH was diluted in phosphate buffered saline (PBS), this was used as a negative control for MAH and applied to 12 wells instead of MAH to check for non-specific binding.

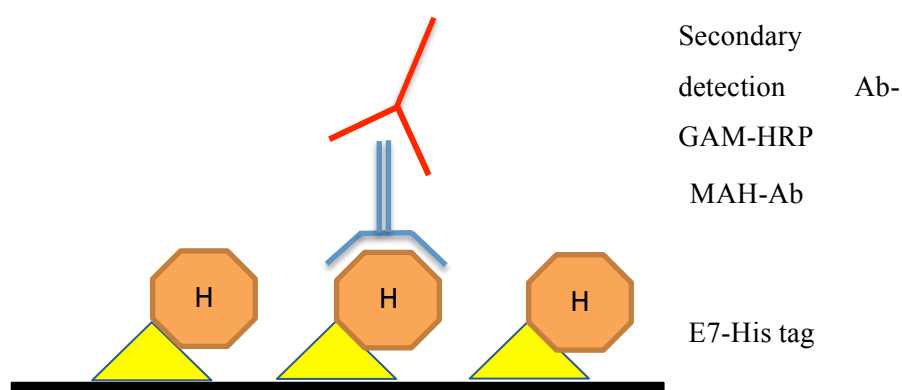


Figure 4.1 Representation of determination of binding control for E7. The E7 protein was His-tagged and the Mouse Anti-His antibody (MAH) was used as the primary detection antibody determining the binding of E7 to the plate, this was further detected by secondary detection antibody, Goat Anti-Mouse-HRP antibody.

Two independent experiments of the optimisation ELISA run (Figure 4.2a,b) unexpectedly showed that the highest readings were from the wells coated with carbonate buffer alone, although some binding of E7 was detected. The wells which had the MAH-Ab replaced with PBS as negative control also demonstrated binding, suggesting non-specific binding of the goat anti-mouse secondary detection antibody.

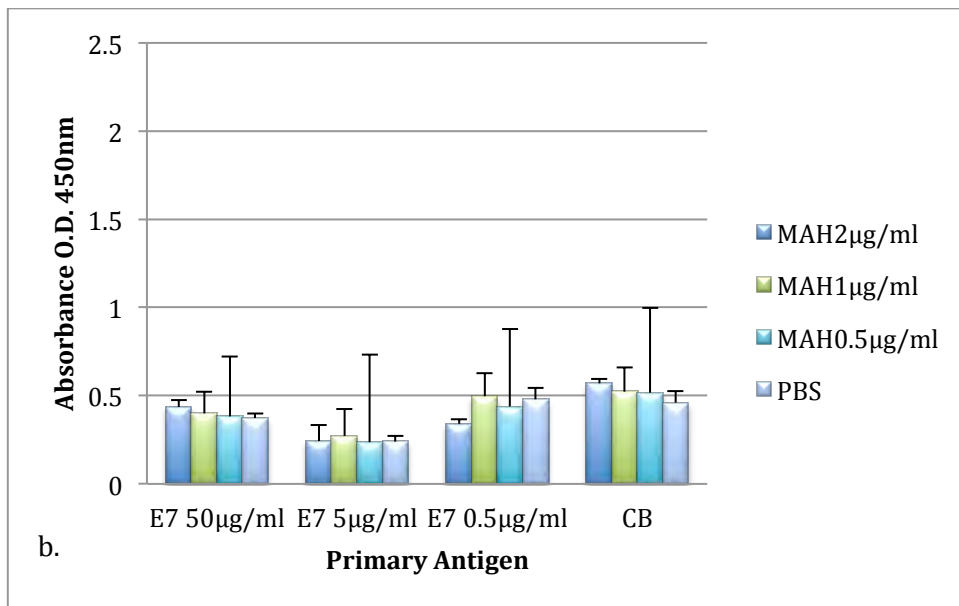
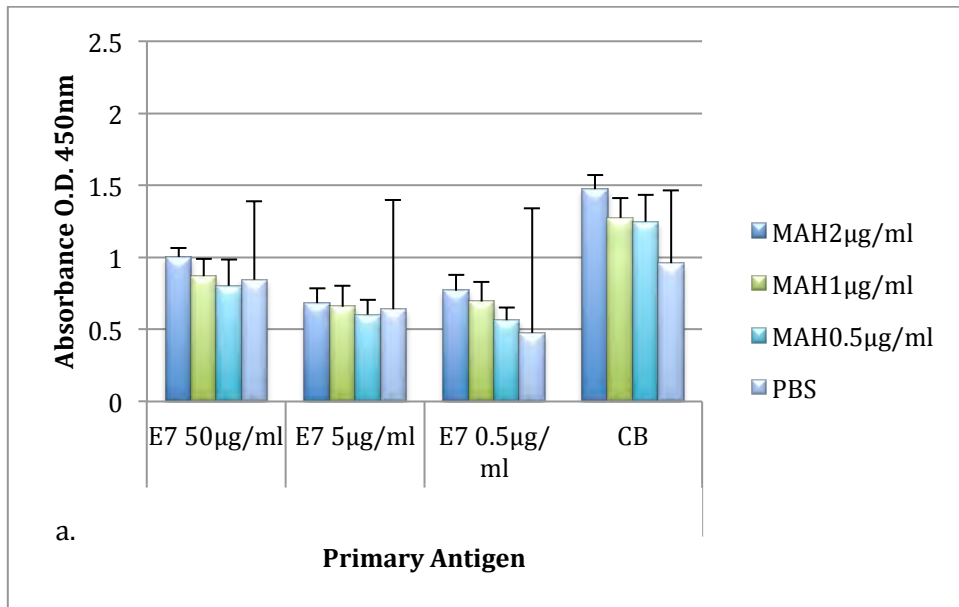


Figure 4.2a&b Absorbance values obtained following ELISA using varying concentrations of both E7 protein and Mouse anti-his (MAH) antibody. Carbonate buffer (CB, 0.05M) and PBS acted as negative controls for E7 and MAH respectively, values calculated from triplicate wells.

The initial results did not conclusively confirm binding of E7 therefore a commercial anti-E7 was purchased to check for the specific presence of E7 on the Maxisorp plate. HPV-16 Anti-E7 antibody (Santa-Cruz) was a mouse monoclonal IgG provided at 200µg/ml raised against amino acids 1-98 which represented the full length of the

HPV-16 E7 protein. The Maxisorp plate (Nunc) was coated with 5 μ g/ml of E7 protein and the ELISA performed as described in section 2.13 but with the use of 1% (w/v) non-fat dried milk (NFDM)-PBS as diluent. As no significant difference in the concentrations of MAH used was demonstrated above, 2 μ g/ml was used in triplicate wells along with anti E7 used at a dilution of 1:200, as recommended by the manufacturer. The negative control for both the MAH and Anti-E7 was the 1% (w/v) NFDM diluent used alone as the primary detection ‘antibody’. Figure 4.3 illustrates the positive reading with anti-E7 that confirmed the binding of the recombinant HPV-E7 to the Maxisorp plate, along with the low readings for the control NFDM. Although a higher reading was expected for the Mouse Anti-HIS antibody this may be explained by the His-protein tag being folded within the protein or by not being exposed on the surface for detection by the MAH-Ab.

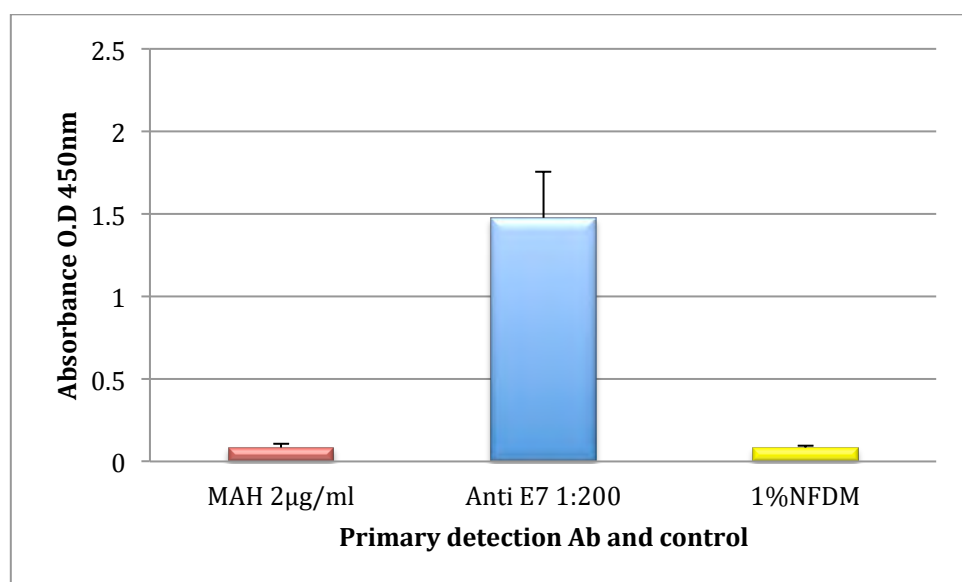


Figure 4.3 Binding control of recombinant HPV-E7 shown with Anti-E7 compared to negative control of 1% NFDM diluent and Mouse Anti-His antibody, representative of three repeat experiments.

4.2.2 Optimisation of E7 concentrations and serum dilutions

Determination of the optimal concentration of recombinant HPV-E7 to use was performed. The purified E7 protein was added to the ELISA plate at differing concentrations (50, 5 and 0.5 μ g/ml) to determine the optimum concentration to use. Local Research Ethics Committee approval was obtained in order to collect serum from healthy individuals to use as controls for the patient serum samples (see section 2.14). Healthy human serum samples (n=3; 100 μ l) were added to duplicate wells at neat and 1:50 dilution in 1% (w/v) NFDMPBS. The same sera were also added to wells coated with carbonate buffer alone to determine the degree of non-specific binding. NFDMPBS (1% w/v) was used in place of the serum to control for non-specific binding of the secondary antibodies.

Figures 4.4a & b illustrate high absorbance readings in all of the neat serums compared with their diluted counterparts showing the presence of antibodies in the serum to the E7 protein, and very little absorbance in comparison was detected when 1%NFDMPBS was substituted for the serum; confirming that the binding of the secondary antibody was specific. When comparing the differences in E7 concentration; no significant difference in the binding was seen between 50 and 5 μ g/ml, a lower reading with 0.5 μ g/ml E7 was observed. Therefore it was determined that 5 μ g/ml was the optimum dilution to proceed with as there was evidence of binding and would maximize the number of assays that could be undertaken. The E7 at 50 μ g/ml did not demonstrate higher proportional readings as expected, this may be due the prozone effect as presence of excess analyte reduces actual binding secondary to competition. Some non-specific binding of the serum was observed in the wells coated with CB alone, demonstrating the need for inclusion of NFDMPBS in the blocking buffers.

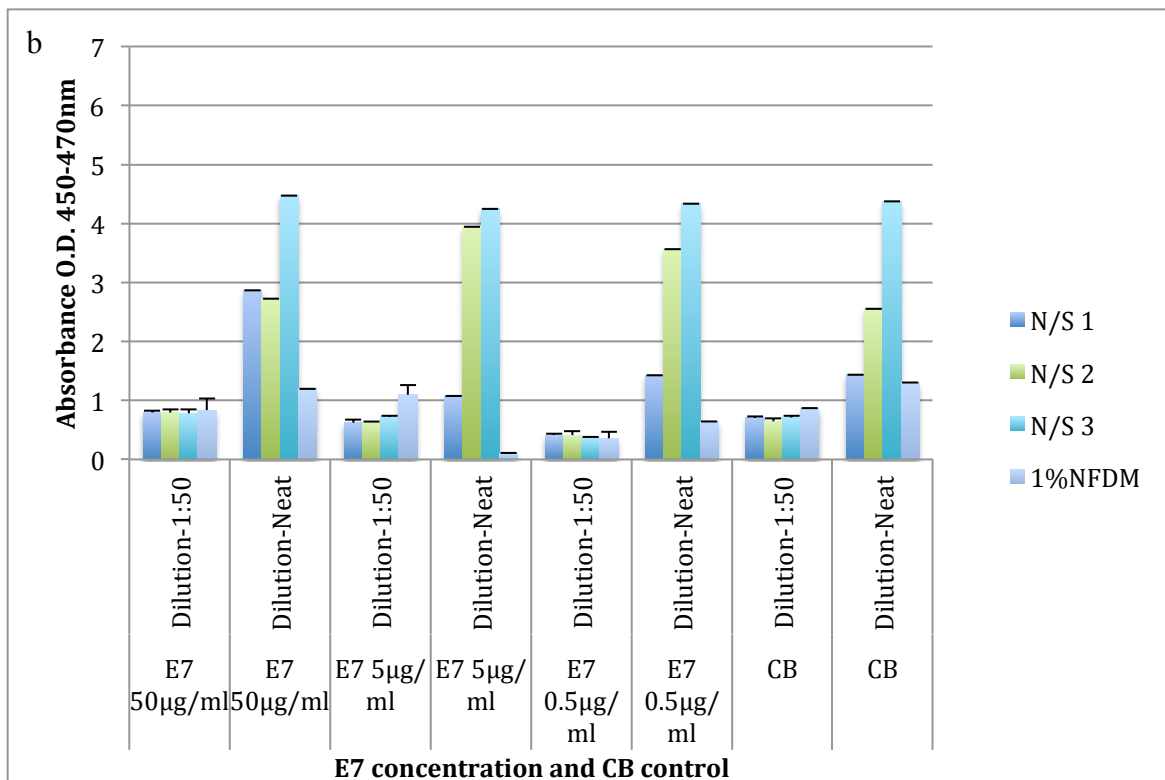
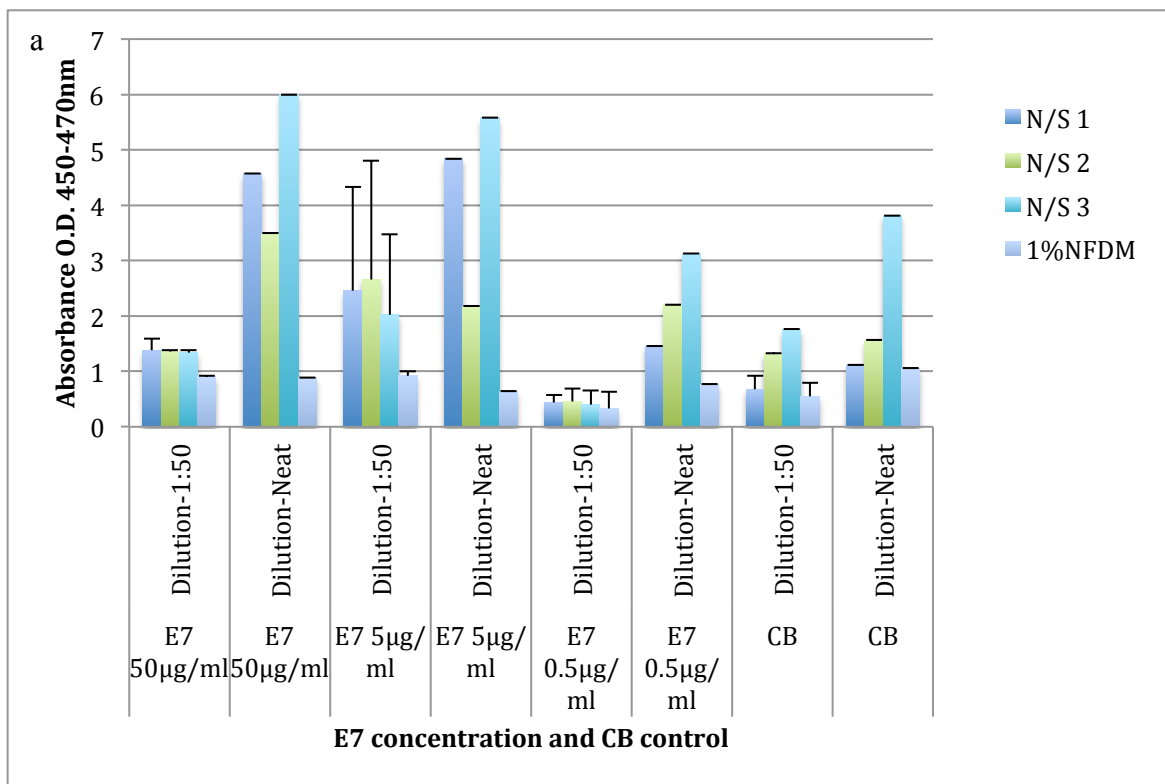


Figure 4.4a and b. Determination of optimum concentration of HPV-E7. Serum from healthy controls (N/S) was used neat and diluted 1:50 and average readings of triplicate wells is displayed, the E7 at 50µg/ml did not sure high readings as may be expected. Figures a and b are representative of duplicate repeat experiments.

4.2.3 Reducing non-specific binding

In order to reduce the non-specific binding of the serum antibodies to the ELISA plate further, the diluents used and the type and concentration of blocking buffer were altered, in addition to performing a wash after the insertion of blocking buffer or omitting this step.

Each well of a 96-well Maxisorp plate was coated with 100µl 0.05M carbonate buffer and incubated overnight at 4°C. Blocking buffer (300µl; 10% (v/v) Normal Goat Serum, 3%, 5% and 10% (w/v) NFDM in PBS) was added to duplicate wells and incubated for 2 hours at 37°C. Following incubation half of the plate (Figure 4.5) was washed with the automated plate washer using PBS & 0.05% Tween 20 (section 2.13), the remainder of the plate was blotted to remove excess blocking buffers.

PBS or 1% (w/v) NFDM diluents were added to the 96-well plate as indicated (Figure 4.5) and incubated for 1 hour at 37°C. A variety of diluents were used as the human sera was diluted in 1% (w/v) NFDM and the detection antibody was diluted in PBS. Following incubation goat anti-mouse HRP was used in the PBS and Goat anti-human HRP was used in the 1% (w/v) NFDM treated wells respectively at concentrations of 1:5000, 1:10,000 and 1:20,000 (Figure 4.5) so that the optimum concentration at which to use the secondary detection antibody could be identified.

Diluent added with secondary detection Anti HRP (diluent/anti-HRP)

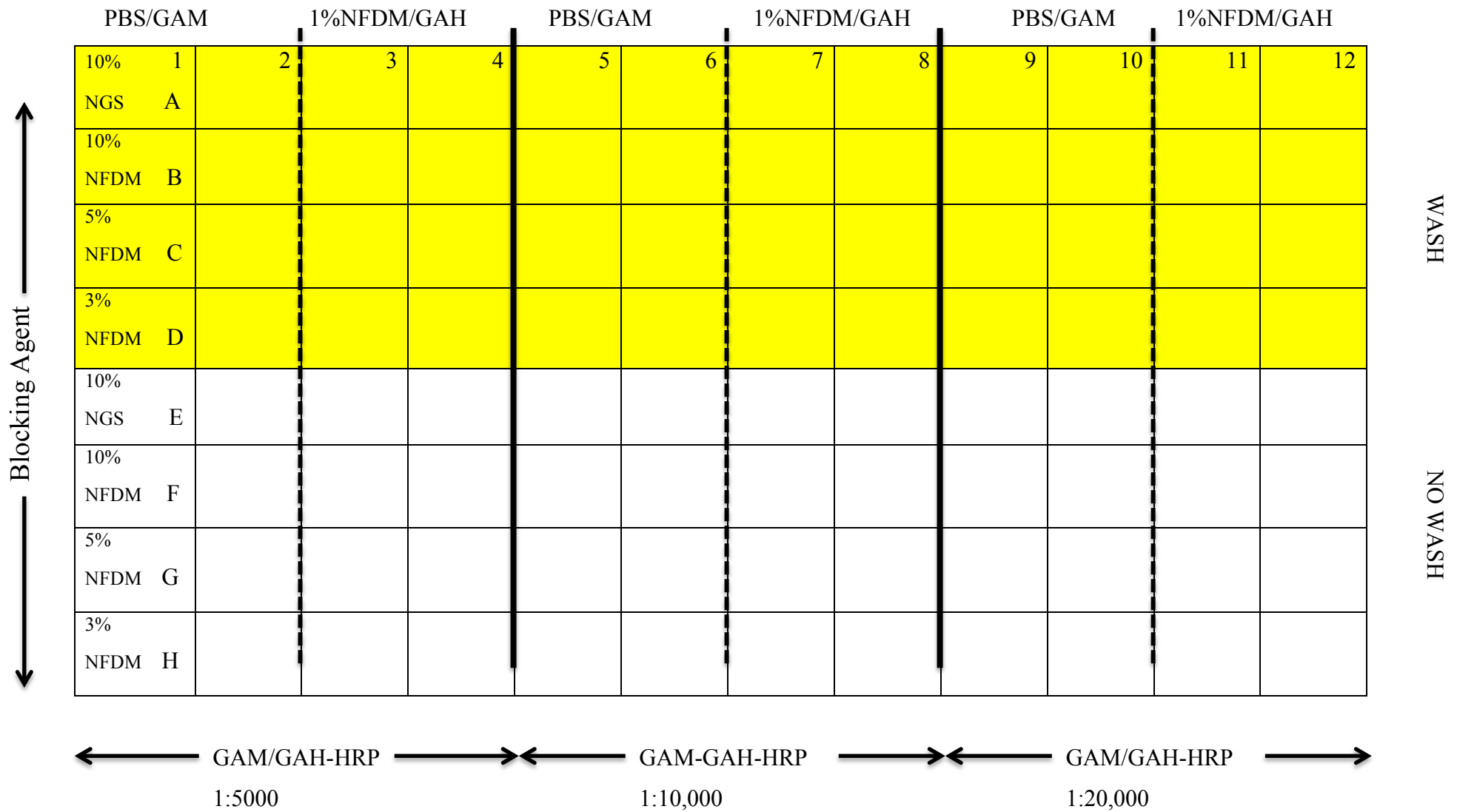


Figure 4.5 Plate set up for reducing non-specific binding of detection antibody and optimizing use of Anti-GAM/GAH-HRP . After coating the plate in Carbonate buffer, the plate set up was duplicated with rows A-D being washed after incubation and E-H not being washed with the various blocking agents. GAM-Goat anti-mouse and GAH-Goat anti-human HRP was added at differing concentrations as illustrated.

The optimum secondary detection antibody (GAH and GAM) concentration to use was the 1:10,000 as this gave minimal non-specific binding (<0.1 a.u.; Figure 4.6), and there was little difference between the 1:10,000 and 1:20,000 for both the GAM and GAH. There was no major difference observed in the level of non-specific binding observed between the blocking agents, NGS and NFDM or between the concentrations of NFDM used. Non-specific binding was slightly lower in the PBS group compared with the 1% NFDM diluent group, this may be that the 1% NFDM adsorbed to the Maxisorp plate was lost when the Maxisorp plate was washed after blocking, although there was reduced non-specific binding with PBS compared to 1% NFDM in the 'No wash' plate (see Figure 4.5b) the difference was less so, suggesting that the blocking agents were having some effect on non-specific binding. The results for the blocking agents were inconclusive therefore further experiments were performed to study the blocking agents (section 4.3.4). To reduce loss of blocking reagent the plates were not washed but rather blotted on paper to remove excess reagent. No significant difference was observed between the 10% normal goat serum blocking reagent and between the 3, 5 and 10% NFDM, therefore it was decided to use the 3% blocking reagent for all future studies.

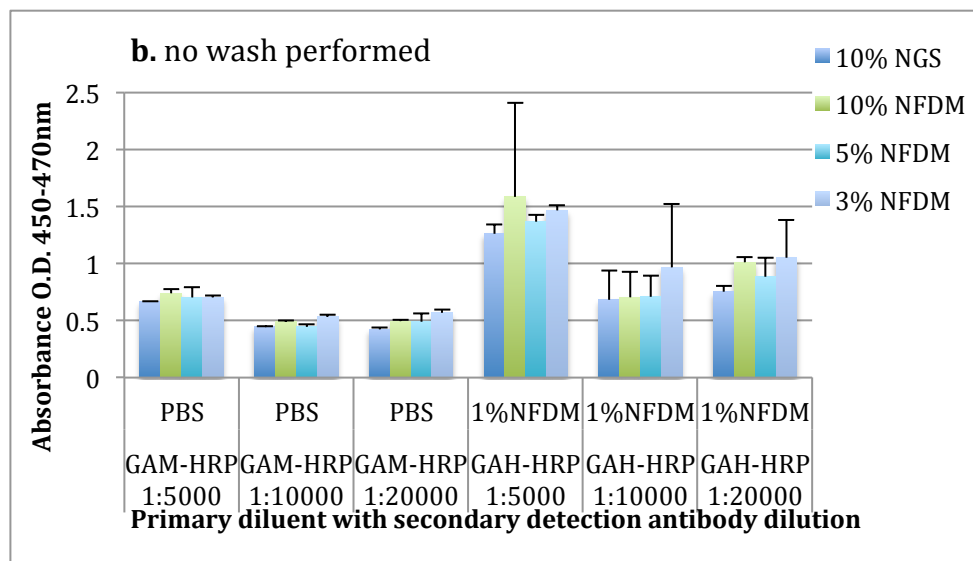
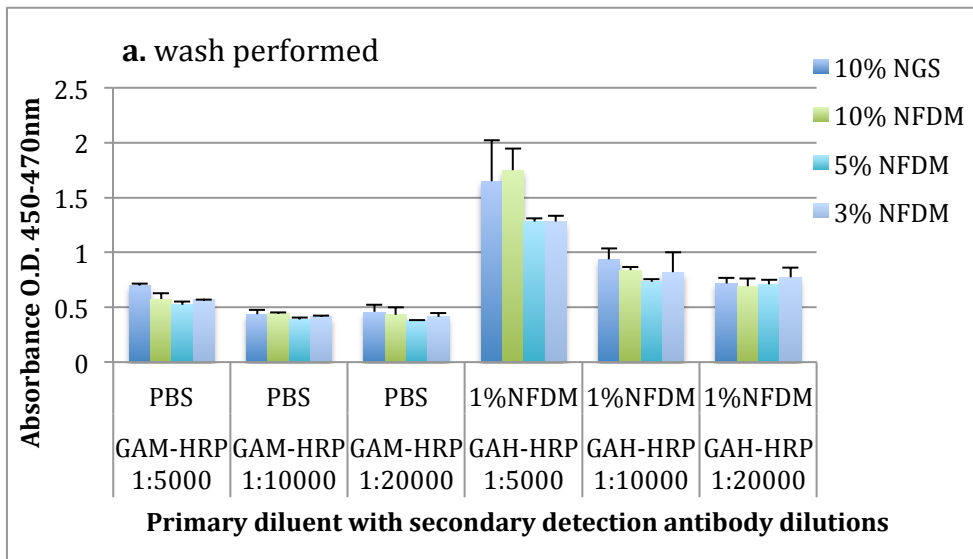


Figure 4.6 a and b. Comparison of blocking buffers, diluents and detection with variable dilutions of Goat-anti mouse or Goat-anti human HRP. There was a wash performed after blocking in figure a and no wash was performed after blocking in figure b.

4.2.4 Determination of optimum blocking reagents and diluents in Human sera

The initial diluents and blocking reagents and washes were determined with PBS, this

was then translated to use in human sera, this was to determine the optimum diluent and blocking reagent to use in sera.

In order to control for non-specific binding of the human sera to the Maxisorp plate the ELISA was carried out using a 96 well plate in which half of the wells were coated in HPV-E7 protein at 5µg/ml (100µl diluted in 0.05M carbonate buffer) and the other half was coated in 0.05M carbonate buffer alone. Human serum from healthy controls (n=3) and patients (n=3) were diluted in both PBS and 1% (w/v) NFDM (1:50) and added to triplicate wells to determine the best diluent. A blocking agent of 3% (w/v) NFDM was used and the ELISA was performed as described previously (section 2.13).

When serum was incubated with carbonate buffer alone the absorbance obtained was the same as when the E7 protein was used to coat the plate and this was apparent with both NFDM and PBS as the serum diluents (see Figure 4.7a and b), strongly suggesting that there was non-specific binding of the serum to the plate. This was confirmed as when 1% NFDM and PBS were used in place of the serum the readings were low both with CB and E7; this also showed that it was not non-specific binding of the secondary antibody which was the problem.

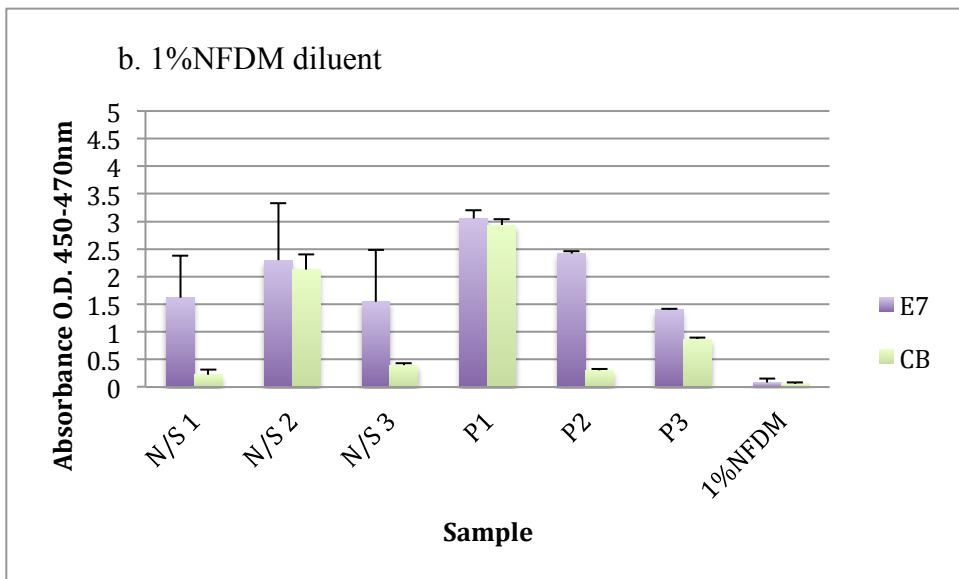
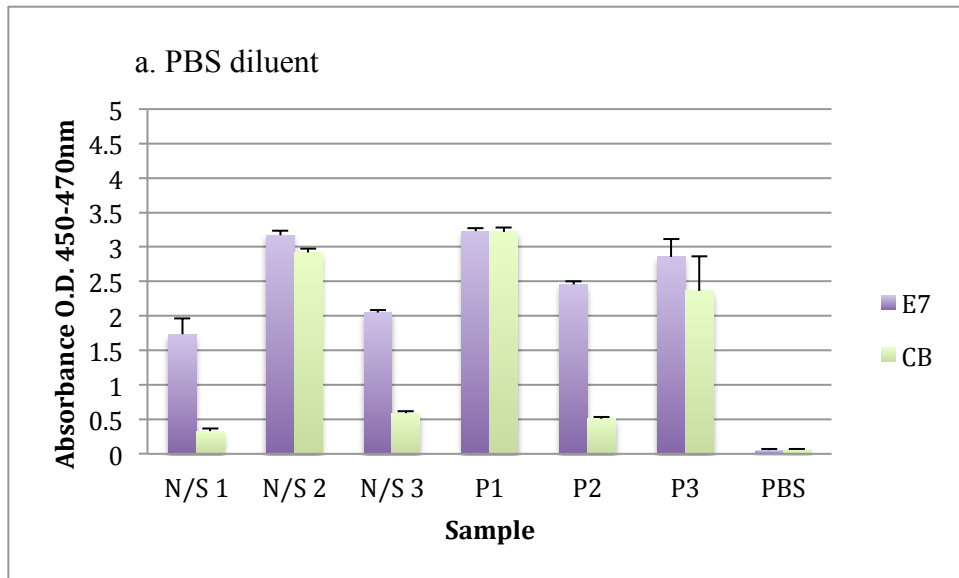
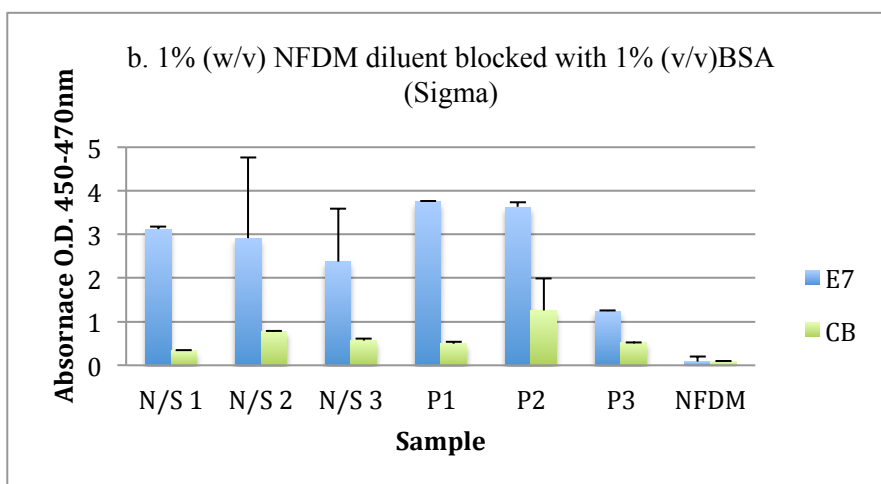
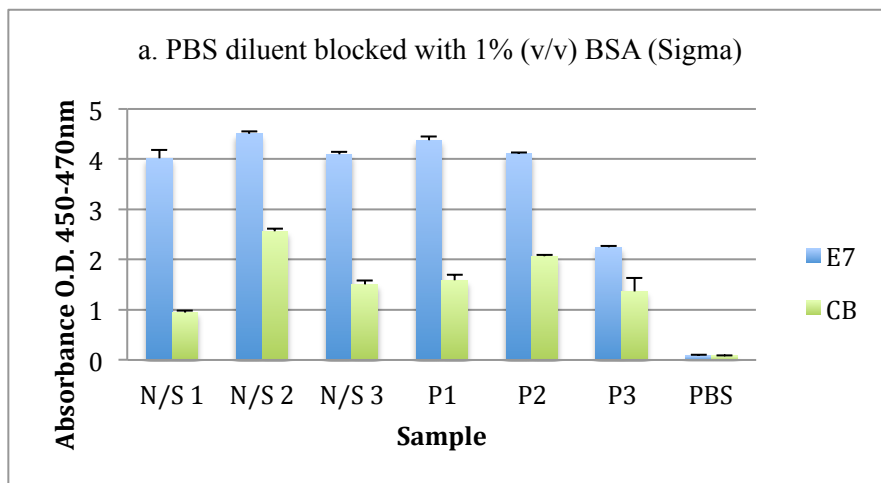


Figure 4.7a and b. Optimising diluents with human sera where N/S – normal serum from healthy controls and P represented patient sample serums. There was no significant difference in the absorbances for E7 or CB alone when either diluent was used.

The experiment was repeated using the same conditions except the blocking agent was changed to 1% bovine serum albumin (BSA) from two sources: Sigma and R&D systems. The R&D preparation was $\geq 98\%$ purity as compared with $\geq 96\%$ percentage from Sigma.

A higher level of non-specific binding was observed when PBS was used to dilute the human serum compared with 1% (w/v) NFDM (Figure 4.8a-d), this was opposite to what had been shown in the previous experiment and may be explained by the 1% (w/v) NFDM diluent providing additional blocking when used in human serum compared to PBS. Furthermore compared to previously used blocking agents of 10% (v/v) Normal Goat serum and varying concentrations of NFDM (Marvel), 1% (v/v) BSA (R&D) produced the lowest levels of non-specific binding of the serum components and provided improved blocking to reduce non-specific binding. Therefore it was concluded that the optimum diluent to use for human serum samples was the 1% (w/v) NFDM when blocking with 1% (v/v) BSA (R&D).



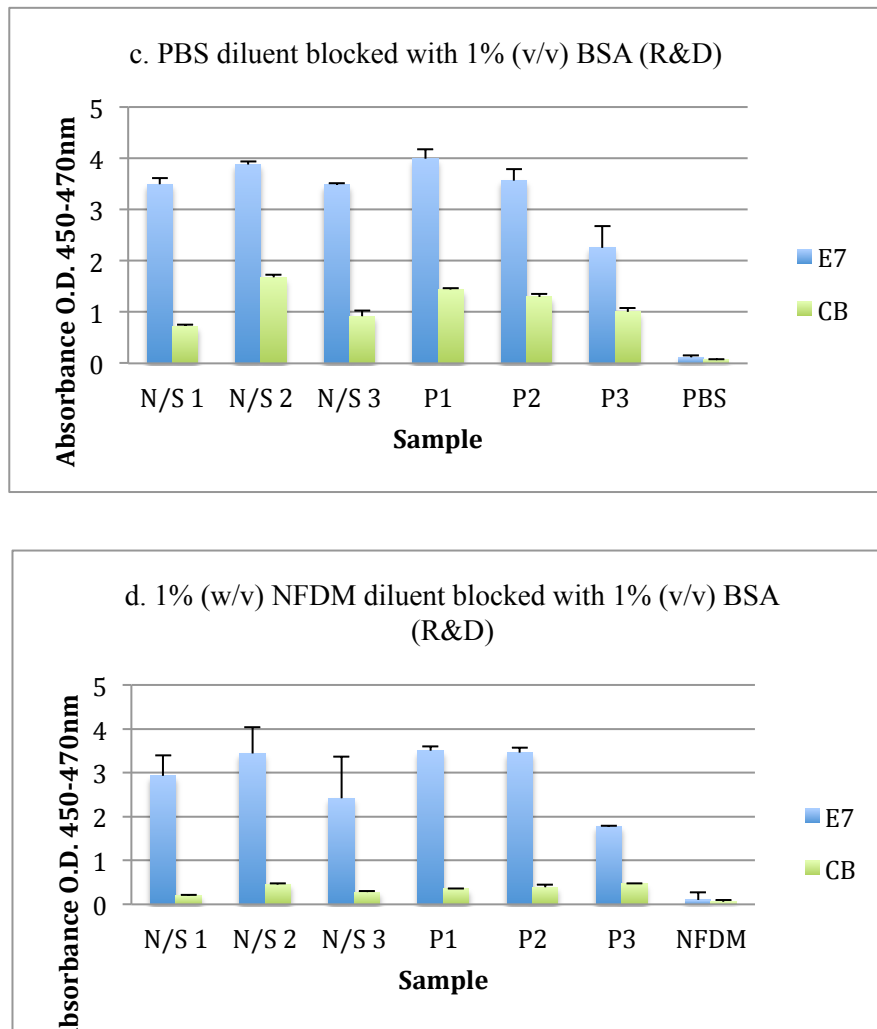


Figure 4.8 a-d illustrate the optimum diluent to use with human sera was 1% (w/v) NFDM and the optimum blocking agent being 1% bovine serum albumin (BSA, R&D), where N/S was healthy control normal samples and P was patient samples, the readings are representative of triplicate well readings.

4.2.5 Use of BSA as a diluent

Experiments were performed to ascertain whether 1% BSA would also improve the binding if used as a diluent as well as a blocking agent, the ELISA was conducted in the same fashion as described in section 4.2. From the results (Figure 4.9a and b) it was established that the optimum diluent to use was still 1% NFDM (Marvel) as this produced the lowest level of non-specific binding (<1.0 a.u) in the wells which had

been coated with carbonate buffer alone compared to the 1% BSA used as a diluent, the experiment was repeated and similar results were obtained.

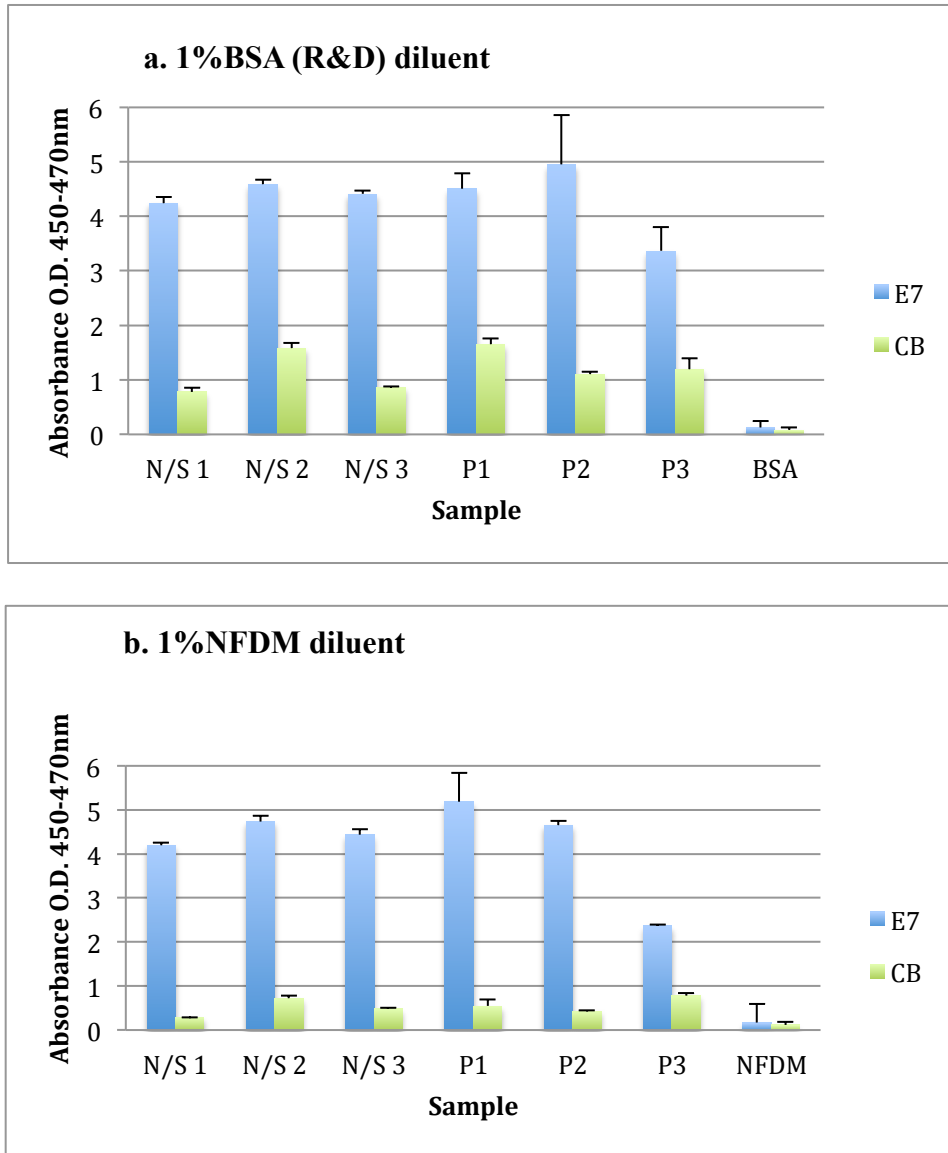


Figure 4.9a & b. Comparison of 1% bovine serum albumin(R&D) versus 1% NFDM as diluent, serum dilutions of 1:50 of healthy controls (N/S) versus patient samples (P).

4.3 Optimising serum concentrations

The next step was to establish the optimum dilution of human serum to use in order to maximize binding but minimize the prozone effect. The prozone effect is when the amount of antibody present in a sample exceeds the level of antigen and therefore antibody-antigen complexes do not form but rather the antigen becomes saturated by univalent antibody binding that gives false negative results due to loss with washing. Increasing dilutions of human serum in 1% NFDM from the healthy control group and patient samples were used (1:50, 1:500 and 1:5000) alongside diluent alone (1%NFDM) as a negative control. The ELISA was carried out as described above using the optimized coating and washing parameters (section 4.2). Briefly, the 96-well Maxisorp plate was coated in 5µg/ml of HPV-E7 and a second plate was coated in 0.05M carbonate buffer alone as control. The blocking agent used was 1% (v/v) BSA (R&D), serum samples were diluted in 1% (w/v) NFDM, the secondary detection antibody GAH-HRP was used at a concentration of 1:10,000 diluted in PBS.

In all of the patient and healthy control samples a decrease in absorbance was observed with increasing dilution of the serum as expected. However there was little difference observed between the patient and normal serum group, however this may have been due to the three patient samples selected not having high concentrations of antibody present (Fig. 4.10). Therefore the experiment was repeated under the same conditions but with the use of increased dilutions of 1:500, 1:5000 and 1:50,000 (Fig. 4.11) and larger cohorts of control (n=14) and patient (n=15) samples hopefully to allow better discrimination between these groups.

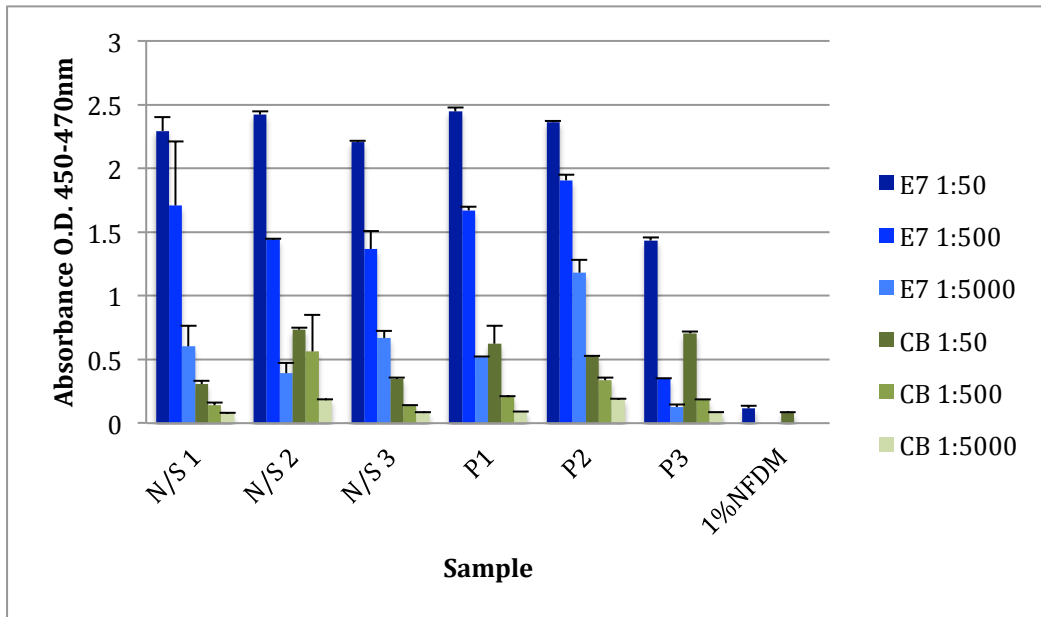


Figure 4.10 Variable serum dilutions (1:50, 1:500 and 1:5000) were added to E7 (5µg/ml) and CB as negative control to assess binding of antibodies, if present, within the serum samples, where N/S was normal serum from healthy controls and P was patient sample, the average from duplicate wells was taken as the absorbance.

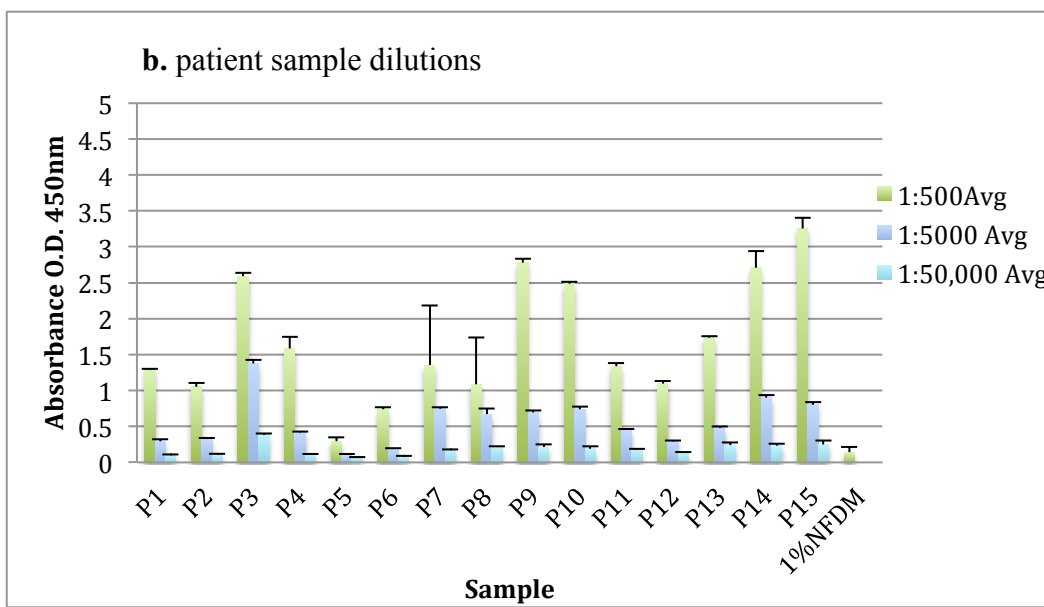
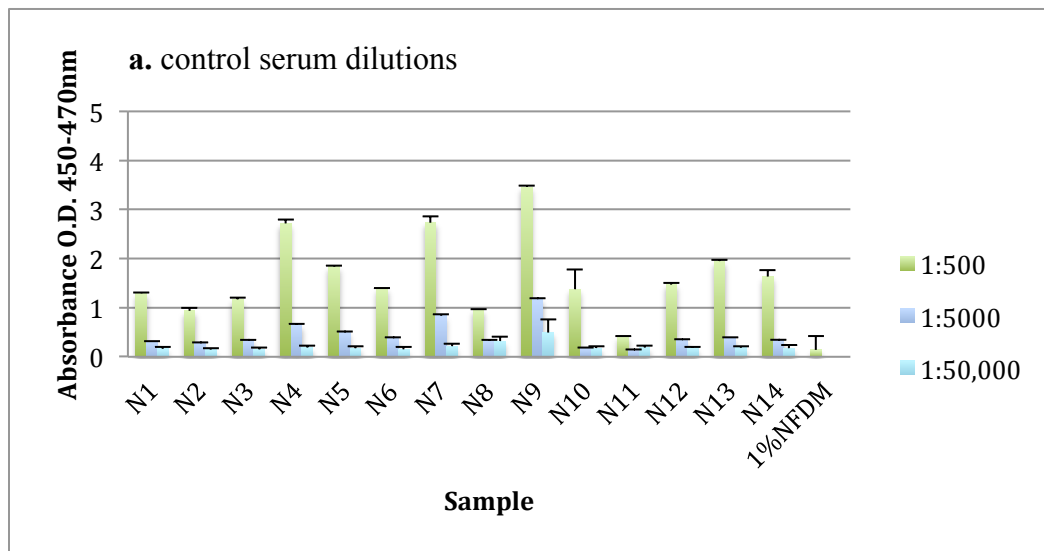


Figure 4.11 a & b. Increased serum dilutions of healthy controls(N) n=14, and patients (P), =15. A greater difference was observed for serum dilutions at greater dilutions compared to the previous 1:50 serum dilution in figure 4.10.

4.4 Determining positive cut off value

In order to establish a cut-off value for the optimised ELISA the average absorbance of triplicate wells of diluent (1% w/v NFDM) against bound E7 (0.5µg/ml) was calculated as 0.13. The cut-off value, above which results would be classed as positive, was then determined as 2 standard deviations above 0.13, which equated to 0.23.

4.5 Use of the optimised E7 ELISA to determine E7 antibody titres in control and HNSCC patient serum

ELISA was undertaken on a total of 86 HNSCC patient samples and 25 healthy controls (Figure 4.12). Two patient samples had to be removed as analysis of clinical records showed one to be a carcinoma of unknown origin, rather than oropharyngeal as labeled, and the other was from a benign mass.

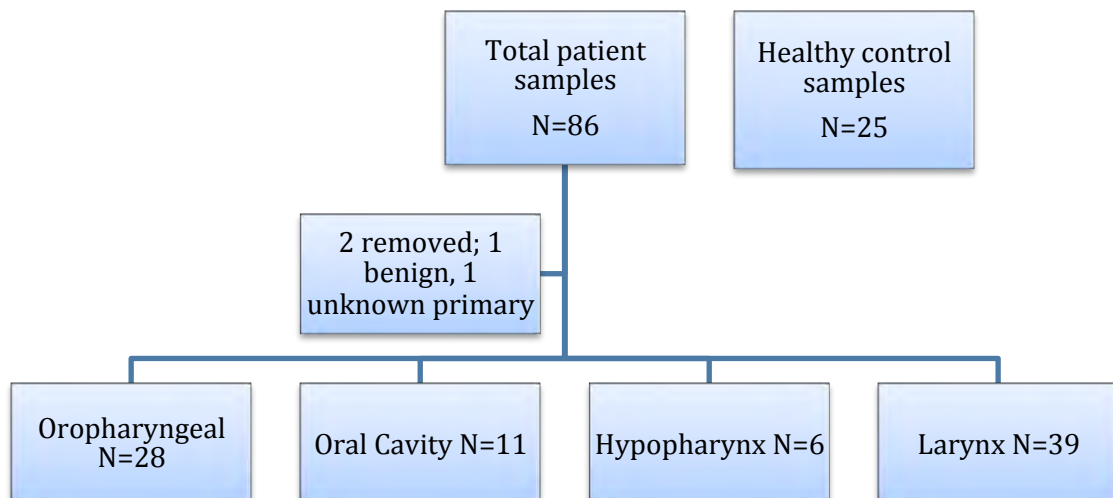


Figure 4.12 Patient and control samples and distribution of subsite of cancer

E7 antibody levels in the sera from healthy controls (n=25) and HNSCC patients (n=84) were determined using the optimised E7 ELISA (Figure 4.13). At 1:500 serum dilution all control samples mounted an immune response above the cut off threshold of 0.23, however this dropped down to 22/25 when serum dilutions of 1:5000 were used. Figure 4.13 illustrates the distribution of absorbance in the control and patient group at 1:500 and 1:5000 dilution around the mean segment. At 1:500 dilution the mean for the healthy control group was 1.88 ± 0.97 compared to 2.37 ± 1.08 for the entire patient group. The mean for the control group at 1:5000 dilution was 0.68 ± 0.67 compared to the patient group at 1.03 ± 0.76 . There was a statistical difference between the mean of the two groups, $t(107) = 2.009$, $p=0.047$ (*students unpaired t-test, IBM SPSS[®] version 19.*).

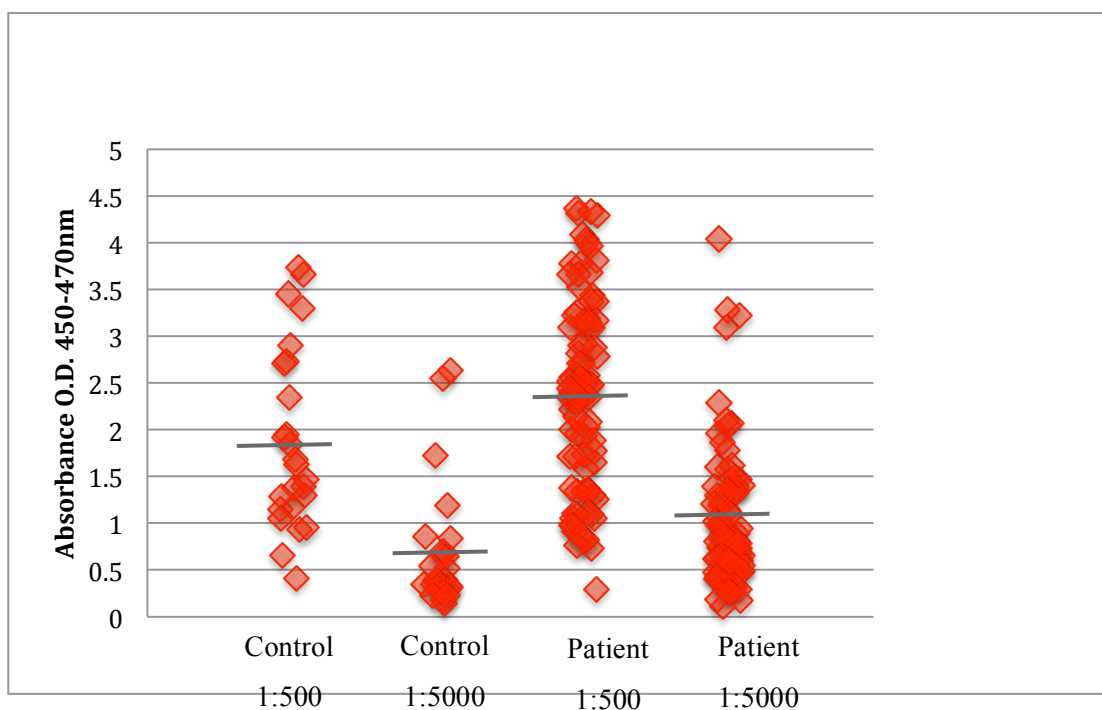


Figure 4.13 Average absorbance for patient (n=84) and control samples (n=25) at 1:500 and 1:5000 dilutions against E7 (5µg/ml) around the mean segment.

Of the 84 patient samples with ELISA performed 76 patients had cancer staging and nodal status available from available clinical records (see Chapter 6). The patient group was therefore further subdivided into Early (T1/T2 clinical stage) versus Late (T3/T4 clinical stage, appendix 1) HNSCC, as well as Node positive vs. Node negative groups (Figure 4.13). Statistical analysis was performed to assess for any difference between the groups. The average absorbance for Early HNSCC was 2.34 ± 1.11 compared with 2.38 ± 1.16 for Late HNSCC, there was no significant difference between the two groups, $p=0.87$ (*unpaired t-test*). For the Node positive (n=40) versus Node negative (n=36) group the average absorbance of E7 was 2.36 ± 1.24 and 2.34 ± 0.99 respectively, again there was no statistically significant difference, $p=0.95$ (*students unpaired t-test*).

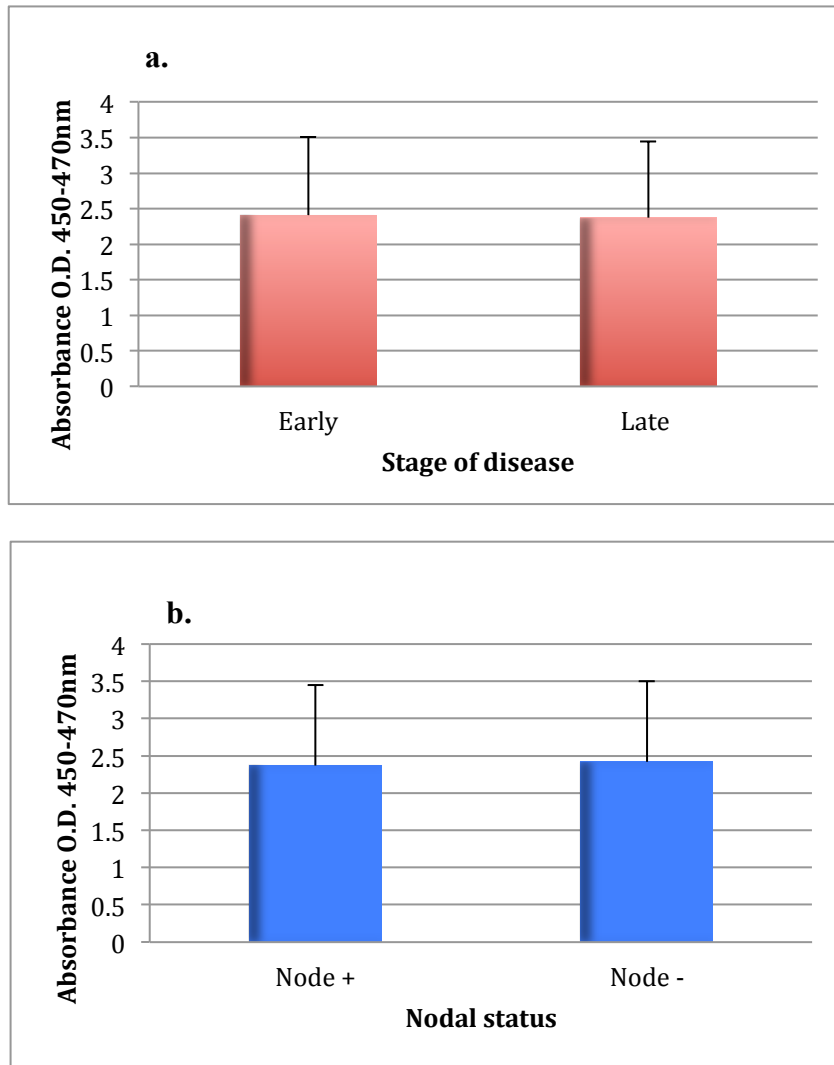


Figure 4.14a and b. Distribution of E7 seropositivity with standard error for early (T1/T2) versus late (T3/T4) HNSCC (a), and node positive versus node negative disease (b).

Due to the sample size the patient samples were divided into individual subsites (Figure 4.15). The average absorbance for each subsite of HNSCC (oral cavity, oropharyngeal, laryngeal and hypopharyngeal) is illustrated with standard deviation. The laryngeal subsite had the greatest absorbance at 1:500 dilution of serum for E7 (2.69 ± 1.10) followed by the Oropharyngeal group (2.19 ± 1.12). The statistical difference was calculated using students unpaired t-test (IBM® SPSS® System, Version 19) where $t(65) = 1.84$, $p = 0.07$. Although the oral cavity and hypopharyngeal group are illustrated on the graph the numbers were too small for statistical analysis ($n = 11$, and $n = 6$ respectively).

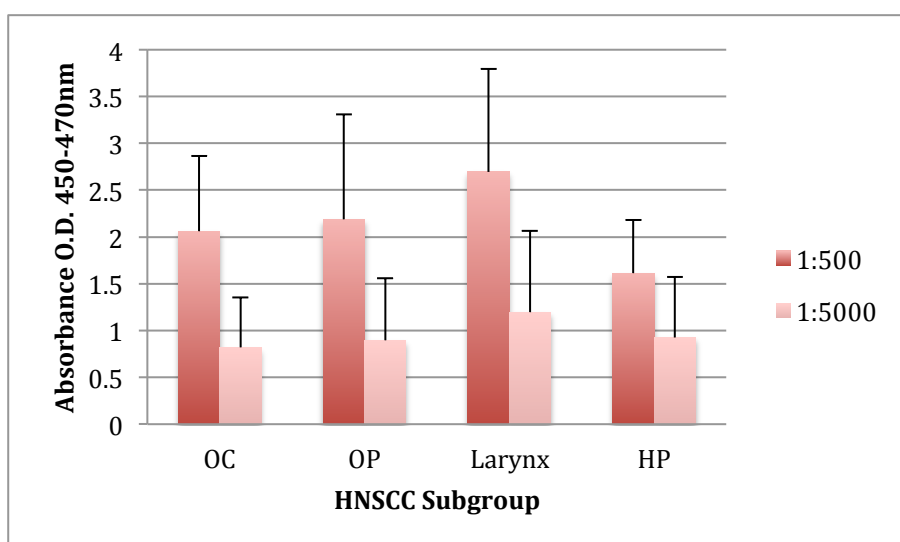


Figure 4.15 Absorbance values for all subgroups of HNSCC at serum dilution 1:500 and 1:5000 for HPV-E7. OC = oral cavity (n=11), OP = oropharyngeal (n=28), HP= hypopharyngeal (n=6) and Larynx =39.

For each subsite the results were further broken down to determine whether there was a relationship between tumour stage and / or nodal status. It was decided to show the results of the 1:500 dilution as all these had values above the cut off.

4.6 E7 Antibody titres for Oropharyngeal SCC

At serum dilutions of 1:500 all 28 oropharyngeal patient samples were seropositive for HPV-E7, however at serum dilutions of 1:5000 the E7 antibody was detected in only 25/28 patients. There was no statistically significant difference in the early (n=16) versus late (n=9) absorbance values for this group, mean 2.17 ± 1.09 vs. 2.30 ± 1.40 $p=0.8$ (students unpaired t-test) (See Figure 4.16a). However when comparing the nodal status although there was a slightly larger difference between the Node +ve (2.15 ± 1.31) compared with the Node -ve (2.43 ± 0.69), however this was not statistically significant, $p=0.63$ (students unpaired t-test) (Figure 4.16b).

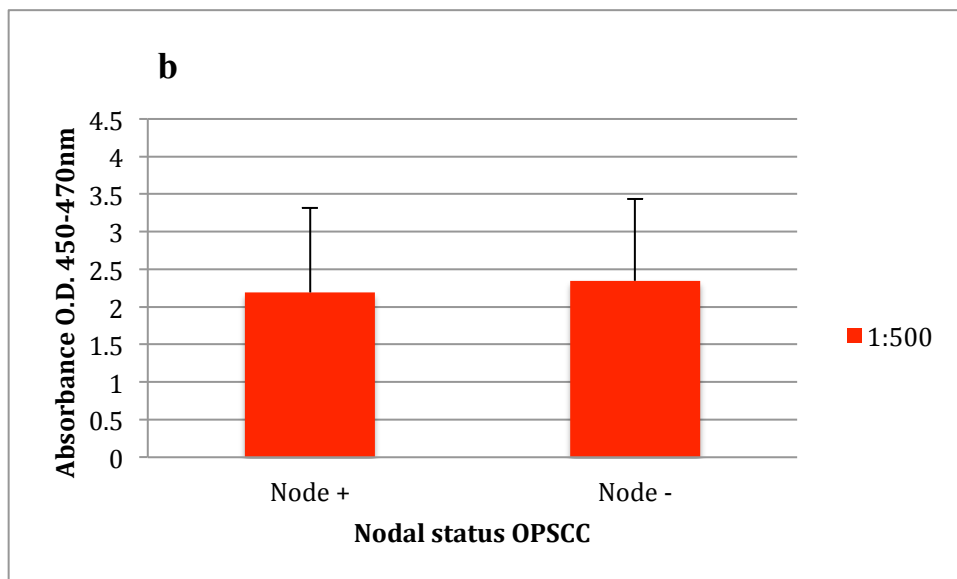
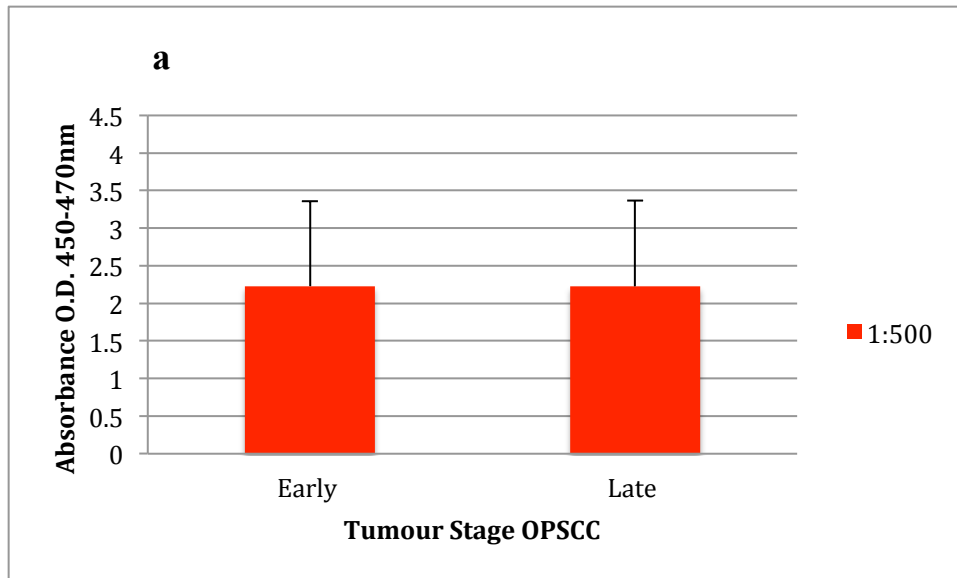


Figure 4.16 a & b. Average absorbance of anti-E7 for early (T1/T2) versus late (T3/T4) OPSCC (a) as determined by ELISA of patient sera, and Nodal status (b) at 1:500 serum dilution (n=28).

Although in the initial analysis of healthy controls versus all patient samples there was a significant difference between the absorbance, when comparing the absorbance for the OP subsite compared to healthy controls, there was no significant difference in the absorbance at 1:500 dilution, 2.19 ± 1.12 versus 1.88 ± 0.97 , $t(51) = -1.06$, $p=0.29$.

4.7 E7 Antibody titres for Oral Cavity SCC

There were only 11 patient samples available for the oral cavity (OC) group, making statistical analysis difficult, therefore general trends were observed. It was observed that with increasing grade of disease there was a greater amount of antibody present within the serum of patient samples, 10/11 patients mounted an antibody response based on the cut off value of 0.23 at a serum dilution of 1:500. Analysis of nodal status illustrated that the Node positive patients had a higher antibody level compared to the node negative as illustrated in the graph below (Fig. 4.17).

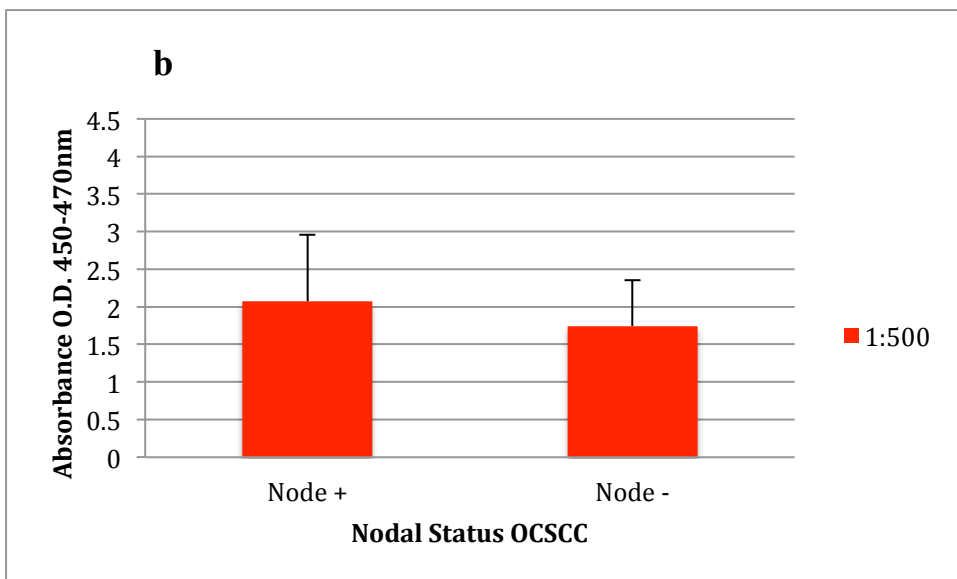
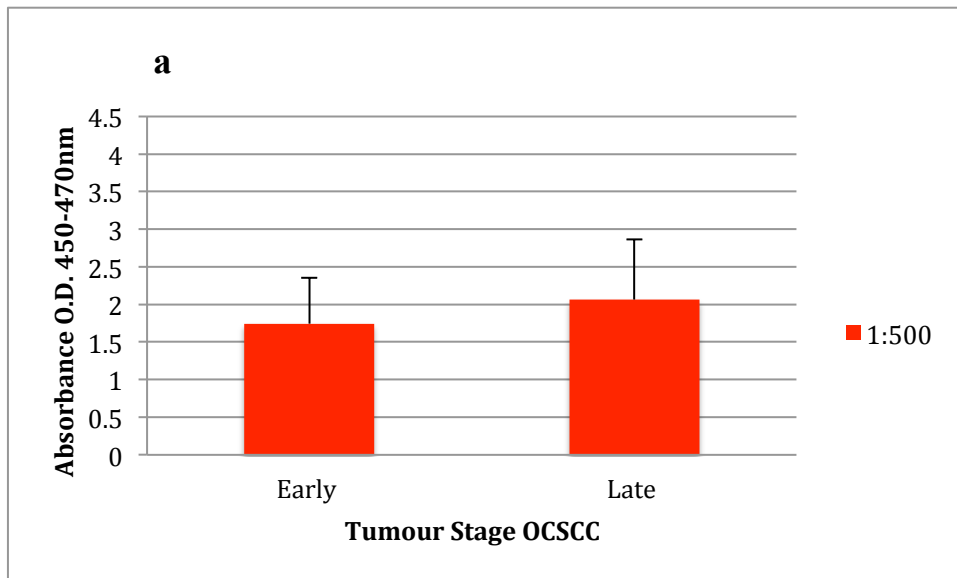


Figure 4.17 a & b. Average absorbance of OCSCC (n=11) at 1:500 dilution and comparison of nodal status. The average absorbance for node positive(n=5) was 2.07 a.u. and 1.75 a.u. for node negative (n=5). The average absorbance for early (n=6) stage was 1.74 a.u. and 2.06 a.u. for late stage (n=4), clinical data was not available for one sample.

4.8 E7 Antibody titres for Laryngeal SCC

There were a total of 39 laryngeal samples, Table 4.1 illustrates the distribution of samples according to grade of disease (see Appendix 1 for grades of disease).

Grade of laryngeal cancer	No. of patient samples
T1	10
T2	6
T3	11
T4	8
Unknown (Records not available)	4

Table 4.1 Distribution of Grade of Laryngeal SCC

Early laryngeal cancer (T1/T2; n=16) tended not to be associated with nodal disease, the average absorbance was 2.70 ± 1.22 compared with late (T3/T4, n=19) stage disease, 2.67 ± 1.12 , $p=0.93$ (students unpaired t-test). There was no significant difference between node positive and node negative disease status, with average absorbance for node positive disease (n=11) at 3.10 ± 1.22 compared with node negative (n=24) at 2.49 ± 1.09 , $p=0.15$ (students unpaired t-test).

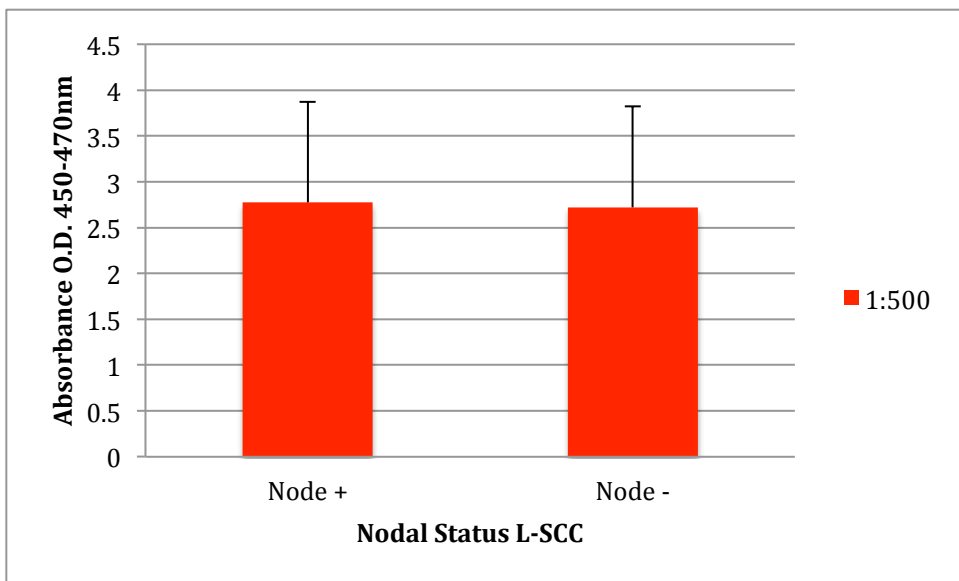
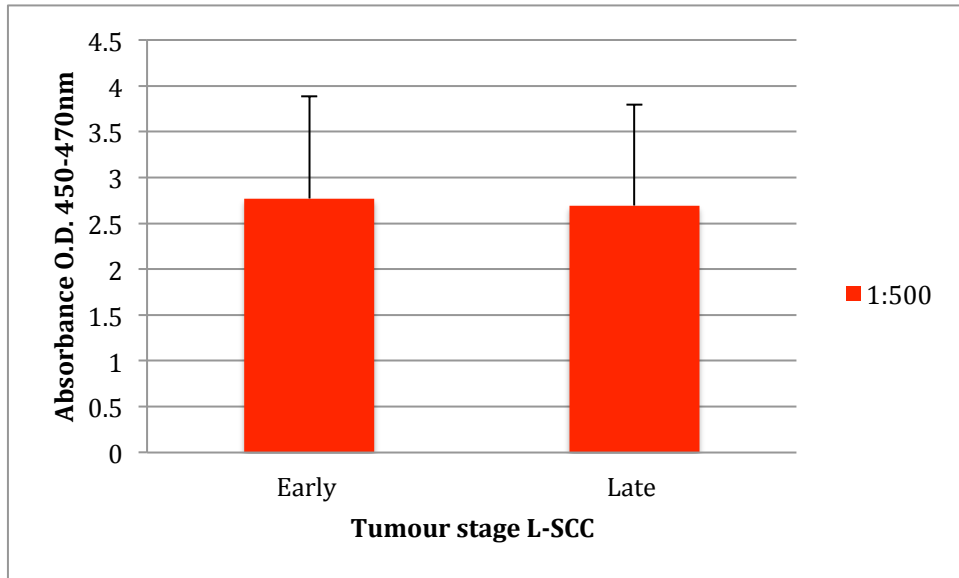


Figure 4.18 a and b Absorbance levels determined by ELISA of anti-E7 against early and late stage of disease and nodal status for Laryngeal SCC at 1:500 serum dilution.

4.9 E7 Antibody titres for Hypopharyngeal SCC

There were a total of 6 hypopharyngeal SCC patient samples, of which 1 sample was T3 and 5 were grade T4. All samples were seropositive and above the cut off threshold of 0.23 at serum dilution of 1:500. The average serum antibody level for

hypopharyngeal cancer was 1.61 ± 0.56 (Fig.1.9). Due to the small sample size statistical analysis was not performed.

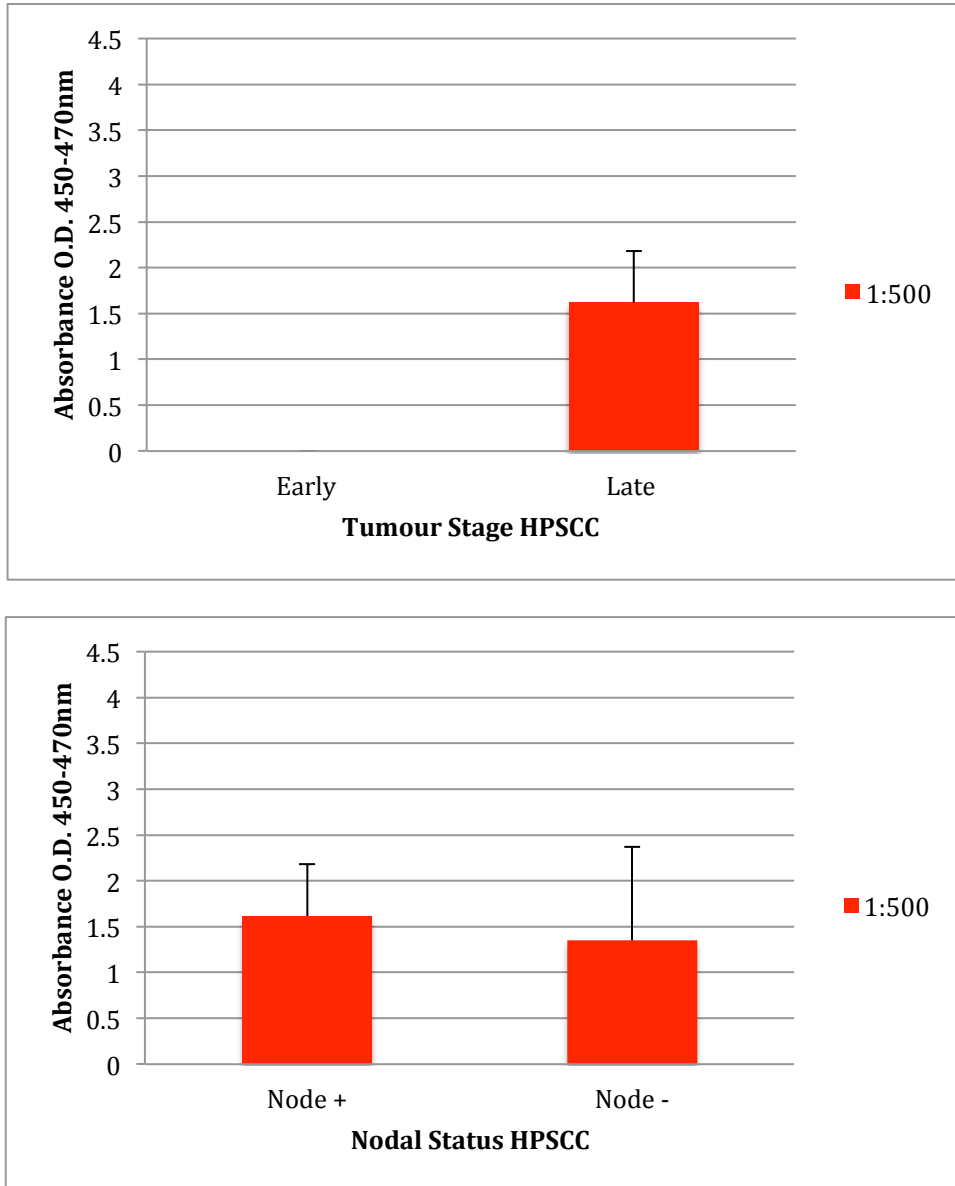


Figure 4.19 Average absorbance for E7 determined by ELISA for late HPSCC (n=6) was 1.61 a.u. and for Node positive (n=5) this was 1.61 a.u. compared to 1.35 a.u. for node negative (n=1) disease, there were no early HPSCC in this cohort.

4.10 Development of the HPV-E6 ELISA

Recombinant viral HPV-E6 was purchased (Boston Biochem, R&D) due to the difficulties with harvesting and purifying HPV-E6 in-house despite extensive experimentation (Chapter 3). The recombinant HPV-E6 had a molecular mass of 19kDa, it was derived from *E.coli* and had 6 cysteine to serine substitutions at positions 23, 58, 87, 104, 118 and 147. It had a purification of >98% which was achieved by SDS-PAGE under reducing conditions and visualised by Colloidal Coomassie® Blue stain.

The ELISA for the E6 antibody was based around the same model that was developed for HPV-E7 (section 4.3), with some modifications. The recombinant E6 for coating the ELISA plate was used at lower concentrations during optimization based on the manufacturer's recommendation. In order to establish the optimum concentration of E6 for binding to the Maxisorp plate, it was coated with 50µl of E6 (1µg/ml, 0.5µg/ml and 0.25µg/ml) diluted in carbonate buffer, and a negative control of 0.05M carbonate buffer alone was used to coat the remaining half of the plate (Fig. 4.20). E6 was allowed to bind to the plate overnight at 4°C before washing as described for the E7 ELISA. The plate was then blocked with 1% (v/v) BSA (R&D) and incubated at 37°C for 4 hours. No wash was performed after this stage. An anti-E6 (Santa-Cruz) antibody was used at 1:200 to detect the binding of the E6 to the plate and 1% (w/v) NFDM was used to control for non-specific binding of the secondary GAM-HRP.

Anti-E6 (Santa Cruz) was added to two wells (B1, B2) to firstly check for E6 binding to the Maxisorp plate and also to two others as a negative control to rule out non-specific binding of anti-E6 as these wells contained carbonate buffer (E6 diluent) only

and not the recombinant E6 protein. Blocking buffer (1% (w/v) NFDM) was added to columns A3-6, this was to check for non-specific binding of this diluent, with both secondary detection antibodies GAM-HRP (which was used to detect Anti-E6) and GAH-HRP (this was used for serum anti-E6 detection), the ELISA was conducted in the same way as described for E7 (section 4.3).

	E6 1µg/ml		E6 0.5µg/ml		E6 0.25µg/ml		CB	
	1	2	3	4	5	6	7	8
A	Anti-E6 1:200	Anti-E6 1:200	1% NFDM	1% NFDM	1% NFDM	1% NFDM	Anti-E6 1:200	Anti-E6 1:200

Figure 4.20 Optimisation of use of E6 protein and testing negative controls. Anti E6 was added to A1-2 to check for binding control and to B7-8 as negative control. The variable dilution of E6 and CB control are indicated above row A. 1% NFDM was added to row A3-6.

The initial results illustrated that there was some binding of recombinant E6 to the Maxisorp plate as there was an increased absorbance when the anti-E6 was added to wells coated in E6 (0.55 a.u.) compared to those coated with carbonate buffer alone (0.16 a.u), figure 4.21 is representative of three repeats of this experiment.

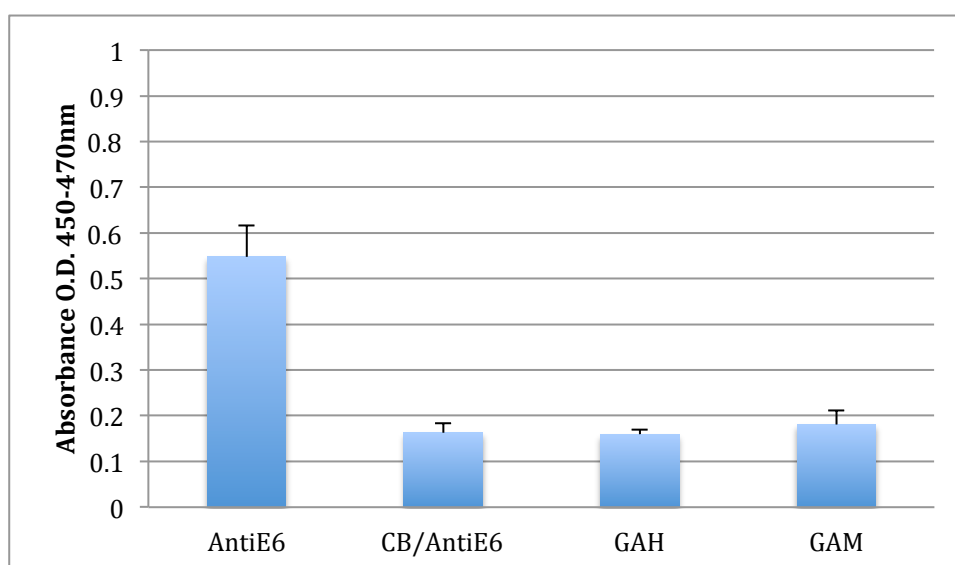


Figure 4.21 Average absorbance values for E6; binding control for E6 antigen was shown by anti-E6 absorbance levels compared to the negative control of carbonate buffer (CB) alone, (representative of three repeats).

4.11 Using the optimised E6 ELISA to determine E6 antibody titres in control and HNSCC patient serum

Experimentation on the optimum level of E6 protein to use on the Maxisorp plate revealed no significant difference between the E6 concentrations of 1µg/ml, 0.5µg/ml and 0.25µg/ml (results not shown), therefore it was decided to proceed with the 0.25µg/ml as this would allow multiple repeat experiments to be undertaken. Half of a 96-well plate (Nunc) was coated with 0.25µg/ml of E6 (Boston Biochem) with the remainder being coated with 0.05M carbonate buffer as control. Healthy control serum and patient samples were tested in the E6 ELISA at dilutions of 1:500, 1:5000 and 1:50,000. Negative controls using 1% (w/v) NFDM were also used to check for non-specific binding of the serum. The same standardized conditions and steps were performed as described in section 4.3.

No difference in absorbance was observed between the control groups and patient samples. The negative controls for the control (N9) and patient (T171) serum samples added to wells coated in carbonate buffer only, gave high levels of absorbance compared with the same samples added to wells coated in the E6 protein. Anti-E6 showed less binding with E6 at a concentration of 0.25µg/ml compared to the 1.0µg/ml previously.

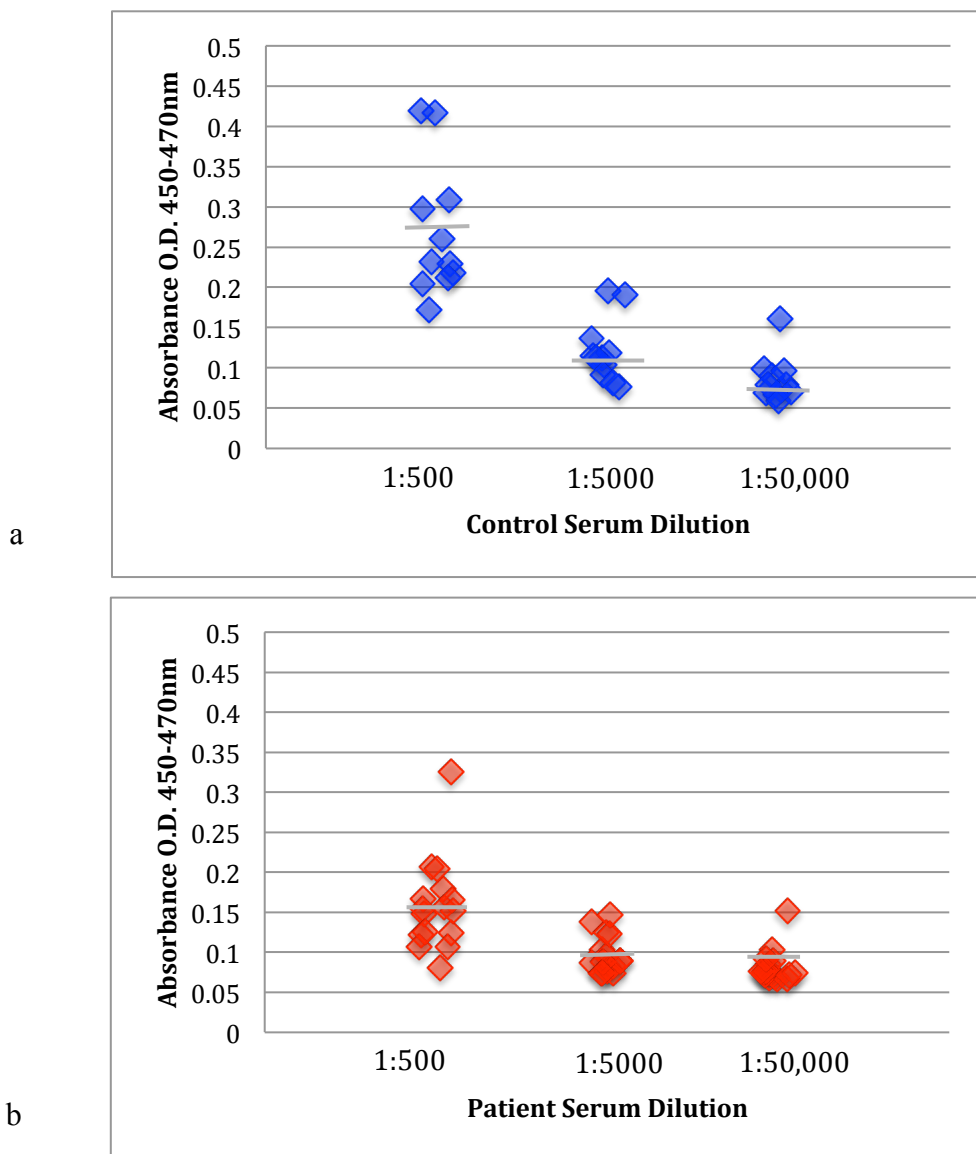


Figure 4.22 a and b. Healthy control and patient absorbance levels for E6 determined by ELISA around the mean segment at serum dilutions of 1:500, -5000 and -50,000. There was no significant difference between the two groups.

A control experiment was conducted to analyse whether the results obtained for control and patient samples in Figure 4.22 were spurious or not. A random control and patient sample were selected and tested against E6 and CB on the Maxisorp plate as for E7 (section 4.3), negative controls for the secondary detection antibodies GAM and GAH were also tested, in addition to Anti-E6 (Santa-Cruz) to check for binding control of E6. The results (see Figure 4.23) illustrated that with increasing serum

dilution the absorbance values were reducing, therefore there was no sample overload. However it was interesting to observe that the negative control samples for both the healthy control and patient sample showed increased absorbance values when tested against CB alone compared to E6. Furthermore although the absorbance of Anti-E6 was higher than when tested against the negative control CB alone (0.14 vs 0.11), this was not significant. Therefore it was concluded that there might not have been enough E6 protein bound to the Maxisorp plate and the higher absorbance readings for the negative controls could be explained by non-specific binding.

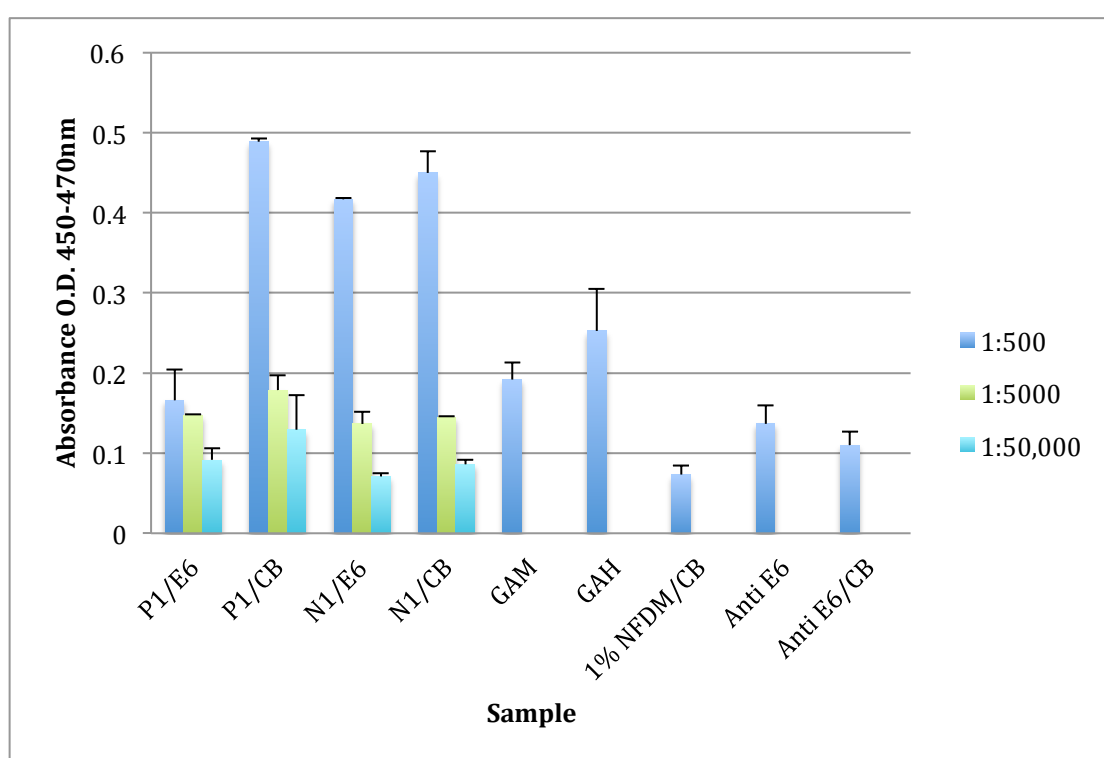


Figure 4.23 Absorbance values for control and patient sample when tested against E6 and negative control CB alone with variable sample dilution.

In order to try and maximize binding the experiment was repeated with a higher concentration (0.75µg/ml) of E6 recombinant protein to coat the plate. A single

patient sample was used (T171) at varying concentrations of 1:500, 1:5000 and 1:50,000. Blocking agent BSA (R&D) was used at concentrations of 1% and 2%. The absorbance values obtained from the negative control of carbonate buffer alone were still comparable to readings with recombinant E6 (see Figure 4.24) suggesting that the recombinant protein was low therefore within the wells containing CB alone, this could be explained by non-specific binding of serum to the Maxisorp plate. Anti-E6 did not show high readings compared with its negative control, 0.13 ± 0.01 a.u. compared to 0.09 ± 0.01 a.u. The experiment was repeated using higher concentrations of E6. There was increased absorbance when 2% BSA was used as blocking agent compared to 1% BSA, however this was also true for the control CB, $p=0.49$ (student's unpaired t-test).

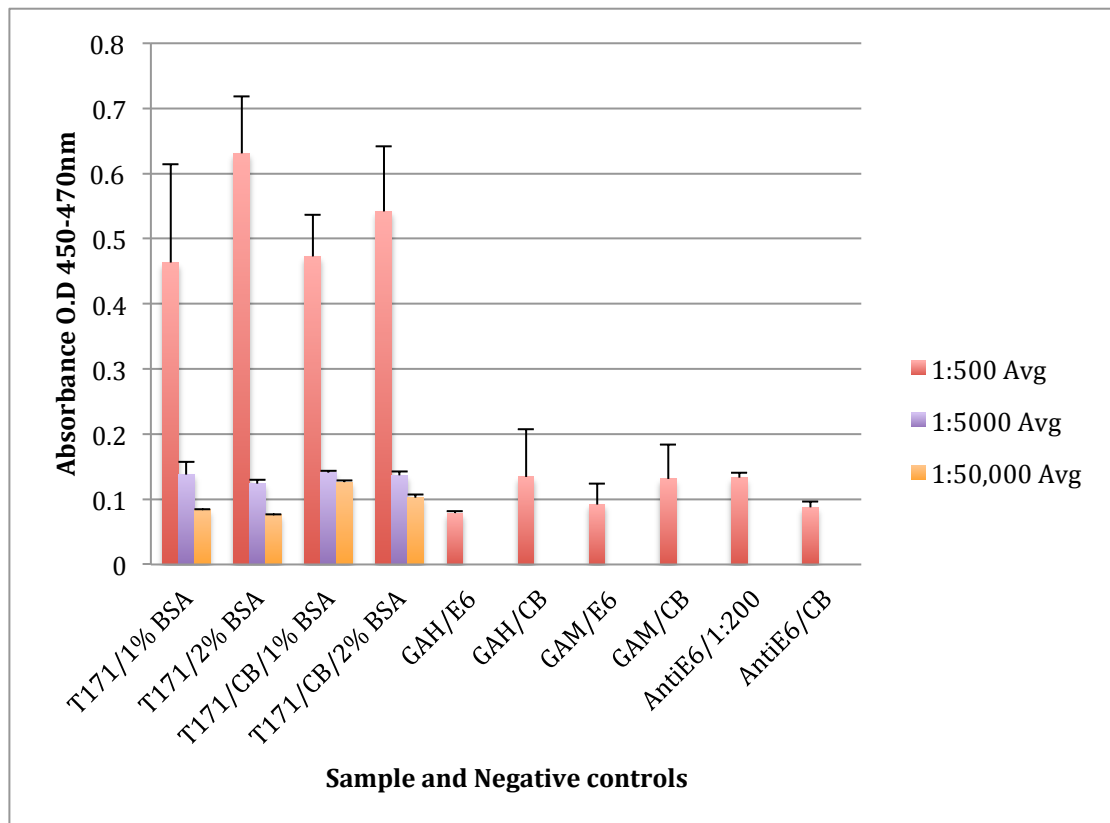


Figure 4.24 Absorbance values for a single patient sample and negative controls with $0.75\mu\text{g/ml}$ of E6 to check for serum and non-specific binding. Anti-E6 was also added to check for binding control for E6.

4.12 Increasing concentrations of plate bound E6

Although there was some evidence of E6 binding to the plate (section 4.10), no significance difference was observed for the serum samples when compared to CB alone. The experiment was repeated under the same standardized conditions but with increasing concentrations of bound E6 (1 μ g/ml, 2 μ g/ml) and CB alone. As demonstrated in Figure 4.24 no significant difference was observed when using 1% BSA compared to 2% BSA, therefore 1% BSA was used from this point onwards.

The previous experiment showed that there was reducing absorbance with increasing serum dilution therefore the 1:500 serum dilution was used from this point onwards. Two patient serum samples were used during this optimization. All remaining steps were carried out as described in section 4.10. Negative controls for each step of the ELISA were also carried out to ascertain where, if non-specific binding was occurring.

Figure 4.25 shows that all negative controls for the secondary detection antibodies and diluents were at a minimum level, thereby ruling out non-specific binding. Although there was an increase in absorbance detected following coating with 2 μ g/ml compared to 1 μ g/ml, this difference was not significant, $p > 0.5$ (student's unpaired t-test). Although the absorbance detected for CB compared E6 was lower (0.35a.u.) this difference was not significant, $p > 0.5$ (student's unpaired t-test).

A higher reading was detected for Anti-E6 when 2 μ g/ml compared to 1 μ g/ml of recombinant protein was used, however the Anti-E6 negative control tested against CB also detected absorbance levels which were not significantly different, $p > 0.5$

(student's unpaired t-test). Although some binding of E6 was illustrated by Anti-E6 with increasing concentrations this was not translated when serum was added, thereby it was difficult to interpret whether this was secondary to insufficient concentration of E6 present and bound to the plate or whether there was a problem with serum antibodies binding to the recombinant protein.

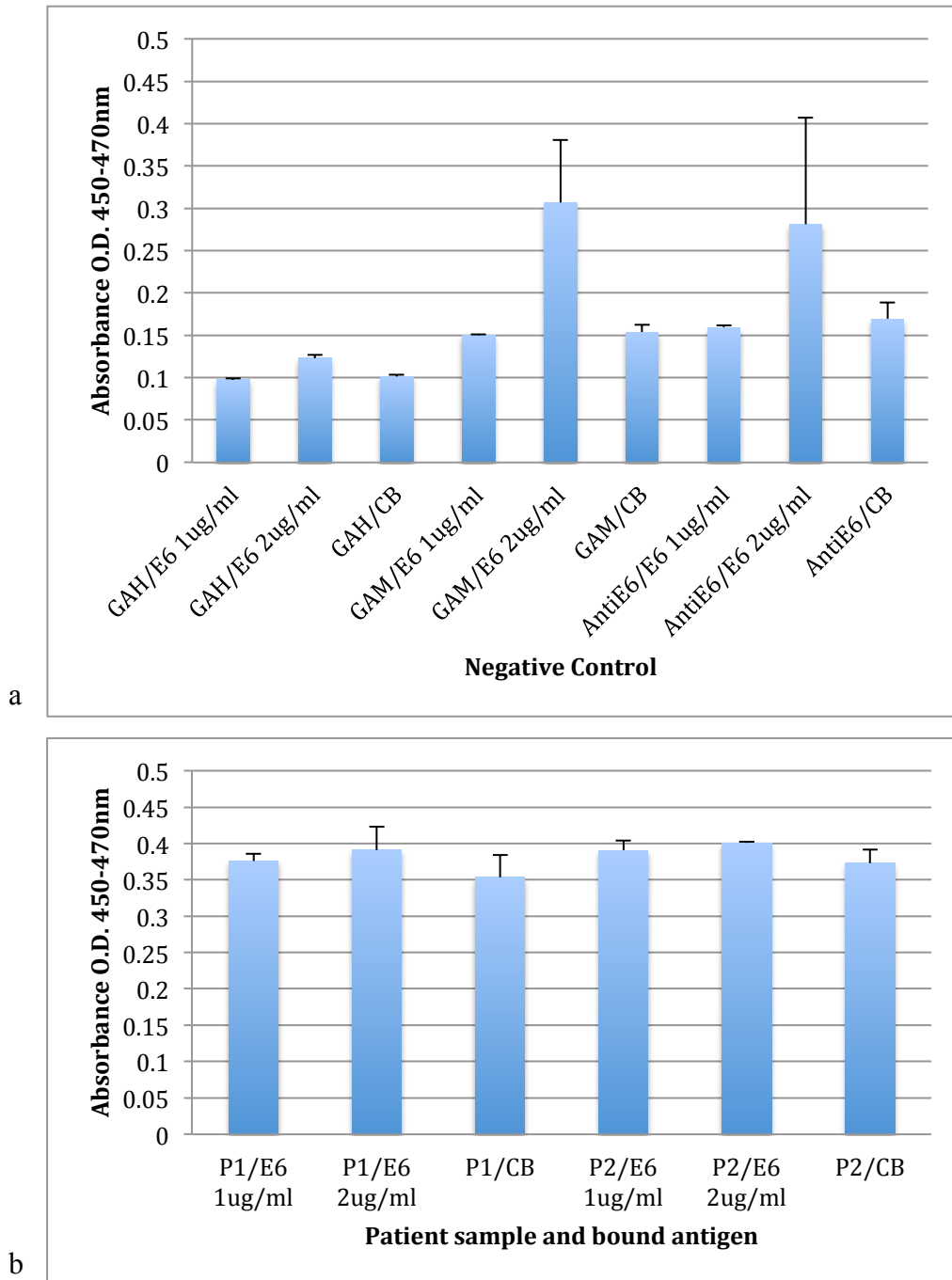


Figure 4.25a & b The negative controls (a) remain low when the E6 concentration is increased, the GAM added to 2µg/ml showed higher absorbance, this may be secondary to non-specific binding. Graph (b) illustrates patient samples tested against variable E6 concentrations and negative control CB.

Therefore the experiment was repeated under the same conditions except for a higher concentration of E6 was used, namely 5µg/ml, a greater number of patient serum samples were tested at a dilution of 1:5000, this was used instead of the previous 1:500 dilution to maximize the binding potential of any potential antibody present and to reduce any prozone effect. The Anti-E6 was retested against recombinant E6 at both 2µg/ml and at 5µg/ml at a dilution of 1:50 in addition to 1:200 (Figure 4.26).

There was little difference between the absorbance of Anti-E6 when 1:50 compared to 1:200 dilution was used (Fig.4.26a), furthermore there was no significant difference between serum absorbance levels for E6 compared to the control of CB alone.

The repeat experiments did not show any difference between the plates coated with E6 compared to CB alone, furthermore Anti-E6 used at concentrated levels showed no difference between the negative controls, this implied that the recombinant E6 was not binding to the Maxisorp plate although the initial experiment suggested it was. The recombinant protein used had previously been used for Western blotting, however this was, to our knowledge, the first use in ELISA, therefore the experiment was abandoned at this stage.

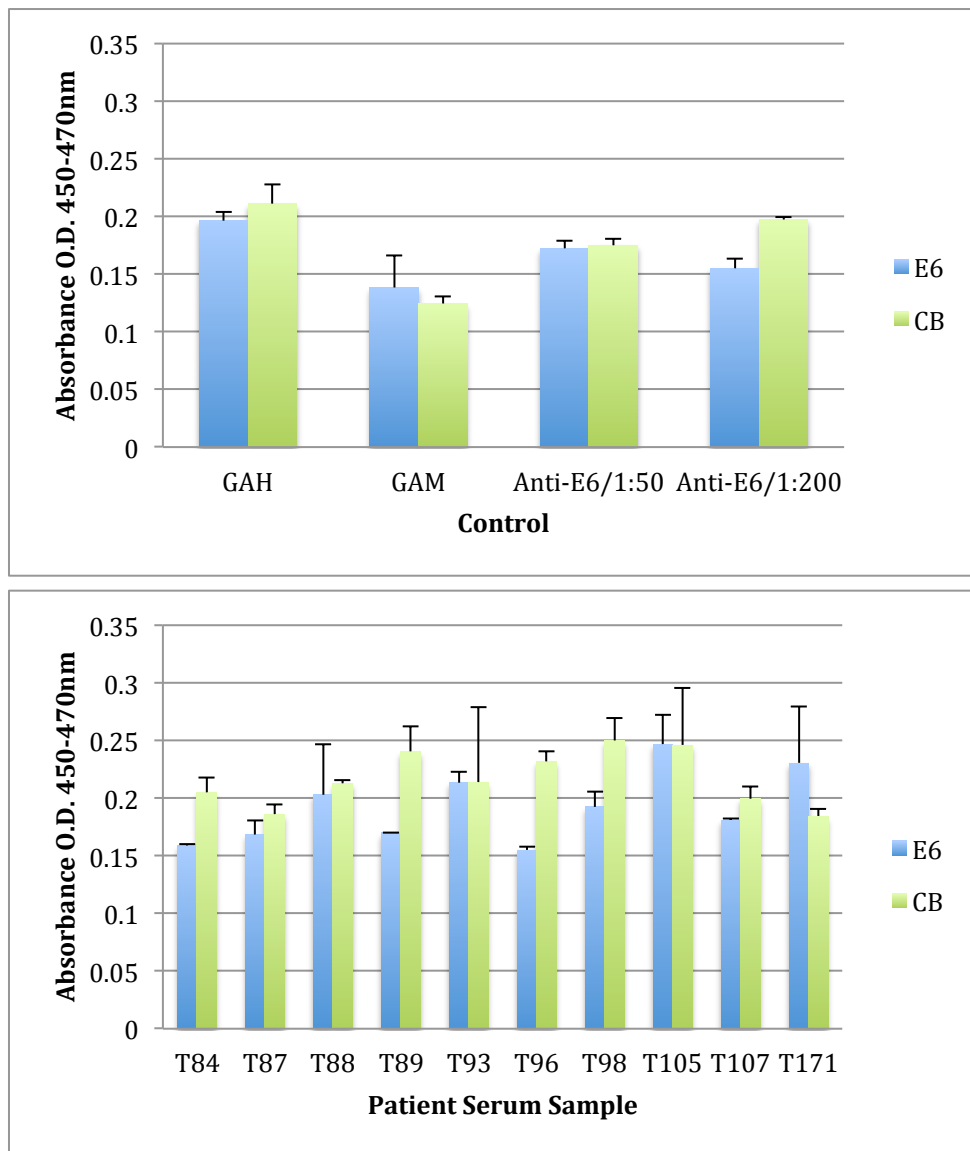


Figure 4.26a & b E6 was used at a concentration of 5µg/ml with negative control of carbonate buffer (CB). Graph (a) illustrates negative control values, little difference is seen for absorbance values of Anti E6 when dilution of 1:50 compared to 1:200 were used. Figure (b) illustrates the absorbance of serum when added to wells coated with E6 compared to CB alone.

4.13 Discussion

Analysis of results indicated that an antibody response to HPV-E7 was observed in both healthy individuals and those with HNSCC. Although when the two groups

were compared initial results indicated a statistical difference (1.88 ± 0.97 compared to 2.37 ± 1.08 , $p=0.047$), in the level of the response when these were subdivided into the individual subtypes of HNSCC there was no difference amongst the control and patient samples.

Within the oropharyngeal group it was noted that with increasing grade of disease there were increasing levels of serum antibodies, however within the subgroups of Oral Cavity and Hypopharyngeal HNSCC the numbers were too small to determine statistical significance. Conversely in the laryngeal squamous cell cancer group no significant difference between the increasing grades of disease and antibody level was observed, although it was noted that within each grade of disease the level of antibody was increased with nodal disease compared to no nodal disease within the same group. This may be accounted for by the sparse lymphatics of the laryngeal framework compared to the immune rich tonsils of the oropharynx and hence, once there is nodal spread the antibody levels increase due to activation of the immune response.

Zumbach *et al.* tested for seropositivity to both E6 and E7 and found that the number of seropositive HNSCC patients (12/92; 13%) was greater compared to the number of seropositive healthy controls (10/288; 3.5%) (Zumbach et al., 2000). There were a number of differences in the way the Zumbach study was conducted that could explain the results. Firstly the cut off value for the control was calculated by taking the difference in O.D. in wells with and without antigen present, however 'positive' or spurious results were removed before positive cut off values were calculated, furthermore on initial analysis there were a higher number of positive results and on

retesting and calculating the mean the number of positive results was reduced, this was true also for HNSCC. ELISA was performed for antigens to HPV 16 E6, -16 E7, -18 E6 and -18 E7 and it was interesting to observe that the higher prevalence of seropositivity was amongst the HPV 16 group. It was noted that although the rate of seropositivity was less prevalent than in the current study, the distribution of seropositivity amongst the HNSCC subtypes was similar compared to the current study. In fact 50% (6/12) of the seropositive HPV 16 E6/E7 were from the larynx and the remaining 33.3% (4/12) from the tonsils and 16.7% (2/12) from the base of tongue. In addition samples for the Zumbach study, were taken up to 6 months after diagnosis compared to the current study in which samples were taken at the time of diagnosis, introduction of treatment may possibly account for reduced antibody levels and therefore apparent reduced seropositivity in the study by Zumbach *et al.*

Di Bonito *et al.* (Di Bonito et al., 2006) developed an ELISA to assess seropositivity to HPV 16 proteins L1, L2, E4, E6 and E7 in Papanicolaou smear test (PAP) abnormal smear patients and found that there was high seropositivity (82% of patients) amongst the HPV16 positive patients for these proteins, however in the patients infected with other HPV types there was 89% seropositivity to HPV 16 proteins, this could be accounted for by a number of cross reactive linear epitopes that exist across the different HPV subtypes, of which not all are high risk HPVs, this may explain the high percentage of seropositivity observed against HPV-E7 amongst healthy controls in this current study. Di-Bonito *et al.* performed an avidity test to rule out non-specific binding. However the variation in antibody levels amongst different patient groups and the optimization of the ELISA to reduce non-specific binding was used to rule out non-specific binding as one would expect similar

antibody levels across all samples for non-specific binding. The results from the Di Bonito (Di Bonito et al., 2006) study showed that although the avidity test was performed there was still a high level of seropositivity amongst HPV 16 positive and those infected with other HPV genotypes. Cross reactive linear epitopes may suggest high seropositivity in our samples as many may be non-high risk.

Direct binding of protein antigens to the hydrophobic polystyrene plates can cause partial or total denaturation of the bound protein and therefore loss of the conformational epitopes (Darst et al., 1988). Previous work done on cervical cancer and seropositivity has shown that antibodies to HPV 16 and 18 E6 and E7 are directed to the conformational epitopes. Sehr *et al.* showed that expressing recombinant GST-tagged HPV proteins increased the specificity of ELISA (Sehr et al., 2001), as GST-fusion caused proteins to become increasingly soluble, increased the purification with single step glutathione attached to a solid support, and since the GST-glutathione involves attachment of GST in its native form it may allow for selection of fusion proteins in their native conformation. Sehr *et al.* performed ELISA by firstly attaching glutathione casein to the 96-well ELISA plate and then adding the GST tagged HPV-X protein to this, the idea being that the conformational shape of the HPV proteins were maintained and hence the antibodies directed to the conformational epitopes would provide increased specificity and sensitivity. Although GST-tagged proteins were not expressed successfully in this study the same principle can be applied to His-tagged proteins which were expressed, therefore to prevent protein degradation, which Meschede *et al.* stated could potentially happen when native proteins are applied to the Maxisorp plate (Meschede et al., 1998), a His-tag capture antibody can be firstly applied to the plate if time had allowed and the experiment was repeated.

The cut off value for our study was determined by the non-specific binding of blocking buffers and secondary detection antibodies to the 96-well plate plus 2 s.d. However Sehr *et al* measured the median absorbance at 450nm of the control sera plus 3 standard deviations (Sehr et al., 2001). The positive outliers for control sera were removed and the median results recalculated after each reading above the control median was omitted. Furthermore the absolute value for each reading was calculated by subtracting the reading of wells where GSTtag as antigen alone was used from the GST – X- tag protein, the idea being to measure the background reactivity of the serum to the GST tag. This certainly increased the specificity of the binding affinity, furthermore Sehr *et al.* also performed an avidity test. These differences in ELISA could potentially explain the higher number of seropositive patients within this group, it may possibly be that the cut off value in this study was set too low and therefore a higher number of samples were recorded as seropositive.

Rosales *et al.*, although looking at cervical cancer patients stated that the use of serum antibody levels could be used as a screening assessment in patients with HPV infection and carcinogenesis (Rosales et al., 2001). They also performed an ELISA to look for serum antibody titres against HPV proteins E2, E6 and E7. However there were a number of differences in the way the experiment was conducted compared to the current study. Firstly the antigens used were not the full-length protein or protein in its native form, peptides from E2, E6 and E7 were used as the target. There are a number of possible problems that could arise from this, firstly it has been previously shown that linear epitopes do exist between different HPV subtype proteins, including non-high risk papillomaviruses, therefore the antibody binding could be non-specific

as Rosales *et al.* showed that although in patients with HPV 6, -11 and -16 DNA the antibodies were specific, this was less so when HPV-18 or -33 were present, suggesting that linear epitopes do exist between different HPV types. Furthermore Sehr *et al.* have shown that it is better to use conformational protein antigens in their native form as this is what the antibodies are directed against (Sehr *et al.*, 2001), short peptides were used in the study by Rosales *et al.*, which may have given false positive results. ELISA performed by using the entire E6 and E7 prototype protein under native conditions has a sensitivity and specificity higher than those of assays using denatured proteins or linear peptides (Nindl *et al.*, 1994, Meschede *et al.*, 1998). Furthermore the cut-off values for determination of seropositivity were different to this study, cut off values were based on any measurement of absorbance at a reading of 405nm of >0.1. Based on this it was found that between 40-47.5% of patients were seropositive to the E2 peptides, however between 45-65% of healthy control individuals with no HPV-DNA present (as determined by In Situ Hybridisation) also were seropositive to HPV-E2 peptides. E2 is an early HPV protein, which is involved with the regulation of HPV DNA synthesis and down regulation of E6 and E7, low levels would therefore be expected in carcinogenesis. Between 30-40% of control patients were seropositive to the HPV- E7 peptides, although at low levels compared to 20-25% of HPV DNA positive at low levels, up to 32% of HPV DNA positive patient samples were seropositive to HPV-E7 peptides at moderate levels and up to 10% at higher levels. For HPV-E6 peptide the results were similar in that 40% of control patients were seropositive to HPV-E6 peptide at low levels (absorbance 0.1-0.15) compared to HPV- DNA positive patients at 37.5% for low levels, 22.5% at moderate levels (0.15-0.6) and at 2.5% at higher levels (>0.6). These results indicate that although at lower levels there was some seropositivity in HPV-DNA negative

patients to the HPV-Proteins it was difficult to determine whether this was secondary to previous exposure or to linear epitopes to the non-high risk papillomaviruses.

Although Rosales *et al.* did show that increasing titres of antibodies against E2, E6 and E7 peptides (as determined by levels of absorbance) were observed in the HPV DNA positive patients (Rosales *et al.*, 2001). These were patients that were selected from PAP smear positive results and had evidence of cervical HPV infection but not necessarily HPV associated carcinogenesis. Therefore the use of serum antibody status is not necessarily an indication of HPV DNA status and this is also dependent on the host immune status.

HPV-16 protein variants can occur, and it has been shown that sequence variants can be as high as 50-90% in some cervical cancer patients with amino acid variations of up to 56% with HPV-E6. However Nindl *et al.* showed that despite sequence or amino acid variants present amongst HPV-E6 this would not affect the seropositivity (Nindl *et al.*, 1994) and that a cross reactivity of antibodies occur hence this would not account for the lack of seropositive results noted in this experiment. The possibility that there were sequence variations in E6 amongst the HPV-positive HNSCC patients would not account for the lack of a seropositive response in this study, as cross reactions amongst variable sequences do exist (Nindl *et al.*, 2000).

Evidence shows that it may be more useful to monitor disease progression and the immune status rather than HPV status alone. Furthermore seropositivity to HPV-E6 and E7 are not markers of HPV infection but the host immune status, therefore it may be more useful to measure serial levels of antibodies amongst the same patient group

during their treatment as marker of disease progression and immune status rather than absolute values of antibody levels. Furthermore a correlation between serum antibody levels and cervical carcinoma has been shown with increasing levels with advanced disease however this has not yet been shown in HNSCC. This study showed that antibodies against HPV-E7 were also present in the healthy control group, therefore supporting that rather than measuring antibodies levels as static it may be more useful to measure serial levels during treatment as response to treatment rather than as a marker of disease status.

Chapter 5 - P16 Immunohistochemistry and In-Situ Hybridisation for HPV 16/18 detection in HNSCC FFPE sections

5.1 Introduction

Although HPV status is becoming increasingly important as a guide to treatment, some Centre's, including Hull and East Yorkshire Hospitals, do not (or at least, did not at the time of the experiments performed in the current study between September 2012 –March 2014) routinely test HNSCC samples for HPV infection. There is currently no single confirmatory test for the presence of HPV therefore necessitating the use of two or more methods of detection (Thavaraj et al., 2011b). In the current study formalin fixed paraffin embedded (FFPE) archived sections of HNSCC were tested for the presence of p16 by immunohistochemistry (IHC), which gave an indication of infection with HPV-16 as a causative factor for tumorigenesis (Hamid et al., 2009). Positive results were further tested with In-situ hybridisation (ISH) at the National HPV screening Centre in Newcastle to confirm the HPV gene presence.

It has been established that the HPV viral oncoproteins E6 and E7 are implicated in the pathogenesis of cancer by inactivating the tumour suppressor proteins p53 and pRb respectively (section 1.8). Chronic infection with high risk HPV, namely HPV 16 results in E7 binding to and inactivating pRb preventing its binding to E2F. This results in uncontrolled transcription of numerous genes and proliferation of cells due to the loss of the negative feedback mechanisms and leading to over expression of the

p16 protein (Hamid et al., 2009, Leemans et al., 2011). The p16 protein (p16, also known as p16^{INK4a}) is a cyclin-dependant kinase (CDK) inhibitor. Its function is to inactivate the CDKs that phosphorylate the retinoblastoma protein (Rb), namely CDK-4 and CDK-6, thus preventing cells from entering the G1 –S phase of the cell cycle, this is described in detail in section 1.8.2.

Over-expression of p16 is a sensitive biomarker of tumour activity as high levels are expressed only when the oncogenic process has started rather than just due to infection with high risk HPV alone (Schache et al., 2011, Thavaraj et al., 2011b). For example up to 30% of the population can be infected with the HPV virus and do not go on to form cancer as in most cases the infection is cleared by the immune system (Skinner et al., 2016), however it is not clear why some patients do not mount an immune response against HPV. The analysis of p16 staining is not based on a simple positive or negative result but must also take into account the staining pattern since p16 is a cellular protein that may be expressed in dysplastic and other lesions, albeit at differing levels.

As described in section 1.10, there is no internationally recognised standard for the detection of HPV, but there are two documented algorithms: 1) the use of p16 IHC followed by PCR, and 2) the use of p16 immunohistochemistry followed by ISH. PCR is very sensitive and can identify the smallest number of viral genes within a sample which may not be clinically relevant and also this process is time consuming and expensive, therefore In-Situ Hybridisation (ISH) was used as a confirmatory test which is also a well recognised algorithm (Singhi and Westra, 2010).

5.1.1 P16^{INK4a} staining patterns

A positive p16 staining pattern is one where there is continuous brown staining in the basal or parabasal layers, covering greater than 70% of the tumour area, and this is consistent with HPV mediated oncogenesis (Figure 5.1a-c). Staining is classified as negative when there is no or a non-continuous staining pattern, or focal areas of staining but not covering the majority of the tumour areas (figure 5.1 d-e).

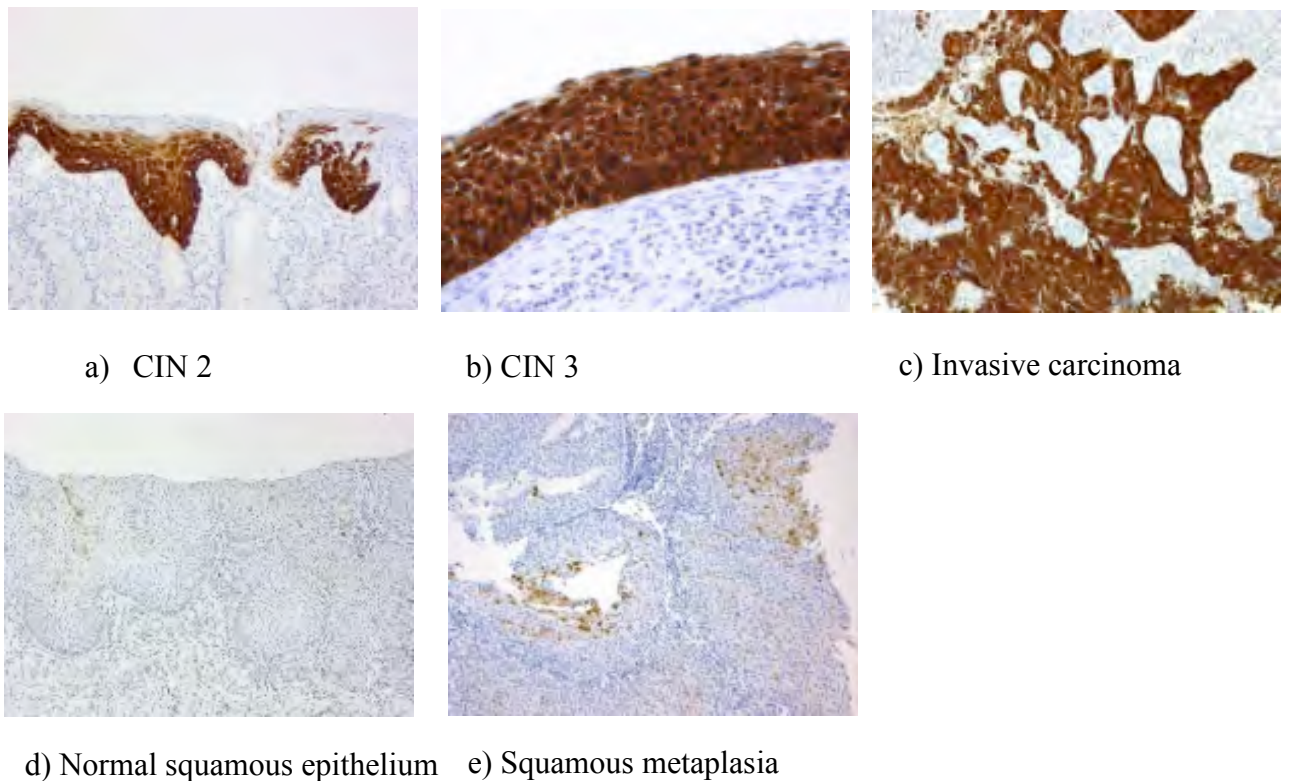


Figure 5.1 Images adapted from CINtec[®] Staining Atlas (mtm laboratories), of p16 positive staining (a-c) in cervical tissue showing the cervical intraepithelial neoplasia (CIN) staging level. Negative staining in cervical specimens are shown in d and e. The same staining patterns are observed in head and neck tissue samples.

Weinberger *et al.* developed a model for the molecular classification of biologically relevant HPV infection (Weinberger *et al.*, 2006), many studies have previously

documented the presence of HPV within HNSCC, ranging from 10%-100%, these were dependant on site of tumour and also on the detection method used. However the presence of HPV within a sample does not indicate a causal relationship and therefore the model was developed with p16 being a good surrogate marker for presence of HPV. The molecular classification allows for the prediction of disease free survival (DFS) and overall survival (OS), this classification can be useful for use in epidemiological studies and research trials. The model is based on four classes which are determined by the presence of HPV-DNA and p16 status (see Fig. 5.2).

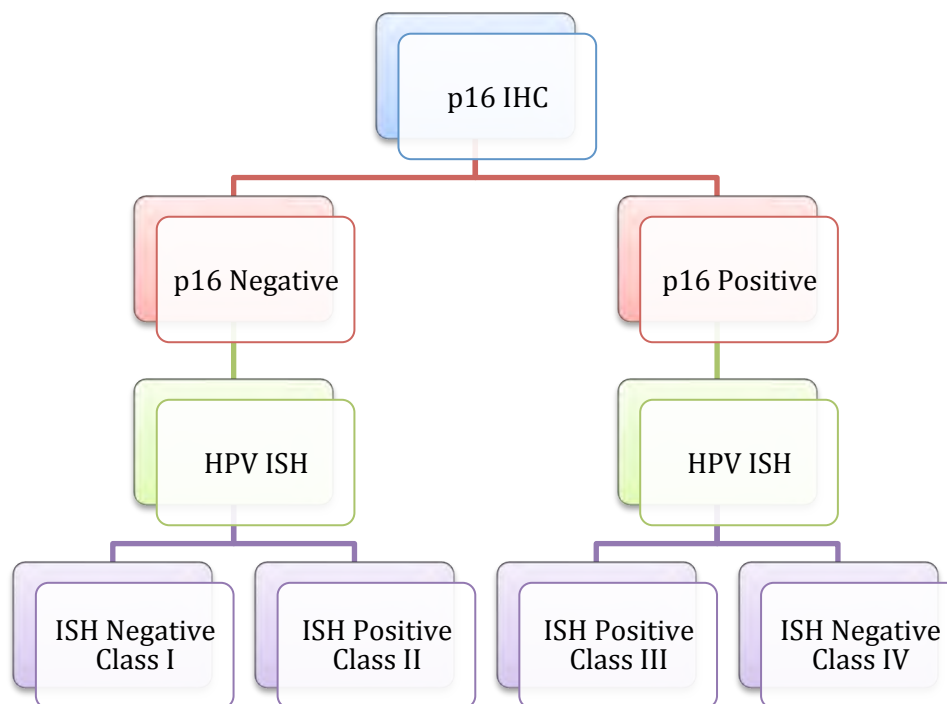


Figure 5.2 Molecular classification using p16 IHC and ISH, the flow chart illustrates the molecular classifications ranging from Class I-IV. The classifications are firstly based on the p16 immunohistochemistry, and then for the presence of HPV-DNA as measured by in-situ hybridisation.

5.2 Methods

5.2.1 P16 immunohistochemistry

The proprietary kit CINtec® Histology (Roche, mtm Laboratories, Heidelberg, Germany) was used with a few minor alterations to the protocol (section 2.11) for immunohistochemical staining (IHC) of p16. The kit uses a mouse monoclonal antibody directed against human p16^{INK4a} protein. Histoclear was used for deparaffinisation with serial washes after 2 minutes rather than insertion in xylene for 5 minutes as recommended by the manufacturer's protocol. For each batch of IHC performed, a negative control was also included by the use of isotype control.

Haematoxylin and Eosin (H&E) staining was also performed on serial sections to allow identification of the tumour areas. Figure 5.3 illustrates connective tissue with diffuse tumour cell infiltration with infiltration of inflammatory cells, and the strong cytoplasmic and nuclear staining for p16^{INK4a} within the tumour cells. Therefore both H&E and p16 staining were carried out in head and neck samples to ensure authenticity of results obtained.

Staining was visualised using a Nikon E800 microscope at both x100 and x400 magnification, so that the whole section could be observed. The results were analysed manually by comparing p16 slides with H&E slides and assessing staining in the tumour area. A staining pattern showing greater than 70% staining was regarded as a positive result. Results were verified with the help of pathologist Dr Laslo Karsai (Hull and East Yorkshire NHS Trust).

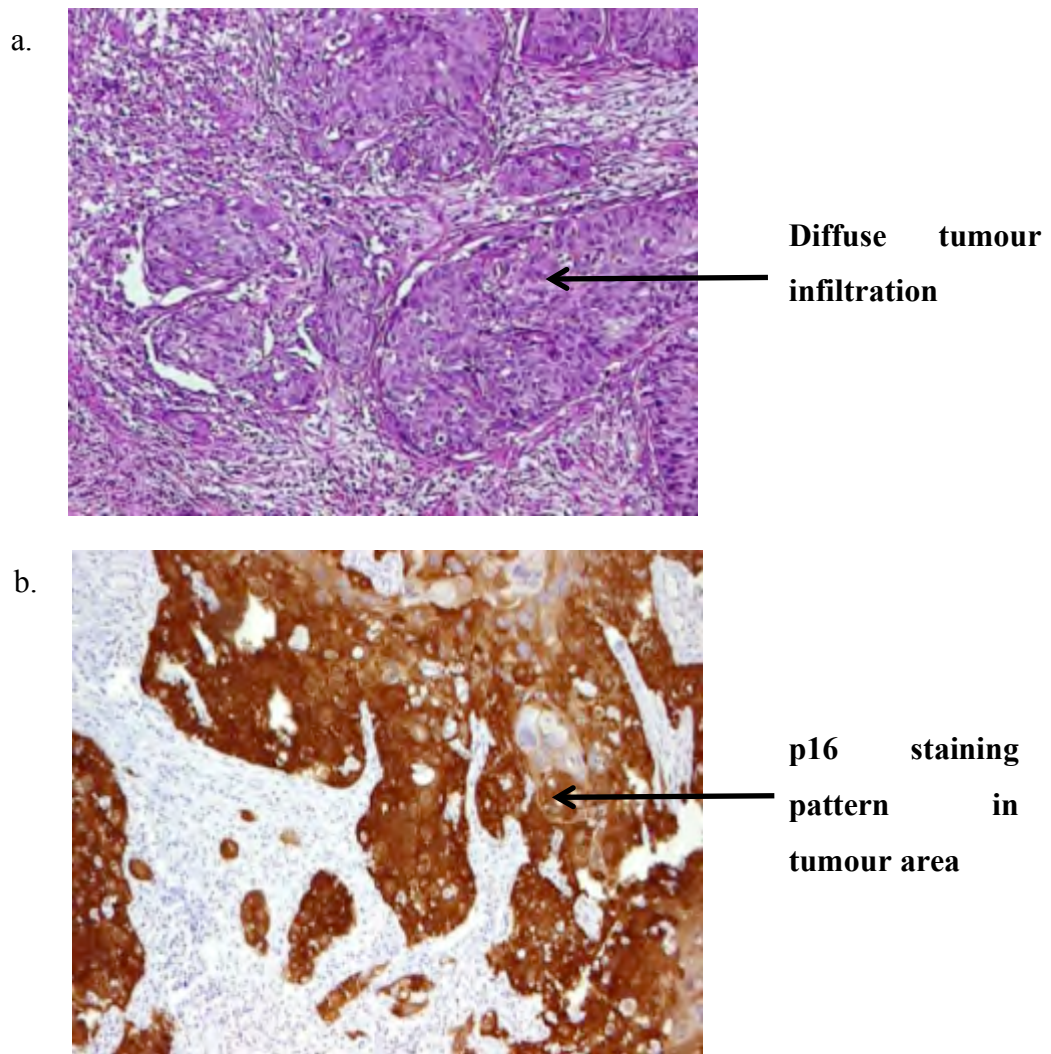


Figure 5.3 a) H&E staining showing connective tissue with tumour infiltration and diffuse infiltration of inflammatory cells b) p16 staining showing cytoplasmic and nuclear staining in the tumour area.

5.2.2. In situ hybridisation of HPV16

The ISH work was carried out by Dr Max Robinson, Senior Lecturer in Oral Pathology (Centre for Oral Health Research, Newcastle University, Framlington Place, Newcastle-upon-Tyne). This is a tertiary referral centre for HPV testing in clinical practice and for research purposes. A total of 48 samples were sent for both

IHC analysis and for ISH testing for verification of HPV positivity, in addition to this a selection of p16 stained samples were sent to verify results obtained in-house . Of the 48 samples sent a selection of negative results were also included to ensure validity of results obtained and reduce false positive results. Dr Robinson analysed the results and then explained the scoring to the author making it clear what was classed as a positive and what was classed as a negative result.

The method for ISH was adapted from the published method by Dr Robinson (Thavaraj et al., 2011a). ISH for high-risk HPV was carried out by using a proprietary reagent – Inform HPV III Family 16 Probe [B] (Ventana Medical Systems, Tucson, Arizona). The Inform HPV III Family 16 Probe [B] detects high risk genotypes HPV- 16, -18, -31, -33, -35, -39, -51, -52, -56, -58 and -66. For each batch of ISH performed, three controls were used, these were FFPE CaSki cells (HPV-16 Positive, 200-400 copies per cell), HeLa cells (HPV-18 positive; 10-50 copies per cell) and C-33A cells (HPV-negative; Ventana Medical Systems). The CaSki cells are a commercially available cell line derived from a small bowel metastasis from the cervix and are reported to contain an integrated human papillomavirus type 16 genome as well as sequences related to HPV-18 (Pattillo et al., 1977). The C-33 A cell line is another cell line derived by N. Auersperg from cervical cancer biopsies, it is negative for HPV DNA and RNA, however the expression of p53 is elevated and the pRB is present but abnormal in size. The HeLa cell line is again derived from cervical carcinoma biopsies (adenocarcinoma type), the HeLa cells have been reported to contain human papilloma virus 18 (HPV-18) sequences, p53 expression was reported to be low, and they contain normal levels of pRB (Boshart et al., 1984)(ATCC. LGC Standards, UK).

The ISH was assessed by Dr Robinson and was regarded as positive, if there was any blue staining reaction in the nuclei of malignant cells, diffuse nuclear and cytoplasmic staining or if there was any ‘punctate’ nuclear (‘integrated’ pattern) staining (Figure 5.4). Negative results were given when there was diffuse staining of tumour and stromal tissues, thought to be caused by non-specific chromogen precipitate. Furthermore pale staining and occasional staining of nuclei and occasional leucocytes was regarded as negative as guided by the manufacturer’s instructions. The samples were then grouped into the four classes as described previously based on both the p16 and the ISH results (section 5.1.1).

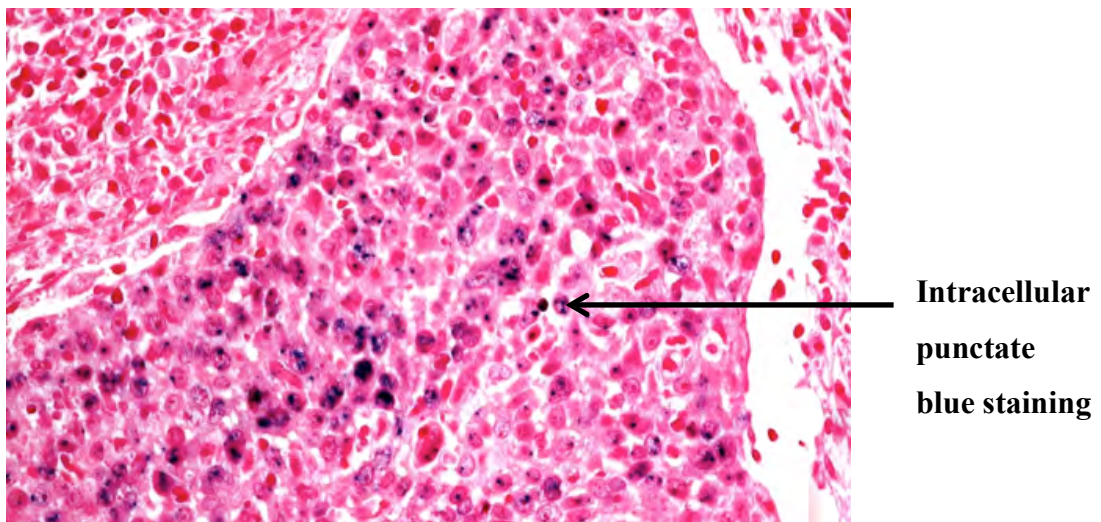


Figure 5.4 Photomicrograph of OPSCC showing ISH positive HPV-DNA, Inform HPV III Family 16 Probe [B] (Ventana Medical Systems, Tucson, Arizona), the blue integrated punctate signals are present throughout the tumour area.

5.3 Results

A total of 89 formalin fixed paraffin embedded (FFPE) HNSCC patient samples were

available for analysis (Figure 5.5) and were stained for both p16 and H&E (section 2.11 and 2.12).

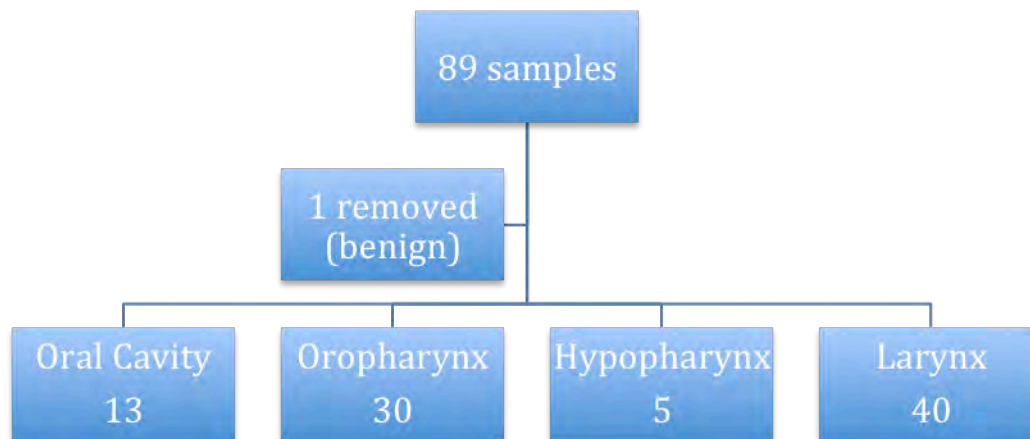


Figure 5.5 Distribution of patient samples available for IHC analysis. On further analysis one sample was found to be benign disease and was therefore removed from analysis.

5.3.1 Analysis of p16 immunohistochemistry

Variable staining patterns for p16 were observed amongst the HNSCC patient cohort (section 5.2.1), these are illustrated in Figure 5.6 which show the positive staining patterns for p16 (a-b) with nuclear and cytoplasmic staining within the tumour area. The negative staining patterns are illustrated by sparse non-continuous staining for p16 within the tumour area (c-d).

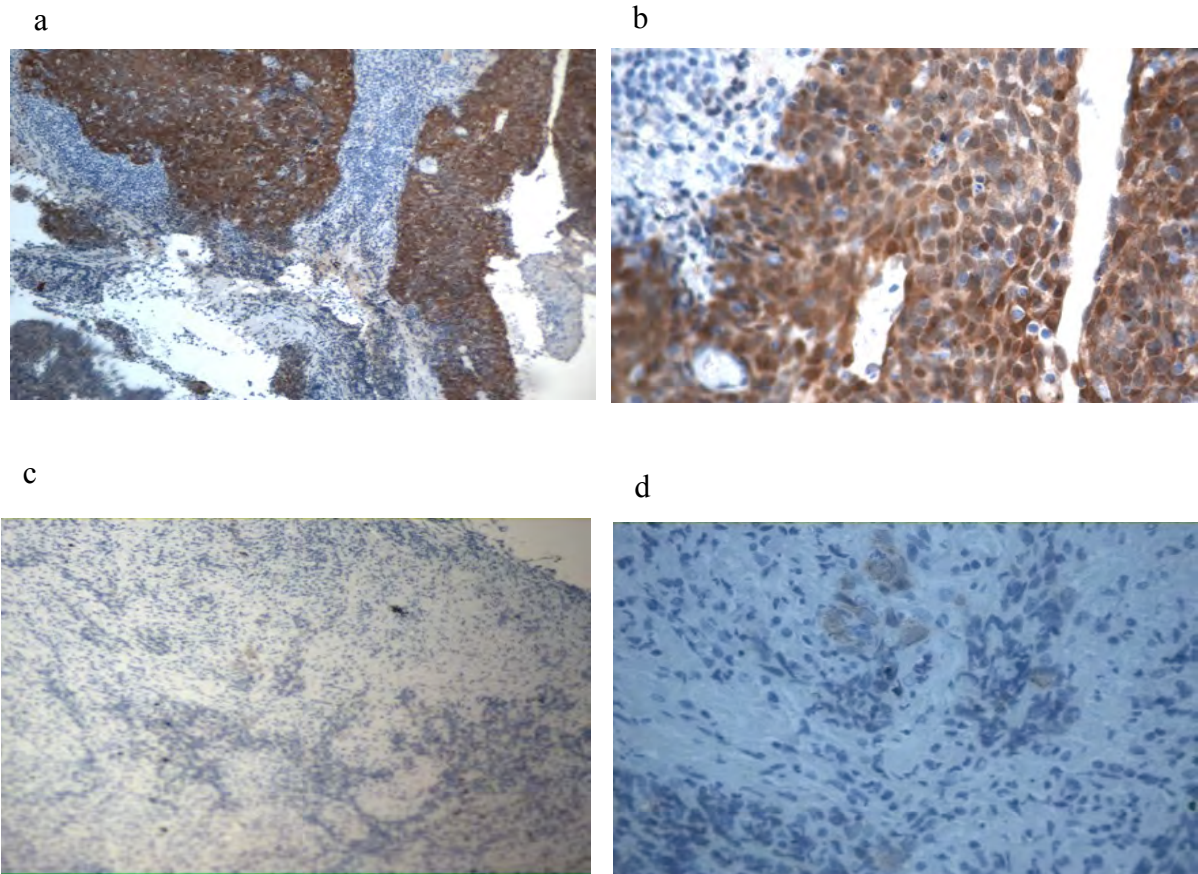


Figure 5.6a-d p16 immunohistochemical staining patterns; a. Representative p16 positive staining at x10 magnification illustrating widespread brown staining in the tumour area of oropharyngeal scc. b. At x40 magnification this shows diffuse cytoplasmic and nuclear staining within the tumour field (representative of 24 positive samples). c. Oropharyngeal p16 negative staining showing focal staining patterns for p16 at x10 magnification, there are some focal staining patterns however these are less than 70% of the tumour area and do not cover the basal or parabasal areas. d. Oropharyngeal SCC at x40 magnification showing little staining for p16 (representative of 64 negative samples).

Of the 88 samples analysed 24 were p16 positive indicating oncogenic transformation with HPV-16. Figure 5.7 illustrates the number of p16 positive tumours compared to the total number within each group according to subtype of HNSCC. The oropharyngeal subgroup was the one which had the greatest percentage of positive p16 samples (70%) and the laryngeal subgroup had the lowest percentage of positive

tumours (2.5%), however both the oral cavity and the hypopharynx groups had sample sizes which were too small to make any valid comments regarding levels of p16 positivity and thus HPV positivity.

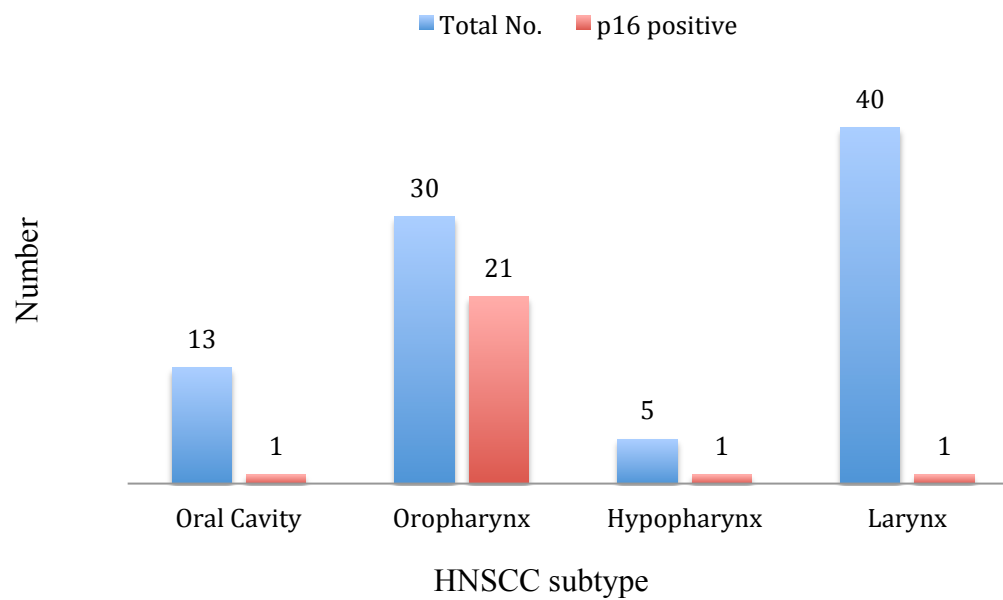


Figure 5.7 Bar chart illustrating the total number of IHC samples per subtype and those that were p16 positive.

5.3.2 Analysis of in-situ hybridisation for the presence of HPV in HNSCC

Out of the 48 HNSCC samples investigated for HPV positivity by ISH the oropharyngeal group again had the highest percentage of samples which were positive (78%) compared with both the laryngeal and the oral cavity subgroups in which only 11% of samples were HPV positive (Figure 5.8).

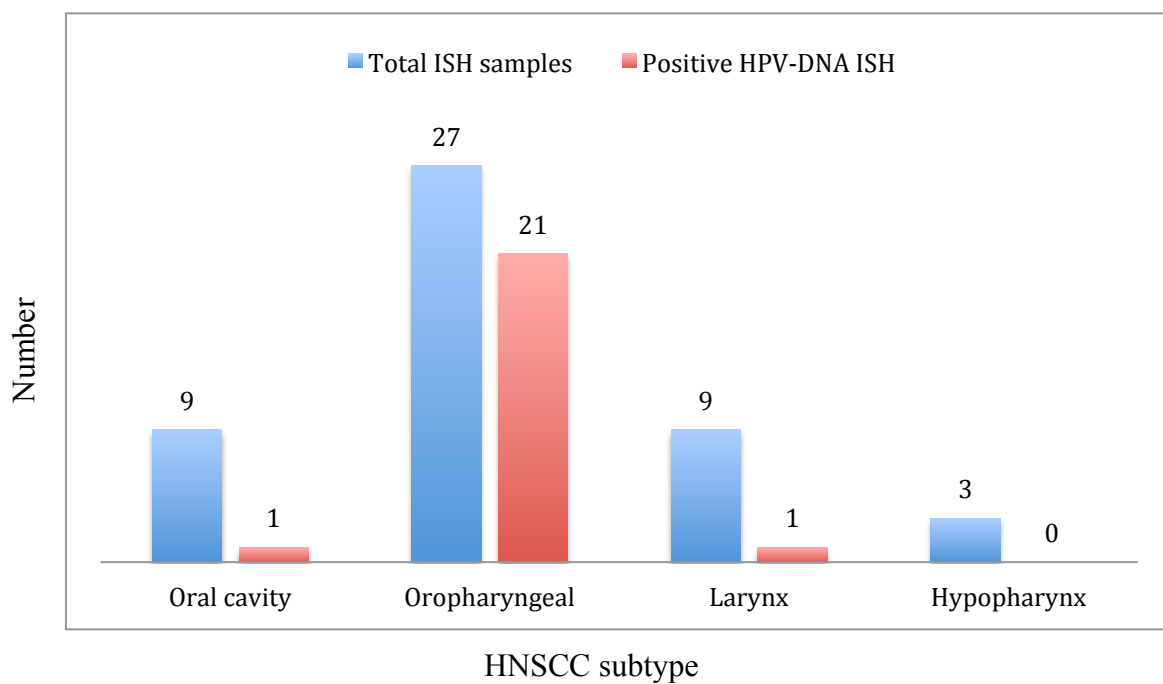


Figure 5.8 A bar chart illustrating the total number of samples per subset tested for in-situ hybridisation and the number of samples that were positive for HPV DNA.

5.3.3 Molecular Classification of HPV status

Only 43 out of the 48 samples were able to have a complete molecular classification

performed based on both the p16 and the ISH results. Five tests failed for the following reasons:

- 1 test had failed High Risk-HPV ISH (this was from the oral cavity group)
- 2 tests had p16 performed but the slide had inadequate tumour for ISH (one laryngeal sample and one hypopharyngeal)
- 1 test had failed p16 and failed ISH secondary due to insufficient tumour (from the oropharyngeal group)
- 1 test had failed p16 staining due to inadequate tumour but positive ISH (from the oropharyngeal group)

In keeping with previous studies the results of this study show that the highest number of HPV positive tumours were seen within the oropharyngeal group. Within this group 76% of tumours were Class III indicating positivity to both p16 IHC and by the presence of HPV DNA detected by ISH. In the remaining HNSCC subsets the levels of Class III were low, however as illustrated by the table the numbers are too small to extrapolate any statistical significance; 4/25 were negative for both p16 and ISH (class I) and only two samples showed a discrepancy between the p16 and the ISH (Table 5.1). Both the laryngeal and oral cavity cohorts (n=8) showed no discrepancy between the tests with 7/8 being negative for both p16 and ISH (class I) and the other sample being positive for both (class II). Out of the whole cohort of tumour samples there were only three which showed discrepancy between the tests.

Table 5.1 Complete molecular classifications of HNSCC samples based on p16 IHC and ISH

	Oropharyngeal		Larynx		Hypopharynx		Oral Cavity	
	No	%	No	%	No	%	No	%
Class I <i>p16</i> negative, <i>ISH</i> negative	4	16%	7	87.5%	1	50%	7	87.5%
Class II <i>p16</i> negative, <i>ISH</i> positive	1	4%	0	0%	0	0%	0	0%
Class III <i>p16</i> positive, <i>ISH</i> positive	19	76%	1	12.5%	0	0%	1	12.5%
Class IV <i>p16</i> positive, <i>ISH</i> negative	1	4%	0	0%	1	50%	0	0%
Total	25		8		2		8	

5.4 Discussion

P16 immunohistochemistry is a useful marker for the screening of HPV, however it is not specific for HPV-16 and therefore results have to be analysed based on degree of staining in the tumour area rather than staining alone (Thavaraj et al., 2011b). In those samples that stain positive for p16, ISH for high risk HPVs is performed to detect those patients in whom molecular active HPV is present. The results from the current study indicate that from all the HNSCC subsets almost half (48.8%) were HPV positive (Class III) but the majority of these were from the oropharyngeal

subgroup (76%), 44.1% of all patients were Class I (HPV negative), where staining for p16 was negative and no HPV DNA was detected on ISH meaning. Only 2.3% were Class II and 4.7% were Class IV, meaning the results of the two tests did not come to the same conclusion; i.e. Class II was negative for p16 IHC however ISH was positive, and in Class IV the opposite was true where p16 was positive on IHC however on ISH no HPV DNA was detected. The discrepancies identified for Class II could be secondary to transient infection with papillomavirus but with no transformation to tumour. Also another explanation could be the infection within a tumour by HPV but with an inactivated p16 gene, which could occur by deletion or methylation (Pim and Banks, 2010). The discrepancies for Class IV could be due to overexpression of p16 by loss of pRb, although this is considered a rare event (Pim and Banks, 2010). The result could also be explained by deviation of the pRb/p16 cell cycle regulation by HPV independent pathways (Thavaraj et al., 2011a). Robinson *et al.* (Robinson et al., 2010) performed a pooled analysis which looked at the rates of p16 positive/HPV negative tumours and p16 negative/HPV positive, these were 5% and 8% respectively, therefore discordant result findings of this study were similar. Although p16 is currently doubted as a good screen for HPV infection alone due to non-specificity, in this study it was found that 93% (40/43) of samples were in agreement between the tests.

When comparing p16 IHC 24/88 (27.3%) patients were p16 positive, most of these were from the oropharyngeal group where 21/30 (70%) were p16 positive. Although the sample size for oropharyngeal SCC was smaller, the results were comparable to other studies where a rate of 62-64% HPV positivity as determined by p16 IHC and ISH was observed (Robinson et al., 2010, Thavaraj et al., 2011a). The laryngeal

group had the least amount of positivity; 1/40, 2.5%. The sample sizes for the oral cavity and hypopharyngeal group were small (13 and 5 respectively), however the order of HPV prevalence within the groups from highest to lowest was oropharyngeal, hypopharyngeal, oral cavity and larynx.

The results of this study are comparable to previous studies looking at HPV positivity amongst OPSCC patients. Of the 25 patients in this study with OPSCC, 76% were p16+/HPV+ (Class III). Thevraj *et al.*, looked at 142 tonsil patients of which 62% were HPV positive, Ang *et al.* found 64% out of 315 tonsils were HPV positive using p16 and ISH (Ang *et al.*, 2010a). Lewis *et al.*, used p16/ISH/PCR to demonstrate that 66% of 239 patients were HPV positive. These findings illustrate that it is useful to perform p16 as screening and ISH as confirmatory and furthermore in unequivocal cases to use PCR which is more expensive and more labour intensive to perform. PCR was not used in this study, however there was one unequivocal ISH case (Class IV).

Weinberger *et al.* reported that patients with a Class III oropharyngeal SCC had a 5-year OS of 79% versus 20% for Class I and 18% for Class II ($p=0.0095$) (Weinberger *et al.*, 2006). For DFS a similar relationship was found with Class III tumours demonstrating a 5-year DFS of 75% versus 15% for Class I tumours and 13% for patients with Class II tumours ($p=0.0025$). Furthermore it was demonstrated that Class III tumours had a significantly lower disease recurrence rate compared to Class I and Class II. Molecular classification is a useful tool for comparison as when comparing HPV-positive versus HPV-negative tumours alone there is little difference between rates of local recurrence (Weinberger *et al.*, 2006).

It may seem logical to test for HPV specifically, however the presence of HPV-DNA per se does not necessarily demonstrate a causal relationship between HPV infection and oncogenic transformation and may be secondary to transient infection alone (Snijders *et al* 2003). HPV DNA is found widely in head and neck dysplasia, SCC and in other cancer types, in benign lesions such as papillomas, and also in some histologically normal tissue (Syrjanen S 2005). Therefore it has been shown that the use of a three-tier system is more effective in reducing false-positive results as measuring p16 detects transcriptionally active HPV. When assessing a HPV DNA positive tumour Thevraj *et al.*, suggested two possible methods, using p16 IHC as an initial screen for both methods and then either in-situ hybridisation or PCR to look for patients with high risk HPV. However, as PCR can pick up a single copy of HPV DNA (section 1.10.1.1) it is thought that it may not be clinically relevant. Thevraj *et al.*, found that there was a higher rate of false positives with PCR at 9% compared to ISH at 1%. Furthermore Lewis *et al.*, found that the survival rates in patients that were p16 positive and HPV-negative were similar to those that were p16 positive and HPV positive, therefore raising the question whether further confirmation of HPV infection is relevant. Another potential problem that could arise with p16 IHC as screening is the inter-observer variability at analysis; Thevraj *et al.*, had a 97% concordance amongst pathologists and 11% inter-observer variation with ISH results. This shows that it may be useful to have at least two pathologists for the analysis of results, figure 5.9 illustrates the diagnostic algorithm for diagnosis of HPV positive HNSCC.

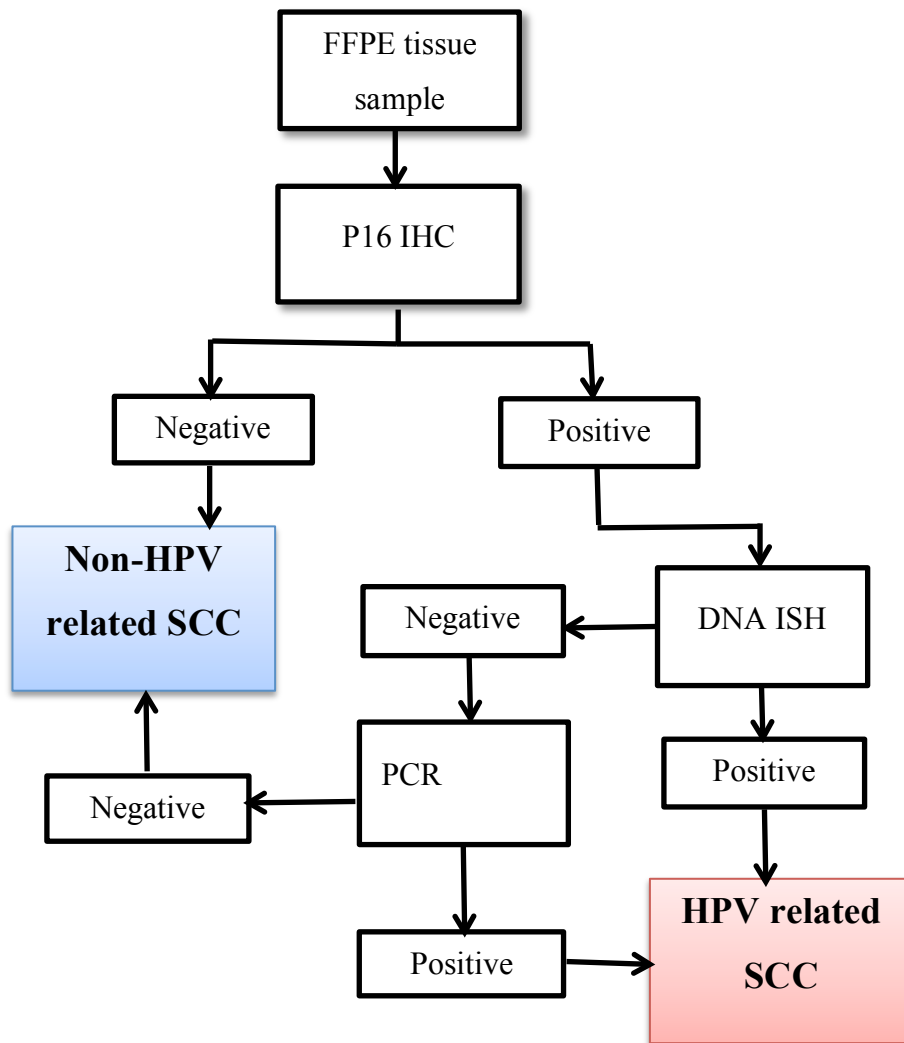


Figure 5.9 Diagnostic algorithm for the detection of biologically active HPV from fresh frozen paraffin embedded head and neck samples.

There is no set standard that is used for the detection of HPV, there is increasing evidence in the literature which states that those with a HPV positive cancer fair much better than those with a HPV negative cancer and therefore the importance of HPV detection is increasingly becoming more apparent. Although there is no set standard for HPV detection clinically when using a screening tool it must fulfil certain criteria which include availability, ease of use and interpretation, cost and low rates of false negatives. P16 is thus used as an initial screening tool, Thevraj et al. (Thavaraj et al.,

2011b) have suggested a model for HPV diagnosis which begins with p16 staining and includes the use of ISH of the high risk HPVs in those with p16 positivity, as was used in this study and in those unequivocal cases to use PCR, this has been suggested by a number of studies (Robinson et al., 2010, Schache et al., 2011, Singhi and Westra, 2010). Table 5.2 was adapted from Lewis Jr' s (Head and Neck pathology 2012) review which compares the correlations of HPV positivity amongst the various tests available; for the purpose of this study the p16 IHC and DNA-ISH were analysed. There was between 60-96% rate of correlation between p16 IHC and DNA-ISH. This study demonstrated a 93% concordance between p16 and DNA ISH.

Study	No. p16 positive patients	HPV DNA ISH
Ang et al.	206	192 (93.2%)
Lewis Jr. et al.	187	139 (74.3%)
Ukpo et al.	148	119 (75.8%)
Schlecht et al.	11	6/10 (60%)
Thavaraj et al.	90	75 (83.3%)
Doxtader et al.	25	24 (96%)

Table 5.2 Adapted from James S. & Lewis Jr. (Head and Neck Pathology, 2012) illustrating the concordance rates between p16 positivity and DNA In-situ-hybridisation.

The current suggestions are to use p16 as an initial screening test to identify transcriptionally active HPV and then to perform a further confirmatory test such as DNA PCR or DNA ISH which was used in this study (Westra, 2009). The reasoning behind confirmation of HPV presence rather than using p16 alone is secondary to what is known already about tumour biology and that p16 is overexpressed in other cancers such as undifferentiated sinonasal carcinoma, where p16 is high however

HPV is not detected, furthermore some non-small cell cancers of the lung have been found to express p16 in upto 60% but with no HPV detected (Westra et al., 2008).

Lewis (Lewis, 2012) reviewed a number of studies which compared p16 with p16 plus a HPV specific test (eg ISH or PCR) and found that the addition of a HPV specific test did not alter the risk stratification for a p16 positive tumour alone. Therefore negating the need for HPV specific testing when comparing disease free or overall survival. RNA testing, such as real time-PCR, is also becoming increasingly used but given its cost and availability at present it is not currently widely used. The diagnostic algorithm illustrated in Fig. 5.9 was used in this study, although no 'Gold Standard' is available this algorithm is accepted by a number of studies as a reasonable diagnostic algorithm (Westra, 2009, Smeets et al., 2007, Thavaraj et al., 2011a). The use of a multimodal algorithm allows for the utilisation of the strengths of the various tests such as p16 which has a sensitivity approaching 100%, but specificity of 79% (Smeets et al., 2007) and ISH which has a specificity of 100% (Westra, 2009).

The clinical need to develop standardised diagnostic algorithms is increasing since there is increasing evidence from early results of de-escalation trials that HPV positive tumours do not require as intensive treatment as compared to HPV negative SCC in terms of chemoradiotherapy. Current trials which are in progress include De-ESCALaTE Trial (Prof. Hisham Mehanna, University of Warwickshire) which compares the efficacy of Cetuximab versus Cisplatin in early and late HPV positive OPSCC (Appendix 3).

Chapter 6 - Clinical Correlations of Tumour Infiltrating Lymphocytes and Peripheral Circulating Cytokines with HPV Status and Survival in HNSCC

6.1 Introduction

The interplay of immune factors has often been looked at to differentiate and identify the variability between survival and prognosis in HPV positive HNSCC versus HPV negative. The Human Papilloma Virus oncoproteins E6 and E7 have been shown to be involved in tumourigenesis of head and neck squamous cell carcinoma, particularly those originating in the oropharynx and oral cavity (Leemans et al., 2011, Westra, 2009, Gillison et al., 2008). These proteins appear to act through inactivating both the p53 and retinoblastoma (pRb) genes, as silencing of these viral proteins results in re-expression of these two suppressor pathways (Ang et al., 2010a). However, paradoxically it is now widely accepted that infection with HPV confers **better** outcomes and survival rates in HNSCC patients (80% 5 year survival) compared with HPV-negative counterparts (50% 5 year survival), regardless of treatment modality (Ang et al., 2010a, Ragin and Taioli, 2007). It is hypothesised that the increased immune response against the HPV infection contributes to better survival, however the exact mechanisms involved remain unknown and do not appear to fully explain the data. Seropositivity in HNSCC has been quoted to range between 24-67%; with rates in oropharyngeal being highest (81.6%), followed by oral cavity (15.8%). Seropositivity is less frequent in hypopharyngeal/laryngeal HPV positive cancers (2.6%) (Rubenstein et al., 2011, Smith et al., 2010). Recent reports have

demonstrated that seropositivity to E6 and E7 in HNSCC patients is also correlated with lower mortality compared with seronegative HNSCC patients (13.6 vs. 40.2%) (Rubenstein et al., 2011) even when corrected for smoking and alcohol history.

The limited previous work investigating different immune parameters and the role of the host immune response in HPV-positive HNSCC has shown both improved survival outcomes in patients with high levels of CD8 cells and low CD4:CD8 ratios (Wansom et al., 2010); and raised circulating levels of interleukin 10 (Bolpetti et al., 2010). However, to the author's knowledge, no systematic study has been carried out in which the relationship between HPV seropositivity and a panel of host immune response parameters (circulating and tumour-specific) and patient outcome has been reported.

Our group has undertaken previous ethically approved studies (see Fig. 6.1), in which serum and peripheral blood mononuclear cells (PBMC) have been collected and stored from newly presenting HNSCC patients prior to and post-treatment. These have been assessed for ten Th1/Th2 related cytokines (Quantibody array based ELISA) and the percentage of peripheral CD4⁺ and Treg (CD4⁺CD25^{high}FOXP3⁺) cells (flow cytometry) respectively. In addition the CD4, CD8 and Treg status of the tumour microenvironment has been determined in archival sections of the resected tumour by immunohistochemistry. Key findings of these studies were: a significant decrease in the serum levels of the Th2 cytokines IL-4, IL-5, IL-6 and IL-10 and the Th1 cytokines IL-2 and IL-8 from pre to post-treatment (Green et al., 2011) and an increase in the percentage of circulating Treg cells from pre to post-treatment with a

positive correlation between circulating Tregs and those in the tumour microenvironment (Green et al., 2013).

The aim of the present study was to investigate and correlate the presence of HPV status with the panel of cellular and soluble immune parameters, and furthermore correlate this with clinical outcomes to highlight the potential interplay of these immune factors and effects on clinical outcomes, e.g. disease free survival.

6.2 Method

A previous study conducted within the School of Biological Biomedical & Environmental Sciences (University of Hull), with Ethical approval of 05/Q1105/55 had data available for the subjects studied in this study for tumour infiltrating lymphocytes (TIL) determined by immunohistochemistry, and also data available for peripheral circulating cytokines as determined by ELISA of serum (see Fig.6.1). The data were analysed together with the data collected from this study to assess if there were any correlations between the TIL, peripheral circulating cytokines (Th1 and Th2) and HPV status of patients together with the antibody status as determined by ELISA against HPV-E7 (see section 4.0) and disease free survival.

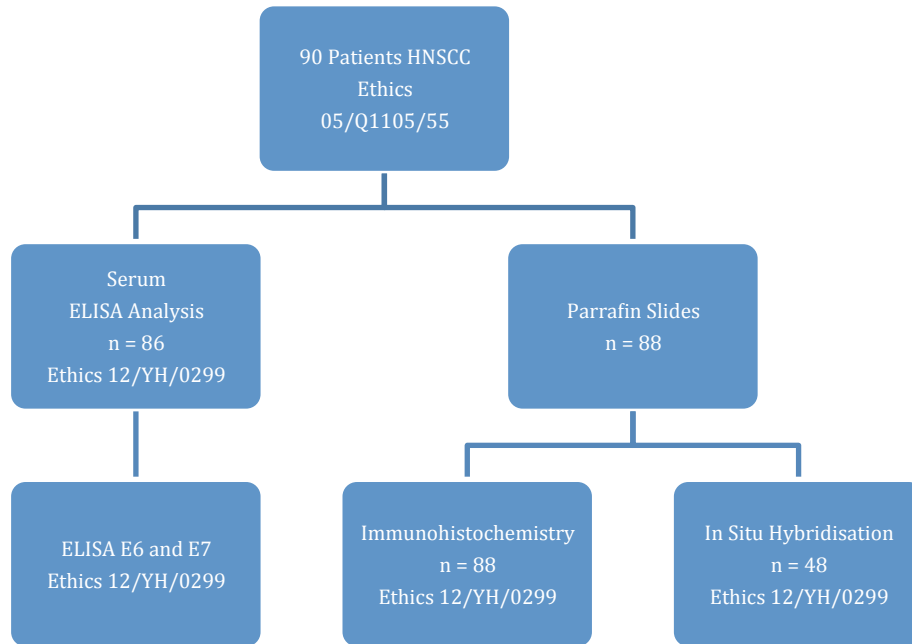


Figure 6.1 Flow chart for HPV diagnostic tests and Ethical approvals. Both studies also have NHS R&D approval

The TIL that were analysed included CD4⁺ helper, CD8⁺ cytotoxicity and FoxP3⁺ve regulatory cells. The CD4⁺ cells proliferate and respond principally to extracellular antigens presented by dendritic cells via MHC II. CD8⁺ cells recognise intracellular peptides presented by the MHC I molecules; CD8⁺ T cells are important for immune defence against intracellular pathogens and malignant cells. Three major mechanisms are utilised to kill infected or malignant cells; the first is by secretion of cytokines such as Interferon gamma (IFN γ), secondly by the production and release of cytotoxic granules containing granzymes and lastly by destruction of infected cells via the apoptotic *Fas* receptor (Brint et al., 2013, Mittrucker et al., 2014). FoxP3 is a key transcription factor expressed by the majority of T regulatory cells (T-Reg), previously known as T-suppressor cells, whose role is to dampen the immune response (O'Connor and Anderton, 2015).

Representative candidates from each of the Th1 and Th2-like cytokines were analysed. The Th1 cytokines are pro-inflammatory cytokines that are responsible for the cellular immune response. In particular interleukin 2 (IL-2) is expressed by activated T-cells, stimulates the growth, differentiation and survival of antigen selected cytotoxic T-cells, in addition to being necessary for T-cell memory development and recognition (Futosi et al., 2013). IFN γ works by activating macrophages and inhibiting Th2 lymphocyte proliferation; furthermore it stimulates B cells to produce receptors that enhance the attachment of microbes to phagocytes (Futosi et al., 2013, Gomez et al., 2015).

The Th2 cytokines work by activating the humoral antibody mediated immune response most effective against extracellular pathogens. They also counteract the Th1 cytokines and generally dampen the immune response in order to reduce collateral damage to non-infected tissue. IL-4 inhibits the proliferation of Th1 cells and stimulates B-cell proliferation and maturation into plasma cells. IL-10 inhibits the secretion of various cytokines by Th1 cells, macrophages and dendritic cells (Saxena et al., 2015).

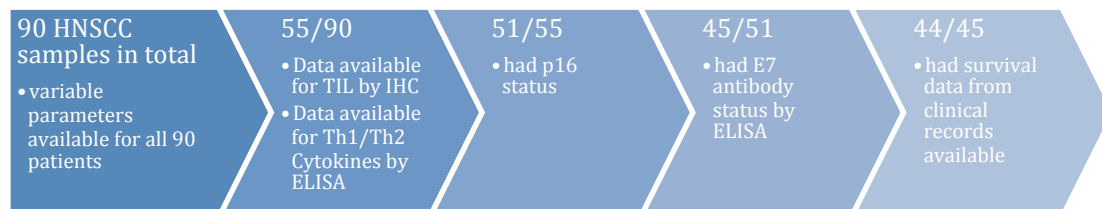
The combination of Th1 (IL-2 and IFN γ) and Th2 (IL-4 and IL-10) cytokines and tumour infiltrating lymphocytes (CD4⁺, CD8⁺ and FoxP3⁺ cells) were selected as a representative of the immune status of the patient and tumour. These were analysed together with the p16 status and E7 antibody status against disease free survival. Data were analysed using IBM SPSS[®] Statistics (Version 23.0), survival data were available for each patient for at least 3 years after the completion of treatment.

6.3 Results

A total of 44/90 patients had complete data available for all of the following parameters (see Fig. 6.2):

- HPV status as determined by surrogate marker p16
- TIL, namely CD4⁺, CD8⁺ and FoxP3⁺ cells
- Th1 cytokines (IL-2 and IFN γ)
- Th2 cytokines (IL-4 and IL-10)
- E7 antibody status
- Survival data from clinical records

Figure 6.2 Patient samples available with complete data set



Of the 44 patient samples from all subsites (oral cavity, oropharynx, larynx and hypopharynx) 11/44 were p16 positive and 33/44 were p16 negative. Of the 11 that were p16 positive 9 of these were from the oropharynx, 1 was from the hypopharynx and the other was from the larynx.

6.3.1. TIL in HPV-positive HNSCC versus HPV-negative HNSCC

The tumour infiltrating lymphocytes were higher in HPV positive HNSCC compared to HPV negative. The CD4 T-lymphocytes were detected in 10/11 HPV positive

patients and the average was 22 ± 37.50 compared to 7.93 ± 8.09 in HPV-negative tumours; however 29/33 HPV negative tumours had detectable CD4⁺ cells within the tumour sample. Although the detectability of cells was similar, the difference in the CD4⁺ count was significant $p=0.05$ (student's independent t-test)

The CD8⁺ cell count was on average 17 ± 20.09 in HPV-positive cases compared to 10 ± 12.79 in HPV-negative tumours, again CD8⁺ cells were detected in 10/11 (91%) HPV positive tumours compared with 30/33 (90%) HPV-negative tumours. In this case there was no statistically significant difference ($p=0.22$, student's independent t-test).

The average FoxP3⁺ cell count was 6.64 ± 11.7 in HPV positive (n=11) compared with 4.24 ± 4.7 in HPV-negative tumours (n=29), $p=0.36$ (student's independent t-test). The differences between the TIL in HPV+HNSCC and HPV-HNSCC are shown in Fig. 6.3a and b.

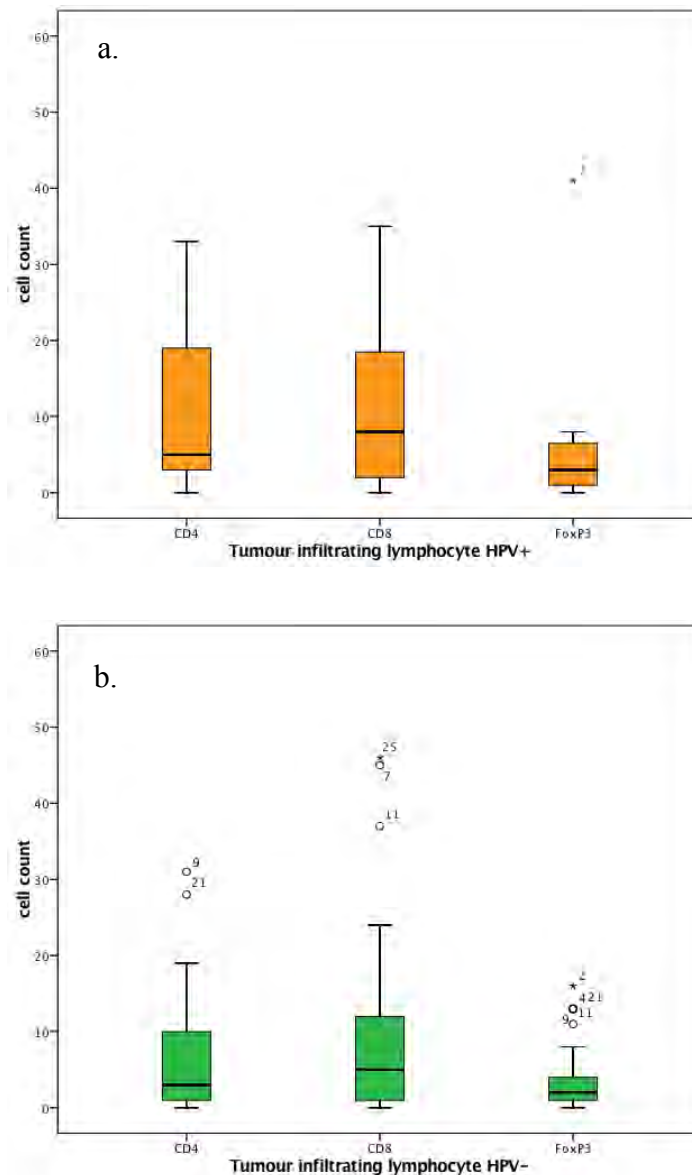


Figure 6.3a & b Tumour infiltrating lymphocytes in HPV positive (a) HNSCC compared to HPV negative (b) HNSCC. The levels of TIL were generally higher in the HPV positive group although statistical significance was shown with CD4 only. The two outliers for the HPV positive group are not shown, but these were 122 for CD4⁺ and 65 for CD8⁺.

The average CD4:CD8 cell ratio was 1.29 in HPV-positive HNSCC compared to 0.79 in HPV-negative HNSCC. It has been previously shown that the lower the CD4:CD8 ratio the better the prognosis is in terms of disease free survival (Wansom et al.,

2010), however in the current study this disagrees with the literature that says that HPV+ve HNSCC has the better outcome. Although the mean ratio was higher in HPV+ve HNSCC it is shown in the boxplot in Figure 6.4 that the distribution amongst HPV-negative HNSCC is much higher.

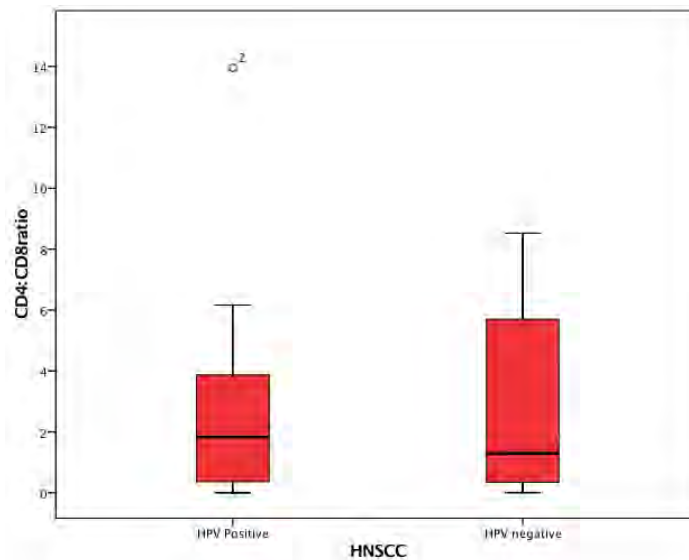


Figure 6.4 Boxplot showing the distribution of CD4:CD8 ratio amongst HPV-positive and HPV-negative HNSCC, the outlier from the HPV negative is excluded (CD4:CD8 ratio 26).

The CD8⁺:Foxp3 cell ratio was 2.56 in HPV positive-HNSCC compared to 2.36 in HPV-negative HNSCC, although these levels showed no statistical difference it is observed in Figure 6.5 that the distribution amongst the HPV-positive group was higher compared to the HPV-negative group.

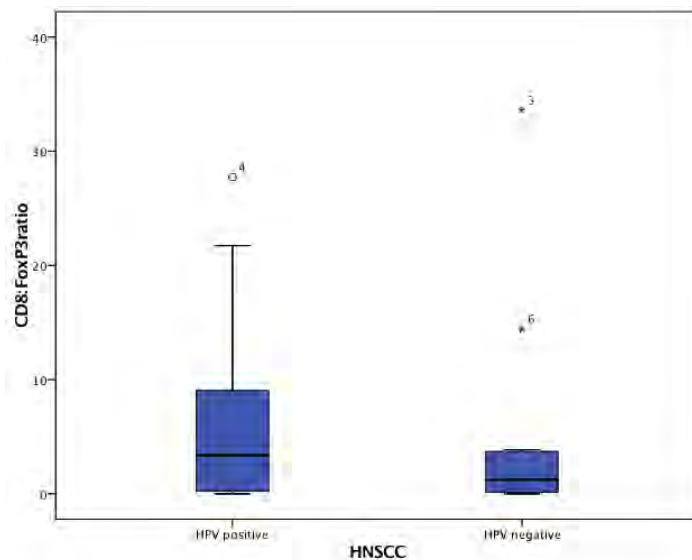


Figure 6.5 Boxplot illustrating the distribution of CD8⁺:FoxP3 ratio amongst HPV-positive versus HPV-negative HNSCC.

6.3.2. Th1 and Th2 cytokines in HPV-positive HNSCC versus HPV-negative HNSCC

Th1 Cytokines

Serum was analysed for quantitative analysis by ELISA, IL-2 was detected in 5/11 (45.5%) HPV-positive HNSCC compared to 18/33 (54.5%) HPV-negative HNSCC. The average IL-2 level was 7.16 ± 4.05 in HPV-positive group (n=5) compared with 28.80 ± 45.7 in the HPV-negative group (n=18). The numbers were too small for meaningful statistical analysis (statistical analysis not shown).

IFN γ was detected in 11/11 (100%) HPV positive HNSCC compared with 26/33 (78.8%) HPV-negative HNSCC. The average level was 410.6 ± 1191 compared to 338.7 ± 849 in HPV-negative HNSCC. This is illustrated in Figure 6.6a along with the Th2 (see Fig.6.6b) cytokines.

Th2 Cytokines

IL-4 was detected in 7/11 (64%) HPV-positive HNSCC compared to 13/33 (39%) HPV-negative HNSCC. The average IL-4 level was 22.8 ± 29.8 in HPV-positive compared to 90.5 ± 138.7 in HPV-negative HNSCC. Statistical analysis was not representative given the small sample size (data not shown). Interleukin 10 (IL-10) was detected in 9/11 (82%) HPV-positive HNSCC compared to 24/33 (73%) HPV negative-HNSCC, the average IL-10 level was 27.1 ± 39.9 in HPV-positive compared to 75.1 ± 121.6 in HPV-negative HNSCC. No discernable difference in the levels of Th1 and Th2 cytokines was observed amongst the two groups.

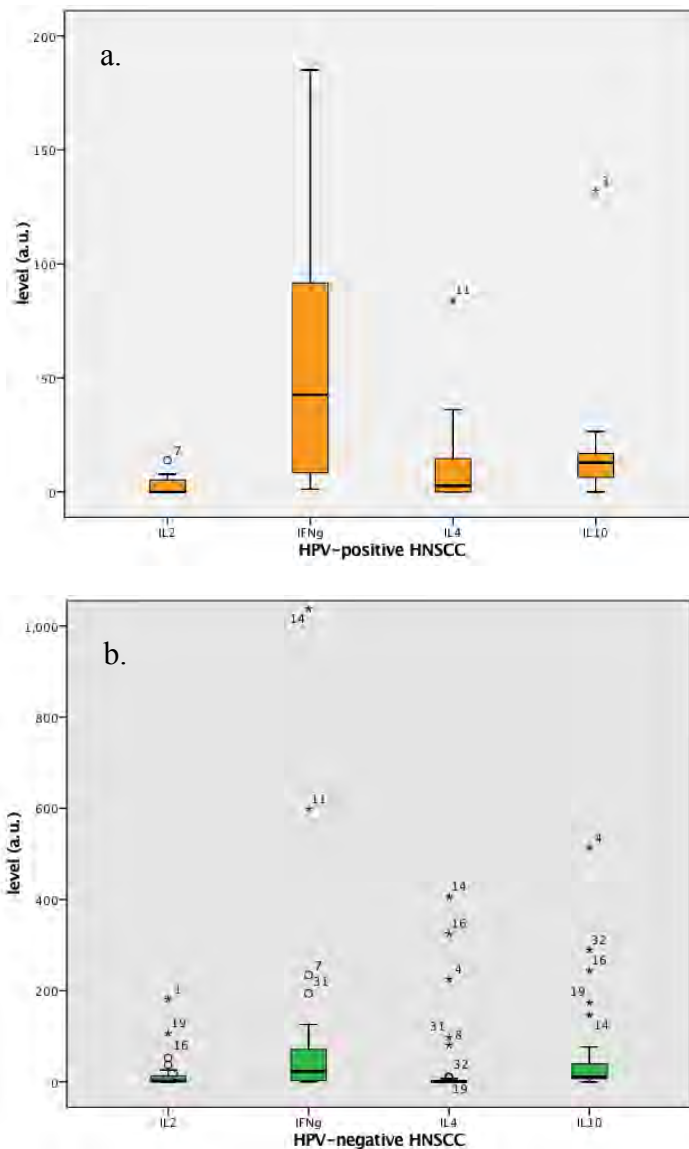


Figure 6.6a and b Distribution of Th1 cytokines (IL-2 and IFN γ) and Th2 cytokines (IL-4 and IL-10) in HPV+ (a) and HPV- (b) HNSCC. The outlier for the (a) HPV-positive IFN γ was at 4000 (not shown), and for the (b) HPV-negative IFN γ group these were 2100 and 3900 (not shown).

6.3.3. Anti-E7 antibody levels in HPV-positive HNSCC compared to HPV-negative HNSCC

The average E7-antibody level, as determined by ELISA (see section 4.0) in HPV-positive (n=11) was 2.10 ± 1.28 a.u. compared to 2.41 ± 1.14 a.u. in HPV-negative

(n=33) HNSCC, there was no statistical significance between the two groups, $p= 0.45$ (student's independent t-test). The groups were further subdivided into 'good' or 'poor' prognosis depending on the length of survival; survival of 3 years or more was defined as good and that less than 3 years was defined as poor. The distribution of E7 antibody levels amongst the groups is shown in Fig.6.7, and although poor prognosis showed higher levels of antibodies against E7 regardless of HPV status, no statistical difference was observed amongst the groups.

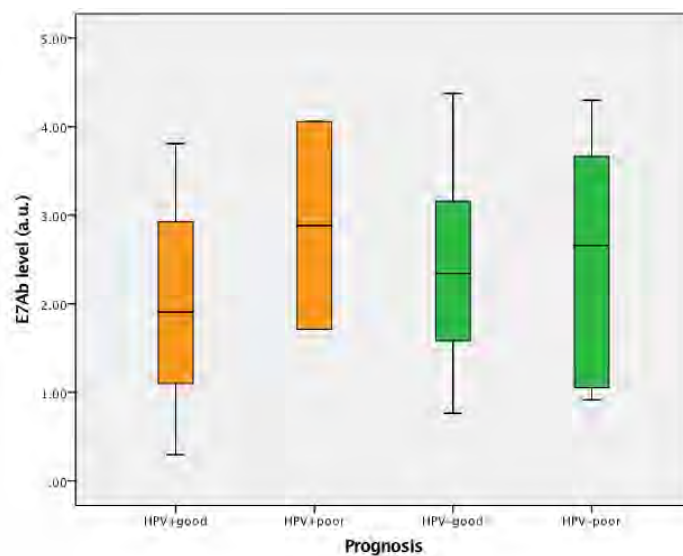


Figure 6.7 E7 antibody status as determined by ELISA (section 4.0) in HPV-positive and HPV-negative HNSCC. Good prognosis was defined as that of 3 years or more and poor prognosis was less than 3 years. There was cross over amongst the distribution of E7 antibody levels amongst the different groups.

6.3.4 Survival Curves in HPV-positive HNSCC versus HPV-negative HNSCC

Survival data was available for a minimum period of 3 years for each patient from analysis of clinical records, this was calculated as the period of time for each patient

before either the disease recurred or death was noted (disease free survival; DFS). Kaplan-Meier curves were plotted for each group. Good prognosis was that in which DFS was 3 years or more and poor prognosis was defined as DFS less than 3 years.

There were a total of 16 deaths in the patient cohort, 13 were in the HPV-negative group and 3 were in the HPV-positive group. The Chi-squared Wilcoxon test showed no significance in the DFS between all HPV-positive and negative HNSCC, $p=0.37$, however the numbers for sample size were small therefore care needs to be taken in analysis. The Kaplan Meier survival curve illustrates the difference in DFS between HPV-positive and HPV-negative HNSCC, the 5 year DFS was 50% in HPV-negative group compared to the 72% 5-year DFS in the HPV-positive.

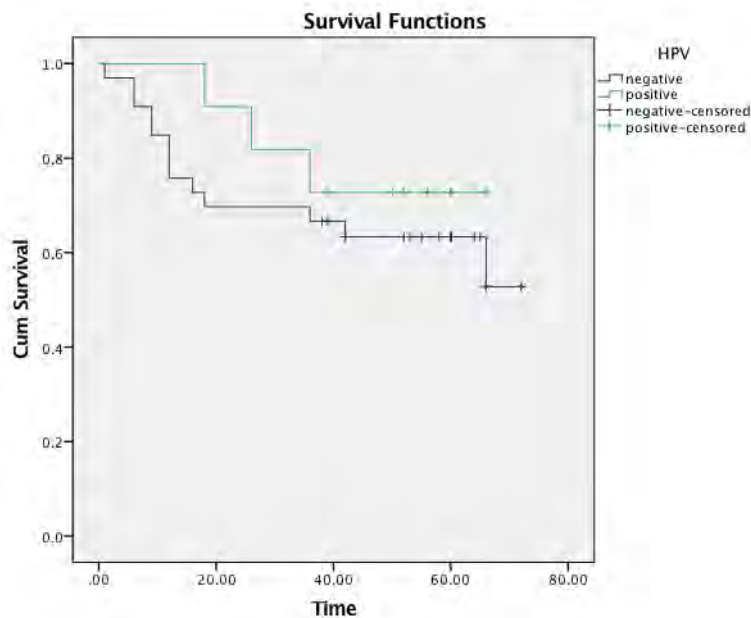


Figure 6.8 Kaplan Meier survival curve illustrating greater DFS in the HPV positive group compared to the HPV-negative group.

6.3.5 Survival Outcomes Regardless of HPV status

Of the 44 samples with complete data set, 32 had good prognosis, this was defined as that of 3 years or more DFS. The good prognosis group had survival outcomes of around 75% 5 year DFS compared to a maximal survival of 24 months in the poor prognosis group (see Fig. 6.9)

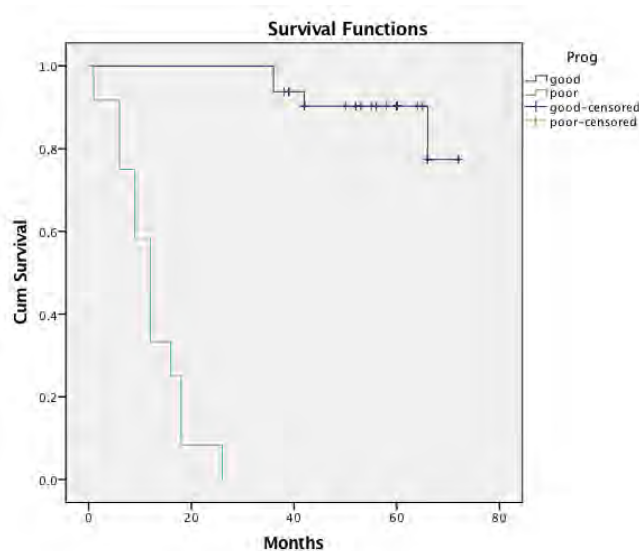


Figure 6.9 Disease free survival in good (≥ 3 -years) compared to poor prognosis (< 3 -years).

The mean counts for each of the TIL, cytokines and E7 antibody level for patients separated into good and poor prognosis are illustrated in Table 6.1. Levels of TIL were similar for both groups except for $CD4^+$ cells; the mean difference between the two groups was statistically different ($p=0.05$), with levels being higher in the good prognosis group. Although not significant general trends of greater levels of circulating cytokines were observed in those with a poorer prognosis, and there was no difference in the levels of E7 antibodies amongst the two groups.

	Prognosis 1=good 2=poor	N	Mean levels (cell count/ absorbance a.u.)	Std. Deviation	Sig.(2-tailed) (p)
CD8 ⁺	Good	32	9.53	14.49	0.42
	Poor	12	13.67	14.99	
FoxP3	Good	32	4.78	7.82	0.53
	Poor	12	3.58	4.44	
IL2	Good	32	11.49	32.19	0.70
	Poor	12	15.73	32.42	
IL4	Good	32	24.10	74.31	0.51
	Poor	12	47.30	108.55	
IL10	Good	32	33.25	57.78	0.28
	Poor	12	85.83	156.12	
IFN γ	Good	32	203.75	717.08	0.34
	Poor	12	566.77	1204.06	
E7Ab	Good	32	2.25	1.11	0.51
	Poor	12	2.55	1.35	
CD4 ⁺	Good	32	12.53	22.61	0.05
	Poor	12	4.25	3.86	

Table 6.1 Mean levels of TIL, cytokines and E7 antibody based on DFS survival, good prognosis ≥ 3 -year DFS and poor prognosis was DFS < 3-years.

6.4 Survival Outcomes in Oropharyngeal SCC

The survival outcomes for HPV-positive OPSCC and HPV-negative OPSCC were assessed, the results indicated that the HPV-positive OPSCC had an improved DFS outcome of 85% at 5-year compared to 65% 5-year DFS for HPV-negative OPSCC (see Fig.6.10), the Chi-squared Wilcoxon showed survival difference not to be statistically different however numbers especially in the HPV- group were small (n=3), p=0.56.

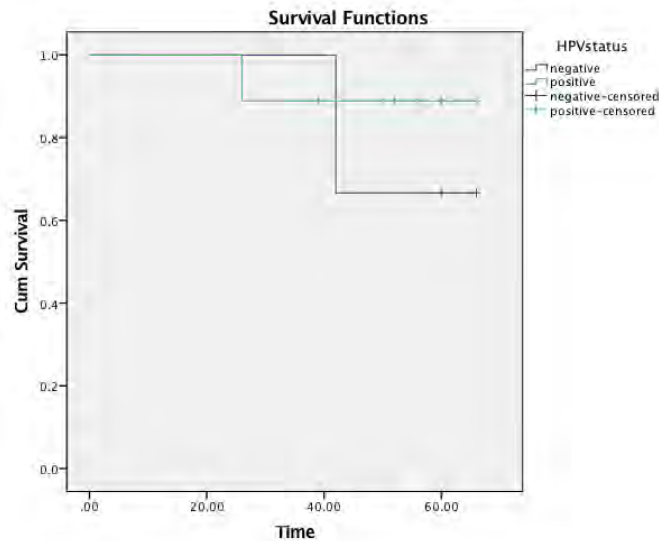


Figure 6.10 Five-year disease free survival in HPV+ versus HPV- OPSCC.

6.4.1 Tumour infiltrating lymphocytes and Anti-E7 antibodies in OPSCC

The mean CD4⁺ cell count was higher in the HPV-positive OPSCC (n=9) compared to the HPV-negative (n=3), the difference being 23.4 ± 39.6 compared to 15.3 ± 14.3 , the difference was not statistical ($p=0.74$). However the boxplot in Fig.6.11a shows that the distribution amongst the HPV-negative group was higher.

The CD8⁺ count appeared considerably higher in the HPV+ group compared to the HPV-negative group, 16.4 ± 21.1 versus 1.7 ± 2.1 , although statistical difference was not shown ($p=0.26$), the boxplot in Fig.6.11b illustrates the higher levels in HPV+ OPSCC. When the ratios of CD4⁺:CD8⁺ were analysed the HPV-positive group had a greater ratio, however the sample size of the HPV-negative group was small, thus statistical analysis was not possible (see Figure 6.12).

Levels of FoxP3 amongst the two groups were comparable, 7.9 ± 12.7 in HPV+

versus 6.3 ± 5.9 in the HPV- group, $p=0.85$ (Fig.6.11c). However when the ratios of CD8:FoxP3 were calculated a clear difference was noted between the two groups with the HPV+ group having 7.8 ± 10 compared to 0.21 ± 0.18 in the HPV- group, $p=0.05$ (see Fig. 6.13).

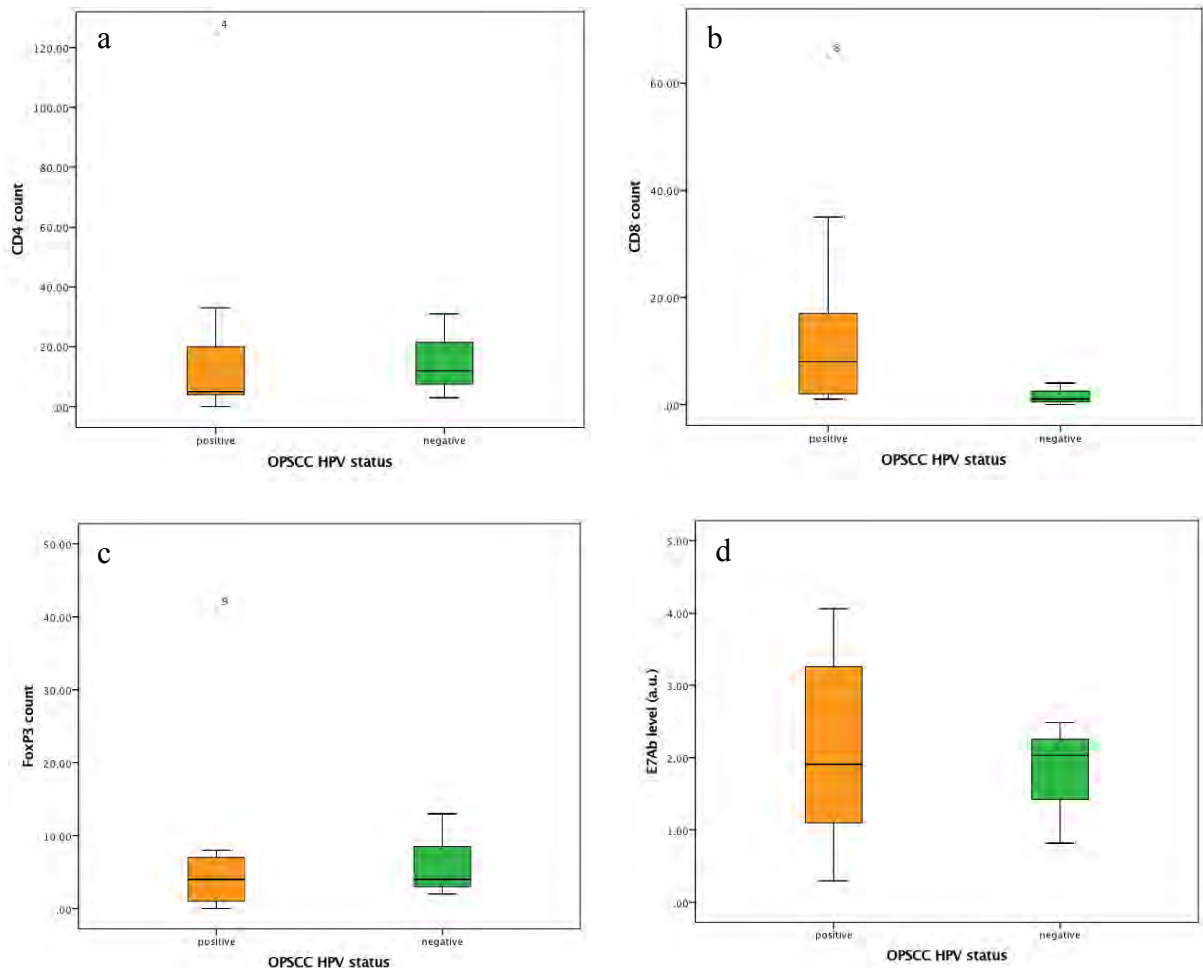


Figure 6.11a-d. Boxplots to illustrate levels of TIL CD4⁺, CD8⁺ and FoxP3, and of anti-E7 antibodies in HPV+ OPSCC compared to HPV- OPSCC.

(a) CD4⁺ cell count was higher in the HPV-positive OPSCC, 23.4 ± 39.6 (n=9) compared to the HPV-negative 15.3 ± 14.3 (n=3). (b) CD8⁺ count appeared considerably higher 16.4 ± 21.1 in the HPV+ group compared to the HPV- group 1.7 ± 2.1 . (c) Levels of FoxP3 were 7.9 ± 12.7 in HPV+ versus 6.3 ± 5.9 in HPV- group.

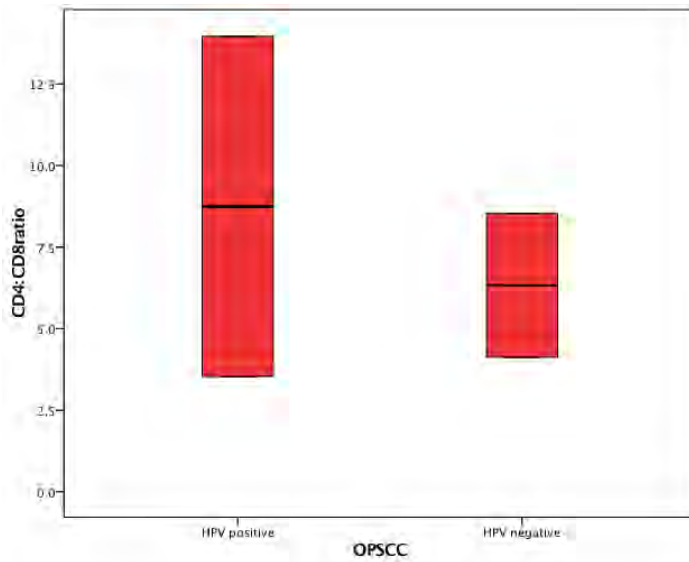


Figure 6.12 Boxplot illustrating the CD4:CD8 ratio amongst the HPV+ compared to the HPV- group, although the graph illustrates higher levels amongst the HPV+ group the numbers were small (n=3) in the HPV- group.

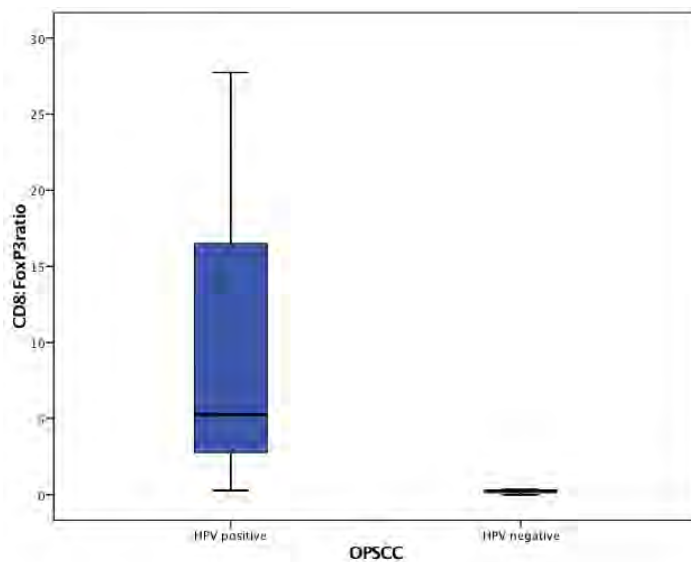


Figure 6.13 Boxplot illustrating the distribution of CD8:FoxP3 ratio amongst HPV+ compared to HPV- OPSCC.

6.4.2 Th1 and Th2 cytokines in OPSCC

The Th1 cytokines (IL-2 and IFN γ) and Th2 cytokines (IL-4 and IL-10) in OPSCC were analysed to assess if there was any difference amongst the two groups. Figure 6.14a and b illustrate the distribution of cytokine levels amongst the two groups. There was a significant difference in the level of IL-2 amongst the two groups ($p=0.038$), there was no discernable difference in the levels of the remaining cytokines amongst the two groups, this is illustrated in Table 6.2 with the mean and standard deviations also shown for each cytokine together with the p value for significance.

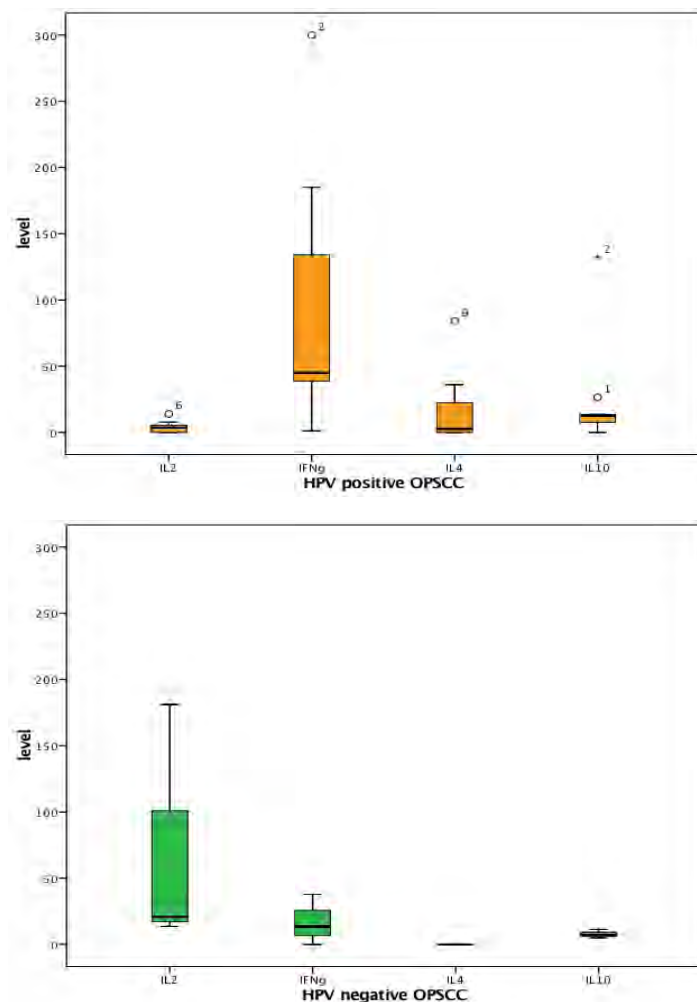


Figure 6.14a and b illustrating levels of Th1 and Th2 cytokines in HPV+ and HPV- OPSCC.

	OP HPV status	N	Mean	Std. Deviation	Sig.(2-tailed) (<i>p</i>)
IFN γ	positive	9	500.16	1313.80	0.551
	negative	3	17.10	19.16	
IL-10	positive	9	24.87	40.87	0.502
	negative	3	7.87	3.25	
IL-4	positive	9	16.94	28.14	0.336
	negative	3	0.0	0.0	
IL-2	positive	9	3.98	4.74	0.038
	negative	3	71.80	94.72	

Table 6.2 The mean and standard deviations for each of the Th1 and Th2 cytokines in OPSCC, these are further subdivided into HPV-positive and HPV-negative for each group. The Independent t-test for each of the Th1 and Th2 cytokines is also illustrated, the only cytokine with significant difference between the two groups was IL-2.

6.5 Discussion

The interplay of variable immune parameters certainly has an impact on improved prognosis in HPV-positive HNSCC compared to HPV-negative, these differences are more apparent with the oropharyngeal subset of HNSCC. This may be due to fact that HPV-16 is implicated in the aetiology of OPSCC as compared to other HNSCC. Although HPV is present within most OPSCC and some HNSCC, other studies have shown the presence of HPV within tumours such as lung cancer but the causation is arguable (Zhai et al., 2015).

This study found that TIL were higher in HPV-positive HNSCC compared to HPV-negative. However not all those within the HPV-positive group exhibited TIL within the sample, the reason as to why some HPV-positive tumours exhibit TIL and some

do not remain unanswered, perhaps this may be due to the overall health and immune status of the patient rather than due to the nature of the tumour itself.

Low ratio of CD4⁺:CD8⁺ have been shown to have favourable outcomes regarding prognosis (Wansom et al., 2010), although this study showed that the CD4⁺:CD8⁺ count was higher in the HPV-positive HNSCC, the sample size was small. The CD4⁺ count was higher in the good (≥ 3 -years) prognosis group, studies previously performed that looked at the role of CD4⁺ cells in vaccinations have shown increased potency of the vaccinations when CD4⁺ cells are stimulated (Hung et al., 2007, Wu et al., 2010, Wu et al., 2011), Song *et al.* showed by stimulating the levels of CD4⁺ cells by intra-tumour injection increased levels of CD4⁺ specific T-cells and thus increased anti-tumour activity (Song et al., 2014).

The CD8⁺:Foxp3 ratio has also been associated with favorable outcomes (Näsman et al., 2012), with higher levels associated with better prognosis, this was found to be true in this study with higher levels in the HPV-positive group, in particular in the OPSCC group. TILs have been shown to have improved prognosis regardless of tumour site and HPV status or viral association (Galon et al., 2006, Sato et al., 2005). In particular infiltrating CD8⁺ cells are shown to have prognostic effects, however the role of the T-regulatory cells - FoxP3, is to dampen the immune response and therefore high levels of these can have a reverse effect, in particular higher levels of T-reg cells have been associated with poorer prognosis (Bates et al., 2006).

Näsman *et al.* showed that high levels of CD8⁺:FoxP3 were associated with a positive clinical outcome in HPV+ tonsillar SCC, however this was also observed for

high levels of CD8⁺:FoxP3 regardless of HPV status(Nasman et al., 2012). CD8⁺ infiltration in particular is associated with improved outcomes, much of this work has been done on cervical cancer where the majority are caused by HPV-16/18, it has been shown that higher levels of CD8⁺ T-cells and high CD8⁺:regulatory T-cells were associated with improved survival and reduced level of lymph node metastases (Piersma et al., 2007).

However some studies have found that increased levels of T-reg cells within the tumour are associated with improved prognosis, this has been shown in colorectal carcinoma, malignant melanoma and lymphoma (Ladanyi et al., 2004, Ladoire et al., 2011, Alvaro et al., 2005). The paradoxical role of T-reg cells within HNSCC tumour tissue associated with favourable outcomes has been explained by Lukesova *et al.*, they demonstrated that the translocation of oral microbes to HNSCC tissue can provoke a T-cell mediated antimicrobial inflammatory response, this involves Th17 cells which can then promote cancer growth, however the infiltration of T-reg cells can dampen this response and thus reduce cancer growth stimulation (Lukesova et al., 2014). Furthermore it has been postulated that the T-reg cells within HNSCC may help to maintain the HPV+ status of some of the HNSCC and thereby stimulate the immune response against viral infected cells (Lukesova et al., 2014).

The levels of peripheral circulating cytokines were variable amongst the two groups, not all patients in either the HPV-positive or HPV-negative group exhibited peripheral circulating cytokines. However when the levels of peripheral circulating cytokines were analysed based on good (≥ 3 -years) or poor (< 3 years) prognosis regardless of HPV status it was noted that the levels of circulating cytokines, both Th1 and Th2,

were much higher in the poor prognosis group. This may be due to a proinflammatory response against the tumour which may then have collateral damaging effects, the fact that both types of cytokines increased would tend to argue against a specific response.

HPV+ OPSCC express foreign viral antigens, although the immune response has failed to prevent the cancer formation there is still an attempt to control or kill the disease by immune reaction. Lack of antigen to present in HPV- tumours or these tumours not being recognized as foreign may explain a lack of immune response in such tumours. There may be a role for increasing recognition of these non-HPV cancer cells when oncogenes, such as p53 and Rb are mutated due to carcinogens in such tumours.

The exact role of HPV infection in the various subsets of HNSCC is not known, it is well recognised that infection with high risk HPV has a causative role in tonsillar OPSCC. HNSCC are a group of heterogeneous cancers that are often grouped together due to locality rather than due to tumour biology or behaviour. Therefore the levels of TIL, circulating cytokines and anti-E7 antibodies together with survival outcomes were analysed in the OPSCC group. There was greater than 85% 5-year DFS in the HPV-positive OPSCC compared to 65% 5-year DFS in the HPV-negative group. The ratio of CD8⁺:FoxP3 was higher in the HPV+ group compared to the HPV- group. There was no significant difference in the levels of circulating cytokines amongst the two groups except for IL-2, which was higher in the HPV- group. IL-2 actions include the stimulation, growth and differentiation of antigen selected cytotoxic cells, it is also necessary for T-cell development, therefore higher

levels in the HPV-negative OPSCC may be due to the lower immune response in these tumours compared to HPV+ OPSCC. Lin *et al.* showed that IL-2 enhanced the potency of DNA vaccine against HPV-E7 expressing tumours by increasing the frequency of CD8⁺ T-cells. There may be a role in antigen presentation in HPV-negative tumours to allow for immune directed therapy in such tumours (Lin et al., 2007).

Improved adaptive immunity may play a role in the favourable prognosis of patients with HPV-16 positive HNSCC tumours. However what is not known is the broader picture of the interplay of other immune parameters and the response to HPV infection, knowledge of which may lead to the development of combined targeted immunotherapy.

Chapter 7. Concluding Remarks

Head and neck squamous cell cancers are often grouped together due to the locality of the anatomy, however within this group there is a heterogeneous group of tumour subtypes, which have similar causative factors, but highly variable clinical behaviour. High risk HPV, especially HPV-16/18 are increasingly implicated in the causation of HNSCC, in particular OPSCC. The trends of which have steadily been increasing over the last 40-years, epidemiological studies in the West have shown large increases in the incidence of OPSCC as compared to the remaining subtypes of HNSCC, this is especially true in the younger population (<40 years age) (Hammarstedt et al., 2006, Genden et al., 2013). The upward trend in OPSCC is attributed to an increasingly younger, sexually active population and changes in sexual behaviour (Smith et al., 2004). High-risk strains of HPV are recognised in the pathogenesis of some HNSCC and have been detected in up to 67% of OPSCC (Smith et al., 2004, Sivasithamparam et al., 2013). It is well recognised now that survival with HPV associated cancers is greater as compared with HPV negative tumours (Ang et al., 2010a).

The aims of this thesis were to investigate further the interplay of various immune parameters to assess what effect these have on survival outcomes, and whether this knowledge can be extrapolated to non-HPV tumours and help de-escalate treatment regimens of radiotherapy and chemotherapy, which although curative, can leave devastating collateral damage.

The primary difficulty in diagnosis of HPV associated tumours is to determine whether HPV infection is causative or if infection with HPV is a coincidental finding. Detection of the HPV virus alone does not indicate causation, the detection of an active virus is required and diagnostic tests can be challenging in terms of use in clinical practice and also expense in the current NHS climate. Although no 'Gold Standard' diagnostic test is available, it is accepted that concordance between p16 staining by immunohistochemistry and In-situ Hybridisation detection of high risk-HPV mRNA can be used clinically. This study showed 93% concordance, this was similar if not greater concordance to what previous studies had found (Thavaraj et al., 2011b, Lewis, 2012).

Robinson *et al.* performed a pooled analysis which looked at the rates of p16 positive/HPV negative tumours and p16 negative/HPV positive, these were 5% and 8% respectively (Robinson et al., 2010), therefore the results of this study for the discordant results was similar. Although p16 is currently doubted as a good screen for HPV infection alone due to non-specificity, in the current study it was found that 93% (40/43) of samples were in agreement between the tests. Furthermore it has been shown previously that molecular classification of HPV tumours is better at distinguishing prognosis than p16 staining alone (Weinberger et al., 2006). Weinberger *et al.*, reported that patients with a Class III oropharyngeal SCC had a 5-year overall survival of 79% versus 20% for Class I and 18% for Class II ($p=0.0095$) (Weinberger et al., 2006), thereby clinically rather than just classifying a HPV associated tumour as negative or positive the molecular classification based on p16 staining and a confirmatory test should be used.

Previous studies have shown seropositivity to the HPV oncoproteins E6 and E7 confers improved survival benefits (Rubenstein et al., 2011); this study also showed that there was seropositivity to E7 present in healthy control subjects. There was cross-over in terms of distribution of levels of E7 antibody across HPV positive and HPV negative HNSCC with good and poor prognosis, however when the OPSCC subtype was reviewed, greater levels of E7 antibody were present in the HPV positive group in this study. This may be secondary to presentation of the virus to the surface of the tumour by antigen-presenting cells. The use of seropositive monitoring may be a useful marker for disease progression or treatment efficacy in HNSCC, or especially OPSCC. This was not looked at in this study however such monitoring is already being trialled in cervical cancer. Although the immune reaction to the HPV virus is different in oropharyngeal and cervical cancer due to the differences in the immune rich tissue in the oropharynx, this is something that could be further developed by analysing the differences in presentation of the virus in cervical versus OP tissue. The use of E7 antibody levels alone are not a useful prognostic indicator as this study showed that these were also present in healthy control subjects.

The interplay of the various immune parameters have an overall prognostic effect, it has been shown that CD4⁺ and CD8⁺ counts are associated with improved survival benefits, however the overall relationships of these have been contradictory in the literature. The work in this thesis found a higher ratio of CD8⁺:FoxP3 and CD4⁺:CD8⁺ TIL in HPV+HNSCC compared to HPV- HNSCC. Although this study did not look at circulating T-regulatory cells (T-regs) per se, previous work in this department showed that there was an increase in circulating T-regs from pre- to post-treatment, and there was a positive correlation between T-regs and TIL (Green et al.,

2013). However Lukesova *et al.*, have shown that lower levels of circulating CD8:Treg have improved prognosis (Lukesova et al., 2014). Some authors have shown lower levels of circulating T-regs (Hoffmann et al., 2002), whilst others have not demonstrated such results (Schaefer et al., 2005, Strauss et al., 2007). Some studies have shown elevated levels of TIL within the tumour microenvironment (Nasman et al., 2012, Wansom et al., 2012). The interplay of immune parameters is variable, work on immunodeficient or immunosuppressed patients previously has shown an increase in HPV associated cancers (Kreimer et al., 2004, Shamanin et al., 1996) and increased immune response is also associated with pro-inflammatory responses which can be associated with pro-angiogenesis and pro-metastatic effects, as chronic inflammation is often associated with neoplasia (Pikarsky et al., 2004, Coussens and Werb, 2002). It may be postulated that as HPV has different methods of immune evasion, which is variable amongst the head and neck sub-sites, this is why the immune response is varied amongst subjects with HPV related HNSCC and thus explains why results of so many studies are contradictory. Much of the work on the characterisation of HPV associated cancers has been carried out on cervical cancer cell lines, the natural history of HPV infection in the head and neck has been poorly characterised, although studies on gene alteration and expression, and miRNA have shown similarities between cervical and HNSCC they have also shown differences between the two sites in terms of tissue biochemistry (Wilting et al., 2009, Pyeon et al., 2007), therefore it is increasing important to delineate the natural history of HPV infection in the head and neck region and how this is different to cervical tissue where most tumors are associated with HPV infection.

At present HPV positive and HPV negative tumours have the same treatment regimen, although HPV positive cancers have been shown to have a different histological and biological profile, and improved survival rates (Ang et al., 2010a) this is especially true of OPSCC, however these two distinct groups are treated with surgery, chemotherapy and fractionated radiotherapy, or often a combination of all three. Recent phase II trials of the use of vaccines in HPV associated vulval-intra-epithelial neoplasia (VIN) have shown promising results (Kenter et al., 2009, Daayana et al., 2010). This has promising hope for increasing immune therapy across HNSCC rather than targeting with chemotherapy or radiation therapy alone, which can have damaging collateral effects.

Acute and late toxicities are associated with most chemotherapy regimens for HNSCC and can pose significant problems for such patients (Lee et al., 2011). These include early complications of nausea, vomiting, immunosuppression, hair loss, skin burns, radiation toxicity to late effects of pain, scarring, osteoradionecrosis, dental decay, gastric tube dependency, infertility, hypothyroidism, carotid stenosis, neurotoxicity and nephrotoxicity. As patients with HPV positive HNSCC tend to be younger (40-60 years) effects of such toxicities can have lasting effects on the overall well being of the patient. The aims of de-escalation treatments are to try to reduce such effects and also to reduce risks of morbidity associated with extensive surgical resections, such that neo-adjuvant treatment protocols can reduce surgical resection fields. De-escalation trials are based around three main points; 1) Exploring Cetuximab (EGFR inhibitor) as an alternative to cisplatin when given with radiotherapy; 2) reduction of radiation dose when given in combination with chemotherapy and 3) Reduction of adjuvant radiotherapy or chemotherapy following

primary treatment with surgical resection (Masterson et al., 2014). At present there are a number of ongoing trials (see appendix 3) which have promising hope of development of treatment protocols to reduce iatrogenic morbidity associated with current treatment protocols, in particular radiotherapy.

The HPV E2 open reading frame (ORF) keeps the expression of HPV oncoproteins E6 and E7 suppressed however when this ORF is disrupted, due to viral integration into host genome, this control mechanism is lost and over expression of E6 and E7 occur and thus progression to carcinogenesis (Doorbar et al., 2012, Lehoux et al., 2009). This may be a target for future treatment, instead of targeting the E6 and E7 oncoproteins vaccinations can be developed or immunotherapy developed which can keep this E2 ORF stable or to reintroduce this back into HPV infected cells to allow for expression of E2 and thus inhibition of the driving force of HPV oncogenesis - E6 and E7.

Although HPV-E6 and E7 are recognised as oncoproteins, the roles of the other HPV proteins can be further evaluated and possible treatment targets against these developed. One such HPV protein is the E5 protein, the function of which is viral replication by helping to replicate the episomal DNA. E5 plays an early role in tumorigenesis as it is lost when the viral DNA integrates into the host DNA (Ganguly, 2012) and therefore targeting this protein may help in the prevention of viral DNA integration and thus cancer formation.

Various studies, some of which have been examined in this thesis, have investigated the role of variable immune markers such as CD4⁺, CD8⁺, FoxP3, IL's and p16

positivity for the clinical prognosis or disease status monitoring. However large clinical trials are needed for the development of clinically relevant biomarkers to be examined.

The rates of non-oropharyngeal HPV positive HNSCC in the current study were found to be low. The immune profiling of non-OP HPV positive HNSCC and the role of HPV positivity to disease progression in such sub-sites remains to be fully determined as the tissue type between the oropharynx, especially tonsil, is different. The increased response to chemo/radiotherapy in HPV positive HNSCC may be explained by an intact p53 gene, which may become re-activated, furthermore chemo/radiotherapy cause cell injury and local inflammation which make the tumour more sensitive to the immune system by increasing the presentation of tumour antigens.

Immunotherapy has a promising role in HPV-associated cancers, it is associated with reduced treatment associated toxicity and also can be varied to the changing tumour type, and as it can be administered systemically it can target possible metastatic cells (Rapidis and Wolf, 2009). The role of possible immune therapy in HPV-HNSCC is yet to be fully determined and potential future research can focus on whether this knowledge can be extrapolated to non-HPV associated HNSCC, treatments such as adoptive immune transfer, which include expansion and re-infusion of patients own immune cells have been studied, also the use of cytokine therapy has been studied, in addition to the development of cancer vaccines based on nucleic acids, dendritic cells, peptide based or a combination of all these (Rapidis and Wolf, 2009).

The hallmark of HNSCC is the tumour heterogeneity and genetic diversity, and certainly HPV associated tumours are thought of as a biologically distinct tumour compared to smoking & alcohol related HNSCC. HPV associated cancers have been shown to have heterogeneous responses in terms of adaptive immunity, however overall there is promising hope that such tumours can be treated with reduced toxicity of current intense treatments and the quality of life for such patients can be increased, who are often younger than the general typical phenotype of HNSCC. There is much to be learned yet on the biology of HPV and cancer but there is promising hope that future advances can be extrapolated to our understanding and treatment of HPV-associated and non-HPV associated HNSCC.

The use of xenograft mice as personal avatars in personalized cancer care are gaining momentum once again, they were first described in 1988 by Fiebig (Fiebig, 1988) but the idea was soon abandoned as the time from implantation to discernable tumour formation in mice and then trialing of drugs was felt to be too long for use in clinical practice. Furthermore, the rate of tumour implantation into the mouse model was around 60-70% at best, however it was concluded that mouse models provided a useful and more accurate model for drug testing compared to cell cultures as they provided information on the biology of tumour response. Recent work by David Sidransky at John Hopkins University has shown implantation rates of greater than 90% and also have shown some promising use of patient derived xenograft (PDX) mice in tailoring cancer treatment. It has been shown that avatar response to treatment predicted tumour response in patients, Garralda *et al.* used avatar directed treatment in 13 subjects and found that 11/13 had avatar response that mimicked tumour response in the patient (Garralda et al., 2014). The work on immune

parameters in this study showed a variable response amongst the different sub-sites of HNSCC, in particular the greatest yield of TIL was observed amongst the OPSCC group. The use of PDX mice in the treatment of HNSCC could provide advantageous as yet there is great heterogeneity in the immune response in HNSCC, immune therapies can be tailored according to the immune status that is not static. Bench testing of PDX has already been shown to correlate with clinical response and may help to select treatment in some patients with no actionable mutations (Garralda et al., 2014), such as those in HPV+ HNSCC. The main advantage being that treatments could be tailored to individuals based on their immune status as determined by levels of TIL and circulating cytokines and seropositivity as was shown in this study, these parameters could then help tailor a specific prescription of immune parameters as adjuncts for the treatment of HNSCC, thereby reducing the patient mortality associated with current homologous treatment regimes for such cancers.

References

- ACCARDI, L., DONA, M. G., DI BONITO, P. & GIORGI, C. 2005. Intracellular anti-E7 human antibodies in single-chain format inhibit proliferation of HPV16-positive cervical carcinoma cells. *Int J Cancer*, 116, 564-70.
- AJCC, A. J. C. O. C. 2002. *AJCC Cancer Staging Manual*, Unites States of America, Springer.
- ALVARO, T., LEJEUNE, M., SALVADO, M. T., BOSCH, R., GARCIA, J. F., JAEN, J., BANHAM, A. H., RONCADOR, G., MONTALBAN, C. & PIRIS, M. A. 2005. Outcome in Hodgkin's lymphoma can be predicted from the presence of accompanying cytotoxic and regulatory T cells. *Clin Cancer Res*, 11, 1467-73.
- ANG, K. K., HARRIS, J., WHEELER, R., WEBER, R., ROSENTHAL, D. I., NGUYEN-TAN, P. F., WESTRA, W. H., CHUNG, C. H., JORDAN, R. C., LU, C., KIM, H., AXELROD, R., SILVERMAN, C. C., REDMOND, K. P. & GILLISON, M. L. 2010a. Human papillomavirus and survival of patients with oropharyngeal cancer. *N Engl J Med*, 363, 24-35.
- ANG, K. K., HARRIS, J., WHEELER, R., WEBER, R., ROSENTHAL, D. I., NGUYEN-TAN, P. F., WESTRA, W. H., CHUNG, C. H., JORDAN, R. C., LU, C., KIM, H., AXELROD, R., SILVERMAN, C. C., REDMOND, K. P. & GILLISON, M. L. 2010b. Human papillomavirus and survival of patients with oropharyngeal cancer. *New England Journal of Medicine*, 363, 24-35.
- BADOUAL, C., HANS, S., RODRIGUEZ, J., PEYRARD, S., KLEIN, C., AGUEZNAY NEL, H., MOSSERI, V., LACCOURREYE, O., BRUNEVAL, P., FRIDMAN, W. H., BRASNU, D. F. & TARTOUR, E. 2006. Prognostic value of tumor-infiltrating CD4+ T-cell subpopulations in head and neck cancers. *Clin Cancer Res*, 12, 465-72.
- BAKER, C. C., PHELPS, W. C., LINDGREN, V., BRAUN, M. J., GONDA, M. A. & HOWLEY, P. M. 1987. Structural and transcriptional analysis of human papillomavirus type 16 sequences in cervical carcinoma cell lines. *J Virol*, 61, 962-71.
- BATES, G. J., FOX, S. B., HAN, C., LEEK, R. D., GARCIA, J. F., HARRIS, A. L. & BANHAM, A. H. 2006. Quantification of regulatory T cells enables the identification of high-risk breast cancer patients and those at risk of late relapse. *J Clin Oncol*, 24, 5373-80.
- BLOT, W. J., MCLAUGHLIN, J. K., WINN, D. M., AUSTIN, D. F., GREENBERG, R. S., PRESTON-MARTIN, S., BERNSTEIN, L., SCHOENBERG, J. B., STEMHAGEN, A. & FRAUMENI, J. F., JR. 1988. Smoking and drinking in relation to oral and pharyngeal cancer. *Cancer Research*, 48, 3282-7.
- BOFFETTA, P., HECHT, S., GRAY, N., GUPTA, P. & STRAIF, K. 2008. Smokeless tobacco and cancer. *Lancet Oncology*, 9, 667-75.
- BOLPETTI, A., SILVA, J. S., VILLA, L. L. & LEPIQUE, A. P. 2010. Interleukin-10 production by tumor infiltrating macrophages plays a role in Human Papillomavirus 16 tumor growth. *BMC Immunology*, 11, 27.

- BOSHART, M., GISSMANN, L., IKENBERG, H., KLEINHEINZ, A., SCHEURLLEN, W. & ZUR HAUSEN, H. 1984. A new type of papillomavirus DNA, its presence in genital cancer biopsies and in cell lines derived from cervical cancer. *EMBO J*, 3, 1151-7.
- BRENNAN, P., LEWIS, S., HASHIBE, M., BELL, D. A., BOFFETTA, P., BOUCHARDY, C., CAPORASO, N., CHEN, C., COUTELLE, C., DIEHL, S. R., HAYES, R. B., OLSHAN, A. F., SCHWARTZ, S. M., STURGIS, E. M., WEI, Q., ZAVRAS, A. I. & BENHAMOU, S. 2004. Pooled analysis of alcohol dehydrogenase genotypes and head and neck cancer: a HuGE review. *American Journal of Epidemiology*, 159, 1-16.
- BRENNER, J. C., GRAHAM, M. P., KUMAR, B., SAUNDERS, L. M., KUPFER, R., LYONS, R. H., BRADFORD, C. R. & CAREY, T. E. 2010. Genotyping of 73 UM-SCC head and neck squamous cell carcinoma cell lines. *Head Neck*, 32, 417-26.
- BRINT, E., O'CALLAGHAN, G. & HOUSTON, A. 2013. Life in the Fas lane: differential outcomes of Fas signaling. *Cell Mol Life Sci*, 70, 4085-99.
- BROOKS, P. J. & THERUVATHU, J. A. 2005. DNA adducts from acetaldehyde: implications for alcohol-related carcinogenesis. *Alcohol*, 35, 187-93.
- BRUNELLE, J. L. & GREEN, R. 2014. One-dimensional SDS-polyacrylamide gel electrophoresis (1D SDS-PAGE). *Methods Enzymol*, 541, 151-9.
- BUNDGAARD, T., WILDT, J., FRYDENBERG, M., ELBROND, O. & NIELSEN, J. E. 1995. Case-control study of squamous cell cancer of the oral cavity in Denmark. *Cancer Causes & Control*, 6, 57-67.
- CASTELLSAGUE, X., QUINTANA, M. J., MARTINEZ, M. C., NIETO, A., SANCHEZ, M. J., JUAN, A., MONNER, A., CARRERA, M., AGUDO, A., QUER, M., MUNOZ, N., HERRERO, R., FRANCESCHI, S. & BOSCH, F. X. 2004. The role of type of tobacco and type of alcoholic beverage in oral carcinogenesis. *International Journal of Cancer*, 108, 741-9.
- CAUDELL, J. J., SCHANER, P. E., MEREDITH, R. F., LOCHER, J. L., NABELL, L. M., CARROLL, W. R., MAGNUSON, J. S., SPENCER, S. A. & BONNER, J. A. 2009. Factors associated with long-term dysphagia after definitive radiotherapy for locally advanced head-and-neck cancer. *Int J Radiat Oncol Biol Phys*, 73, 410-5.
- CHATURVEDI, A. K., ENGELS, E. A., ANDERSON, W. F. & GILLISON, M. L. 2008. Incidence trends for human papillomavirus-related and -unrelated oral squamous cell carcinomas in the United States. *J Clin Oncol*, 26, 612-9.
- CHATURVEDI, A. K., ENGELS, E. A., PFEIFFER, R. M., HERNANDEZ, B. Y., XIAO, W., KIM, E., JIANG, B., GOODMAN, M. T., SIBUG-SABER, M., COZEN, W., LIU, L., LYNCH, C. F., WENTZENSEN, N., JORDAN, R. C., ALTEKRUSE, S., ANDERSON, W. F., ROSENBERG, P. S. & GILLISON, M. L. 2011. Human papillomavirus and rising oropharyngeal cancer incidence in the United States. *Journal of Clinical Oncology*, 29, 4294-301.
- CHEN, P. C., KUO, C., PAN, C. C. & CHOU, M. Y. 2002. Risk of oral cancer associated with human papillomavirus infection, betel quid chewing, and cigarette smoking in Taiwan--an integrated molecular and epidemiological study of 58 cases. *Journal of Oral Pathology & Medicine*, 31, 317-22.
- CHOMCZYNSKI, P. & SACCHI, N. 1987. Single-step method of RNA isolation by acid guanidinium thiocyanate-phenol-chloroform extraction. *Anal Biochem*, 162, 156-9.

- CHOMCZYNSKI, P. & SACCHI, N. 2006. The single-step method of RNA isolation by acid guanidinium thiocyanate-phenol-chloroform extraction: twenty-something years on. *Nat Protoc*, 1, 581-5.
- CHU, N. S. 2001. Effects of Betel chewing on the central and autonomic nervous systems. *Journal of Biomedical Science*, 8, 229-36.
- CONWAY, D. I., STOCKTON, D. L., WARNAKULASURIYA, K. A., OGDEN, G. & MACPHERSON, L. M. 2006. Incidence of oral and oropharyngeal cancer in United Kingdom (1990-1999) -- recent trends and regional variation. *Oral Oncol*, 42, 586-92.
- COUSSENS, L. M. & WERB, Z. 2002. Inflammation and cancer. *Nature*, 420, 860-7.
- D'SOUZA, G., KREIMER, A. R., VISCIDI, R., PAWLITA, M., FAKHRY, C., KOCH, W. M., WESTRA, W. H. & GILLISON, M. L. 2007. Case-control study of human papillomavirus and oropharyngeal cancer. *New England Journal of Medicine*, 356, 1944-56.
- DAAYANA, S., ELKORD, E., WINTERS, U., PAWLITA, M., RODEN, R., STERN, P. L. & KITCHENER, H. C. 2010. Phase II trial of imiquimod and HPV therapeutic vaccination in patients with vulval intraepithelial neoplasia. *Br J Cancer*, 102, 1129-36.
- DAHNO 2013. National Head and Neck Cancer Audit *In: CENTRE, H. A. S. C. I.* (ed.).
- DARST, S. A., ROBERTSON, C. R. & BERZOFSKY, J. A. 1988. Adsorption of the protein antigen myoglobin affects the binding of conformation-specific monoclonal antibodies. *Biophys J*, 53, 533-9.
- DE COSTA, F., BARBER, C. J., PUJARA, P. T., REED, D. W. & COVELLO, P. S. 2016. Purification of a Recombinant Polyhistidine-Tagged Glucosyltransferase Using Immobilized Metal-Affinity Chromatography (IMAC). *Methods Mol Biol*, 1405, 91-7.
- DE VOS VAN STEENWIJK, P. J., HEUSINKVELD, M., RAMWADHDOEBE, T. H., LOWIK, M. J., VAN DER HULST, J. M., GOEDEMANS, R., PIERSMA, S. J., KENTER, G. G. & VAN DER BURG, S. H. 2010. An unexpectedly large polyclonal repertoire of HPV-specific T cells is poised for action in patients with cervical cancer. *Cancer Research*, 70, 2707-17.
- DENIS, F., GARAUD, P., BARDET, E., ALFONSI, M., SIRE, C., GERMAIN, T., BERGEROT, P., RHEIN, B., TORTOCHAUX, J., OUDINOT, P. & CALAIS, G. 2003. Late toxicity results of the GORTEC 94-01 randomized trial comparing radiotherapy with concomitant radiochemotherapy for advanced-stage oropharynx carcinoma: comparison of LENT/SOMA, RTOG/EORTC, and NCI-CTC scoring systems. *Int J Radiat Oncol Biol Phys*, 55, 93-8.
- DI BONITO, P., GRASSO, F., MOCHI, S., ACCARDI, L., DONA, M. G., BRANCA, M., COSTA, S., MARIANI, L., AGAROSI, A., CIOTTI, M., SYRJANEN, K. & GIORGI, C. 2006. Serum antibody response to Human papillomavirus (HPV) infections detected by a novel ELISA technique based on denatured recombinant HPV16 L1, L2, E4, E6 and E7 proteins. *Infect Agent Cancer*, 1, 6.
- DIKSHIT, R. P. & KANHERE, S. 2000. Tobacco habits and risk of lung, oropharyngeal and oral cavity cancer: a population-based case-control study in Bhopal, India. *International Journal of Epidemiology*, 29, 609-14.
- DOORBAR, J. 2005. The papillomavirus life cycle. *J Clin Virol*, 32 Suppl 1, S7-15.

- DOORBAR, J., FOO, C., COLEMAN, N., MEDCALF, L., HARTLEY, O., PROSPERO, T., NAPHTHINE, S., STERLING, J., WINTER, G. & GRIFFIN, H. 1997. Characterization of events during the late stages of HPV16 infection in vivo using high-affinity synthetic Fabs to E4. *Virology*, 238, 40-52.
- DOORBAR, J., QUINT, W., BANKS, L., BRAVO, I. G., STOLER, M., BROKER, T. R. & STANLEY, M. A. 2012. The biology and life-cycle of human papillomaviruses. *Vaccine*, 30 Suppl 5, F55-70.
- DUONG-LY, K. C. & GABELLI, S. B. 2014. Salting out of proteins using ammonium sulfate precipitation. *Methods Enzymol*, 541, 85-94.
- FAKHRY, C. & GILLISON, M. L. 2006. Clinical implications of human papillomavirus in head and neck cancers. *Journal of Clinical Oncology*, 24, 2606-11.
- FIEBIG, H. H. 1988. 'Comparison of tumor response in nude mice and in patients', Human Tumour Xenografts in Anticancer Drug Development. *ESO Monographs*, 25-30.
- FISCHER, C. A., ZLOBEC, I., GREEN, E., PROBST, S., STORCK, C., LUGLI, A., TORNILLO, L., WOLFENBERGER, M. & TERRACCIANO, L. M. 2010. Is the improved prognosis of p16 positive oropharyngeal squamous cell carcinoma dependent of the treatment modality? *International Journal of Cancer*, 126, 1256-62.
- FLORIN, L., SAPP, C., STREECK, R. E. & SAPP, M. 2002. Assembly and translocation of papillomavirus capsid proteins. *J Virol*, 76, 10009-14.
- FRATTINI, M. G., HURST, S. D., LIM, H. B., SWAMINATHAN, S. & LAIMINS, L. A. 1997. Abrogation of a mitotic checkpoint by E2 proteins from oncogenic human papillomaviruses correlates with increased turnover of the p53 tumor suppressor protein. *EMBO Journal*, 16, 318-31.
- FUTOSI, K., FODOR, S. & MOCSAI, A. 2013. Reprint of Neutrophil cell surface receptors and their intracellular signal transduction pathways. *Int Immunopharmacol*, 17, 1185-97.
- GALON, J., COSTES, A., SANCHEZ-CABO, F., KIRILOVSKY, A., MLECNIK, B., LAGORCE-PAGES, C., TOSOLINI, M., CAMUS, M., BERGER, A., WIND, P., ZINZINDOHOUE, F., BRUNEVAL, P., CUGNENC, P. H., TRAJANOSKI, Z., FRIDMAN, W. H. & PAGES, F. 2006. Type, density, and location of immune cells within human colorectal tumors predict clinical outcome. *Science*, 313, 1960-4.
- GANGULY, N. 2012. Human papillomavirus-16 E5 protein: oncogenic role and therapeutic value. *Cellular Oncology*, 35, 67-76.
- GARRALDA, E., PAZ, K., LOPEZ-CASAS, P. P., JONES, S., KATZ, A., KANN, L. M., LOPEZ-RIOS, F., SARNO, F., AL-SHAHROUR, F., VASQUEZ, D., BRUCKHEIMER, E., ANGIUOLI, S. V., CALLES, A., DIAZ, L. A., VELCULESCU, V. E., VALENCIA, A., SIDRANSKY, D. & HIDALGO, M. 2014. Integrated next-generation sequencing and avatar mouse models for personalized cancer treatment. *Clin Cancer Res*, 20, 2476-84.
- GENDEN, E. M., SAMBUR, I. M., DE ALMEIDA, J. R., POSNER, M., RINALDO, A., RODRIGO, J. P., STROJAN, P., TAKES, R. P. & FERLITO, A. 2013. Human papillomavirus and oropharyngeal squamous cell carcinoma: what the clinician should know. *Eur Arch Otorhinolaryngol*, 270, 405-16.
- GILLISON, M. L., D'SOUZA, G., WESTRA, W., SUGAR, E., XIAO, W., BEGUM, S. & VISCIDI, R. 2008. Distinct risk factor profiles for human papillomavirus

- type 16-positive and human papillomavirus type 16-negative head and neck cancers. *J Natl Cancer Inst*, 100, 407-20.
- GILLISON, M. L., ZHANG, Q., JORDAN, R., XIAO, W., WESTRA, W. H., TROTTI, A., SPENCER, S., HARRIS, J., CHUNG, C. H. & ANG, K. K. 2012. Tobacco smoking and increased risk of death and progression for patients with p16-positive and p16-negative oropharyngeal cancer. *Journal of Clinical Oncology*, 30, 2102-11.
- GIROGLOU, T., FLORIN, L., SCHAFFER, F., STREECK, R. E. & SAPP, M. 2001. Human papillomavirus infection requires cell surface heparan sulfate. *J Virol*, 75, 1565-70.
- GOMEZ, J. C., YAMADA, M., MARTIN, J. R., DANG, H., BRICKEY, W. J., BERGMEIER, W., DINAUER, M. C. & DOERSCHUK, C. M. 2015. Mechanisms of interferon-gamma production by neutrophils and its function during *Streptococcus pneumoniae* pneumonia. *Am J Respir Cell Mol Biol*, 52, 349-64.
- GORR, T. A. & VOGEL, J. 2015. Western blotting revisited: critical perusal of underappreciated technical issues. *Proteomics Clin Appl*, 9, 396-405.
- GREEN, V. L., MICHNO, A., GREENMAN, J. & STAFFORD, N. D. 2011. Effect of treatment on systemic cytokines in head and neck squamous cell carcinoma patients. *Results Immunol*, 2, 1-6.
- GREEN, V. L., MICHNO, A., STAFFORD, N. D. & GREENMAN, J. 2013. Increased prevalence of tumour infiltrating immune cells in oropharyngeal tumours in comparison to other subsites: relationship to peripheral immunity. *Cancer Immunol Immunother*, 62, 863-73.
- GRONBAEK, M., BECKER, U., JOHANSEN, D., TONNESEN, H., JENSEN, G. & SORENSEN, T. I. 1998. Population based cohort study of the association between alcohol intake and cancer of the upper digestive tract. *BMJ*, 317, 844-7.
- HAFKAMP, H. C., MANNI, J. J., HAESEVOETS, A., VOOGD, A. C., SCHEPERS, M., BOT, F. J., HOPMAN, A. H., RAMAEKERS, F. C. & SPEEL, E. J. 2008. Marked differences in survival rate between smokers and nonsmokers with HPV 16-associated tonsillar carcinomas. *International Journal of Cancer*, 122, 2656-64.
- HAMID, N. A., BROWN, C. & GASTON, K. 2009. The regulation of cell proliferation by the papillomavirus early proteins. *Cellular & Molecular Life Sciences*, 66, 1700-17.
- HAMMARSTEDT, L., LINDQUIST, D., DAHLSTRAND, H., ROMANITAN, M., DAHLGREN, L. O., JONEBERG, J., CRESON, N., LINDHOLM, J., YE, W., DALIANIS, T. & MUNCK-WIKLAND, E. 2006. Human papillomavirus as a risk factor for the increase in incidence of tonsillar cancer. *Int J Cancer*, 119, 2620-3.
- HASHIDA, T. & YASUMOTO, S. 1991. Induction of chromosome abnormalities in mouse and human epidermal keratinocytes by the human papillomavirus type 16 E7 oncogene. *J Gen Virol*, 72 (Pt 7), 1569-77.
- HAYFLICK, L. 1965. The Limited in Vitro Lifetime of Human Diploid Cell Strains. *Experimental Cell Research*, 37, 614-36.
- HEUSINKVELD, M., GOEDEMANS, R., BRIET, R. J., GELDERBLUM, H., NORTIER, J. W., GORTER, A., SMIT, V. T., LANGEVELD, A. P., JANSEN, J. C. & VAN DER BURG, S. H. 2012. Systemic and local human papillomavirus 16-specific T-

- cell immunity in patients with head and neck cancer. *International Journal of Cancer*, 131, E74-85.
- HIRANO, F., KANEKO, K., TAMURA, H., DONG, H., WANG, S., ICHIKAWA, M., RIETZ, C., FLIES, D. B., LAU, J. S., ZHU, G., TAMADA, K. & CHEN, L. 2005. Blockade of B7-H1 and PD-1 by monoclonal antibodies potentiates cancer therapeutic immunity. *Cancer Res*, 65, 1089-96.
- HOFFMANN, D. & DJORDJEVIC, M. V. 1997. Chemical composition and carcinogenicity of smokeless tobacco. *Advances in Dental Research*, 11, 322-9.
- HOFFMANN, T. K., DWORACKI, G., TSUKIHIRO, T., MEIDENBAUER, N., GOODING, W., JOHNSON, J. T. & WHITESIDE, T. L. 2002. Spontaneous apoptosis of circulating T lymphocytes in patients with head and neck cancer and its clinical importance. *Clin Cancer Res*, 8, 2553-62.
- HOFFMANN, T. K., NAKANO, K., ELDER, E. M., DWORACKI, G., FINKELSTEIN, S. D., APPELLA, E., WHITESIDE, T. L. & DELEO, A. B. 2000. Generation of T cells specific for the wild-type sequence p53(264-272) peptide in cancer patients: implications for immunoselection of epitope loss variants. *J Immunol*, 165, 5938-44.
- HUNG, C. F., TSAI, Y. C., HE, L. & WU, T. C. 2007. DNA vaccines encoding li-PADRE generates potent PADRE-specific CD4+ T-cell immune responses and enhances vaccine potency. *Mol Ther*, 15, 1211-9.
- INTERNATIONAL AGENCY FOR RESEARCH ON CANCER, I. 2004. Monographs on the Evaluation of Carcinogenic Risks to Humans, Betel-Quid and Areca-nut Chewing and Some Areca-nut-derived Nitrosamine. In: ORGANIZATION, W. H. (ed.). Lyon, France.
- ISAYEVA, T., LI, Y., MASWAHU, D. & BRANDWEIN-GENSLER, M. 2012. Human papillomavirus in non-oropharyngeal head and neck cancers: a systematic literature review. *Head and neck pathology*, 6 Suppl 1, S104-20.
- ISRAELS, E. D. & ISRAELS, L. G. 2000. The cell cycle. *Oncologist*, 5, 510-3.
- JAMES, M. A., LEE, J. H. & KLINGELHUTZ, A. J. 2006. HPV16-E6 associated hTERT promoter acetylation is E6AP dependent, increased in later passage cells and enhanced by loss of p300. *International Journal of Cancer*, 119, 1878-85.
- JENG, J. H., CHANG, M. C. & HAHN, L. J. 2001. Role of areca nut in betel quid-associated chemical carcinogenesis: current awareness and future perspectives. *Oral Oncology*, 37, 477-92.
- JOHNSON, N. 2001. Tobacco use and oral cancer: a global perspective. *Journal of Dental Education*, 65, 328-39.
- KASTAN, M. B. & BARTEK, J. 2004. Cell-cycle checkpoints and cancer. *Nature*, 432, 316-23.
- KENTER, G. G., WELTERS, M. J., VALENTIJN, A. R., LOWIK, M. J., BERENDS-VAN DER MEER, D. M., VLOON, A. P., ESSAHSAH, F., FATHERS, L. M., OFFRINGA, R., DRIJFHOUT, J. W., WAFELMAN, A. R., OOSTENDORP, J., FLEUREN, G. J., VAN DER BURG, S. H. & MELIEF, C. J. 2009. Vaccination against HPV-16 oncoproteins for vulvar intraepithelial neoplasia. *N Engl J Med*, 361, 1838-47.

- KO, Y. C., HUANG, Y. L., LEE, C. H., CHEN, M. J., LIN, L. M. & TSAI, C. C. 1995. Betel quid chewing, cigarette smoking and alcohol consumption related to oral cancer in Taiwan. *Journal of Oral Pathology & Medicine*, 24, 450-3.
- KREIMER, A. R., ALBERG, A. J., DANIEL, R., GRAVITT, P. E., VISCIDI, R., GARRETT, E. S., SHAH, K. V. & GILLISON, M. L. 2004. Oral human papillomavirus infection in adults is associated with sexual behavior and HIV serostatus. *J Infect Dis*, 189, 686-98.
- KREIMER, A. R., CLIFFORD, G. M., BOYLE, P. & FRANCESCHI, S. 2005. Human papillomavirus types in head and neck squamous cell carcinomas worldwide: a systematic review. *Cancer Epidemiology, Biomarkers & Prevention*, 14, 467-75.
- KURIEN, B. T. & SCOFIELD, R. H. 2015. Western blotting: an introduction. *Methods Mol Biol*, 1312, 17-30.
- LADANYI, A., SOMLAI, B., GILDE, K., FEJOS, Z., GAUDI, I. & TIMAR, J. 2004. T-cell activation marker expression on tumor-infiltrating lymphocytes as prognostic factor in cutaneous malignant melanoma. *Clin Cancer Res*, 10, 521-30.
- LADOIRE, S., MARTIN, F. & GHIRINGHELLI, F. 2011. Prognostic role of FOXP3+ regulatory T cells infiltrating human carcinomas: the paradox of colorectal cancer. *Cancer Immunol Immunother*, 60, 909-18.
- LAJER, C. B. & VON BUCHWALD, C. 2010. The role of human papillomavirus in head and neck cancer. *APMIS*, 118, 510-9.
- LASSEN, P., ERIKSEN, J. G., HAMILTON-DUTOIT, S., TRAMM, T., ALSNER, J. & OVERGAARD, J. 2009. Effect of HPV-associated p16INK4A expression on response to radiotherapy and survival in squamous cell carcinoma of the head and neck. *Journal of Clinical Oncology*, 27, 1992-8.
- LEE, J. J., JENG, J. H., WANG, H. M., CHANG, H. H., CHIANG, C. P., KUO, Y. S., LAN, W. H. & KOK, S. H. 2005. Univariate and multivariate analysis of prognostic significance of betel quid chewing in squamous cell carcinoma of buccal mucosa in Taiwan. *Journal of Surgical Oncology*, 91, 41-7.
- LEE, M. K., NALLIAH, R. P., KIM, M. K., ELANGO VAN, S., ALLAREDDY, V., KUMAR-GAJENDRAREDDY, P. & ALLAREDDY, V. 2011. Prevalence and impact of complications on outcomes in patients hospitalized for oral and oropharyngeal cancer treatment. *Oral Surg Oral Med Oral Pathol Oral Radiol Endod*, 112, 581-91.
- LEEMANS, C. R., BRAAKHUIS, B. J. & BRAKENHOFF, R. H. 2011. The molecular biology of head and neck cancer. *Nature Reviews. Cancer*, 11, 9-22.
- LEHOUX, M., D'ABRAMO, C. M. & ARCHAMBAULT, J. 2009. Molecular mechanisms of human papillomavirus-induced carcinogenesis. *Public Health Genomics*, 12, 268-80.
- LEWIN, F., NORELL, S. E., JOHANSSON, H., GUSTAVSSON, P., WENNERBERG, J., BIORKLUND, A. & RUTQVIST, L. E. 1998. Smoking tobacco, oral snuff, and alcohol in the etiology of squamous cell carcinoma of the head and neck: a population-based case-referent study in Sweden. *Cancer*, 82, 1367-75.
- LEWIS, J. S., JR. 2012. p16 Immunohistochemistry as a standalone test for risk stratification in oropharyngeal squamous cell carcinoma. *Head Neck Pathol*, 6 Suppl 1, S75-82.

- LI, M., BEARD, P., ESTES, P. A., LYON, M. K. & GARCEA, R. L. 1998. Intercapsomeric disulfide bonds in papillomavirus assembly and disassembly. *J Virol*, 72, 2160-7.
- LIN, C. T., TSAI, Y. C., HE, L., YEH, C. N., CHANG, T. C., SOONG, Y. K., MONIE, A., HUNG, C. F. & LAI, C. H. 2007. DNA vaccines encoding IL-2 linked to HPV-16 E7 antigen generate enhanced E7-specific CTL responses and antitumor activity. *Immunol Lett*, 114, 86-93.
- LIU, X., DAKIC, A., ZHANG, Y., DAI, Y., CHEN, R. & SCHLEGEL, R. 2009. HPV E6 protein interacts physically and functionally with the cellular telomerase complex. *Proceedings of the National Academy of Sciences of the United States of America*, 106, 18780-5.
- LUCE, D., LECLERC, A., BEGIN, D., DEMERS, P. A., GERIN, M., ORLOWSKI, E., KOGEVINAS, M., BELLI, S., BUGEL, I., BOLM-AUDORFF, U., BRINTON, L. A., COMBA, P., HARDELL, L., HAYES, R. B., MAGNANI, C., MERLER, E., PRESTON-MARTIN, S., VAUGHAN, T. L., ZHENG, W. & BOFFETTA, P. 2002. Sinonasal cancer and occupational exposures: a pooled analysis of 12 case-control studies. *Cancer Causes & Control*, 13, 147-57.
- LUKESOVA, E., BOUCEK, J., ROTNAGLOVA, E., SALAKOVA, M., KOSLABOVA, E., GREGA, M., ECKSCHLAGER, T., RIHOVA, B., PROCHAZKA, B., KLOZAR, J. & TACHEZY, R. 2014. High level of Tregs is a positive prognostic marker in patients with HPV-positive oral and oropharyngeal squamous cell carcinomas. *Biomed Res Int*, 2014, 303929.
- LYFORD-PIKE, S., PENG, S., YOUNG, G. D., TAUBE, J. M., WESTRA, W. H., AKPENG, B., BRUNO, T. C., RICHMON, J. D., WANG, H., BISHOP, J. A., CHEN, L., DRAKE, C. G., TOPALIAN, S. L., PARDOLL, D. M. & PAI, S. I. 2013. Evidence for a role of the PD-1:PD-L1 pathway in immune resistance of HPV-associated head and neck squamous cell carcinoma. *Cancer Res*, 73, 1733-41.
- MAITLAND, B. A. 2005. Human Papillomaviruses and Cancer. *Microbiology Today*, Aug 2005, 116=120.
- MANNERVIK, B. & DANIELSON, U. H. 1988. Glutathione transferases--structure and catalytic activity. *CRC Crit Rev Biochem*, 23, 283-337.
- MARTINEZ, L. A., CHEN, Y., FISCHER, S. M. & CONTI, C. J. 1999. Coordinated changes in cell cycle machinery occur during keratinocyte terminal differentiation. *Oncogene*, 18, 397-406.
- MARUR, S., D'SOUZA, G., WESTRA, W. H. & FORASTIERE, A. A. 2010. HPV-associated head and neck cancer: a virus-related cancer epidemic. *Lancet Oncol*, 11, 781-9.
- MASTERSON, L., MOUALED, D., LIU, Z. W., HOWARD, J. E., DWIVEDI, R. C., TYSOME, J. R., BENSON, R., STERLING, J. C., SUDHOFF, H., JANI, P. & GOON, P. K. 2014. De-escalation treatment protocols for human papillomavirus-associated oropharyngeal squamous cell carcinoma: a systematic review and meta-analysis of current clinical trials. *Eur J Cancer*, 50, 2636-48.
- MATEO, C., FERNANDEZ-LORENTE, G., PESSELA, B. C., VIAN, A., CARRASCOSA, A. V., GARCIA, J. L., FERNANDEZ-LAFUENTE, R. & GUISAN, J. M. 2001. Affinity chromatography of polyhistidine tagged enzymes. New dextran-coated immobilized metal ion affinity chromatography matrices for prevention of undesired multipoint adsorptions. *J Chromatogr A*, 915, 97-106.

- MCKAIG, R. G., BARIC, R. S. & OLSHAN, A. F. 1998. Human papillomavirus and head and neck cancer: epidemiology and molecular biology. *Head Neck*, 20, 250-65.
- MESCHEDE, W., ZUMBACH, K., BRASPENNING, J., SCHEFFNER, M., BENITEZ-BRIBIESCA, L., LUANDE, J., GISSMANN, L. & PAWLITA, M. 1998. Antibodies against early proteins of human papillomaviruses as diagnostic markers for invasive cervical cancer. *J Clin Microbiol*, 36, 475-80.
- MIDDLETON, K., PEH, W., SOUTHERN, S., GRIFFIN, H., SOTLAR, K., NAKAHARA, T., EL-SHERIF, A., MORRIS, L., SETH, R., HIBMA, M., JENKINS, D., LAMBERT, P., COLEMAN, N. & DOORBAR, J. 2003. Organization of human papillomavirus productive cycle during neoplastic progression provides a basis for selection of diagnostic markers. *J Virol*, 77, 10186-201.
- MISSERO, C., CALAUTTI, E., ECKNER, R., CHIN, J., TSAI, L. H., LIVINGSTON, D. M. & DOTTO, G. P. 1995. Involvement of the cell-cycle inhibitor Cip1/WAF1 and the E1A-associated p300 protein in terminal differentiation. *Proc Natl Acad Sci U S A*, 92, 5451-5.
- MITTRUCKER, H. W., VISEKRUNA, A. & HUBER, M. 2014. Heterogeneity in the differentiation and function of CD8(+) T cells. *Arch Immunol Ther Exp (Warsz)*, 62, 449-58.
- MORK, J., LIE, A. K., GLATTRE, E., HALLMANS, G., JELLUM, E., KOSKELA, P., MOLLER, B., PUKKALA, E., SCHILLER, J. T., YOUNGMAN, L., LEHTINEN, M. & DILLNER, J. 2001. Human papillomavirus infection as a risk factor for squamous-cell carcinoma of the head and neck. *N Engl J Med*, 344, 1125-31.
- MUNGER, K., BASILE, J. R., DUENSING, S., EICHTEN, A., GONZALEZ, S. L., GRACE, M. & ZACNY, V. L. 2001. Biological activities and molecular targets of the human papillomavirus E7 oncoprotein. *Oncogene*, 20, 7888-98.
- NASMAN, A., ROMANITAN, M., NORDFORS, C., GRUN, N., JOHANSSON, H., HAMMARSTEDT, L., MARKLUND, L., MUNCK-WIKLAND, E., DALIANIS, T. & RAMQVIST, T. 2012. Tumor infiltrating CD8+ and Foxp3+ lymphocytes correlate to clinical outcome and human papillomavirus (HPV) status in tonsillar cancer. *PLoS One*, 7, e38711.
- NINDL, I., BENITEZ-BRIBIESCA, L., BERUMEN, J., FARMANARA, N., FISHER, S., GROSS, G., LOPEZ-CARILLO, L., MULLER, M., TOMMASINO, M., VAZQUEZ-CURIEL, A. & ET AL. 1994. Antibodies against linear and conformational epitopes of the human papillomavirus (HPV) type 16 E6 and E7 oncoproteins in sera of cervical cancer patients. *Arch Virol*, 137, 341-53.
- NINDL, I., ZUMBACH, K., PAWLITA, M., TELLER, K., SCHNEIDER, A. & DURST, M. 2000. Absence of antibody against human papillomavirus type 16 E6 and E7 in patients with cervical cancer is independent of sequence variations. *J Infect Dis*, 181, 1764-7.
- NORTON, S. A. 1998. Betel: consumption and consequences. *Journal of the American Academy of Dermatology*, 38, 81-8.
- NSDUH 2010. Results from the 2009 National survey on drug Use and Health. In: STUDIES, O. O. A. (ed.) *Summary of National Findings*. USA.
- O'CONNOR, R. A. & ANDERTON, S. M. 2015. Inflammation-associated genes: risks and benefits to Foxp3+ regulatory T-cell function. *Immunology*, 146, 194-205.

- OZBUN, M. A. & MEYERS, C. 1998. Human papillomavirus type 31b E1 and E2 transcript expression correlates with vegetative viral genome amplification. *Virology*, 248, 218-30.
- PARK, J. S., PARK, D. C., KIM, C. J., AHN, H. K., UM, S. J., PARK, S. N., KIM, S. J. & NAMKOONG, S. E. 1998. HPV-16-related proteins as the serologic markers in cervical neoplasia. *Gynecol Oncol*, 69, 47-55.
- PARKIN DM, W. S., FERLAY J, TEPPLO L & THOMAS DB 2003. Cancer Incidence in Five Continents *IARC Scientific Publications, IARC Press*, VIII.
- PASYK, K. A. & HASSETT, C. A. 1989. Modified hematoxylin and eosin staining method for epoxy-embedded tissue sections. *Pathol Res Pract*, 184, 635-8.
- PATTILLO, R. A., HUSSA, R. O., STORY, M. T., RUCKERT, A. C., SHALABY, M. R. & MATTINGLY, R. F. 1977. Tumor antigen and human chorionic gonadotropin in CaSki cells: a new epidermoid cervical cancer cell line. *Science*, 196, 1456-8.
- PIERSMA, S. J., JORDANOVA, E. S., VAN POELGEEST, M. I., KWAPPENBERG, K. M., VAN DER HULST, J. M., DRIJFHOUT, J. W., MELIEF, C. J., KENTER, G. G., FLEUREN, G. J., OFFRINGA, R. & VAN DER BURG, S. H. 2007. High number of intraepithelial CD8+ tumor-infiltrating lymphocytes is associated with the absence of lymph node metastases in patients with large early-stage cervical cancer. *Cancer Res*, 67, 354-61.
- PIKARSKY, E., PORAT, R. M., STEIN, I., ABRAMOVITCH, R., AMIT, S., KASEM, S., GUTKOVICH-PYEST, E., URIELI-SHOVAL, S., GALUN, E. & BEN-NERIAH, Y. 2004. NF-kappaB functions as a tumour promoter in inflammation-associated cancer. *Nature*, 431, 461-6.
- PIM, D. & BANKS, L. 2010. Interaction of viral oncoproteins with cellular target molecules: infection with high-risk vs low-risk human papillomaviruses. *APMIS*, 118, 471-93.
- PORICHIS, F., KWON, D. S., ZUPKOSKY, J., TIGHE, D. P., MCMULLEN, A., BROCKMAN, M. A., PAVLIK, D. F., RODRIGUEZ-GARCIA, M., PEREYRA, F., FREEMAN, G. J., KAVANAGH, D. G. & KAUFMANN, D. E. 2011. Responsiveness of HIV-specific CD4 T cells to PD-1 blockade. *Blood*, 118, 965-74.
- PROMEGA. 2016. *Bacterial Strain JM109* [Online]. Available: <http://www.promega.co.uk> [Accessed].
- PUISSANT, C. & HOUDEBINE, L. M. 1990. An improvement of the single-step method of RNA isolation by acid guanidinium thiocyanate-phenol-chloroform extraction. *Biotechniques*, 8, 148-9.
- PYEON, D., NEWTON, M. A., LAMBERT, P. F., DEN BOON, J. A., SENGUPTA, S., MARSIT, C. J., WOODWORTH, C. D., CONNOR, J. P., HAUGEN, T. H., SMITH, E. M., KELSEY, K. T., TUREK, L. P. & AHLQUIST, P. 2007. Fundamental differences in cell cycle deregulation in human papillomavirus-positive and human papillomavirus-negative head/neck and cervical cancers. *Cancer Res*, 67, 4605-19.
- RAGIN, C. C. & TAIOLI, E. 2007. Survival of squamous cell carcinoma of the head and neck in relation to human papillomavirus infection: review and meta-analysis. *Int J Cancer*, 121, 1813-20.
- RAJJOUB, S., BASHA, S. R., EINHORN, E., COHEN, M. C., MARVEL, D. M. & SEWELL, D. A. 2007. Prognostic significance of tumor-infiltrating lymphocytes in oropharyngeal cancer. *Ear Nose Throat J*, 86, 506-11.

- RAPIDIS, A. D. & WOLF, G. T. 2009. Immunotherapy of head and neck cancer: current and future considerations. *J Oncol*, 2009, 346345.
- RAVAGGI, A., ROMANI, C., PASINETTI, B., TASSI, R. A., BIGNOTTI, E., BANDIERA, E., ODICINO, F. E., RAGNOLI, M., DONZELLI, C., FALCHETTI, M., CALZA, S., SANTIN, A. D. & PECORELLI, S. 2006. Correlation between serological immune response analyzed by a new ELISA for HPV-16/18 E7 oncoprotein and clinical characteristics of cervical cancer patients. *Arch Virol*, 151, 1899-916.
- ROBINSON, K. L. & MACFARLANE, G. J. 2003. Oropharyngeal cancer incidence and mortality in Scotland: are rates still increasing? *Oral Oncol*, 39, 31-6.
- ROBINSON, M., SLOAN, P. & SHAW, R. 2010. Refining the diagnosis of oropharyngeal squamous cell carcinoma using human papillomavirus testing. *Oral Oncol*, 46, 492-6.
- ROMANCZUK, H. & HOWLEY, P. M. 1992. Disruption of either the E1 or the E2 regulatory gene of human papillomavirus type 16 increases viral immortalization capacity. *Proceedings of the National Academy of Sciences of the United States of America*, 89, 3159-63.
- ROSALES, R., LOPEZ-CONTRERAS, M. & CORTES, R. R. 2001. Antibodies against human papillomavirus (HPV) type 16 and 18 E2, E6 and E7 proteins in sera: correlation with presence of papillomavirus DNA. *J Med Virol*, 65, 736-44.
- RUBENSTEIN, L. M., SMITH, E. M., PAWLITA, M., HAUGEN, T. H., HANSIKOVA, E. & TUREK, L. P. 2011. Human papillomavirus serologic follow-up response and relationship to survival in head and neck cancer: a case-comparison study. *Infect Agent Cancer*, 6, 9.
- SANCHEZ-PEREZ, A. M., SORIANO, S., CLARKE, A. R. & GASTON, K. 1997. Disruption of the human papillomavirus type 16 E2 gene protects cervical carcinoma cells from E2F-induced apoptosis. *Journal of General Virology*, 78, 3009-18.
- SANO, T., OYAMA, T., KASHIWABARA, K., FUKUDA, T. & NAKAJIMA, T. 1998. Expression status of p16 protein is associated with human papillomavirus oncogenic potential in cervical and genital lesions. *American Journal of Pathology*, 153, 1741-8.
- SATO, E., OLSON, S. H., AHN, J., BUNDY, B., NISHIKAWA, H., QIAN, F., JUNGBLUTH, A. A., FROSINA, D., GNJATIC, S., AMBROSONE, C., KEPNER, J., ODUNSI, T., RITTER, G., LELE, S., CHEN, Y. T., OHTANI, H., OLD, L. J. & ODUNSI, K. 2005. Intraepithelial CD8⁺ tumor-infiltrating lymphocytes and a high CD8⁺/regulatory T cell ratio are associated with favorable prognosis in ovarian cancer. *Proc Natl Acad Sci U S A*, 102, 18538-43.
- SAXENA, A., KHOSRAVIANI, S., NOEL, S., MOHAN, D., DONNER, T. & HAMAD, A. R. 2015. Interleukin-10 paradox: A potent immunoregulatory cytokine that has been difficult to harness for immunotherapy. *Cytokine*, 74, 27-34.
- SCHACHE, A. G., LILOGLOU, T., RISK, J. M., FILIA, A., JONES, T. M., SHEARD, J., WOOLGAR, J. A., HELLIWELL, T. R., TRIANTAFYLLOU, A., ROBINSON, M., SLOAN, P., HARVEY-WOODWORTH, C., SISSON, D. & SHAW, R. J. 2011. Evaluation of human papilloma virus diagnostic testing in oropharyngeal squamous cell carcinoma: sensitivity, specificity, and prognostic discrimination. *Clin Cancer Res*, 17, 6262-71.

- SCHAEFER, C., KIM, G. G., ALBERS, A., HOERMANN, K., MYERS, E. N. & WHITESIDE, T. L. 2005. Characteristics of CD4+CD25+ regulatory T cells in the peripheral circulation of patients with head and neck cancer. *Br J Cancer*, 92, 913-20.
- SCHEFFNER, M., HUIBREGTSE, J. M., VIERSTRA, R. D. & HOWLEY, P. M. 1993. The HPV-16 E6 and E6-AP complex functions as a ubiquitin-protein ligase in the ubiquitination of p53. *Cell*, 75, 495-505.
- SCHEFFNER, M., WERNES, B. A., HUIBREGTSE, J. M., LEVINE, A. J. & HOWLEY, P. M. 1990. The E6 oncoprotein encoded by human papillomavirus types 16 and 18 promotes the degradation of p53. *Cell*, 63, 1129-36.
- SEBELIUS, K. 2010. *How Tobacco Smoke Causes Disease: The Biology and Behavioral Basis for Smoking-Attributable Disease: A Report of the Surgeon General*, Atlanta, GA: U.S., U.S. Department of Health and Human Services, Centers for Disease Control and Prevention, National Center for Chronic Disease Prevention and Health Promotion, Office on Smoking and Health.
- SEHR, P., ZUMBACH, K. & PAWLITA, M. 2001. A generic capture ELISA for recombinant proteins fused to glutathione S-transferase: validation for HPV serology. *J Immunol Methods*, 253, 153-62.
- SHAMANIN, V., ZUR HAUSEN, H., LAVERGNE, D., PROBY, C. M., LEIGH, I. M., NEUMANN, C., HAMM, H., GOOS, M., HAUSTEIN, U. F., JUNG, E. G., PLEWIG, G., WOLFF, H. & DE VILLIERS, E. M. 1996. Human papillomavirus infections in nonmelanoma skin cancers from renal transplant recipients and nonimmunosuppressed patients. *J Natl Cancer Inst*, 88, 802-11.
- SHIBOSKI, C. H., SCHMIDT, B. L. & JORDAN, R. C. 2005. Tongue and tonsil carcinoma: increasing trends in the U.S. population ages 20-44 years. *Cancer*, 103, 1843-9.
- SINGHI, A. D. & WESTRA, W. H. 2010. Comparison of human papillomavirus in situ hybridization and p16 immunohistochemistry in the detection of human papillomavirus-associated head and neck cancer based on a prospective clinical experience. *Cancer*, 116, 2166-73.
- SIRIANNI, N., HA, P. K., OELKE, M., CALIFANO, J., GOODING, W., WESTRA, W., WHITESIDE, T. L., KOCH, W. M., SCHNECK, J. P., DELEO, A. & FERRIS, R. L. 2004. Effect of human papillomavirus-16 infection on CD8+ T-cell recognition of a wild-type sequence p53264-272 peptide in patients with squamous cell carcinoma of the head and neck. *Clin Cancer Res*, 10, 6929-37.
- SIVASITHAMPARAM, J., VISK, C. A., COHEN, E. E. & KING, A. C. 2013. Modifiable risk behaviors in patients with head and neck cancer. *Cancer*, 119, 2419-26.
- SKINNER, S. R., WHEELER, C. M., ROMANOWSKI, B., CASTELLSAGUE, X., LAZCANO-PONCE, E., DEL ROSARIO-RAYMUNDO, M. R., VALLEJOS, C., MINKINA, G., PEREIRA DA SILVA, D., MCNEIL, S., PRILEPSKAYA, V., GOGOTADZE, I., MONEY, D., GARLAND, S. M., ROMANENKO, V., HARPER, D. M., LEVIN, M. J., CHATTERJEE, A., GEERAERTS, B., STRUYF, F., DUBIN, G., BOZONNAT, M. C., ROSILLON, D., BARIL, L. & GROUP, V. S. 2016. Progression of HPV infection to detectable cervical lesions or clearance in adult women: Analysis of the control arm of the VIVIANE study. *Int J Cancer*, 138, 2428-38.

- SMEETS, S. J., HESSELINK, A. T., SPEEL, E. J., HAESEVOETS, A., SNIJDERS, P. J., PAWLITA, M., MEIJER, C. J., BRAAKHUIS, B. J., LEEMANS, C. R. & BRAKENHOFF, R. H. 2007. A novel algorithm for reliable detection of human papillomavirus in paraffin embedded head and neck cancer specimen. *Int J Cancer*, 121, 2465-72.
- SMITH, B. J. 1994. SDS polyacrylamide gel electrophoresis of proteins. *Methods Mol Biol*, 32, 23-34.
- SMITH, D. B. & JOHNSON, K. S. 1988. Single-step purification of polypeptides expressed in *Escherichia coli* as fusions with glutathione S-transferase. *Gene*, 67, 31-40.
- SMITH, E. M., PAWLITA, M., RUBENSTEIN, L. M., HAUGEN, T. H., HANSIKOVA, E. & TUREK, L. P. 2010. Risk factors and survival by HPV-16 E6 and E7 antibody status in human papillomavirus positive head and neck cancer. *Int J Cancer*, 127, 111-7.
- SMITH, E. M., RITCHIE, J. M., SUMMERSGILL, K. F., KLUSMANN, J. P., LEE, J. H., WANG, D., HAUGEN, T. H. & TUREK, L. P. 2004. Age, sexual behavior and human papillomavirus infection in oral cavity and oropharyngeal cancers. *Int J Cancer*, 108, 766-72.
- SONG, L., YANG, M. C., KNOFF, J., WU, T. C. & HUNG, C. F. 2014. Cancer immunotherapy employing an innovative strategy to enhance CD4+ T cell help in the tumor microenvironment. *PLoS One*, 9, e115711.
- SPANOS, W. C., NOWICKI, P., LEE, D. W., HOOVER, A., HOSTAGER, B., GUPTA, A., ANDERSON, M. E. & LEE, J. H. 2009. Immune response during therapy with cisplatin or radiation for human papillomavirus-related head and neck cancer. *Arch Otolaryngol Head Neck Surg*, 135, 1137-46.
- SPITZ, M. R., FUEGER, J. J., GOEPFERT, H., HONG, W. K. & NEWELL, G. R. 1988. Squamous cell carcinoma of the upper aerodigestive tract. A case comparison analysis. *Cancer*, 61, 203-8.
- STACEY, S. N., JORDAN, D., WILLIAMSON, A. J., BROWN, M., COOTE, J. H. & ARRAND, J. R. 2000. Leaky scanning is the predominant mechanism for translation of human papillomavirus type 16 E7 oncoprotein from E6/E7 bicistronic mRNA. *J Virol*, 74, 7284-97.
- STANDRING, S. 2009. *Gray's Anatomy: The Anatomical Basis of Clinical Practice*, Elsevier.
- STANLEY, M. A. 2012. Epithelial cell responses to infection with human papillomavirus. *Clin Microbiol Rev*, 25, 215-22.
- STRAUSS, B., RABKIN, S., SAGHER, D. & MOORE, P. 1982. The role of DNA polymerase in base substitution mutagenesis on non-instructional templates. *Biochimie*, 64, 829-38.
- STRAUSS, L., BERGMANN, C., GOODING, W., JOHNSON, J. T. & WHITESIDE, T. L. 2007. The frequency and suppressor function of CD4+CD25highFoxp3+ T cells in the circulation of patients with squamous cell carcinoma of the head and neck. *Clin Cancer Res*, 13, 6301-11.
- SULLIVAN, R. J. & HAGEN, E. H. 2002. Psychotropic substance-seeking: evolutionary pathology or adaptation? *Addiction*, 97, 389-400.
- TABOR, S. & RICHARDSON, C. C. 1989. Effect of manganese ions on the incorporation of dideoxynucleotides by bacteriophage T7 DNA polymerase and *Escherichia coli* DNA polymerase I. *Proc Natl Acad Sci U S A*, 86, 4076-80.

- TECHNOLOGIES, L. 2012. [Accessed].
- TERMINE, N., PANZARELLA, V., FALASCHINI, S., RUSSO, A., MATRANGA, D., LO MUZIO, L. & CAMPISI, G. 2008. HPV in oral squamous cell carcinoma vs head and neck squamous cell carcinoma biopsies: a meta-analysis (1988-2007). *Annals of Oncology*, 19, 1681-90.
- THAVARAJ, S., STOKES, A., GUERRA, E., BIBLE, J., HALLIGAN, E., LONG, A., OKPOKAM, A., SLOAN, P., ODELL, E. & ROBINSON, M. 2011a. Evaluation of human papillomavirus testing for squamous cell carcinoma of the tonsil in clinical practice. *Journal of Clinical Pathology*, 64, 308-12.
- THAVARAJ, S., STOKES, A., GUERRA, E., BIBLE, J., HALLIGAN, E., LONG, A., OKPOKAM, A., SLOAN, P., ODELL, E. & ROBINSON, M. 2011b. Evaluation of human papillomavirus testing for squamous cell carcinoma of the tonsil in clinical practice. *J Clin Pathol*, 64, 308-12.
- THERMOSCIENTIFIC. 2012. *2XReddyMix PCR mastermix* [Online]. USA. [Accessed].
- THOMAS, M., LAURA, R., HEPNER, K., GUCCIONE, E., SAWYERS, C., LASKY, L. & BANKS, L. 2002. Oncogenic human papillomavirus E6 proteins target the MAGI-2 and MAGI-3 proteins for degradation. *Oncogene*, 21, 5088-96.
- THURLOW JK, M. C., HUNTER KD ET AL 2010. Spectral clustering of microarray data elucidates the roles of microenvironment remodeling and immune responses in survival of head and neck squamous cell carcinoma. *Journal of Clinical Oncology*, 28, 2881-2888.
- TUYNS, A. J., ESTEVE, J., RAYMOND, L., BERRINO, F., BENHAMOU, E., BLANCHET, F., BOFFETTA, P., CROSIGNANI, P., DEL MORAL, A. & LEHMANN, W. 1988. Cancer of the larynx/hypopharynx, tobacco and alcohol: IARC international case-control study in Turin and Varese (Italy), Zaragoza and Navarra (Spain), Geneva (Switzerland) and Calvados (France). *International Journal of Cancer*, 41, 483-91.
- UICC 2009. *TNM Classification of malignant Tumours*, Wiley-Blackwell.
- VENUTI, A. & PAOLINI, F. 2012. HPV detection methods in head and neck cancer. *Head and neck pathology*, 6 Suppl 1, S63-74.
- VIERBOOM, M. P., ZWAVELING, S., BOS, G. M. J., OOMS, M., KRIETEMEIJER, G. M., MELIEF, C. J. & OFFRINGA, R. 2000. High steady-state levels of p53 are not a prerequisite for tumor eradication by wild-type p53-specific cytotoxic T lymphocytes. *Cancer Res*, 60, 5508-13.
- WANSOM, D., LIGHT, E., THOMAS, D., WORDEN, F., PRINCE, M., URBA, S., CHEPEHA, D., KUMAR, B., CORDELL, K., EISBRUCH, A., TAYLOR, J., MOYER, J., BRADFORD, C., D'SILVA, N., CAREY, T., MCHUGH, J., WOLF, G. & PROGRAM, U. M. H. N. S. 2012. Infiltrating lymphocytes and human papillomavirus-16--associated oropharyngeal cancer. *Laryngoscope*, 122, 121-7.
- WANSOM, D., LIGHT, E., WORDEN, F., PRINCE, M., URBA, S., CHEPEHA, D. B., CORDELL, K., EISBRUCH, A., TAYLOR, J., D'SILVA, N., MOYER, J., BRADFORD, C. R., KURNIT, D., KUMAR, B., CAREY, T. E. & WOLF, G. T. 2010. Correlation of cellular immunity with human papillomavirus 16 status and outcome in patients with advanced oropharyngeal cancer. *Arch Otolaryngol Head Neck Surg*, 136, 1267-73.
- WARD, M. J., THIRDBOROUGH, S. M., MELLOWS, T., RILEY, C., HARRIS, S., SUCHAK, K., WEBB, A., HAMPTON, C., PATEL, N. N., RANDALL, C. J., COX, H.

- J., JOGAI, S., PRIMROSE, J., PIPER, K., OTTENSMEIER, C. H., KING, E. V. & THOMAS, G. J. 2014. Tumour-infiltrating lymphocytes predict for outcome in HPV-positive oropharyngeal cancer. *Br J Cancer*, 110, 489-500.
- WATANABE, Y., KATOU, F., OHTANI, H., NAKAYAMA, T., YOSHIE, O. & HASHIMOTO, K. 2010. Tumor-infiltrating lymphocytes, particularly the balance between CD8(+) T cells and CCR4(+) regulatory T cells, affect the survival of patients with oral squamous cell carcinoma. *Oral Surg Oral Med Oral Pathol Oral Radiol Endod*, 109, 744-52.
- WEBSTER, K., PARISH, J., PANDYA, M., STERN, P. L., CLARKE, A. R. & GASTON, K. 2000. The human papillomavirus (HPV) 16 E2 protein induces apoptosis in the absence of other HPV proteins and via a p53-dependent pathway. *Journal of Biological Chemistry*, 275, 87-94.
- WEINBERGER, P. M., YU, Z., HAFFTY, B. G., KOWALSKI, D., HARIGOPAL, M., BRANDSMA, J., SASAKI, C., JOE, J., CAMP, R. L., RIMM, D. L. & PSYRRI, A. 2006. Molecular classification identifies a subset of human papillomavirus--associated oropharyngeal cancers with favorable prognosis. *J Clin Oncol*, 24, 736-47.
- WELLS, S. I., FRANCIS, D. A., KARPOVA, A. Y., DOWHANICK, J. J., BENSON, J. D. & HOWLEY, P. M. 2000. Papillomavirus E2 induces senescence in HPV-positive cells via pRB- and p21(CIP)-dependent pathways. *EMBO Journal*, 19, 5762-71.
- WESTRA, W. H. 2009. The changing face of head and neck cancer in the 21st century: the impact of HPV on the epidemiology and pathology of oral cancer. *Head Neck Pathol*, 3, 78-81.
- WESTRA, W. H., TAUBE, J. M., POETA, M. L., BEGUM, S., SIDRANSKY, D. & KOCH, W. M. 2008. Inverse relationship between human papillomavirus-16 infection and disruptive p53 gene mutations in squamous cell carcinoma of the head and neck. *Clin Cancer Res*, 14, 366-9.
- WHO 2012. GLOBOCAN: Estimated Cancer Incidence, Mortality and Prevalence Worldwide. In: CANCER, I. A. F. R. O. (ed.). Lyon, France: World Health Organisation.
- WILKE, C. M., WU, K., ZHAO, E., WANG, G. & ZOU, W. 2010. Prognostic significance of regulatory T cells in tumor. *International Journal of Cancer*, 127, 748-58.
- WILTING, S. M., SMEETS, S. J., SNIJDERS, P. J., VAN WIERINGEN, W. N., VAN DE WIEL, M. A., MEIJER, G. A., YLSTRA, B., LEEMANS, C. R., MEIJER, C. J., BRAKENHOFF, R. H., BRAAKHUIS, B. J. & STEENBERGEN, R. D. 2009. Genomic profiling identifies common HPV-associated chromosomal alterations in squamous cell carcinomas of cervix and head and neck. *BMC Med Genomics*, 2, 32.
- WORLD-HEALTH-ORGANIZATION 2007. IARC monographs on the evaluation of carcinogenic risks to humans. Human Papillomavirus ed. Lyon.
- WU, A., ZENG, Q., KANG, T. H., PENG, S., ROOSINOVICH, E., PAI, S. I. & HUNG, C. F. 2011. Innovative DNA vaccine for human papillomavirus (HPV)-associated head and neck cancer. *Gene Ther*, 18, 304-12.
- WU, C. Y., MONIE, A., PANG, X., HUNG, C. F. & WU, T. C. 2010. Improving therapeutic HPV peptide-based vaccine potency by enhancing CD4+ T help and dendritic cell activation. *J Biomed Sci*, 17, 88.

- YIP, T. T., NAKAGAWA, Y. & PORATH, J. 1989. Evaluation of the interaction of peptides with Cu(II), Ni(II), and Zn(II) by high-performance immobilized metal ion affinity chromatography. *Anal Biochem*, 183, 159-71.
- ZHAI, K., DING, J. & SHI, H. Z. 2015. HPV and lung cancer risk: a meta-analysis. *J Clin Virol*, 63, 84-90.
- ZHOU, J., MICHAUD, D. S., LANGEVIN, S. M., MCCLEAN, M. D., ELIOT, M. & KELSEY, K. T. 2013. Smokeless tobacco and risk of head and neck cancer: evidence from a case-control study in New England. *International Journal of Cancer*, 132, 1911-7.
- ZUMBACH, K., KISSELJOV, F., SACHAROVA, O., SHAICHAEV, G., SEMJONOVA, L., PAVLOVA, L. & PAWLITA, M. 2000. Antibodies against oncoproteins E6 and E7 of human papillomavirus types 16 and 18 in cervical-carcinoma patients from Russia. *Int J Cancer*, 85, 313-8.

Appendix 1. TNM Staging of HNSCC

Staging of Head and Neck Cancer

Stage	Definition
TX	Primary tumour cannot be assessed
T0	No evidence of primary tumour
Tis	Carcinoma in situ

Staging of Tumours of the Oral Cavity

Stage	Boundaries
T1	≤2 cm
T2	>2 cm to 4 cm
T3	>4 cm
T4a	Through cortical bone, deep/extrinsic muscle of tongue, maxillary sinus, skin
T4b	Masticator space, pterygoid plates, skull base, internal carotid artery

Staging of tumours of the Oropharynx

Stage	Boundaries
T1	≤2 cm
T2	>2 cm to 4 cm
T3	>4 cm
T4a	T4a Larynx, deep/extrinsic muscle of tongue, medial pterygoid, hard palate, mandible
T4b	T4b Lateral pterygoid muscle, pterygoid plates, lateral nasopharynx, skull base, carotid artery

Staging of tumours of the Hypopharynx

Stage	Boundaries
T1	≤2 cm and limited to one subsite
T2	>2 cm to 4 cm or more than one subsite
T3	>4 cm or with hemilarynx fixation
T4a	Thyroid/cricoid cartilage, hyoid bone, thyroid gland, oesophagus, central compartment soft tissue
T4b	Prevertebral fascia, carotid artery, mediastinal structures

Staging of tumours of the Larynx

Stage	Boundaries
Supraglottis	
T1	One subsite, normal vocal cord mobility
T2	Mucosa invaded of more than one adjacent subsite of supraglottis or glottis or adjacent region outside the supraglottis; without fixation of the larynx
T3	Tumour limited to larynx with cord fixation or invades postcricoid area, pre-epiglottic tissues, paraglottic space, thyroid cartilage erosion
T4a	Tumour invades thyroid cartilage; trachea, soft tissues of neck: deep/extrinsic muscle of tongue, strap muscles, thyroid, oesophagus
T4b	Tumour invades prevertebral space, encases carotid artery, or involves mediastinal structures
Glottis	

T1 T1a T1b	Limited to vocal cord(s), normal mobility
T2	Tumour extends to supraglottis, subglottis, impaired cord mobility
T3	Tumour limited to larynx with vocal cord fixation
T4a	Tumour invades thyroid or cricoid cartilage; trachea, soft tissues of neck: deep/extrinsic muscle of tongue, strap muscles, thyroid, oesophagus
T4b	Tumour invades prevertebral space, encases carotid artery, or involves mediastinal structures,
Subglottis	
T1	Limited to subglottis
T2	Extends to vocal cord(s) with normal/impaired mobility
T3	Tumour limited to larynx with vocal cord fixation
T4a	Tumour invades cricoid or thyroid cartilage; trachea, soft tissues of neck: deep/extrinsic muscle of tongue, strap muscles, thyroid, oesophagus
T4b	Tumour invades prevertebral space, encases carotid artery, or involves mediastinal structures

Cervical Nodal Staging in the TNM system

Stage	Boundaries
NX	Regional lymph nodes cannot be assessed
N0	No regional lymph nodes metastasis
N1	Ipsilateral single ≤ 3 cm
N2 a b c	Ipsilateral single > 3 to 6 cm Ipsilateral multiple ≤ 6 cm Bilateral, contralateral ≤ 6 cm
N3	> 6 cm

Staging of Metastases in the TNM staging system

Stage	Definition
MX	Distant metastasis cannot be assessed
M0	No distant metastasis
M1	Distant metastasis

Tables adapted from AJCC Cancer Staging Manual (AJCC, 2002)

AJCC, A. J. C. O. C. 2002. *AJCC Cancer Staging Manual*, Unites States of America, Springer.

Appendix 2. Buffers and Solutions

50 x TAE Electrophoresis Buffer (ThermoScientific)

1X 40mM Tris
 20mM Acetic Acid
 1mM EDTA

LB Broth High Salt (Melford)

Tryptone 10g/L
Sodium Chloride 10g/L
Yeast Extract 5g/L
pH 7.2 ± 0.2

STE Buffer

2.5mls 1mM Tris pH 7.6
0.292g Sodium Chloride >99.5%
0.4mls 0.5M EDTA
0.25g SDS
Made up to 50mls with dH₂O

All ingredients from Sigma

Talon Buffer

10mM Tris
300mM NaCl
pH 8.0

10x SDS Running Buffer

1L 30.3g Tris Base
 144.2g Glycine
 10g SDS
 d₂H₂O to 1L

4x Tris-HCL/SDS pH 8.8

500mls 1.5M Tris-HCL

Tris Base 91g

d₂H₂O 300mls – pH to 8.8 using concentrated HCL

d₂H₂O Top up to 500mls

0.4% SDS

SDS 2g

Stored at 4°C

4x Tris-HCL/SDS pH 6.8

100ml 0.4M Tris-HCL

Tris Base 6.05g

d₂H₂O 40mls – pH to 6.8 using concentrated HCL

d₂H₂O Top up to 100ml

0.4% SDS

SDS 0.4g

4x SDS Loading Buffer

50ml 4x Tris-HCL pH6.8 25ml

Glycerol 20ml

SDS 4g

Bromophenol Blue 0.5mg

d₂H₂O up to 50ml

2x Urea/SDS Loading Buffer

4x SDS Loading Buffer 1ml

Urea 1g

β-mercaptoethanol 400μl

d₂H₂O 400μl

Used at 1x concentration

Appendix 3: Current on-going Trials in De-escalation of Treatment in HNSCC

Adapted from MASTERSON et al., De-escalation treatment protocols for human papillomavirus-associated oropharyngeal squamous cell carcinoma: a systematic review and meta-analysis of current clinical trials. *Eur J Cancer*. 2014;50(15):2636-48.

RCT	Trial Design	Study Type	Site/Stage	Start Date	End Date	Study Location
<i>Replacement of cisplatin by cetuximab</i>						
RTOG-1016 (NCT01302834)	Radiation therapy (70Gy for 6/52) with weekly cetuximab or cisplatin (administered on day 1 and day 22)	Interventional Phase III RCT Multi site Open label	OPSCC Stage III-IV	June 2011	June 2020	USA
De-ESCALaTE (ISRCTN33522080)	Radiation therapy (70Gy for 6/52) with weekly cetuximab or cisplatin (administered on day 1, 22 and 43)	Interventional Phase III RCT Multi site Open label	OPSCC Stage III-IV	Oct 2012	Feb 2015	UK
TROG-12.01 (NCT01855451)	Radiation therapy (70Gy in 35 fractions) with weekly cetuximab or cisplatin	Interventional Phase III RCT Multi site Open label	OPSCC Stage III-IV	May 2013	May 2019	Australia
<i>Induction chemotherapy followed by decreased chemo-radiotherapy dose in good responders</i>						
ECOG-1308 (NCT01084083)	Induction chemotherapy followed by low dose (54Gy) radiotherapy or standard dose (70Gy) IMRT with cetuximab depending on initial response to induction. chemotherapy	Interventional Phase II RCT Multi site Open label	OPSCC Stage III-IV	March 2010	March 2015	USA
University of Chicago (NCT01133678)	Patients randomized to receive induction chemotherapy with everolimus or placebo in combination with cisplatin, paclitaxel and cetuximab. Those with positive field undergo attenuated radiation field.	Interventional Phase II RCT Multi site Double-blind	HNSCC stage III-IV	May 2010	May 2016	USA
Quarterback trial (NCT01706939)	Patients who respond to induction chemotherapy will be randomized to low dose (54Gy) IMRT with weekly carboplatin or standard dose IMRT (70Gy) with weekly carboplatin.	Interventional Phase III RCT Multi site Single blinded	OP/unknown primary/nasopharynx Stage III-IV	Sept 2012	Sept 2019	USA

<i>Surgical resection with or without neo-adjuvant chemo-radiotherapy (based on histological features)</i>						
ADEPT (NCT01687413)	Intensity of adjuvant therapy required in p16+ OPSCC after removal of all disease with minimally invasive approach. After surgery patients randomized to radiotherapy alone or radiotherapy and cisplatin	Interventional Phase III RCT Multi site Open label	OPSCC Stage III-IV	Sept 2012	Sept 2017	USA
ECOG-3311 (NCT01898494)	Transoral surgery and neck dissection, followed by histological stratification into low, intermediate and high risk. Low risk-no adjuvant therapy, intermediate-randomised between 50-60Gy IMRT, high risk-IMRT (66Gy) with weekly cisplatin)	Interventional Phase II RCT Multi site Open label	OPSCC Stage III-IV	Jul 2013	Oct 2016	USA
PATHOS	Transoral surgery and neck dissection, followed by histological stratification into low, intermediate and high risk. Low risk-no adjuvant therapy, intermediate-randomised between 50 and 60Gy IMRT. High risk-IMRT with or without weekly cisplatin	Interventional Phase II RCT Multi site Open label	OPSCC Stage III-IV	Sept 2014	Sept 2019	UK

RCT; randomised controlled trial; ECOG, Eastern Co-operative oncology Group; RTOG, Radiation Therapy Oncology Group; De-ESCALaTE, Determination of Epidermal growth factor receptor inhibitor (cetuximab) versus Standard Chemotherapy (cisplatin) early And Late Toxicity Events in HPV positive OPSCC; TROG, Tasman Radiation Oncology Group; ADEPT, Adjuvant Therapy De-Intensification Trial for HPV-related, p16+ OPSCC; PATHOS, Post operative Adjuvant Treatment for HPV positive tumours.

Appendix 4. Ammonium sulphate precipitation tables

The table below provides multiplication factors for use in calculating the required volume of a 100% saturated solution of ammonium sulfate solution. The table values are independent of temperature.

Desired Final Ammonium Sulfate Percent Saturation

	10	15	20	25	30	35	40	45	50	55	60	65	70	75	80	85	90	95
0	0.111	0.176	0.250	0.333	0.429	0.538	0.667	0.818	1.000	1.222	1.500	1.857	2.333	3.000	4.000	5.667	9.000	19.000
10		0.059	0.125	0.200	0.286	0.385	0.500	0.636	0.800	1.000	1.250	1.571	2.000	2.600	3.500	5.000	8.000	17.000
15			0.063	0.133	0.214	0.308	0.417	0.545	0.700	0.889	1.125	1.429	1.833	2.400	3.250	4.667	7.500	16.000
20				0.067	0.143	0.231	0.333	0.455	0.600	0.778	1.000	1.286	1.667	2.200	3.000	4.333	7.000	15.000
25					0.071	0.154	0.250	0.364	0.500	0.667	0.875	1.143	1.500	2.000	2.750	4.000	6.500	14.000
30						0.077	0.167	0.273	0.400	0.556	0.750	1.000	1.333	1.800	2.500	3.667	6.000	13.000
35							0.083	0.182	0.300	0.444	0.625	0.857	1.167	1.600	2.250	3.333	5.500	12.000
40								0.091	0.200	0.333	0.500	0.714	1.000	1.400	2.000	3.000	5.000	11.000
45									0.100	0.222	0.375	0.571	0.833	1.200	1.750	2.667	4.500	10.000
50										0.111	0.250	0.429	0.667	1.000	1.500	2.333	4.000	9.000
55											0.125	0.286	0.500	0.800	1.250	2.000	3.500	8.000
60												0.143	0.333	0.600	1.000	1.667	3.000	7.000
65													0.167	0.400	0.750	1.333	2.500	6.000
70														0.200	0.500	1.000	2.000	5.000
75															0.250	0.667	1.500	4.000
80																0.333	1.000	3.000
85																	0.500	2.000
90																		1.000
95																		

Initial Ammonium Sulfate Percent Saturation

Adapted from Sigma-Aldrich, product information sheet A 5479